

Lubricant-Derived Ash – In-Engine Sources and Opportunities for Reduction

by

Simon A.G. Watson

B.A.Sc. Mechanical Engineering
University of Toronto, 2003

M.A.Sc. Mechanical Engineering
University of Toronto, 2005

Submitted to the Department of Mechanical Engineering in partial fulfillment of the requirements for the degree of

DOCTOR OF PHILOSOPHY IN MECHANICAL ENGINEERING

AT THE

MASSACHUSETTS INSTITUTE OF TECHNOLOGY

June 2010

© 2010 Massachusetts Institute of Technology
All rights reserved.

Signature of Author:
Department of Mechanical Engineering
April 30, 2010

Certified by:
Wai K. Cheng
Professor of Mechanical Engineering
Committee Chair

Certified by:
Victor W. Wong
Principal Research Scientist and Lecturer in Mechanical Engineering
Thesis Supervisor

Accepted by:
David Hardt
Chairman, Department Committee on Graduate Students

(This page intentionally left blank)

Lubricant-Derived Ash – In-Engine Sources and Opportunities for Reduction

by

Simon A.G. Watson

Submitted to the Department of Mechanical Engineering on
April 30, 2010 in partial fulfillment of the requirements for the
degree of Doctor of Philosophy in Mechanical Engineering

ABSTRACT

Diesel particulate filters (DPF) are an effective means for meeting increasingly stringent emissions regulations that limit particulate matter. Over time, ash primarily derived from metallic additives in the engine oil accumulates in DPFs. Lubricant-derived ash increases pressure drop and reduces fuel economy. After long time periods, the accumulation of ash may lead to irreversible plugging in DPFs, which necessitates periodic filter removal and cleaning.

This thesis examines the sources for lubricant-derived ash in engines and explores potential opportunities to reduce ash emissions. The research studies changes in lubricant composition in the engine via advanced in-situ diagnostics and computer modeling of species transport in the power cylinder. These changes are directly related to ash emissions and the effectiveness of the lubricant in protecting engine components.

In the first part of this thesis, sampling techniques are employed to determine the composition of the lubricant in critical locations in the engine system, where oil is lost by liquid oil consumption and vaporization. The first practical in-situ FTIR measurements of lubricant composition at the piston and liner interface are obtained with a novel diagnostics system employing Attenuated Total Reflection (ATR) spectroscopy. This information is used to create a mass balance for ash-related elements and a framework for modeling the distribution of ash-related species in the engine.

In the second part of this thesis, a novel approach to condition the lubricant at a fixed station in the oil circuit is explored as a potential means to reduce ash emissions. This study examines the performance of an innovative oil filter that releases no additives into the lubricant, yet enhances the acid control function typically performed by detergent and dispersant additives. The filter has the potential to be used as a replacement for detergent additives in a lubricant formulation, or enhance additive effectiveness there-by allowing in an increase in oil drain interval. This research will assist in the development of new formulations for diesel lubricants that minimize detrimental effects on DPFs, while providing adequate protection to engine components.

Thesis Supervisor: Victor W. Wong

Title: Principal Research Scientist and Lecturer in Mechanical Engineering

(This page intentionally left blank)

ACKNOWLEDGEMENTS

I thank the following individuals for their contributions to this thesis, patient guidance and unwavering support. I am extremely grateful for all those who made my experience at MIT a rewarding time in my life.

Foremost, I express my utmost gratitude to my advisor Dr. Victor Wong for his guidance and encouragement during this project. I appreciate him affording me the independence flexibility to explore several aspects of this problem. I am also especially grateful for the many opportunities he gave me to present my research at conferences and meetings around the world. Additionally, I would also like to acknowledge Professors Wai K. Cheng, John Heywood, and Bill Green for their advice as members of my thesis committee.

This project was supported of the MIT Consortium to Optimize Lubricant and Diesel Engines for Robust Emission Aftertreatment Systems. I thank all of the current and past consortium members for providing stimulating discussions and for their helpful advice during our consortium meetings. In particular, I acknowledge Darrel Brownawell, Scott Harold, Mark Jarrett and Scott Lockledge for their substantial contributions to this work. I will always be indebted to Professor Wenwei Huang for his assistance while establishing this project. Thanks are also due to Tim McClure at the MIT Center for Materials Science and Engineering for his assistance with spectroscopy. Peter Melling made substantial contributions to the advanced diagnostics developed during this study.

I am appreciative of the support provided by all of members of the Sloan Automotive Laboratory. Raymond Phan was a never ending source of assistance and advice during this project. Thane Dewitt contributed through his technical assistance and ability to solve the tough challenges encountered during the experiments. Janet Maslow deserves special credit for keeping us all organized and making the lab a pleasant place to work.

I am also fortunate to have had the opportunity to develop many lasting friendships with several of my colleges at the Sloan Automotive Lab. Sharing an office with Raul Coral, RJ Scaringe, Kristian Bodek and Walter Hoffman lead to many memories and made my time at MIT an enjoyable experience. I would also like to thank Alexander Sappok, Craig Wildman and Vikram Mittal for their help while preparing for qualifying exams. Additionally, I thank Amir Maria, Arthur Kariya, Kai Liao, Dongkun Lee, Manolis Kasseris, Dr. Kenneth Kar, and Yuichi Kodama for being there to give helpful advice, support and stimulating conversation.

Most of all, I thank the members of my family for their unconditional support and belief in me. I am lucky to be married to my wife Lorna, who provided loving support throughout my studies and encouragement. I am thankful for her patience and unwavering belief that I would eventually finish.

Simon A.G. Watson
April 2010

(This page intentionally left blank)

TABLE OF CONTENTS

ABSTRACT	3
ACKNOWLEDGEMENTS	5
TABLE OF CONTENTS	7
LIST OF FIGURES	11
LIST OF TABLES	18
ACRONYMS AND SYMBOLS	21
NOMENCLATURE	21
SYMBOLS	22
CHAPTER 1 - INTRODUCTION	25
1.0 LUBRICANT-DERIVED ASH	25
1.1 CURRENT KNOWLEDGE BASE	26
1.2 THESIS OBJECTIVES	28
1.3 THESIS SUMMARY	28
1.3.1 Part 1 – The In-Engine Transport and Distribution of Ash-Related Species	29
<i>1.3.1.1 Part 1 - Fundamental Questions:</i>	30
1.3.2 Part 2 – Oil Conditioning as a Potential Means to Lower Additive Requirements	30
<i>1.3.2.1 Part 2 - Fundamental Questions:</i>	31
1.4 CONTRIBUTIONS TO KNOWLEDGE	31
CHAPTER 2 – EFFECTS OF LUBRICANT ADDITIVES IN DIESEL ENGINES	34
2.0 INTRODUCTION	34
2.1 LUBRICANT CHEMISTRY	35
2.1.1 Lubricant Formulations	35
2.1.2 Lubricant-Derived Ash and Sulfated Ash	36
2.1.3 Lubricant Additives that Contribute to Ash	38
<i>2.1.3.1 Detergents and Dispersants</i>	38
<u>2.1.3.1.1 Detergents</u>	39
<u>2.1.3.1.2 Dispersants</u>	41
<i>2.1.3.2 Antiwear Additives</i>	41
<i>2.1.3.3 Antioxidants</i>	45
2.1.4 Lubricant Contamination and Degradation	45
2.1.5 Total Acid Number (TAN) and Total Base Number (TBN)	47
2.2.6 Oil Drain Interval	50
2.3 EFFECTS OF ASH ON DIESEL PARTICULATE FILTERS	51
2.3.1 DPF Operation	51
2.3.2 Exhaust Ash Emissions and Effects on DPFs	53

2.4	LOW SAPS OIL FORMULATIONS	58
2.5	THE LUBRICATION SYSTEM	60
2.5.1	Engine Bulk Oil Flows	62
2.5.2	Power Cylinder Oil Flows	62
2.6	OIL CONSUMPTION	65
2.7	STUDIES OF LUBRICANT COMPOSITION IN DIESEL ENGINES	68
CHAPTER 3 – EXPERIMENTAL AND ANALYTICAL METHODS		74
3.0	TEST ENGINE	74
3.1	OIL SAMPLING	75
3.1.1	Ring Pack Sampling	77
3.1.2	Sump Oil Sampling	80
3.1.2.1	<i>Oil Consumption Measurement</i>	81
3.1.3	Valve Train Sampling	82
3.2	OIL ANALYSIS	83
3.2.1	Inductively Coupled Plasma (ICP) Analysis	83
3.2.2	Total Base Number (TBN)	85
3.2.3	Total Acid Number (TAN)	86
3.2.4	Four Ball Wear Test	87
3.2.5	Fourier Transform Infrared (FTIR) Spectroscopy	88
3.3	IN-SITU FOURIER TRANSFORM INFRARED (FTIR) SPECTROSCOPY	91
3.3.1	Measurement Principle – Attenuated Total Reflectance (ATR)	93
3.3.2	ATR Probe Design	94
3.3.3	Measurement Procedure	99
3.4	FILTER DEBRIS ANALYSIS	103
3.5	LUBRICANTS	104
3.6	FUEL	104
3.7	LUBRICANT SPECIES TRANSPORT MODEL FRAMEWORK	106
3.7.1	Modeling Approach	106
3.7.2	Model Framework	107
3.7.3	Base Oil Evaporation Model	108
3.7.4	Convection Model	109
3.7.5	Oil Model	110
3.7.6	Estimating the Convective Heat Transfer Coefficient	111
CHAPTER 4 - IN-ENGINE DISTRIBUTION AND TRANSPORT OF ASH-RELATED SPECIES		114
4.0	INTRODUCTION	114
4.1	EXPERIMENTAL METHODOLOGY	117
4.1.1	Ring Pack Sampling Experiments	117
4.1.2	Long Duration Sampling Experiments	119
4.1.3	Valve Train Sampling	120
4.1.4	In-Situ FTIR Measurements	121
4.1.5	Lubricant and Fuel Properties	123
4.1.6	Oil Sample Analysis	125
4.2	RESULTS	125

4.2.1 Ring Pack Oil Samples	125
4.2.2 Top Ring Groove Enrichment	127
4.2.3 Crankcase Oil Analysis	128
4.2.4 Comparison of Actual and Expected Loss from the Crankcase	131
4.2.5 Valve Train Oil Samples	133
4.2.6 Filter Debris Analysis	136
4.2.7 Characterization of In-Engine Deposits	138
4.2.8 In-Situ Measurements at the Piston and Liner Interface	138
4.2.8.1 Ring Pack Oil Composition	138
4.2.8.2 Residence time	139
4.3 ANALYSIS OF RESULTS	142
4.3.1 Estimated Ash Emissions	143
4.3.2 Elemental Mass Balance	145
4.3.3 Source of Calcium and Magnesium in Exhaust	148
4.3.4 Source of Zinc and Phosphorus in Exhaust	152
4.4 MODELING LUBRICANT SPECIES DISTRIBUTIONS AND TRANSPORT IN THE ENGINE	153
4.4.1 Power Cylinder Model	153
4.4.2 Model Calibration	155
4.4.3 Alternatives for Reducing Ash Emissions	159
4.4.3.1 Effect of Reduced Base Oil Volatility	160
4.4.3.2 Effect of Shortened Ring Pack Residence time	161
4.5 CONCLUSIONS	161
CHAPTER 5 - FILTER CONDITIONING AS A POTENTIAL MEANS TO REDUCE ADDITIVE REQUIREMENTS	165
5.0 INTRODUCTION	165
5.1 CURRENT ALTERNATIVE TECHNOLOGIES	166
5.2 STRONG BASE FILTER	166
5.3 EFFECT ON AFTERTREATMENT SYSTEM DURABILITY	169
5.4 EXPERIMENTAL APPROACH	170
5.4.1 Test Procedure	171
5.4.2 Lubricant and Fuel Properties	173
5.4.3 Oil Sample Analysis	175
5.5 RESULTS	176
5.5.1 Test Conditions	176
5.5.2 Mobility of Strong Base Material	179
5.5.3 Lubricant Acidity	180
5.5.3.1 Total Acid Number (TAN)	181
5.5.3.2 pH Measurements	183
5.5.4 Total Base Number (TBN) Retention	184
5.5.5 Lubricant Oxidation	187
5.5.6 Viscosity	188
5.5.7 Wear Metal Analysis	189
5.5.8 Four Ball Wear Tests	195
5.5.9 Filter Capacity and Efficiency	196

5.6 ANALYSIS OF RESULTS	197
5.6.1 Proposed Mechanism	197
5.6.2 Effect On Lubricant Acidity	199
5.6.2.1 <i>Proposed Acid Transfer Mechanism</i>	199
5.6.2.2 <i>Acid Neutralization Rate</i>	200
5.6.2.3 <i>Neutralization of Oxidation By-Products</i>	201
5.6.3 Effect on Lubricant Viscosity	202
5.6.4 Effect on Corrosion and Wear	203
5.6.5 Effect on Aftertreatment System Durability	204
5.6.6 Effect on Oil Drain Interval	204
5.7 CONCLUSIONS	205
CHAPTER 6 – CONCLUSIONS AND RECOMMENDATIONS	208
6.0 CONCLUSIONS	208
6.0.1 In-Engine Distribution and Transport of Ash-Related Species	208
6.0.2 Filter Conditioning as a Potential Means to Reduce Additive Requirements	209
6.1 RECOMMENDATIONS	210
6.1.1 Percent Ash Measurement	212
6.2 RECOMMENDATIONS FOR FUTURE WORK	213
6.2.1 In-Situ FTIR Measurements of Lubricant Composition	214
6.2.2 Lubricant Species Distribution and Transport Model	214
6.2.3 Lubricant Conditioning with the Strong Base Filter	215
6.2.4 In-Situ Raman Spectroscopy	216
6.2.1.1 <i>Ultraviolet Raman Spectroscopy</i>	217
REFERENCES	220
APPENDICES	230
APPENDIX A - ESTIMATING SULFATED ASH WITH ELEMENTAL WEIGHTING FACTORS	230
APPENDIX B - CALCULATING BASE OIL PROPERTIES	232
APPENDIX C - STATISTICAL ANALYSIS OF VALVE TRAIN OIL SAMPLES	234
APPENDIX D - STATISTICAL SIGNIFICANCE OF TRENDS IN FILTER TEST RESULTS	235

LIST OF FIGURES

Figure 2.1 – Solubilization of a soot contaminant by surfactant molecules in oil [19].	39
Figure 2.2 – Schematic of Overbased Calcium Sulfonate Detergent [19].	40
Figure 2.3 – Zinc Dialkyldithiophosphate (ZDDP)	42
Figure 2.4 – Forms of ZDDP. <i>Left</i> - dimer. <i>Right</i> - monomer [26].	43
Figure 2.5 - Basic ZDDP, $Zn_4[PS_2(OR)_2]_6O$ [26].	43
Figure 2.6 – The typical change in TBN and TAN over the life of an engine lubricant. The lines show: a) a characteristic decrease in TBN for a fully formulated oil; b) TBN for an oil formulation with a reduced detergent level; c) a reduced rate of TBN depletion due to a lower acidic contamination rate; and d) a typical increase in the TAN.	48
Figure 2.7 – Particle laden flow is filtered by the DPF as it passes through the porous walls of the substrate. A catalyst on the filter walls also reduces emissions of carbon monoxide and hydrocarbons.	52
Figure 2.8 – Typical ash and soot distributions in the channel of a regenerated DPF. The inlet for flow is on the left of the picture. Exhaust passes through to the outlet, on the right of the picture [40].	53
Figure 2.9 – A compilation of studies documented in SAE papers illustrating the dependence of pressure drop on sulfated ash level [49].	54
Figure 2.10 – A comparison of the actual mass of ash recovered from DPF with the expected amount based on sulfated ash for three lubricant formulations. Data compiled from [45].	55
Figure 2.11 – A schematic of the lubrication system in a diesel engine.	61
Figure 2.12 – A simplified schematic of the oil flows in the power cylinder system. Oil is supplied to the cylinder liner and piston ring pack by splashing and sprays. A portion of the oil returns back to the sump. A portion of the oil in the ring pack is lost by oil consumption to the combustion chamber.	63
Figure 2.13 – A schematic of the ring pack geometry in a typical diesel engine. The oil flows between locations on the piston ring pack and liner are highly transient [58].	64
Figure 2.14 – The mechanisms for oil consumption from the power cylinder system; a) Inertia; b) Reverse Gas Flow; c) Evaporation; d) Crankcase Ventilation; and e) Valve Guide Leakage.	66
Figure 3.1 – An image of the experimental setup with major components listed. The engine is loaded by an AC generator operating at 1800, or 1500 rpm. Power is dissipated by a resistor load bank rated at 7 kW.	74
Figure 3.2 – A schematic of the engine system showing the locations where oil was extracted in this study. A different experimental technique was used to	76

obtain samples from each location, while the engine was operating.	
Figure 3.3 – A schematic of the ring pack sampling system used in this study.	77
Figure 3.4 – <i>Left</i> - A picture of the Lister Petter TR1 piston ring pack. <i>Right</i> - A picture of the piston used with the sampling system. The piston rings have been removed to reveal the sampling hole situated in the top ring groove.	78
Figure 3.5 – <i>Left</i> - A schematic showing the connection between the channel inside the piston and the sampling tube. <i>Right</i> - A picture of the tube connector, containing a 0.5 millimeter orifice. Deposits are clearly visible on the face of the orifice and inside the sampling tube.	78
Figure 3.6 – The mass of oil samples collected in one hour by the piston ring pack sampling system, over the duration of a 40 hour experiment.	79
Figure 3.7 – A schematic of the sump oil sampling and oil consumption measurement system. Oil samples are collected after measuring the oil level in the sump.	80
Figure 3.8 – Pictures of the sump oil sampling system.	81
Figure 3.9 – The sampling locations in the valve train system. Lubricant was collected from the valve rockers and simultaneously from the sump.	82
Figure 3.10 – The contact geometry used during a four ball wear test.	87
Figure 3.11 – In a typical FTIR analysis the oil sample is placed between the infrared source and detector. Infrared radiation must pass through the sample to be absorbed.	89
Figure 3.12 – A typical FTIR spectrum of used oil with peaks of interest labeled.	90
Figure 3.13 – Functional groups that correspond with absorbance peaks in FTIR spectra of used oil.	90
Figure 3.14 – A schematic of the FTIR measurement system. Infrared radiation is absorbed from the surface of a zinc sulfide crystal mounted on the cylinder liner.	92
Figure 3.15 – The measurement principle for Attenuated Total Reflectance FTIR spectroscopy.	93
Figure 3.16 – A CAD rendering of the ATR probe developed for this study. The probe obtains FTIR measurements of lubricant composition at the piston and liner interface during engine operation.	94
Figure 3.17 – The ATR crystal. <i>Left</i> - A cutaway of the probe tip and crystal mounting. <i>Right</i> – Internal reflections culminate the infrared radiation towards the probe tip. Two reflections occur at the sample location.	95
Figure 3.18 – The transmission properties of zinc sulfide are relatively constant across the wavelengths in the mid infrared range.	96
Figure 3.19 – A schematic of the ATR probe.	96

Figure 3.20 – An illustration of the sampling region.	97
Figure 3.21 – A picture of the ATR probe attached to the engine.	98
Figure 3.22 – A picture of the optics, interferometer and detector used in the ATR system.	98
Figure 3.23 – A spectrum of used oil at the piston and line interface. The lubricant is contaminated with biodiesel fuel, as indicated by the prominent ester peak. This data was obtained 4.5 minutes after engine shutdown.	100
Figure 3.24 – Raw spectra collected by the ATR system. The engine starts at 30s and is shut down at 199 seconds. The vertical axis is in absorbance units.	101
Figure 3.25 – The raw spectral time series viewed from above.	102
Figure 3.26 – Individual spectra obtained by the ATR system. The spectra obtained at start-up (36 seconds) and 66 seconds may be used to characterize the composition of the lubricant. The spectrum at 78 seconds is noisy and unusable.	102
Figure 3.27 – The data series shown in Figure 3-21 after removal of the noisy spectra.	103
Figure 3.28 – A filter debris micro-patch obtained during the filter debris analysis procedure.	103
Figure 3.29 – A representation of a single zone in the lubricant species transport model. Each zone can communicate with any number of neighboring zones by oil transport. Chemical reactions are modeled as sources, or sinks of a species in each zone.	106
Figure 3.30 – A simple model of the power cylinder system. Left - Lubricant in the engine is separated into three zones. Right – The zones are interconnected by oil flows, many of which model the modes of oil consumption.	108
Figure 3.31 – Distillation curves for the oils used in this study.	110
Figure 4.1 – A simplified representation of the oil flows in the power cylinder	115
Figure 4.2 – The peaks used to compare the chemical composition of the valve train and sump oil.	121
Figure 4.3 – Two FTIR spectra of engine oil measured with ATR spectroscopy. The blue spectrum is a fresh oil sample. The red spectrum is used oil aged for 350 hours with 10 wt% biodiesel. The presence of biodiesel is clearly indicated by the ester peak at approximately 1750 cm^{-1} .	123
Figure 4.4 – Results from a typical ring pack sampling experiment with oil A.	126
Figure 4.5 - The average enrichment factors of metallic element in TRG samples.	127
Figure 4.6 – The measured concentrations of calcium, zinc and phosphorus in the crankcase oil during the long duration engine tests. Results for oils D and E are shown.	129

Figure 4.7 – The total mass lost for elements in the in the crankcase oil.	130
Figure 4.8 - A comparison of the actual and expected mass loss of ash-related elements from the crankcase oil.	131
Figure 4.9 – The differences in the sample means ($\mu_v - \mu_s$) of elemental concentrations measured in the valve train and sump oil samples.	134
Figure 4.10 – Results of the student t-Test, comparing the valve train and sump oil elemental composition. A t-Test significance greater than 0.05 implies that the null hypothesis (H_o) can be accepted to a confidence level of 95%.	134
Figure 4.11 – The differences in the sample means ($\mu_v - \mu_s$) of FTIR absorbance (at specific wavenumbers) measured in the valve train and sump oil samples.	135
Figure 4.12 – Results of the student t-Test, comparing the valve train and sump oil chemical composition. A t-Test significance greater than 0.05 implies that the null hypothesis (H_o) can be accepted to a confidence level of 95%.	136
Figure 4.13 – The mass of individual elements in the debris trapped by a standard full-flow oil filter. The filter was used for 285 hours.	137
Figure 4.14 – In-situ FTIR spectra of the oil in the piston ring zone and sump. The fingerprint region between 1850 and 1000 cm^{-1} is shown.	139
Figure 4.15 – The concentration of biodiesel was measured in-situ as it mixed with the oil in the piston ring zone.	140
Figure 4.16 – A top view of the spectral time series recorded during the tracer experiment. The emergence of an ester peak is clearly visible at 1750 cm^{-1} .	140
Figure 4.17 – The growth of the peak associated with biodiesel.	141
Figure 4.18 – The estimated composition of DPF ash that would result from the long duration engine tests.	144
Figure 4.19 – A comparison of the estimated DPF ash with the total expected ash based on the sulfated ash level of the fresh lubricant.	145
Figure 4.20 – A mass balance for calcium. The letters on the horizontal axis refer to the lubricants used in the long duration engine tests.	146
Figure 4.21 – A mass balance for zinc.	146
Figure 4.22 – A mass balance for phosphorus.	147
Figure 4.23 – A simplified model of the power cylinder system. The concentration of calcium in the TRG, measured with ring pack sampling, may be used to estimate the rate of bulk oil loss. This is the only mode for the emission of calcium into the exhaust.	148
Figure 4.24 – The fractions of total volatile and liquid (bulk) oil consumption during the ring pack sampling experiments. High oil consumption rates occurred during these experiments due to the volatilization of light-end hydrocarbons from the fresh oil.	150

Figure 4.25 – The fractions of oil consumed by volatile and liquid (bulk) oil consumption from the piston ring pack region during the ring pack sampling experiments.	151
Figure 4.26 – A schematic of the framework used to model ash-related lubricant species distribution and transport in the power cylinder.	154
Figure 4.27 – A comparison of the elemental emissions, measured and from the model.	156
Figure 4.28 – The predicted species concentrations during a ring pack (RP) sampling experiment with oil A. The compositions of samples from the ring pack are also plotted.	157
Figure 4.29 – A comparison of the measured enrichment factors and those predicted by the model.	157
Figure 4.30 – A comparison of the sump oil composition for oil A measured in the long duration engine tests and predicted by the model.	158
Figure 4.31 – A comparison of the sump oil composition for oil D measured in the long duration engine tests and predicted by the model.	158
Figure 4.32 – The predicted distillation curves for base oil in the sump and ring pack after 289 hours of engine operation (<i>Left</i> - Oil A, <i>Right</i> - Oil D). The curves shift to the left due to preferential volatilization of lighter hydrocarbons in the mixture.	159
Figure 4.33 – Base oil distillation curves. The higher volatility oil has a NOACK volatility of 15%. The lower volatility oil has a NOACK volatility of 11%.	160
Figure 4.34 – Predicted elemental emissions with higher and lower volatility base oils.	160
Figure 4.35 - Elemental emissions for ring pack residence times of 3 and 1 minute.	161
Figure 5.1 – <i>Left</i> - The standard filter element. <i>Right</i> - The prototype strong base filter. Both filters are full-flow 20 micron filter elements and are reinforced with stainless steel mesh.	167
Figure 5.2 – A TEM image of standard (20 micron) filter paper.	168
Figure 5.3 – A TEM image of the filter paper in the strong base filter.	168
Figure 5.4 – Elemental analysis with ESEM of a strong base particle in the filter. The particles are primarily composed of magnesium oxide.	169
Figure 5.5 – Both filter elements were mounted in a Racor™ full-flow housing. Both filters contained identical oil volumes and similar flow profiles.	171
Figure 5.6 – Total oil consumption.	177
Figure 5.7 – Oil soot content in the first 300 hours, measured with FTIR.	179
Figure 5.8 – The concentration of magnesium measured with ICP (ASTM	180

D5185).	
Figure 5.9 – TAN of the zero-detergent and CI-4 PLUS oil samples measured with ASTM D-664 and colorimetric titration.	182
Figure 5.10 - Lubricant acidity measured in pH units.	184
Figure 5.11 – TBN retention for the tests with the zero-detergent and CI-4 PLUS oils.	185
Figure 5.12 – Oil oxidation in the tests with the CI-4 PLUS oil, measured with FTIR analysis.	187
Figure 5.13 – Viscosity of zero-detergent oil samples.	188
Figure 5.14 – The concentration of iron in the CI-4 PLUS oil samples measured with ICP (ASTM D5185).	190
Figure 5.15 – The concentration of iron in the zero-detergent oil samples measured with ICP.	191
Figure 5.16 – The concentration of copper and chromium in the CI-4 PLUS oil samples measured with ICP.	192
Figure 5.17 – The concentration of copper and chromium in the zero-detergent oil samples measured with ICP.	193
Figure 5.18 – The concentration of tin and lead in the CI-4 PLUS oil samples measured with ICP.	194
Figure 5.19 – The concentration of tin and lead in the zero-detergent oil samples measured with ICP.	194
Figure 5.20 – Four ball wear test results.	195
Figure 5.21 – The proposed mechanism for acid transfer to the strong base filter.	198
Figure 6.1 – Left - A schematic of a multi-zone representation of the piston ring pack. Right - The modes for oil transport through the piston ring pack.	215
Figure 6.2 – The configuration of a proposed Raman system for in-situ measurements of lubricant composition in the power cylinder.	216
Figure 6.3 – Raman spectra of used diesel engine oil with high soot content (1.8%), measured with deep UV (193 nm) laser excitation.	217
Figure 6.3 – Raman spectra of used diesel engine oil with high soot content (1.8%), measured with deep UV (193 nm) laser excitation. <i>Red</i> – Used Oil Spectrum, <i>Blue</i> – Spectrum of quartz sample container subtracted from the raw spectrum.	218

(This page intentionally left blank)

LIST OF TABLES

Table 2.1 – Sources of Sulfur and Ash in Diesel Engine Oil	37
Table 2.2 – Elements Found in Sulfated Ash and Elemental Weighting Factors to Estimate Fresh Oil Sulfated Ash Content	37
Table 2.3 - Major Elements in a Typical SAE 15W40 Oil Formulation	38
Table 2.4 – Ratio of TBN Measured by Different Test Methods for Selected Additives [21]	50
Table 2.5 – The Composition of Ash Collected in a DPF, Compared to the Fresh Oil Elemental Composition [51]	57
Table 3.1 – Relevant Engine Specifications	74
Table 3.2 – Common sources of Elements found in ICP Analysis of Used Oil Samples	84
Table 3.3 – Four Ball Wear Test Parameters	87
Table 3.4 – Diesel Lubricating Oil Condition Monitoring Parameters Used for Direct Trending and Reporting Procedure	91
Table 3.5 – ATR Probe Specifications	95
Table 3.6 – Measurement Parameters	100
Table 3.7 – Lubricant Properties	105
Table 3.8 – Lubricant Elemental Analysis (D4951)	105
Table 4.1 – Long Duration Engine Test Parameters	119
Table 4.2 – FTIR Experimental Parameters	122
Table 4.3 – Properties of Lubricants Used in the Ring Pack Sampling Experiments	124
Table 4.4 Fresh Oil Concentrations of Metallic Elements in the Lubricants Used in Ring Pack Sampling Experiments (ASTM D5185)	124
Table 4.5 – The Sulfated Ash and Oil Consumption for the Lubricants Used in the Long Duration Engine Tests	125
Table 4.6 – TRG Sample Analysis Results	128
Table 4.7 – Emission Rates for Elements Associated with DPF Ash	132
Table 4.8 – Comparison of the Mass of Elements in the Oil Filter and the Sump Oil [†]	138
Table 4.9 – Specified Parameters for Each Zone	154
Table 4.10 – The Specified Volatility for Zinc and Phosphorus	155
Table 4.11 – Elemental Emission Rates (Measured and Predicted by the Model)	156

Table 5.1 – Engine Test Parameters	171
Table 5.2 – Lubricant Properties	173
Table 5.3 – Fresh Lubricant Elemental Analysis (ASTM D4951)	174
Table 5.4 – A Description of the Components in the Zero-Detergent Oil	174
Table 5.5 – A Comparison of the Conditions in the Tests with Zero-Detergent Oil	178
Table 5.6 – A Comparison of the Conditions in the Tests with CI-4 PLUS Oil	178
Table 6.1 – Parameters Used in a Percent Ash Calculation for Selected Additives	213
Table 6.2 – Comparison of Sulfated Ash and Percent Ash Measurements	213
Table A.1 – Elemental Weighting Factors	230
Table A.2 – Elemental Percentages of Lubricant Species that Contribute of Sulfated Ash	230
Table A.3 Calculation of Estimated Sulfated Ash Percentage	231
Table C.1 – Valve Train and Sump Oil ICP Data	234
Table C.2 – Valve Train and Sump Oil FTIR Data	234
Table D.1 – Summary of Regression Parameters	235

(This page intentionally left blank)

ACRONYMS AND SYMBOLS

NOMENCLATURE

ATR	Attenuated Total Reflectance
ATS	Aftertreatment System
ASTM	American Society for Testing and Materials
BMEP	Break Mean Effective Pressure
B	Boron
Ca	Calcium
DPF	Diesel Particulate Filter
EGR	Exhaust Gas Recirculation
ESEM	Environmental Scanning Electron Microscope
FTIR	Fourier Transform Infrared
HgCdTe	Mercury-Cadmium-Telluride
ICP	Inductively Coupled Plasma
IR	Infrared
KOH	Potassium Hydroxide
Mg	Magnesium
MoDTC	Molybdenum Dithiocarbamate
NO _x	Nitrogen Oxides
OCR	Oil Control Ring
OEM	Original Equipment Manufacturer
PM	Particulate Matter
P	Phosphorus
PIBSA	Polyisobutylene Amine Succinimides
SAN	Strong Acid Number
SAPS	Sulfated Ash, Phosphorus and Sulfur
SnDDC	Dibutyl Tin Dioctylldithiocarbamate
TAN	Total Acid Number
TBN	Total Base Number

TDC	Top Dead Center
TEM	Transmission Electron Microscope
TGA	Thermo-Gravimetric Analysis
TRG	Top Ring Groove
TRZ	Top Ring Zone
UDEO	Universal Diesel Engine Oil
VI	Viscosity Index
XRF	X-Ray Fluorescence
XRD	X-Ray Diffraction
ZDDP	Zinc Dialkyldithiophosphate
Zn	Zinc
ZnS	Zinc Sulfide

SYMBOLS

A	Concentration (kg/kg)
A_{eff}	Effective Zone Oil Surface Area (m ²)
CC	Subscript Denoting Crankcase
D_{ah}	Binary Diffusion Coefficient (m ² /s)
g	Convective Mass Flux (kg/m ² ·s)
H_o	Null Hypothesis
i	Lubricant Species Index
j	Interconnecting Zone Index
k	Zone Index
k	Thermal Conductivity (W/K·m)
L	Number of Interconnecting Zones
L	Characteristic Length (m)
m	Mass (kg), Instantaneous Mass Flux (kg/s)
\dot{m}	Mass Flow Rate (kg/s)
M	Number of Zones, Concentration (kg/kg)
mf	Mass Fraction (kg/kg)

\overline{mf}	Mole Fraction (kmol/kmol)
MW	Molecular Weight (kg/kmol)
Nu	Nusselt number
OC	Oil Consumption (kg/s)
P_c	Bulk Gas Pressure (Pa)
Pr	Prandlt number
P_v	Vapor Pressure (Pa)
Re	Reynolds Number
RP	Subscript Denoting Ring Pack
Sc	Schmidt number
Sh	Sherwood Number
t	Time (s)
T	Time Period (s)
T_s	Surface Temperature (Kelvin)
T_{bp}	Boiling Point (Kelvin, or °C)
T_l	Liquid Temperature (Kelvin)
V	Characteristic Velocity (m/s)
VP	Vapour Pressure (mm Hg)
Y	Flow Rate (kg/s)
α	Thermal diffusivity (m ² /s)
β	Composition Modification Factor (0-1)
ρ	Density (kg/m ³)
τ	Time Delay, Residence Time
μ	Sample Mean
ν	Kinematic viscosity (m ² /s)

(This page intentionally left blank)

CHAPTER 1 - INTRODUCTION

1.0 LUBRICANT-DERIVED ASH

Current on-highway North American, European, and Japanese regulations on diesel engines require substantial reductions in particulate matter (PM) and nitrogen oxide (NO_x) emissions. They also specify that modern diesel engines be equipped with diesel particulate filters (DPF), which trap particulate emissions in the exhaust stream. A small fraction of the particulates emitted from diesel engines are inorganic compounds (containing metallic elements) from a variety of sources in the engine. The predominant source of metallic species in the exhaust is the lubricant additive package. Oxidizing these inorganic compounds produces ash, which collects in DPFs and on other components in aftertreatment systems.

The accumulation of ash in DPFs has detrimental effects on engine systems [1]. Lubricant-derived ash increases engine backpressure and reduces fuel economy. Over long time periods, the accumulation of lubricant-derived ash may lead to irreversible plugging in DPFs, which necessitates periodic filter removal and cleaning. Phosphorus and sulfur from the lubricant has also been linked to chemical deactivation of aftertreatment system catalysts. The quantity of lubricant-derived ash in the exhaust is related to the rate of oil consumption and the composition of the lubricant. Ash emitted from diesel engines is primarily composed of metal oxides, sulfates and phosphates. The majority of these compounds originate from the consumption of metallic compounds in the oil additive package.

The lubricants industry is currently focused on developing new lubricant formulations with reduced amounts of the additives containing sulfur, phosphorus and metallic species. However, these additives serve a wide range of beneficial and necessary functions within the engine including acid control, wear and corrosion protection, and oxidation resistance. Lubricant formulators must reduce the amount of ash-related compounds

emitted in the exhaust, while also ensuring that the lubricant provides adequate engine protection [2].

1.1 CURRENT KNOWLEDGE BASE

The impact of a lubricant on aftertreatment systems may be roughly assessed by measuring the sulfated ash content in accordance with the ASTM D874 standard [3]. However, this test does not account for the actual conditions inside the engine, so it tends to overestimate the impact of the lubricant.

Recent studies of ash accumulation in DPFs consistently find that the mass of ash-related elements in filters is less than would be expected based on the ASTM D874 sulfated ash level of the fresh oil and the oil consumption rate [1,4,5,6,7]. Furthermore, the relative fractions of metallic elements in DPF ash are not representative of the crankcase oil composition [1,4,6]. For instance, metallic elements associated with the detergent in the lubricant (i.e. calcium and magnesium) are recovered in exhaust and DPF ash at much lower rates than would be expected considering their concentration in the crankcase oil. A much higher portion of the crankcase phosphorus content from the antiwear additive Zinc Dialkyldithiophosphate (ZDDP) is recovered than any other element. Many fates for metallic compounds in the lubricant are suggested by [4] to account for the lower than expected recovery rates including:

- Accumulation in the crankcase oil due to preferential consumption of the base oil by volatility;
- Penetration through the DPF;
- Deposition on surfaces inside the engine; and
- Formation of antiwear films for the ZDDP elements.

Preferential emission or retention of metallic elements from the additive package is related to the distribution and transport of ash-related compounds in the engine. Up to this point, studies have focused on measuring the amount of ash-related elements in

engine exhaust or collected in DPFs without examining lubricant compositional changes. In this thesis, changes in the elemental composition of the lubricant are measured in the power cylinder of an operating diesel engine. The objective is to ascertain if changes in the oil composition before it is consumed and emitted in the exhaust has a strong effect on the composition of ash found in DPFs.

The most direct means to reduce ash emissions from engines is to lower the concentration of the compounds that contribute to ash in lubricants. However, reductions in additive levels often impair the ability of the lubricant to adequately protect engine components. For instance, considerable research and development has focused on optimizing additive packages to control lubricant acidity and protect components from wear. Dispersants and over-based detergent additives are typically used in diesel lubricants to neutralize acids. These additives are effective; however, new lubricant specifications limit the amount of ash containing additive that can be used in formulations. The recent API CJ-4 specification requires a sulfated ash level at or below 1.0 percent [8]. There is insufficient data to demonstrate that adequate wear protection can be maintained with reduced levels of antiwear additives. Therefore, the concentration of over-based detergents is reduced in these oils because they are the only other significant source of ash. This change decreases the acid neutralization capacity of the lubricant, so the lengths of oil drain intervals have remained constant at best [9].

Acid control remains an important issue especially in modern diesel engines employing advanced emission control technologies [10]. The high EGR rates used by these engines increases the exposure of the lubricant to combustion acids and induces more severe oxidation. However, this increase in acid contamination is balanced by a reduction in the amount of sulfur based acids [11]. The change to ultra-low-sulfur diesel fuel reduces the concentration of sulfur dioxide in exhaust gases. Additionally, the widespread use of biodiesel fuel is especially concerning. Hydrolysis of the esters in biodiesel increases the weak acid concentration in the lubricant, which in turn accelerates the rate of lubricant degradation, and promotes engine wear and corrosion [12,13]. Novel technologies must be developed that supplement, or enhance the performance of additives in lubricant

formulations. These new technologies could be used to extend the oil drain intervals of low ash lubricants, and enable the formulation of lubricants that do not contain any components that contribute to ash.

1.2 THESIS OBJECTIVES

The objectives of this thesis are:

1. To examine the in-engine distribution, in space and time, of ash-related lubricant species, and relate these variations to the mass of ash emitted from diesel engines.
2. To investigate new additive technologies that could enable reductions in the concentrations of ash-related species in the lubricant, while maintaining adequate engine protection.

This research will assist in the development of new formulations for diesel lubricants that minimize detrimental effects on aftertreatment systems, while providing adequate protection to engine components.

1.3 THESIS SUMMARY

This study is divided into two main sections:

1. In-Engine Distribution and Transport of Ash-Related Species
2. Filter Conditioning as a Potential Means to Reduce Additive Requirements

In the first part, the distribution of ash-related species in the engine is examined via oil sampling, in-situ measurements and modeling. Long duration engine tests are employed to measure the emission rates of metallic elements into the exhaust. In-situ measurements of lubricant composition at the piston and liner interface are also obtained using a novel technique developed during this study. Results show that the majority of exhaust ash is derived from over-based detergent additives, even though they are preferentially retained

in the sump oil due to volatilization of other species with lower molecular masses (i.e. base oil and ZDDP). In addition, the conditions in the piston ring pack of the engine strongly influence ash emissions. These results are analyzed with a model of lubricant species distribution and transport in the engine, developed during this study.

In the second part of the thesis, a novel approach that conditions the lubricant at a fixed station in the oil circuit is explored as a potential means to reduce additive requirements. Long duration engine tests explore the implications of using oil with no over-based detergent (ashless) additives in conjunction with an oil filter that performs the acid control function. Significantly lower ash emissions are expected when the detergent is removed from the lubricant formulation.

1.3.1 Part 1 – The In-Engine Transport and Distribution of Ash-Related Species

In this part of the thesis, the chemical composition of the lubricant in the power cylinder was characterized with sampling experiments and in-situ measurements. The composition of the lubricant in a single cylinder heavy-duty diesel engine was measured in three locations; the crankcase, valvetrain and top ring groove of the piston during engine operation. The chemical changes of the lubricant as it flowed through the power cylinder system were related to the emissions of ash-related species in the exhaust.

The results from these measurements showed that the multi-component fluid mechanics of the piston ring pack strongly affects the composition of the oil consumed in the power cylinder system. Emissions of ash-related elements from the lubricant were lower than would be expected based on oil consumption and crankcase oil composition. This occurred partly because in the ring pack inorganic additive compounds are less volatile than light end hydrocarbons in the base oil.

Oil was extracted from the top ring groove of the piston during engine operation with a ring pack sampling system previously used by [14,15,16]. The elemental composition of oil extracted from the top ring groove was significantly different from that of the

crankcase oil. Additive metals were concentrated in the top ring groove of the power cylinder. Detergent compounds (i.e. calcium and magnesium) concentrate due to the valorization of the base oil from the high-temperature piston surfaces. The metals associated with ZDDP (i.e. zinc and phosphorus) are concentrated to a lesser degree. The concentrations of the ZDDP elements appear to be reduced because of the higher volatility of ZDDP thermal degradation products.

A novel diagnostic technique, employing FTIR spectroscopy, was also developed for in-situ measurements of lubricant composition at the piston and liner interface. FTIR spectra of the oil were obtained from the surface of a zinc sulfide crystal, which was installed into the cylinder liner above the top center position of the oil control ring. Measurements of contaminants in the lubricant (combustion acids, soot and water) and oxidation by-products (carboxylic acids) were obtained with this system.

Finally, a model framework for the distribution and transport of ash-related lubricant species in the power cylinder system was developed and validated using the results of the sampling experiments. The formulation models the major sources of ash emissions from the power cylinder system.

1.3.1.1 Part 1 - Fundamental Questions:

1. What is the distribution of ash-related species in the engine?
2. How does this distribution change due to oil aging and degradation?
3. How do these changes influence the mass of ash transported to aftertreatment systems?

1.3.2 Part 2 – Oil Conditioning as a Potential Means to Lower Additive Requirements

In this part of the thesis, an innovative oil filter was demonstrated that releases no additives into the lubricant, yet enhances the acid control function typically performed by

detergent and dispersant additives. The filter chemically conditions the crankcase oil during engine operation by sequestering acidic compounds derived from engine combustion and lubricant degradation.

Long duration tests with a single cylinder diesel engine were performed to determine if oil conditioning with the strong base filter reduces lubricant acidity (Total Acid Number - TAN), improves Total Base Number (TBN) retention, and slows the rate of viscosity increase and oxidation. Effects of the strong base filter on wear and corrosion in the engine were also explored. Tests were performed with two lubricant formulations: an experimental zero-detergent oil and a fully formulated oil. The zero-detergent lubricant contained no detergent additive and is formulated with an ashless antiwear additive. This novel technology has the potential to significantly reduce ash emissions from diesel engines.

1.3.2.1 Part 2 - Fundamental Questions:

1. Is filter conditioning an effective supplement, or replacement for ash-related lubricant additives?
2. What effect is there on lubricant acidity?
3. Does filter conditioning reduce the rate of oil degradation and can it be used to increase oil drain interval?
4. Does filter conditioning reduce engine wear?

1.4 CONTRIBUTIONS TO KNOWLEDGE

This thesis contributes to knowledge in the following ways:

Part 1 – The In-Engine Transport and Distribution of Ash-Related Species

- The first measurements of ring pack oil elemental composition.
- The in-engine measurements of lubricant composition lead to an improved understanding of the sources and fates of ash-related compounds in the engine.

- The first application of a novel diagnostics system for FTIR for measurements of lubricant composition in engines.

Part 2 – In-Situ Measurements of Lubricant Composition at the Piston and Liner Interface

- First demonstration of a novel oil filter technology that supplements the action of detergent additives. This system could be used to substantially reduce lubricant ash levels, or increase oil drain interval.

(This page intentionally left blank)

CHAPTER 2 – EFFECTS OF LUBRICANT ADDITIVES IN DIESEL ENGINES

2.0 INTRODUCTION

Diesel engine oils are a complex mixture of hydrocarbon base oil and several additive compounds carefully designed to perform essential functions in engines. The compositions of lubricant formulations are balanced to maximize synergetic effects between all of the components in the mixture. Engine oils are formulated to provide sufficient protection to engine components over the longest possible oil drain interval.

The increasing use of DPFs and other aftertreatment devices on diesel engines has imposed a new requirement on diesel lubricant formulations; the need to limit ash emissions from the oil. Lubricant interactions within the engine must be better understood to design new lubricants with reduced ash emissions, but also provide adequate engine protection and oil drain interval. This information is also essential to assess the effect of new lubricant formulations on aftertreatment devices.

Up to this point, there have been several studies focused on lubricant degradation and the effect of specific additives inside the engine. The impact of candidate lubricant formulations on aftertreatment systems has also been evaluated by measuring the amount of ash-related elements in engine exhaust, or collected in DPFs during dynamometer and field tests. These experiments do not consider the complex interactions occurring within the engine. The mechanisms for the emission of ash-related species from the engine are not well understood.

This chapter reviews the areas of knowledge, from both chemistry and engineering, that relate to lubricant performance in diesel engines and the effect of lubricants on aftertreatment systems. This thesis builds upon previous studies of lubricant interactions in diesel engines.

2.1 LUBRICANT CHEMISTRY

Diesel lubricants must operate in extremely aggressive environments with high temperatures, acidic contaminants and in contact with compounds that cause oil degradation. Under such conditions, it must efficiently perform a number of vital roles, such as lubrication of moving interfaces, cooling of engine components and removal of debris from tribological interfaces. Lubricants are also expected to maintain this performance for ever increasing periods of time before it is replaced. To meet these expectations, the base oil must be combined with a number of additives, which must be carefully selected to provide the final lubricant with the desired performance.

2.1.1 Lubricant Formulations

Lubricating oils perform a number of important functions in diesel engines:

- Friction reduction for components in hydrodynamic and boundary lubrication;
- Reduction of wear in the valve train and components such as bearings, pistons, piston rings, and cylinder liners;
- Prevention of corrosion due to acids and moisture;
- Reduction of piston deposits and prevention of sludge build-up on internal surfaces;
- Cooling of pistons and other components;
- Maintaining adequate seal lubrication and controlling swelling to prevent leakage

Lubricants are a complex mixture of components that are optimized to provide the maximum level of protection to engine components. They consist of a hydrocarbon base oil (typically 75 – 83 wt%), viscosity modifier (5 – 8 wt%) and an additive package (12 – 18 wt%) [17]. The base oil alone cannot provide all of the functions required in modern engines. Therefore, additive packages have evolved to play an increasingly important role in the oil formulation.

Additive packages consist of a number of different additives that impart or enhance properties that protect engine surfaces, modify oil properties, or protect the base oil. There are several types of additives commonly found in modern diesel oils. Some additives perform multiple functions in the lubricant (i.e. ZDDP, detergents and dispersants). They can be classified as follows:

- Engine surface protection additives:
 - Detergents and detergent/inhibitors that neutralize acidic contaminants and keep engine surfaces clean (sulfonates, phenates, salicylates)
 - Dispersants (nitrogen and hydrocarbon based)
 - Antiwear additives (ZDDP)
 - Rust and corrosion inhibitors (detergents, ZDDP, triazoles, thiodiazoles)
 - Friction modifiers
 - Agents that control seal swelling
- Oil property modification additives:
 - Antifoam agents (silicone oils)
 - Viscosity improvers and pour point depressants (hydrocarbon and oxygen based)
- Base oil protection:
 - Antioxidants and metal deactivators (ZDDP, phenates, phosphonates, salicylates, phenolics, amines, carbamates, copper compounds, molybdenum compounds)

2.1.2 Lubricant-Derived Ash and Sulfated Ash

Lubricant-derived ash is the mineral matter remaining after engine oil has been burned and the residue is further heated to remove any remaining carbon. It is composed primarily of matter that is bound to the metallic elements in the oil. The amount of ash produced by burning fresh oils depends on the nature and quantity of the various metallic compounds in the additive package (see Table 2.1). Used oil produces additional ash due to presence of metal particles derived from engine wear and inorganic contaminants.

Table 2.1 – Sources of Sulfur and Ash in Diesel Engine Oil

Component	Sulfur (wt%)	Approximate Ash Contribution (wt% of oil)
Detergent	0.05-0.25	0.6-1.3
ZDDP	0.20-0.25	0.15
Other (Antioxidants, viscosity improvers, friction modifiers)	0.0-0.10	0.0-0.15
Total	0.25-0.60	0.75-1.6
Typical Group II base oil	0.0001-0.003	0.0

Sulfated ash is property of lubricants that has increased in importance since the introduction of diesel aftertreatment systems. It is currently used in industry to determine the propensity of a lubricant formulation to form ash. The standardized method used to measure sulfated ash of oils ASTM D874. In this method, the residue remaining after burning a sample is treated with sulfuric acid and then it is further heated. This procedure converts volatile ash compounds that would be lost during the final heating phase into less volatile sulfates or oxides.

Table 2.2 – Elements Found in Sulfated Ash and Elemental Weighting Factors to Estimate Fresh Oil Sulfated Ash Content

Elements Found in Sulfated Ash	Elemental Weighting Factors for Sulfated Ash [Multiply fresh oil metal percentages by]
Calcium	3.4
Magnesium	4.95
Zinc	1.5
Phosphorus	0.0
Barium	1.7
Sodium	3.09
Lead	1.464
Boron	3.22
Potassium	2.33
Lithium	7.92
Manganese	1.291
Molybdenum	1.5
Copper	1.252

The use of ASTM D874 as a measure of the propensity of an oil to form ash has been criticized by several researchers. The ash derived from the procedure has a different

composition than the ash typically found in aftertreatment systems [4,7,18]. Table 2.2 lists the metallic elements that contribute to sulfated ash along with weighting facts that can be used to estimate the sulfated ash level of a lubricant formulation. Boron contributes to sulfated ash but is absent from aftertreatment system ash. On the other hand, phosphorus does not contribute to sulfated ash but it is found in abundance in aged aftertreatment systems.

2.1.3 Lubricant Additives that Contribute to Ash

The additive package is the source of vast majority of ash that accumulates in diesel aftertreatment systems. The metallic elements in ash found at the highest concentrations are calcium, magnesium zinc and phosphorus [4,7,18]. Table 2.3 lists the metallic elements found in a typical oil formulation and the additive compound associated with each element. Of the many components in additive packages, detergents, ZDDP and Antioxidants are the main contributors to ash.

Table 2.3 - Major Elements in a Typical SAE 15W40 Oil Formulation

Element	Level (ppm)	Main Contributor
Calcium	400-3800	Detergents
Magnesium	0-1500	Detergents
Zinc	1300	ZDDP
Phosphorus	1200	ZDDP, Antioxidants
Sulfur	2000-7000	Base oil, ZDDP, Detergents
Boron	0-800	Dispersants, Antiwear
Silicon	20-40	Antifoam
Copper	0-50	Antioxidants
Nitrogen	600-2000	Dispersants
Total Base Number (TBN)	8-13 mgKOH/g	Detergents

2.1.3.1 Detergents and Dispersants

Detergent and dispersant additives control acidic contaminants in the oil, keep oil-insoluble combustion products such as soot in suspension and also prevent the agglomeration of high molecular weight oxidation products into solid particles. These

additives prevent corrosion, oil thickening, sludge and varnish deposition on metal surfaces.

Detergents and dispersants are surfactant molecules having a large oleophilic hydrocarbon “tail” which allows the compound to dissolve in the base oil and a polar hydrophilic head that is attracted to contaminants in the lubricant. Solid contaminants (i.e. soot, oxidation by-products and acids) are enveloped by the surfactant, which forms micelles in the oil (Figure 2.1). The nonpolar tails on the outside of the micelles prevent adhesion of the particles on metal surfaces as well as agglomeration into larger particles.

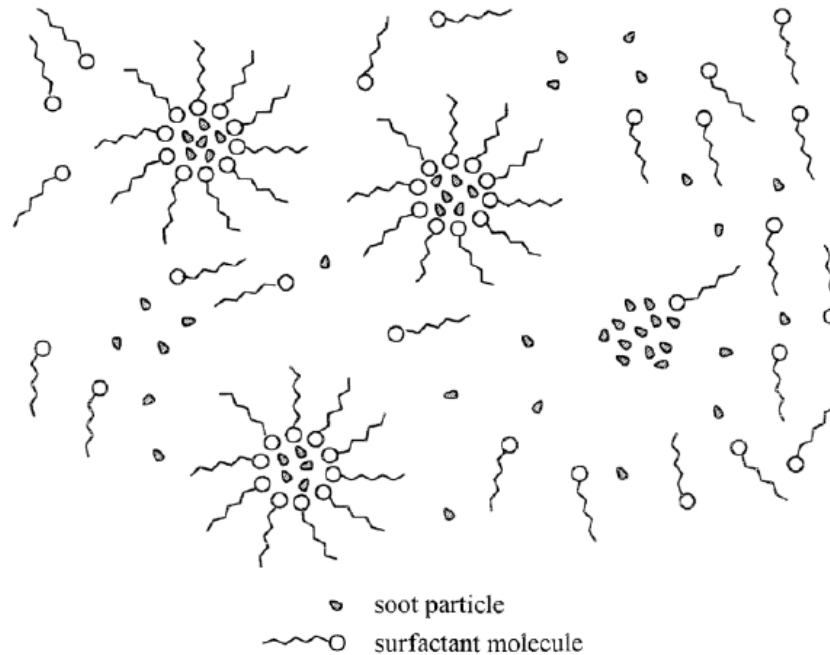


Figure 2.1 – Solubilization of a soot contaminant by surfactant molecules in oil [19].

2.1.3.1.1 Detergents

The most important role of detergents is to prevent corrosive wear by neutralizing acidic contaminants in the lubricant. Detergent additives are typically metal-containing compounds with high alkaline reserve. Acids can also be neutralized by ashless dispersants that do not contain any metals. Ashless dispersants perform cleaning properties and are similar to detergents.

Detergents can be classified as neutral, basic or overbased. A neutral detergent consists of two alkyl substituted sulfonate, phenate or salicylate anions attached to a single divalent metal such as calcium or magnesium. A basic detergent consists of an alkyl substituted sulfonate, phenate or salicylate anion and an OH attached to a divalent metal. Overbased detergents consist of colloidal metal carbonate particles surrounded by surfactant molecules (Figure 2.2). The polar head of the surfactant molecule binds to a calcium or magnesium cation to form a metallic soap. This neutral metallic soap stabilizes large amounts of metallic carbonate base that would otherwise be insoluble in oil. The term overbased reflects the fact that the metal cation to surfactant ratio is greater than one. This property results gives the overbased detergent a greater acid neutralizing capacity than neutral or basic detergents. As a result, they are widely used in lubricant formulations especially when oil drain interval is limited by acid neutralization capacity [20].

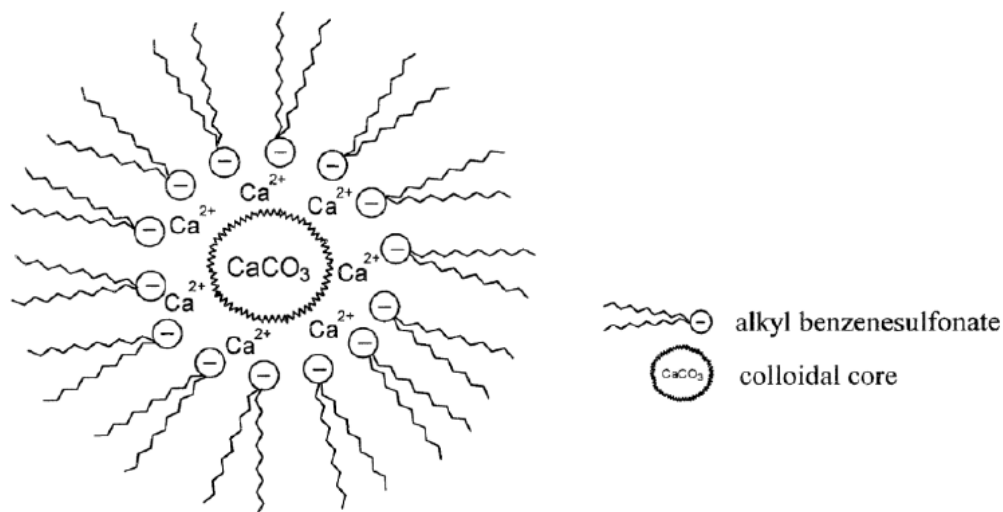


Figure 2.2 – Schematic of Overbased Calcium Sulfonate Detergent [19].

Classes of metal-containing detergents include phenates, salicylates, thiophosphonates and sulfonates. The majority of detergents used in modern diesel lubricants contain calcium and magnesium. Calcium phenates are widely used and besides their good dispersant properties they also possess good acid neutralization properties. Salicylates exhibit antioxidant properties as well. Sulfonates have excellent detergent and acid

neutralization properties and can also have excellent anticorrosion properties. Calcium sulfonates are relatively cheap products with good performance.

Magnesium detergents have the potential to form less ash than calcium detergents due to their lower molecular weight and can be used to reduce sulfated ash levels in lubricants. Magnesium sulfonates have been shown to reduce piston ring wear and corrosion, but they are less effective at neutralizing weak acids and preventing bearing corrosion [21]. For this reason, magnesium detergents are often used in combination with calcium detergents in lubricant formulations.

2.1.3.1.2 Dispersants

The principal function of dispersants is to suspend oil insoluble contaminants and degradation products. They are more effective in this role than detergents especially when temperatures are low. A common class of dispersants is substituted polyisobutylene amine succinimides (PIBSA).

Dispersants contain basic nitrogen that provides its dispersing ability. Basic dispersants are very effective at ensuring soot particles remain dispersed in the oil and cause less soot mediated oil thickening [20]. The basic nitrogen can, however, degrade engine oil seals. For this reason, some of the active nitrogen is “capped” to render it non-basic or neutral. One way to cap the nitrogen is to borate the dispersant [9].

2.1.3.2 Antiwear Additives

Antiwear additives prevent damage and wear to parts experiencing boundary lubrication. They have a polar structure that is attracted to and forms a protective layer on metal surfaces. Antiwear additives react with metal surfaces at elevated temperatures to form a tribochemical protection layer that prevents direct contact between the sliding surfaces. Zinc dialkyldithiophosphates (ZDDP, also abbreviated as ZDTP, ZnDTP or ZDP) are the most widely used antiwear additive in lubricating oils (the structure of ZDDP is shown in

Figure 2.3). It is a dual purpose additive, functioning as both an excellent antiwear agent and an effective antioxidant and metal passivator. This multifunctional nature has made it one of the most commonly used and cost effective additives.

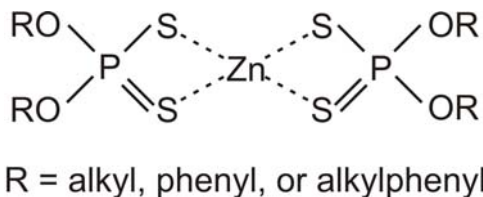


Figure 2.3 – Zinc Dialkyldithiophosphate (ZDDP)

ZDDP forms a zinc oxide glass structure on metal surfaces, which protects rubbing surfaces from wear. These nano-scale films are formed after decomposition of the additive at high temperatures or pressures. Although there is no specific threshold temperature that must be exceeded in order for the thermal film formation, it is generally understood that temperatures exceeding 80°C will induce slow film development and temperatures beyond 150°C will drastically accelerate the rate of formation [22]. Under rubbing the conditions seen in boundary lubrication, films have been found to form at room temperature, although higher temperatures greatly increase the rate of formation [23].

ZDDP exists in many forms, which are used in varying amounts in lubricant formulations to achieve the desired reactivity and thermal stability for the additive. While Figure 2.3 shows ZDDP in its simplest (monomeric) form, it actually exists in equilibrium between a monomer and dimer state in solution (Figure 2.4). Furthermore, ZDDP is often added to lubricating oil in an agglomerate state, called “basic ZDDP”, in contrast to the “neutral” forms described above (Figure 2.5). Past studies have found that basic ZDDP converts to its neutral form and ZnO at high temperatures [24,25]. In general, ZDDP in its neutral form is more reactive and therefore more effective as an antiwear agent. Of the neutral form, the monomer is most reactive. Basic ZDDP is less volatile than the neutral ZDDP, so it is less likely to be emitted from the engine due to volatile oil consumption.

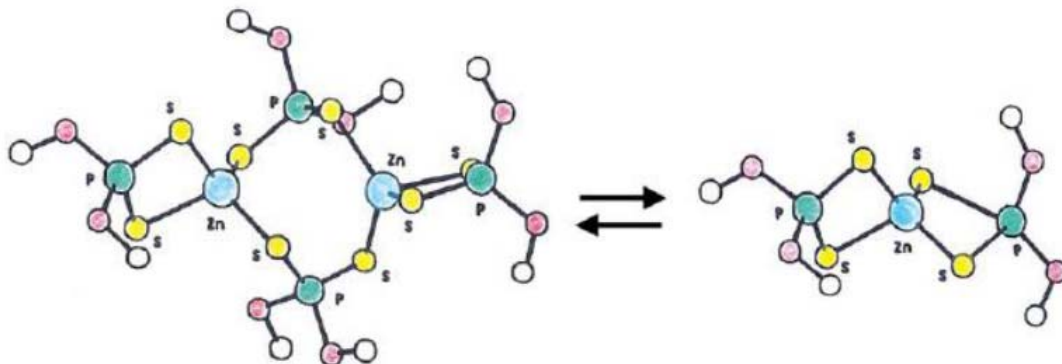


Figure 2.4 – Forms of ZDDP. *Left* - dimer. *Right* - monomer [26].

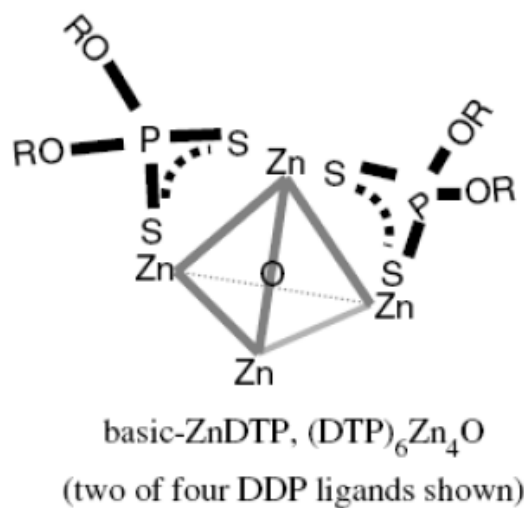


Figure 2.5 - Basic ZDDP, $Zn_4[PS_2(OR)_2]_6O$ [26].

Zinc dialkyldithiophosphates are synthesized by the reaction of primary and secondary alcohols (C3 to C12) or alkylated phenols with phosphorus (V) sulphide to produce zinc dialkyldithiophosphoric acid. The acid is then neutralized with zinc oxide to produce neutral ZDDP. If excess zinc oxide is used, the ZDDP can be made basic (alkaline).

ZDDP is consumed during engine operation. It reacts with oil degradation products such as hydroperoxides or peroxyradicals and thermally decomposes into various phosphorous containing by-products that are volatile [27].

The functional group on the ZDDP molecule (i.e., R in Figure 3) has a large effect on its thermal stability, affecting the decomposition rate for a given lubrication condition. The most common types of ZDDP, defined by their functional groups are secondary alkyl ZDDP, primary alkyl ZDDP and aryl ZDDP. Aryl ZDDP is most thermally stable, followed by primary alkyl and then secondary alkyl ZDDP [28]. In terms of antiwear film formation, high instability is desired as it tends to increase the reactivity. For the range of temperatures generally seen in an engine, experimental evidence shows that alkyl ZDDP forms antiwear film faster, with secondary alkyl being fastest [24].

Long chain primary and short chain secondary ZDDPs are more common in lubricating oils. Typical engine oil formulations contain approximately 85% secondary alkyl and 15% primary alkyl ZDDP [26]. While short chain secondary ZDDP is more active as an antiwear compound, it is also more volatile and less thermally stable. Phosphorous from secondary ZDDP is more likely to be emitted from the engine and be deposited on catalysts in exhaust aftertreatment systems, especially when oil temperatures exceed 165°C. Newer lubricant formulations that are more compatible with catalyzed aftertreatment systems favor not only lower levels of ZDDP, but also a shift from short chain secondary to long chain primary ZDDP. Supplemental antiwear additives that do not contain phosphorus can be used in order to avoid an unacceptable reduction in antiwear performance [29].

Metal dithiocarbamates, such as molybdenum dithiocarbamate (MoDTC) and dibutyl tin dioctylldithiocarbamate (SnDDC), are one such supplemental antiwear additive that can enhance antiwear properties when used in combination with ZDDP. While they contain no phosphorous, because of their metal content they can still contribute to ash accumulation in diesel particulate filters and can have poor thermal stability under severe dynamic loading or at high temperature [30].

Ashless multi-functional additives are currently being developed as possible alternatives to ZDDP. One additive, borate esters, have been described in literature, however, their reactivity with water has limited widespread use. Reaction of the boron-containing

additives with water results in the liberation of oil-insoluble boric acid that can cause corrosion in the engine. Approaches to improve hydrolytic stability have been developed, but have not always proven satisfactory [31,32]. Another study found that borate esters cannot replace ZDDP completely because ZDDP possesses superior antioxidation and corrosion inhibiting properties. However, the partial replacement of ZDDP with borate esters, can decrease wear [33].

2.1.3.3 Antioxidants

Oxidation degrades the quality of the base oil as it is exposed to the high temperatures in an engine. The characteristics of heavily oxidized lubricants include discoloration and a burnt odor. As aging advances, viscosity may rise significantly and acidic oxidation products are formed in the oil. Oxidation products may induce corrosion and other problems.

Antioxidants delay or slow the oxidation process that causes oil aging. Oxidation reactions can produce free radicals, which start chain reactions that accelerate the rate of reaction. Antioxidants terminate these chain reactions by removing free radical intermediates and inhibiting other oxidation reactions by being oxidized themselves.

Most antioxidants used in commercial lubricants are phosphorus and sulfur containing compounds. ZDDP is an effective antioxidant in addition to being a potent antiwear additive. Antioxidants are a significant source of the phosphorus found in the ash.

2.1.4 Lubricant Contamination and Degradation

The quality and effectiveness of lubricants is degraded during use by contamination and thermal (oxidative) degradation. As it degrades, the lubricant functions less efficiently, until it must finally be replaced to maintain engine performance and prevent damage to components.

During use, oil can become contaminated by such things as soot, unburned fuel, metallic particles, water and acid by-products of fuel combustion or lubricant degradation. Before contaminant levels reach a critical level, the oil must be drained and the engine refilled with fresh oil.

The acids that contaminate oils are the source of many lubricant-related problems in diesel engines. During normal engine operation, the lubricant is exposed to combustion and blow-by gases containing nitrogen, sulfur and carbon-based acids. The weak organic (carbon) acids also accumulate in the lubricant due to oxidation of the base oil. Severe problems can occur if these acids remain in the oil and are not neutralized. Accumulation of weak organic acids in the oil can cause engine wear and corrosion, high lubricant viscosity, sludge, varnish and piston deposits. In several cases the capacity of the oil to neutralize and control acids determines the lubricant lifetime and the oil drain interval.

Acid control remains an important issue especially in modern diesel engines employing advanced emission control technologies [10]. The high EGR rate used by these engines increases the exposure of the lubricant to combustion acids and induces more severe oxidation. However, this increase in acid contamination is balanced by a reduction in the amount of sulfur based acids [11]. The change to ultra-low-sulfur diesel fuel reduces the concentration of sulfur dioxide in exhaust gases. The widespread use of biodiesel fuel is especially concerning. Hydrolysis of the esters in biodiesel increases the weak acid concentration in the lubricant, which in turn accelerates the rate of lubricant degradation, and promotes engine wear and corrosion [12,13].

Unburned fuel may also be present in the oil. Fuel dilution may also be reflected in a decrease in viscosity and flash point compared to new oil. Fuel (and especially biodiesel) has poor thermal stability at oil pan temperatures and oxidation can occur. The interaction of deteriorated fuel with bearings can cause corrosion as indicated by elevated levels of lead in used oil.

Soot is entrained in the oil and harmlessly suspended until active additive components become depleted. This condition causes the soot particles to agglomerate into larger particles. Accelerated valve and injector train wear occurs once soot levels in the oil exceed safe levels and result in further increases in soot generation and wear. Elevated levels of iron in the oil as well as sludge build-up on internal surfaces of the engine may result.

2.1.5 Total Acid Number (TAN) and Total Base Number (TBN)

An important property of engine oils is their capacity to neutralize acids. Lubricants must have sufficient capacity over their lifetime to neutralize acids (i.e. alkaline reserve), to prevent the corrosion of corrode engine surfaces by acidic compounds. Inorganic acidity in used oils arises from contamination by acidic products of combustion such as SO_x and NO_x . Organic acidity is a result of oil oxidation. Some oil additives are also weakly acidic. Unused diesel engine oils containing detergent and dispersant additives are normally alkaline. The extent to which alkalinity is reduced in a used oil may be a measure of the loss of dispersancy or alkalinity by additive depletion.

Neutralization value can be used as a measure of the acidity, or alkalinity of oil and is determined by titration. Acidity is determined by titration with potassium hydroxide and alkalinity by titration with hydrochloric acid or perchloric acid. The result is expressed as the amount of potassium hydroxide (KOH) required to neutralize one gram of acidic oil, or as the amount of acid, expressed in terms of the equivalent amount of KOH, required to neutralize one gram of an alkaline oil. The amount of KOH is expressed in milligrams, so the neutralization value is given as mgKOH/g oil. The alternative names for neutralization value are acid number and base number.

The total acidity, expressed as the Total Acid Number (TAN), is a measure of the combined concentration of organic and inorganic acids with dissociation constants greater than 10^{-9} . The strong acid number (SAN) is a measure of the concentration of strong acids, usually inorganic acids. The difference between TAN and SAN is a measure

of the concentration of organic acids. An increase in TAN from its initial value is usually a result of oil oxidation. While it is natural for oils to oxidize, overheating, overextended oil drain intervals, or water or air contamination can accelerate the process. TAN typically increases over the lifetime of a lubricant (Figure 2.6)

The Total Base Number (TBN) is a measure of the amount of available alkaline additives in a lubricant. Engine oils are formulated to contain a reserve alkalinity that enables them to neutralize acidic by-products of oil oxidation and the combustion process. The TBN of engine oil gradually decreases during use (Figure 2.6), which indicates that detergent and dispersant additives are being consumed by acid neutralization. Oils for most diesel engine applications typically have a TBN between 8 and 12 mgKOH/g. However, marine engines burning heavy fuel oil require much higher TBN, in some cases as high as 80 mgKOH/g, to adequately neutralize sulfuric acid generated from the use of fuel containing high levels of sulfur.

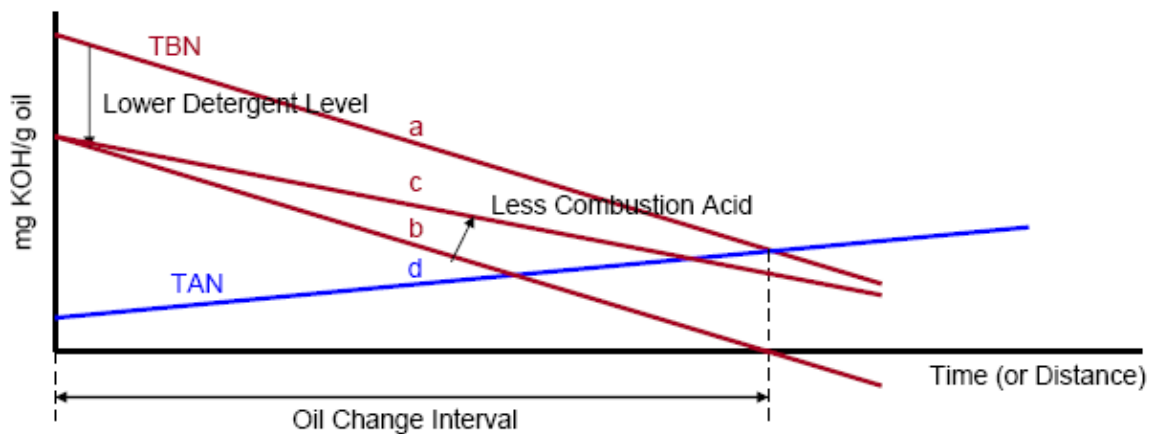


Figure 2.6 – The typical change in TBN and TAN over the life of an engine lubricant. The lines show: a) a characteristic decrease in TBN for a fully formulated oil; b) TBN for an oil formulation with a reduced detergent level; c) a reduced rate of TBN depletion due to a lower acidic contamination rate; and d) a typical increase in the TAN.

For most diesel engine applications, commercial engine oils provide adequate alkalinity to meet recommended oil drain intervals. In applications such as large marine engines

burning high sulfur residual fuel, engine oil BN needs to be matched to the sulfur level of the fuel being used. Insufficient alkalinity will result in engine damage due to corrosion by acid attack. Excessive alkalinity will result in the build-up of deposits of metallic detergent compounds detrimental to engine life.

Another common parameter associated with acidic and alkaline fluids is pH. The pH describes the overall acidity, or alkalinity strength of an oil, not the concentration of acids or base. Acid or base concentrations, not strengths, are of more interest for engine oils. However, pH measurements may be used to verify TAN measurements.

Lubricants simultaneously have an acid and base number because the tests measure different constituents with the two different titration procedures. In some cases, engine oil additives are amphoteric; they can behave as either an acid or a base. Acid and base numbers are not reciprocal in nature, although in most cases TAN does tend to increase and TBN decrease as an oil ages.

Two commonly accepted measurement methods are used to measure TBN, ASTM D-2896 (Standard Test Method for Base Number of Petroleum Products by Potentiometric Perchloric Acid Titration) [34] and ASTM D-4739 (Standard Test Method for Base Number Determination by Potentiometric Hydrochloric Acid Titration) [35]. D-2896 is commonly used for fresh oils and D-4739 for used oils. Both are titration based methods where a measured amount of acid is added to the oil until the base has been consumed. The TBN is calculated from the amount of acid required to completely neutralize the lubricant. The methods differ in the acid used for titration and the solvent into which the oil is dissolved. D2896 uses a stronger acid and a more polar solvent system than D-4739.

D-4739 does not measure all the base reserve available for some additives found in oil. The method tends to measure the TBN contributed mostly from only detergent additives in a sample. D-2896 also measures the contribution of dispersant additives to the TBN of

the oil. Table 2.4 shows some typical values for the ratio of TBN measured by D-4739 and D-2896.

The ratio is close to 1 for the two detergents but significantly less than 1 for ashless additives. For the ashless dispersant shown it is 0.48 and for the amine antioxidant it is zero [21]. Larger differences in TBN between D-2896 and D-4739 indicate higher concentrations of dispersants and antioxidants [9].

Table 2.4 – Ratio of TBN Measured by Different Test Methods for Selected Additives [21]

Additive	ASTM D-4739/D-2896 Ratio
Phenate detergent	0.96
Sulfonate detergent	0.96
Ashless dispersant	0.48
Amine antioxidant	0.00

2.2.6 Oil Drain Interval

Oil drain interval is an important consideration, especially for engines in commercial service where it is undesirable to take a unit out of service to change the oil. Oil drain intervals are determined by numerous factors including oil formulation, engine operating conditions, oil filtration system design and the size of the oil sump.

Oil analysis is often used to determine the appropriate oil drain interval. The drain interval may be set by measuring such properties as viscosity, fuel and water dilution, soot accumulation, TBN, TAN and metals at periodic intervals. The maximum oil drain interval ensures that none of a set of important limits are exceeded for the oil.

The drain interval for modern diesel oils is often limited by the capacity of the lubricant to neutralize acids. The current practice in industry is to change the oil when the used oil TBN is below, or TAN exceeds 2 mgKOH/g oil. The increased use of lubricants with lower detergent levels and reduced fresh oil TBN have convinced several experts to reevaluate this oil drain criteria. It has been suggested that lubricants should be changed

when the TBN and TAN are equal (see Figure 2.6) [9]. This criteria tends to lengthen oil drain interval for lubricants that more efficiently neutralize the oxidation by-products and weak acids reflected by TAN measurement.

2.3 EFFECTS OF ASH ON DIESEL PARTICULATE FILTERS

Diesel particulate filters and advanced catalyzed aftertreatment systems have been adopted by several original equipment manufactures to meet increasingly stringent diesel emissions limits. Since their introduction, DPFs have quickly become the preferred means for meeting current and future particulate matter emission limits. Presently all 2007 and newer on-road diesel engines must be equipped with particulate filters in the United States. DPFs are extremely effective at removing particulate matter from the exhaust, including metallic compounds emitted from the lubricant. These compounds form ash in the filter over time, a process that negatively affects the efficiency and durability of the system.

2.3.1 DPF Operation

While many types of filter media have been developed, cellular ceramic wall-flow particulate filters have found widespread use due to their relatively low cost and high trapping efficiency. The trap consists of a ceramic honeycomb substrate with porous channel walls. The channels in the substrate are blocked on alternate ends by small ceramic plugs. Particulate-laden exhaust, which enters the upstream of the channel open end, must pass through the porous walls before exiting the filter. As the exhaust passes through the walls, the particles are trapped inside the porous material and along the channels walls as depicted in the schematic shown in Figure 2.7. The trapped particles act as an added filtering medium in cellular ceramic traps, further increasing trapping efficiency as the traps are loaded [38].

As soot accumulates inside a DPF there is an increased flow restriction and a corresponding rise in exhaust backpressure, which results in a fuel economy penalty [37].

The trapped particulate matter is removed from the filter by periodic or continuous regeneration. Trap regeneration is usually accomplished by burning off the accumulated soot [38]. Particle trapping efficiency and the pressure drop across the trap are, therefore, the two most important measures of trap performance.

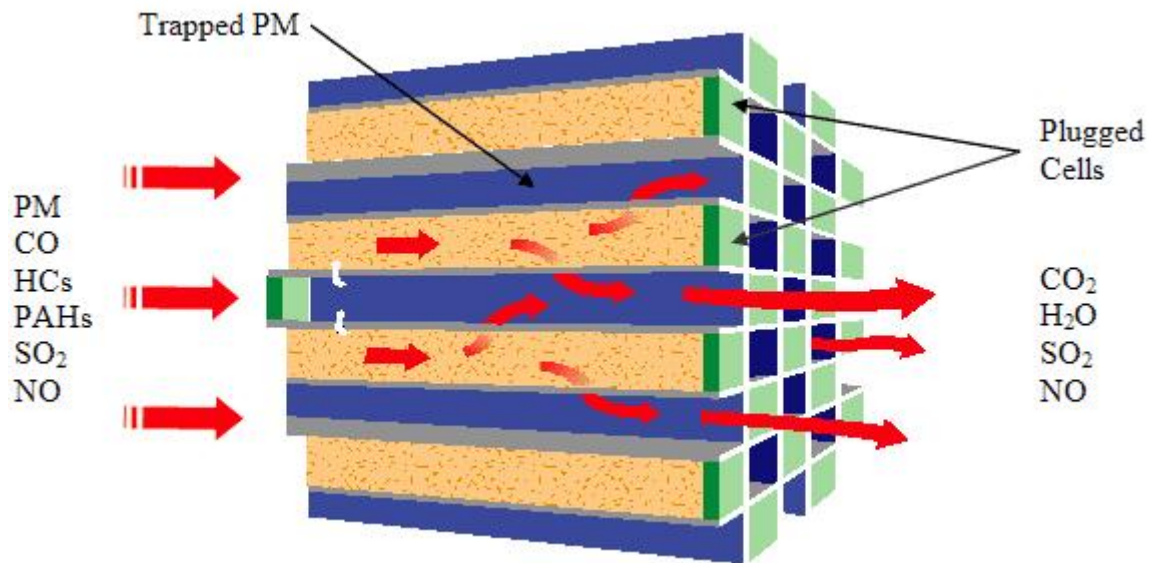


Figure 2.7 – Particle laden flow is filtered by the DPF as it passes through the porous walls of the substrate. A catalyst on the filter walls also reduces emissions of carbon monoxide and hydrocarbons.

Following DPF regeneration, incombustible material (ash) remains and accumulates in the filter over time. The accumulation of ash eventually leads to irreversible plugging of the DPF, limiting the useful service life of the system and requiring filter removal for periodic cleaning or replacement. Current U.S. EPA regulations require manufacturers to certify diesel particulate filters for maintenance intervals of no less than 150,000 miles in heavy-duty applications [39]. Figure 2.8 shows typical ash and soot distributions in a DPF channel.

Ash tends to accumulate in a thin layer along the channel walls as well as in a plug at the end of the channels. The end-plug, formed by the ash, completely fills the channels and reduces the effective length of the filter, while the ash accumulated along the channel

walls restricts the channel diameter and frontal area. Soot accumulated on top of the ash layer is also visible in the Figure 2.8 [37].



Figure 2.8 – Typical ash and soot distributions in the channel of a regenerated DPF. The inlet for flow is on the left of the picture. Exhaust passes through to the outlet, on the right of the picture [40].

2.3.2 Exhaust Ash Emissions and Effects on DPFs

It is extremely difficult to obtain accurate measures of ash emissions directly from the raw exhaust stream. Ash comprises a small fraction of the particulate matter emitted from diesel engines. As a result, several researchers have attempted to deduce the nature of the ash emissions by analyzing the incombustible material that collects in DPFs. The following generally accepted observations have been made by several researchers [37]:

- The mass of ash in DPFs increases with oil consumption and lubricant ash content [1,4, 7,41].
- Lubricant-derived ash is mostly composed of oxides, sulfates, and phosphates of Zn, Ca, and Mg [1,4,7,39,42].
- The use of lubricant sulfated ash levels to predict engine-out ash over-estimates the quantity of ash found in DPFs most likely due to lubricant volatility and differences in speculated oil consumption rates [1,40,41].
- Pressure drop across DPFs does not correlate precisely with the mass of ash in filters [7,24,40,43].

- Specific additive elements, primarily S and P, adversely impact catalyst performance [44,45,46,47].
- Ash accumulation within the DPF is affected by regeneration strategy [48].

The accumulation of ash emissions in DPFs reduces the available filtration area, leading to flow restriction and plugging, commonly causing an increase in the pressure differential across the filter (pressure drop). A number of studies have investigated the effect of ash accumulation in diesel particulate filters on pressure drop increase. The compilation of results in Figure 2.9 shows that the mass of ash found in DPFs increases with the sulfated ash level of the lubricant.

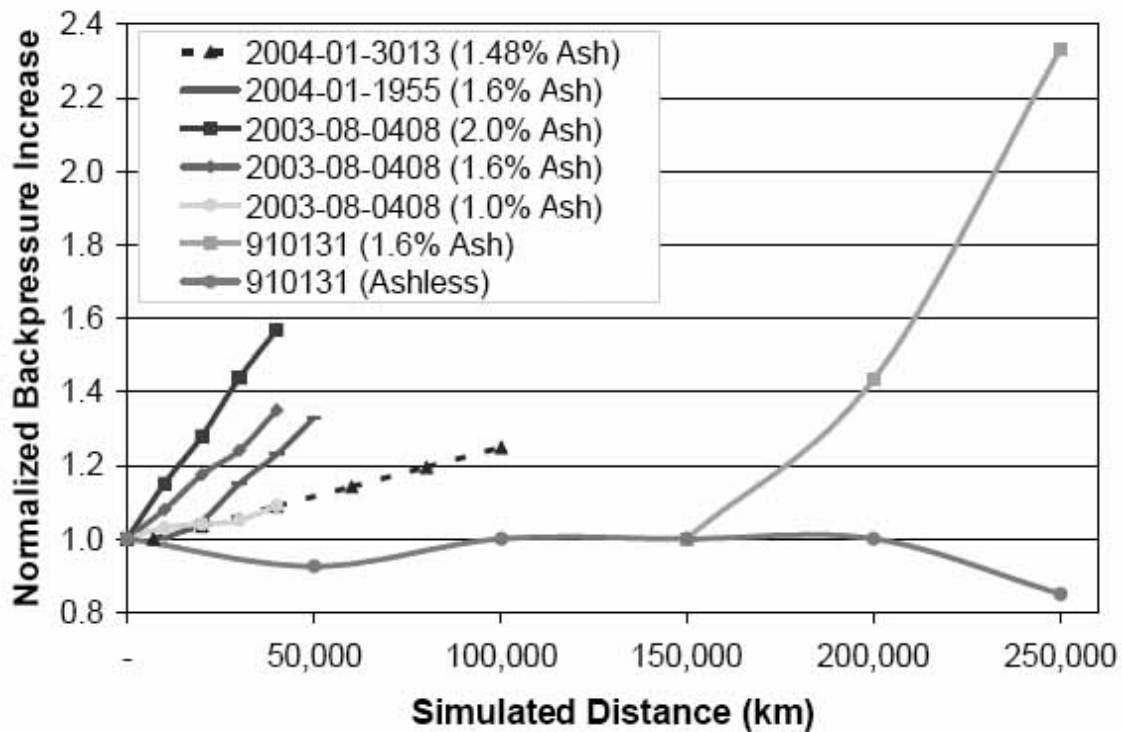


Figure 2.9 – A compilation of studies documented in SAE papers illustrating the dependence of pressure drop on sulfated ash level [49].

Recent studies of ash accumulation in DPFs consistently find that the mass of lubricant-derived ash collected in filters and raw exhaust is less than would be expected based on the sulfated ash level of the fresh oil and the oil consumption rate [1,4,5,50]. Figure 2.10

graphs data measured by [45] that compares the mass of ash collected in DPFs with the expected amount of ash based on the sulfated ash level of the oil.

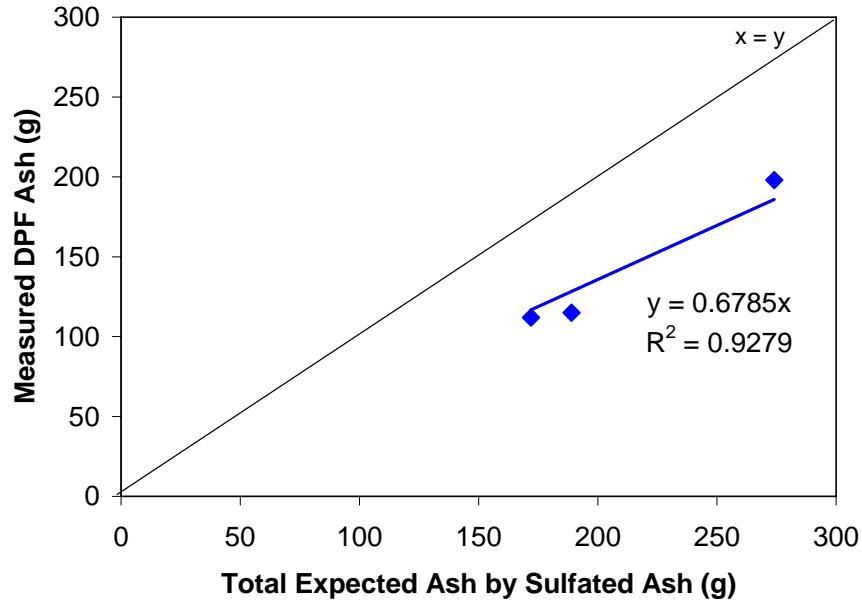


Figure 2.10 – A comparison of the actually mass of ash recovered from DPF with the expected amount based on sulfated ash for three lubricant formulations. Data compiled from [45].

In addition, the relative fractions of metallic elements in DPF ash are not representative of the crankcase oil composition [1,4,50]. For instance, the mass of metallic elements associated with the detergent in the lubricant (i.e. calcium and magnesium) recovered in raw exhaust is significantly less than would be expected from the oil consumption rate and the concentration of detergent in the lubricant. Typically, a much higher portion of the crankcase phosphorus content from the antiwear additive Zinc Dialkyldithiophosphate (ZDDP) is recovered in raw exhaust than any other element. Elemental capture rates in DPFs, based on the fresh oil composition, have been estimated at 27% to 31% for magnesium, 37% to 42% for calcium, 37% to 86% for zinc, and 46% to 86% for phosphorous [1,50].

These observations suggest that a substantial mass of the metallic elements in the lubricant must be retained in the engine system. Four fates for metallic compounds in the

lubricant are suggested by [4] and other researchers to account for the lower than expected recovery rates including:

- Accumulation in the crankcase oil due to preferential consumption of the base oil by volatility;
- Penetration of ash through the DPF;
- Deposition on surfaces inside the engine and exhaust system; and
- Formation of antiwear films on engine surfaces.

The preferential retention of metallic elements due to the relative volatility of the compounds to which these elements are bound is the most likely possible explanation for the lower than expected emission rates [45]. Measurements have shown that more than 95%, and in some cases over 99%, of metals (calcium and zinc) and over 80% of phosphorous leaving the cylinder of a diesel engine are trapped by the DPF [37,45]. Only relatively small amounts of the metals that contribute to ash have been found in engine deposits and on exhaust system components [4].

Ash emissions affect the DPF differently depending on their composition and material properties. [5] examined the effects of various lubricant formulations by utilizing eight different lubricant formulations each containing different levels of boron-based dispersants, ZDDP, and calcium-based detergents. The sulfated ash content of the lubricants ranged from 0.42% to 1.9%. An accelerated ash loading technique was used to load DPFs with ash, by adding 5 wt% of the test oils to the fuel. Calcium was the largest contributor to the DPF ash metallic content. Although, while calcium was observed to be the largest contributor to lubricant sulfated ash content, as measured by ASTM D874, DPF pressure drop increase, due to ash accumulation, appeared to be more closely correlated to zinc and phosphorous concentrations in the lubricant than calcium. Interestingly, no boron was found in the DPF, although it was present in the lubricants. This result indicated that boron was passing through the DPF. It is unlikely that boron was accumulating inside the engine, as the lubricant was doped in the fuel.

Contradictory results have been found in other studies. [7] noted that high lubricant phosphorous concentrations were not directly correlated to an increase in DPF pressure drop. This study utilized ten lubricants with various levels of calcium, magnesium, ZDDP, phosphorous, and boron. The authors further noted an interaction between the platinum levels in the DPF and phosphorous in the ash, possibly creating conditions suitable for reducing the ash particles to a sufficiently small size to pass through the DPF pores. No study has ever directly observed sufficient quantities of ash passing through DPFs. Similar to previous studies, no boron was observed in the ash deposits accumulated in the particulate filter.

Table 2.5 – The Composition of Ash Collected in a DPF, Compared to the Fresh Oil Elemental Composition [51]

Oil	A	B	C
Oil Elemental Composition wt%			
Ca	0.444	0.300	0.231
Zn	0.135	0.148	0.120
P	0.120	0.134	0.110
Mg	< 0.001	< 0.001	< 0.001
Mo	< 0.001	0.011	0.011
S	0.43	0.45	0.47
Ash Composition in DPF, wt%			
CaSO ₄	75 ± 6	66 ± 6	65 ± 14
CaCO ₃	2 ± 1	3 ± 1	3 ± 3
Zn ₂ (PO ₃) ₂	15 ± 3	21 ± 6	24 ± 9
ZnSO ₄	2 ± 1	5 ± 3	< 1
ZnO	5 ± 2	5 ± 3	9 ± 3

A number of studies have attempted to identify and quantify the various lubricant-derived ash components accumulated in the DPF. In general, a large fraction of the ash was found to consist of metallic sulfates and phosphates, with a much smaller contribution from metal oxides. The principal ash component is calcium sulfate (CaSO₄), with zinc phosphates (Zn₃(PO₃)₂) and zinc magnesium phosphate (Zn₂Mg(PO₃)₂) playing an important secondary role. Calcium sulfate is observed to be the predominant lubricant-derived component found in the ash, with concentrations ranging from 59% to 75% of the total mass of ash [45,51] (see Table 2.5). On an elemental basis, it has been demonstrated that uncombusted material collected from a DPF connected to a diesel engine using both

1.4% and 1.0% sulfated ash oils consisted of about 22% Ca, 15% S, 10% Zn and 7%P [51]. Thus detergents and antiwear additives are the main contributors to ash accumulated in DPFs.

The emission of sulfur from lubricant additives contributes to DPF ash as well as being absorbed onto catalyst surfaces. Not all sulfur containing oil additives contribute to sulfur poisoning in the same way. Sulfur converted to SO_2 and then absorbed on a catalyst surface is the main route of sulfur poisoning. [52] found that more than 80% of sulfur contained in the base oil and in ZDDP is converted to SO_2 and therefore has the potential to poison catalysts. Sulfur in calcium sulfonate, a detergent additive, is poorly converted; only about 10% of it is converted to SO_2 . However, calcium sulfonate is a major contributor to ash.

Phosphorus is another critical component in the lubricant that may have deleterious effects on DPFs. Catalyst poisoning by phosphorous can significantly decrease the soot regeneration activity on a DPF. There is some experimental evidence that phosphorus emissions result in a deactivating effect that has been shown to be far more critical in determining DPF durability than thermal aging. Phosphorus was also reported to decrease the filtration efficiency of both catalyzed and uncatalyzed DPF substrates [62].

2.4 LOW SAPS OIL FORMULATIONS

A new oil specification, called API CJ-4 [54], was developed specifically to reduce the impact of oils on aftertreatment systems and address the unique needs of modern diesel engines employing high rates of exhaust gas recirculation. This specification imposes the first chemical limits on the formulation of heavy duty diesel engine oils. To meet the CJ-4 oil specifications, the phosphorus content in the lubricant must be below 1200 ppm, sulfur below 0.4%, and sulfated ash below 1.0%. Volatility is limited to 15% for 10W-30 oils and 13% for all other viscosity grades.

CJ-4 oils have additive systems specially designed to improve the protection of both the engine power system and advanced emissions control systems like DPFs. These oils have been shown to extend the life of the emission control systems, as required for regulatory compliance [54]. CJ-4 oils are qualified utilizing several new engine tests that are more severe than those used for previous specifications, thus it defines a new category of oils with much more robust performance than previous categories. They oils are formulated for improved wear protection, deposit and oil consumption control, soot-related viscosity control, prevention of viscosity loss from shearing, used oil low-temperature pumpability, and protection from thermal and oxidative breakdown when compared to previous formulations.

Limiting sulfated ash, phosphorus and sulfur (SAPS) presents a significant challenge when developing new oil formulations, as many commonly used additives contain sulfur and phosphorous and contribute to sulfated ash. While some additives have organic alternatives containing little or no sulfur and phosphorous and which do not contribute to sulfated ash, some important antiwear and detergent additives do not. ZDDP is one such important sulfur and phosphorous containing antiwear/antioxidant additive that does not have an effective alternative. Also, while low sulfur detergent alternatives are available, they still contribute to sulfated ash [7].

Thus to meet the low SAPS requirements, some additives could be replaced if effective alternatives exist that do not contribute to sulfated ash and higher quality base oils (that require less additives and contain less sulfur) could be used. Until effective replacements are found for detergents and ZDDP, a careful balancing and reduction in the concentrations of SAPS contributing additives is required to ensure that the engine oil meets all the performance requirements over a sufficiently long oil drain interval.

In an example strategy to achieve a low SAPS oil for the Japanese market [55], the amount of ZDDP blended into the oil was maintained at the same level as that for conventional high-ash oils to ensure excellent antiwear performance. The reduction in sulfated ash was achieved by reducing the amount of metallic detergent by roughly 50%.

This reduced not only the amount of calcium, the main component of ash, but also the fresh oil TBN. The amount of ashless antioxidants and dispersants were increased to offset loss of detergency and oxidation resistance resulting from decreased levels of the metallic detergents. Group III base oil was used reduce the sulfur content and improve oxidation resistance.

A lower fresh oil TBN is expected with many low SAPS oil, consistent with the example above. While TBN of fresh oil is important, the ability of oil to retain TBN over its drain interval is arguably more critical than the absolute value of the fresh new oil. Lower rates of TBN depletion are expected in modern diesel engines due to the introduction of ultra low sulfur diesel fuel. Thus it could be argued that the fresh oil base number of low SAPS oils does not need to be as high as for high ash oils meant for engines using diesel fuel with higher levels of sulfur. However, as already mentioned, the lower amounts of sulfur derived acids that the oil is exposed to could be partially compensated for by higher acid dewpoints due to the higher EGR rates, by higher amounts of nitric acid and by more organic acids resulting from higher engine oil temperatures. Therefore, TBN remains a critical property that still must be maintained at a level to provide adequate protection against acids.

2.5 THE LUBRICATION SYSTEM

The lubrication system in a typical diesel engine can be separated into four regions; the crankcase, piston ring pack, valve train and combustion chamber (see Figure 2.11). The crankcase provides a volume in which the crankshaft and connecting rotate. Several liters of oil are stored in the sump of the engine, which is also situated inside the crankcase. The piston ring pack lubricates the contacts between the piston and the cylinder liner. A vary small quantity of resides in this section of the engine. Oil is also supplied to the valve train to lubricate the contacts between valves, rocker arms, pushrods, lifters, and the cam shaft. The components in this region operate under boundary lubrication regime. Antiwear additives in the oil, especially ZDDP, are essential in the valve train to prevent excessive wear and failure of components.

The piston assembly and ring pack forms the boundary between the combustion chamber and the crankcase, therefore it is essential as it provides and maintains a seal for the high pressure combustion gases. Sealing is accomplished by the piston rings that are mounted in ring grooves cut into the face of the piston. The piston rings slide along the liner while the engine is operating. The interactions among liner, piston, and rings during engine operation require sufficient lubrication of the surfaces in relative motion to minimize friction and wear, thereby enhancing the lifetime of the engine. Another task performed by the piston-ring pack is the supply of oil to all surfaces in relative motion (i.e. to all ring grooves and the liner). This supply of oil, however, must be controlled, since excess oil in regions adjacent to the combustion chamber results in high rates of oil consumption.

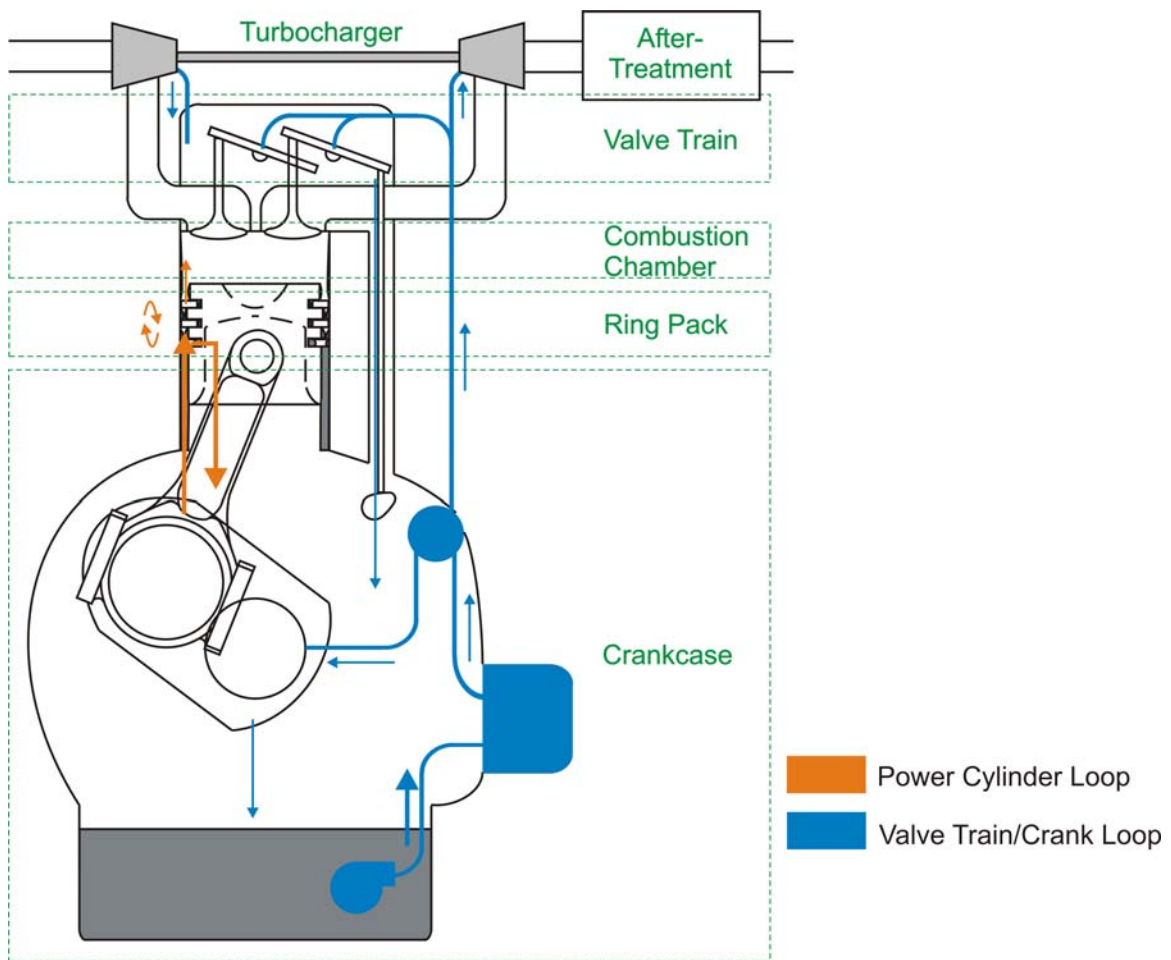


Figure 2.11 – A schematic of the lubrication system in a diesel engine.

2.5.1 Engine Bulk Oil Flows

Lubricant is distributed through the engine to by two main oil circuits: a *primary loop* where a pump drives the lubricant through the engine block, valvetrain, crankshaft and main journal bearings, and a *power cylinder loop* where oil flows through the piston ring pack. Figure 2.11 shows the oil-transport loops. The highest oil flowrates are used in the primary oil circuit. Oil is pumped through an oil filter, which captures wear particles and contaminants before the lubricant is delivered to sensitive engine components.

The operating conditions experienced by the oil in the primary and ring pack loops are quite different. The bulk lubricant in the primary oil loop is typically at temperatures between 100°C and 135°C. There is a small quantity of oil (of the order of a few tenths of a milliliter) that resides in the ring pack. The small volume of oil in the piston ring pack region is exposed to the harshest conditions and must withstand temperatures above 250°C. These high temperatures promote severe oxidation of the base oil. Oil in the ring pack is also subjected to the highest contaminant loading due to exposure to particulates, gaseous emissions, and fuel dilution.

2.5.2 Power Cylinder Oil Flows

A simplified representation of the oil flows in the power cylinder is illustrated in Figure 2.12. To facilitate lubrication of the piston rings and liner, oil is supplied from the crankcase onto the piston liner by splashing or sprays. Excess oil is returned to the crankcase by the oil control ring (OCR). A fraction of the oil supply is transported by various modes past the OCR and into the ring pack where it mixes with the small volume of degraded oil in the ring grooves and on the face of the piston. The lubricant in the ring pack is mixed on the piston face by several oil transport mechanisms that have been observed by [56]. A large portion of this flow is returned to the crankcase through the ring grooves and by interactions with blow-by gas. This exchange between the crankcase and ring pack is manifested as a slow degradation of the crankcase oil. Feedback between the crankcase and the ring pack oil occurs on a timescale of a few minutes [57].

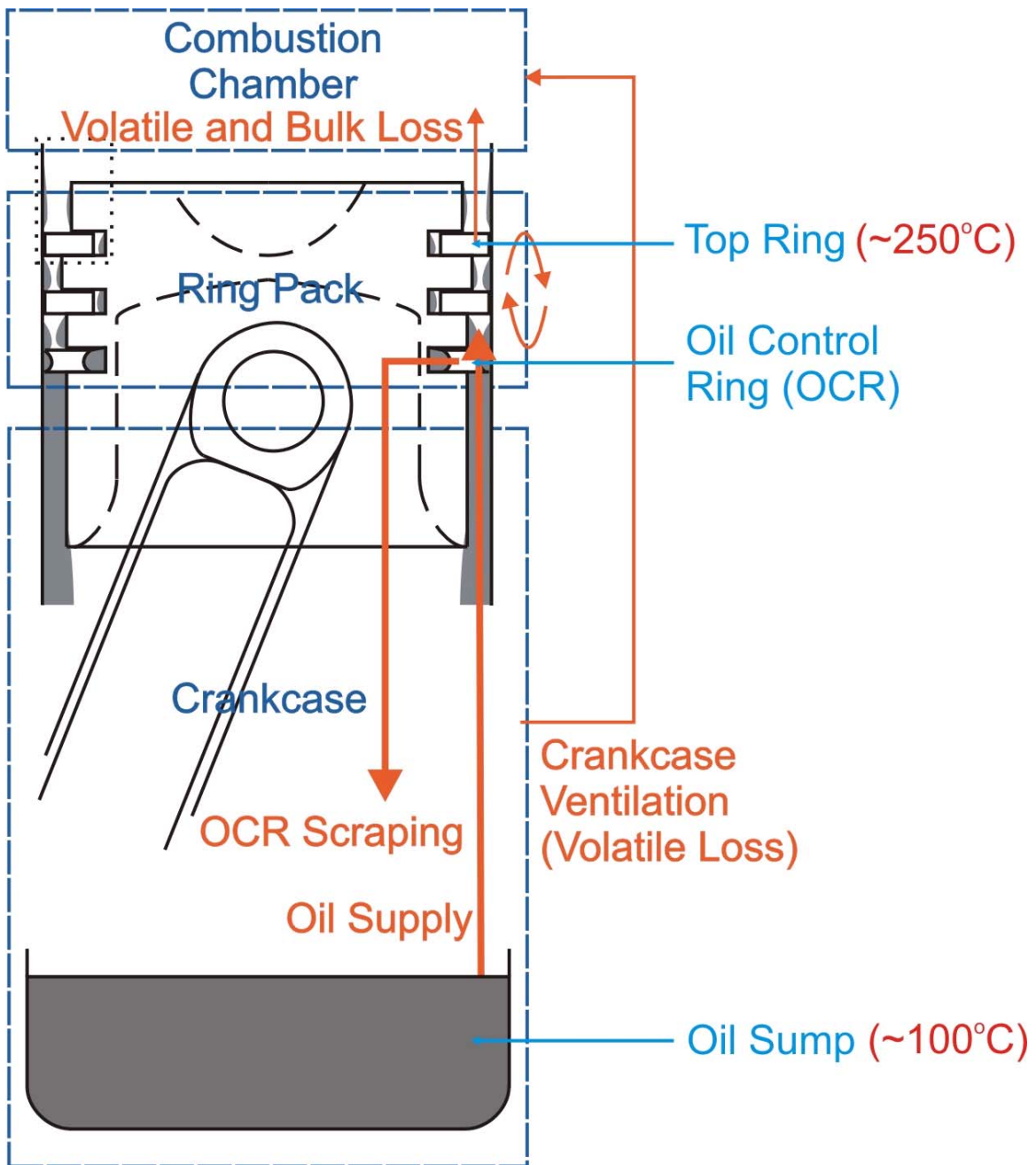


Figure 2.12 – A simplified schematic of the oil flows in the power cylinder system. Oil is supplied to the cylinder liner and piston ring pack by splashing and sprays. A portion of the oil returns back to the sump. A portion of the oil in the ring pack is lost by oil consumption to the combustion chamber.

The composition of the lubricant in the ring pack results from a complex interaction of oxidation, contamination, oil transport, volatilization and mixing on the surfaces of the piston and cylinder liner. The surface of the piston is subdivided into three regions (called “lands”) that are separated by the gaps for piston rings, as shown schematically in Figure 2.13. The sealing action of the piston rings partially isolates the lands such that the composition of the oil films in each zone may be different. Any interaction and mixing of oil between the zones occurs mostly as a result of oil transport along the piston and liner. Oxidation and volatilization on the piston also vary with location, since both are dependent on the surface temperature. The highest temperatures are found on the top land and drop rapidly at positions progressively further away from the combustion chamber.

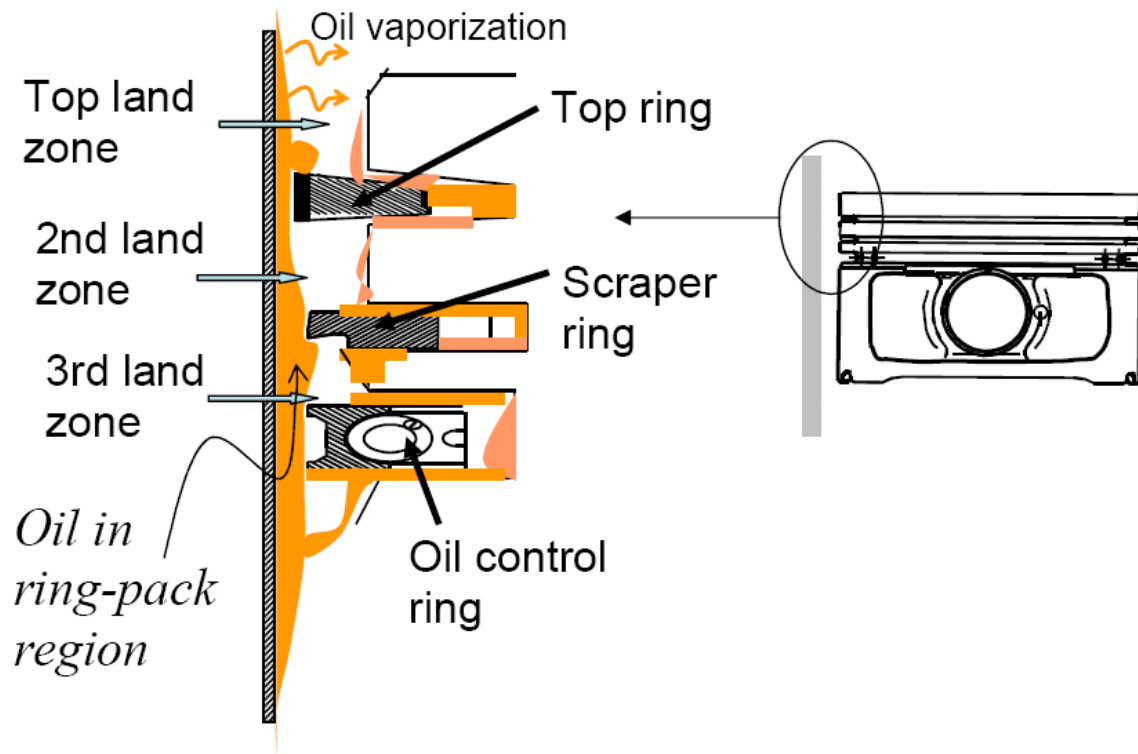


Figure 2.13 – A schematic of the ring pack geometry in a typical diesel engine. The oil flows between locations on the piston ring pack and liner are highly transient [58].

Computer models and direct observations are currently used to examine oil transport in the piston ring pack. An advanced diagnostic system has been used for two-dimensional oil distribution measurements of oil film thickness on the piston employing a multiple die

laser fluorescence technique [56]. Five modes of oil transport are apparent from real-time observations of the oil flow pattern during engine operation [56]:

- Scraping and oil release on the piston rings,
- Inertia driven flows,
- Ring pumping and squeezing,
- Gas dragging, and
- Gas entrainment

The piston ring pack exhibits complex flow behavior. The modes of oil transport listed above are driven to varying degrees by the dynamics of the rings and the gas flows around them, twisting of the rings, piston side motion and bore distortion. Piston and ring dynamics have been modeled in great detail [59,60,61,62].

Of the oil in the ring pack, only a small quantity is transported to the top ring groove (TRG) on the piston, which is in close proximity to the combustion chamber. Oil flowing out of the TRG and onto the piston crown is often regarded as effectively lost to the combustion chamber by oil consumption [56,63]. The mass of ash-related elements emitted from the power cylinder and into the exhaust depends on compositional changes of the lubricant as it flows from the crankcase to the TRG.

2.6 OIL CONSUMPTION

Oil is consumed from several regions in a diesel engine. These areas are all sources of lubricant-derived ash in the exhaust. In particular, the lubrication requirements and dynamics of the piston ring pack result in oil loss through the power cylinder region that makes a major contribution to the total oil consumption. As a result, the mechanisms for oil consumption in the power cylinder determine to a large extent the mass of lubricant-derived metallic elements in the exhaust stream.

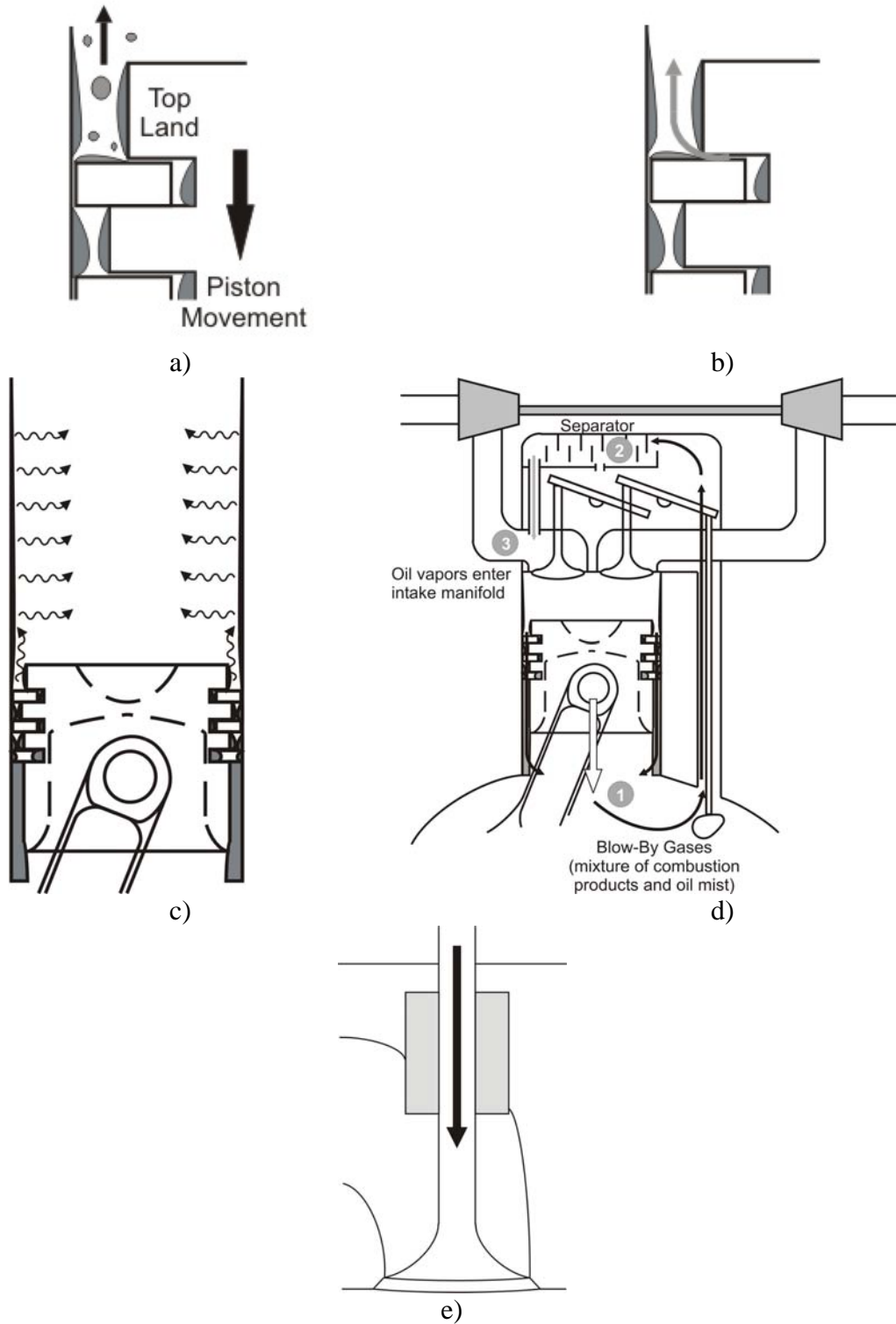


Figure 2.14 – The mechanisms for oil consumption from the power cylinder system; a) Inertia; b) Reverse Gas Flow; c) Evaporation; d) Crankcase Ventilation; and e) Valve Guide Leakage.

Five possible oil consumption mechanisms have been suggested to contribute to the total oil consumption from the power cylinder system [64]. These potential sources of lubricant-derived ash are illustrated in Figure 2.14. As indicated earlier, the oil can accumulate on the piston top land under certain load conditions [65,66]. This oil may be thrown off the top land (Figure 2.14a) and directly into the combustion chamber by inertia forces resulting from the acceleration and deceleration of the piston assembly. The contribution of this driving mechanism to total oil consumption depends on the mass of accumulated oil film on the top land and ring. In other studies, direct oil transport to the combustion chamber was found to depend on gas flow in the piston-ring-liner system. Gas pressures in the second land clearance, i.e. the volume between the top ring and second ring, can become greater than the combustion chamber pressure during some periods of the engine cycle. This pressure gradient will cause a reverse gas flow into the combustion chamber through the top ring gap and around the top ring groove if the top ring loses its stability in the groove. The reverse gas flow may transport oil in both liquid and mist form (Figure 2.14b) into the combustion chamber. This transport mechanism is supported by visualization studies of the oil distribution in the piston-ring pack, when the top ring was pinned. In these studies, oil flow through the top ring gap towards the combustion chamber was observed during low load conditions [67,68].

Oil mist, also present in the recycled blow-by gas flow (Figure 2.14c), has also been found to enter the combustion chamber via the intake manifold system. Experimental studies on different engines quantified the contribution of oil in the crankcase ventilation gases to total oil consumption [69,70]. It was found that, in some engines, this oil consumption source could contribute significantly to total oil consumption.

Oil evaporation (Figure 2.14d) from the piston-ring-liner system is also believed to contribute significantly to total oil consumption, especially during severe operation conditions when the thermal loading of engine components is high. Several experimental results indicated that oil evaporation from the liner and piston might contribute substantially to oil consumption [71,72,73]. In addition, a number of purely theoretical

approaches studied oil evaporation from the liner and found sensitivities in the evaporation process to oil composition and to component temperatures [63,74,75,76].

In older engine designs, oil transport through the valve guides (from the cylinder head into the intake port) (Figure 2.14e) contributed to oil consumption. This effect occurred especially in spark ignition engines operating under part load conditions, when the intake manifold pressure is significantly below atmospheric. However, this oil leak path is effectively sealed in modern engines by positive valve stem seals [69]. Therefore, this oil consumption source is considered to contribute little to the total oil consumption in modern diesel engines.

The final potential source of oil consumption in diesel engines is the turbocharger. Oil can leak into the exhaust, or intake system through damaged turbocharger seals. This mode of oil consumption is not expected to be significant as long as the turbocharger and oil seals are functioning normally.

2.7 STUDIES OF LUBRICANT COMPOSITION IN DIESEL ENGINES

There have been several studies of lubricant composition in engines. It is often assumed that the composition of the lubricant in the sump is representative of the oil condition at all locations in the engine. However, studies of lubricant in the piston ring zone have shown that the oil in this region has a composition that is very different than the sump oil. The lubricant in the top ring zone is exposed to the highest temperatures and greatest contaminant loading in the engine. To some extent, the composition of the oil in the top ring zone affects ash emissions from the engine, since the lubricant in this region is most likely to be lost by oil consumption.

To determine the condition of oil in the top ring zone, sampling studies have been conducted where oil was extracted from this region. This research has been carried out using diesel engines almost exclusively. Early oil sampling was conducted at the cylinder wall, undoubtedly due to the relative ease of implementation compared to sampling via

the piston assembly. [77] undertook this research on a Petter AVB diesel engine. Clear differences were observed between fresh oil and the samples from the top ring top dead center (TDC) position, with a 20% increase in viscosity reported.

A similar investigation was conducted [78], that studied samples obtained through the cylinder wall from the top ring zone at the TDC position. Samples were compared to oil taken from the sump and fresh oil. As with previous work, the oil at the top ring zone position was found to be significantly more degraded than that of the sump. A 73% loss of base oil was reported at the top ring zone with a 50% decrease in the mean molecular weight of the Viscosity Index Improver (VII).

In concurrent studies, other researchers began to extract oil directly from the surface of the piston. In most cases, the lubricant is sampled at the desired sampling point through a small hole drilled from the outer face of the piston to the inside. A flexible tube is used to direct the sample out of the engine. The samples were then analyzed to determine the level of deterioration that occurred during engine operation. [14] used a piston sampling system to extract oil from behind the top ring of a single cylinder diesel engine. Samples were taken from the top ring groove as it was proposed that this oil acts as a reservoir for the upper ring zone and was likely to be directly lost to the combustion chamber. These experiments were carried out with both a Petter AA1 and a Caterpillar 1Y73 diesel engine.

Analysis of the extracted samples showed they were more heavily oxidized than those taken from the sump, with a considerable amount of evaporation being experienced by the oil taken from the top ring groove. This was to be expected as the top ring groove is subjected to much higher temperatures than the sump and is also in contact with the harmful combustion products contained in the blow-by gases. After 50-hour tests, the sampled lubricant viscosity was found to have increased by 10-30%, while it peaked at an increase of 20-65% at around 10 to 15 hours into the test.

[79] also used a similar sampling system to extract oil from the top ring region of the piston, with a flexible tube being used to transport the oil from a sampling hole in the piston to the outside of the engine. Following a 10 hour run using a Petter W1 gasoline engine, the samples from the top ring groove showed a steady degradation throughout the run, while the sump oil showed little change. The observed viscosity of the samples taken from the top ring zone reduced considerably over the test. This condition was attributed to fuel dilution of the oil, an effect that does not occur in diesel engines unless a fuel injection is initiated very early in the cycle.

Experiments to investigate the effect of component wear and engine load on oil degradation have also been conducted by [80]. Long duration engine tests over 350-hours were performed with excessively worn components. An increase in the amount of blow-by through the piston assembly was observed, with a corresponding increase in lubricant degradation. Viscosity, Total Acid Number (TAN) and sludge formation, were all found to increase with increased wear of the components and engine load.

[81] extracted lubricant samples from several positions on the piston of a Caterpillar 3406B engine. A number of analyses were performed on the samples that showed that the lubricant degradation became more severe as the samples were taken from positions progressively closer to the combustion chamber. The Viscosity Index (VI) was found to decrease significantly in the ring pack when compared with the samples taken from the cylinder wall. A similar decrease was observed for the relative volatility of the samples. This indicated that the composition of the oil on the bore wall was different from that of the ring pack, and both of these were different to that of the sump or fresh oil. Experiments with unmodified mineral base oil, a semi-synthetic base oil and a fully synthetic base oil, all with a common additive pack, were also carried out. The synthetic oil was found to have the best performance in this case. All the oils were found to have a significant decrease in Total Base Number (TBN). The synthetic oil gave very little change in relative volatility, while a progressive increase was observed from the semi-synthetic to the mineral oil. This result indicated that the synthetic oil suffered less degradation.

The trends seen in diesel engines were also observed by [82] who investigated oil degradation in the piston assembly of a gasoline engine. As with earlier researchers, they used a sampling tube to extract oil from the second land region on the thrust and anti-thrust sides of the piston. Oil samples were collected during 5-hour tests, at a number of speeds and loads for a 1.6 liter, 4-cylinder engine lubricated with 10W-30 oil. The amount of oil collected was found to increase with engine speed, while a decrease was seen with rising engine load. Changes in TAN and TBN were used to evaluate the extent of oil degradation. Unsurprisingly for the length of test, little change was observed for oil samples from the bulk oil in the sump. For the oil collected from the sump the decrease of TBN and the corresponding increase in TAN were found to be greatest at low speed and to increase with engine load. Additionally, gas from the sampling tube was analyzed for hydrocarbons, oxygen and nitrogen oxides (NO_x). Hydrocarbon levels were found 15 to 55 times higher than in the exhaust, while the levels of NO_x were around 28 times higher.

In-situ measurements of lubricant composition in the top ring zone have also been obtained by [83]. Measurements were obtained with infrared (IR) reflection absorption spectroscopy. The absorption of an IR beam, passed through a window in the engine cylinder and reflected off the surface of the piston, was measured to determine the composition of the lubricant. Changes in the level of the carbonyl ($\text{C}=\text{O}$) group were measured to monitor the level of degradation, since compounds with this group are generated as products of lubricant oxidation. Using this system, tests were carried out on a CAT1Y73 diesel engine, lubricated with a 15W-40 Universal Diesel Engine Oil (UDEO). The experiments were conducted at 1200 rpm/10 bar Brake Mean Effective Pressure (BMEP), with data also being collected for motored and idling conditions. It was found that the carbonyl ratio increased when the engine was operating at high power and that it varied between engine strokes. The IR system utilized in this study required extremely accurate triggering times to coincide with passage of the piston. An extremely high performance interferometer was also required to obtain a spectrum of the oil as the piston passed the window. The signal was also susceptible to thermal radiation from the surface of the hot piston.

Most recently, [15] conducted top ring zone sampling studies with a single cylinder gasoline engine (Ricardo Hydra). Samples were extracted from the engine while it was running at a number of engine loads and speeds. Oxidation was found to increase with higher loads and speeds. There was a significant increase in oxidation over the first 15 minutes of engine operation. Chemical, rheological and tribological analysis of the samples revealed that the lubricant in the top ring zone was significantly degraded relative to the sump oil. The effect of engine speed and load on residence time was also studied. The oil in the ring pack was found to have a relatively short residence time (approximately 3 minutes). Engine speed was found to have a direct relationship with the rate of oil flow through the ring pack and the rate of oil degradation in that region. However, engine speed had little effect on the rate of sump oil degradation. Engine load was found to have little correlation with the residency time in oil in the piston ring pack. Load had a direct relationship with the rate of oil degradation in the ring pack and oil sump.

The previous sampling studies of oil in engines have shown that the properties of a lubricant can be altered significantly as it flows through an engine. Up to this point, the effect of these compositional changes on ash emissions has not been studied. For instance, the elemental composition of the oil in the top ring zone has not been well characterized. Knowledge of lubricant composition in various locations in the engine will also assist in determining what concentrations of additive compounds are required in the oil.

(This page intentionally left blank)

CHAPTER 3 – EXPERIMENTAL AND ANALYTICAL METHODS

3.0 TEST ENGINE

The diesel engine used in this study was a Lister Petter TR-1. The specifications of this single cylinder engine are listed in Table 3.1. This engine was selected because it could easily be modified for extraction of oil samples from several locations in the system.

Table 3.1 – Relevant Engine Specifications

Model	Lister Petter T1
Configuration	Single Cylinder, Air Cooled
Maximum Power	5.5 kW at 1800 rpm
Fuel Injection	Direct Injection
Displacement	0.773 L
Oil Capacity	2.6 L
Oil Change Interval	250 hours



- A. Lister-Petter 1-cyl diesel engine
- B. Oil filter adapter
- C. Intake
- D. Exhaust
- E. Dyno/Generator
- F. Battery
- G. Resistor bank
- H. Voltmeter/ammeter
- I. Fuel tank

Figure 3.1 – An image of the experimental setup with major components listed. The engine is loaded by an AC generator operating at 1800, or 1500 rpm. Power is dissipated by a resistor load bank rated at 7 kW.

Figure 3.1 is an image of the experimental setup, including the Lister Petter T1. The engine is air-cooled and features a crankcase ventilation system, which maintains a slight vacuum in the crankcase during operation. Air cooled engines tend to have higher surface temperatures during operation and larger clearances between components. Considering these attributes, a higher rate of oil consumption due to vaporization was expected.

Several modifications were made to the stock engine to minimize the oil consumption rate. The inlet and exhaust valve guides were fitted with additional o-ring seals to minimize oil consumption through the valve stems. A closed crankcase breather with a separator was also installed on the engine to trap oil mist and return liquid oil to the crankcase. Finally, lubricants with relatively low base oil volatilities were selected for the tests. Reducing oil consumption through the valve guides and crankcase breather system increased the fraction of oil consumed via the piston ring pack. These modifications decreased the average oil consumption rate to 3.56 grams/hour with a commercially available CI-4 PLUS lubricant with a mono viscosity grade (SAE 40).

Advanced emission control technology (EGR and aftertreatment) was not employed on the T1. The lack of EGR on the engine reduced combustion acid contamination of the lubricant relative to modern on-highway engines. However, the absence of NO_x control most likely increased the fraction of nitrogen-based acids. Reduced oxidation and organic acid was also expected due to the moderate oil sump temperatures and the relatively low power output of the engine.

3.1 OIL SAMPLING

Oil sampling was employed in this study to characterize how the composition of the lubricant changes with time and as it flows through different regions in the system. Oil samples were extracted from three regions of the engine:

1. The piston ring pack;
2. oil sump; and
3. valve train.

Figure 3.2 is a schematic of the engine system showing the sampling locations. Different sampling techniques were used to obtain oil samples from each location while the engine was operating. A ring pack sampling system was employed to obtain samples of oil from behind the top ring of the piston. Oil samples were extracted from the sump through the dip stick access hole. Lubricant was obtained from the surfaces in the valve train operating under the boundary lubrication regime. Observations of lubricant composition throughout the engine were important to develop an understanding of ash emissions and additive requirements.

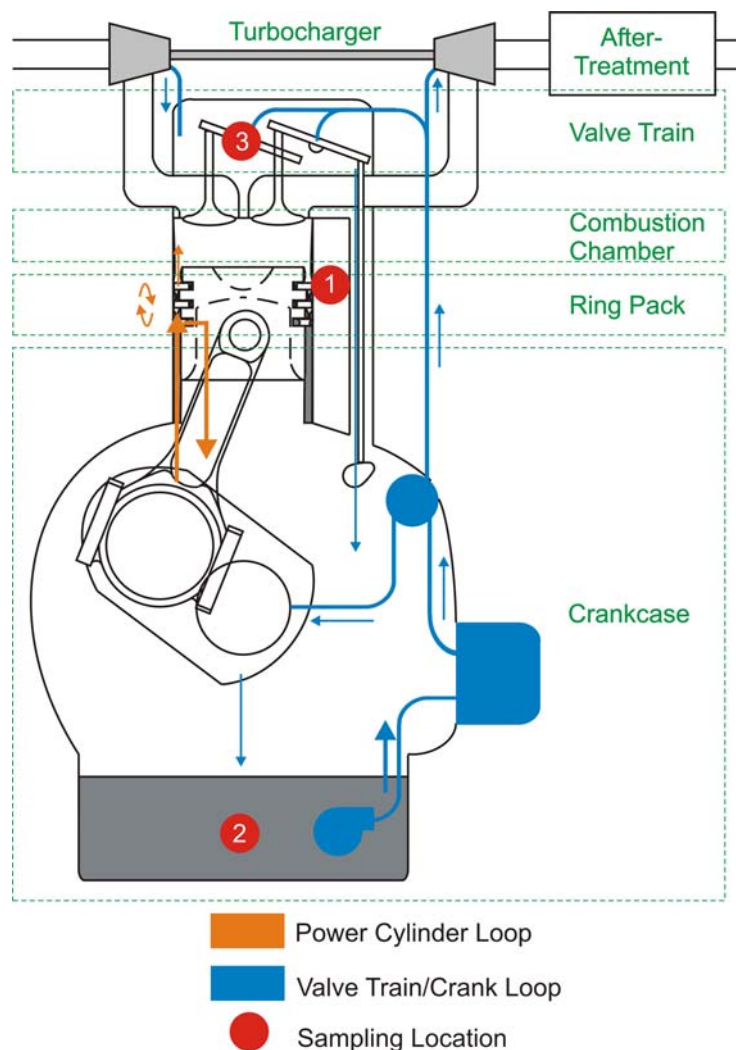


Figure 3.2 – A schematic of the engine system showing the locations where oil was extracted in this study. A different experimental technique was used to obtain samples from each location, while the engine was operating.

3.1.1 Ring Pack Sampling

Ring pack sampling was used in this study to obtain samples of the lubricant from behind the piston rings during engine operation. The lubricant in this region of the engine is subject to the highest temperatures (in excess of 250°C) and contamination from acidic gases in the combustion chamber. The highest rate of oil degradation occurs in the piston ring pack region.

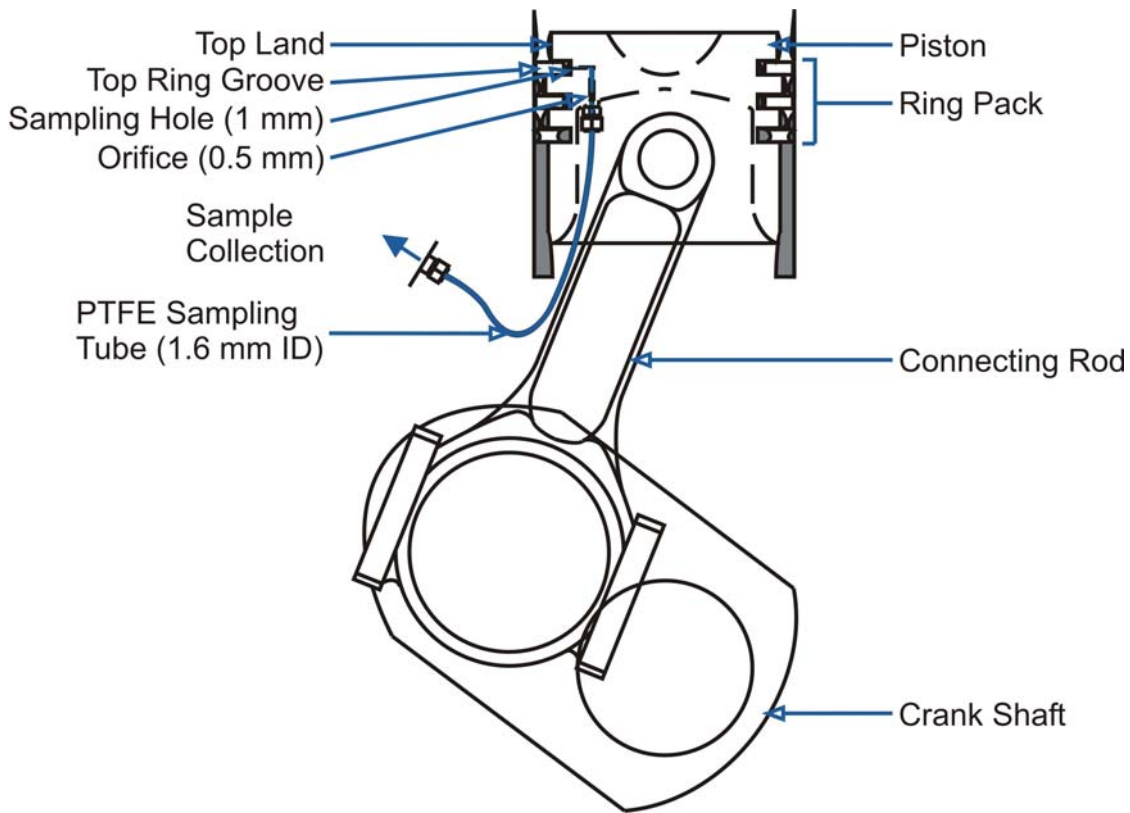


Figure 3.3 – A schematic of the ring pack sampling system used in this study.

A schematic of the ring pack sampling system is shown in Figure 3.3. The system was based on the apparatus developed by [14], and used to study lubricant degradation in [15] and [16]. Oil was extracted from the engine via a small (1 mm diameter) hole drilled into the top ring groove of the piston (see Figure 3.4). The sampling hole was situated on the anti-thrust face of the piston and was centered axially in the groove such that it is covered by the top ring at all times. The channel drilled into the piston was terminated on the

piston under-crown by a fitting that incorporated a 0.5 mm restriction (see Figure 3.5). This orifice limited the sampling rate, thereby minimizing the effect of the sampling system on oil flows and residence times in the ring pack. Finally, a length of Teflon tubing connected the orifice to a sample collection point mounted outside the crankcase.

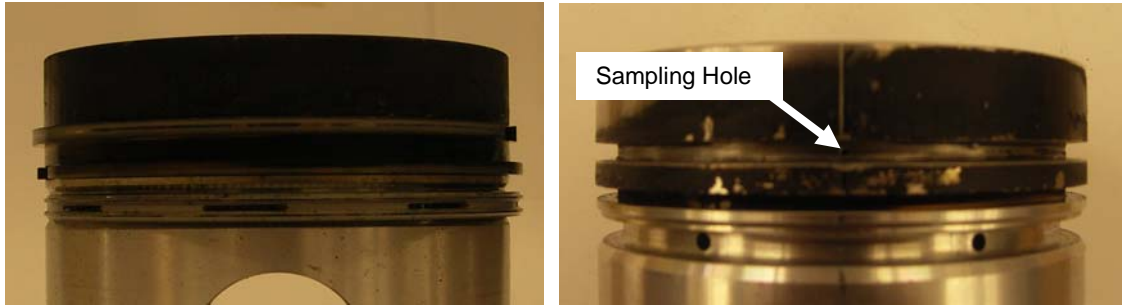


Figure 3.4 – *Left* - A picture of the Lister Petter T1 piston ring pack. *Right* - A picture of the piston used with the sampling system. The piston rings have been removed to reveal the sampling hole situated in the top ring groove.

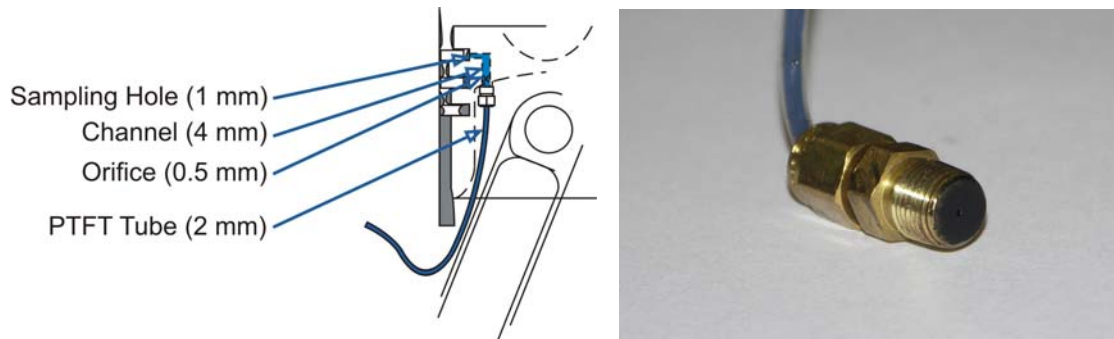


Figure 3.5 – *Left* - A schematic showing the connection between the channel inside the piston and the sampling tube. *Right* - A picture of the tube connector, containing a 0.5 millimeter orifice. Deposits are clearly visible on the face of the orifice and inside the sampling tube.

During each engine cycle, a small quantity of oil from the ring pack was entrained as a mist in the blow-by gas that flows through the sampling hole in the piston. The liquid oil was collected outside of the engine by condensing the oil mist against the side of a chilled sampling vial. The majority of the flow through the sampling tube was comprised of blow-by gases from the combustion chamber. Interaction of the oil sample with blow-by

gas during extraction was expected to have only a small effect on the sample composition since oil in the ring pack is normally subjected to high gas flow rates during engine operation.

The flow rate of oil through the sampling system is highly variable and depends on several factors including the availability of oil in the top ring groove, blow-by gas flow and deposition inside the sampling system. The mass of oil samples collected by the ring pack sampling system over a 40 hour experiment is shown in Figure 3.6. Each sample was collected over one hour of engine operation. The flow rate of oil through the sampling system fluctuated between 10-20 mg per minute. A gradual reduction in the oil flow rate was often observed over the duration of sampling experiments. This effect could be attributed to the accumulation of deposits inside the sampling hole, orifice and sampling tube (deposits can be clearly seen in Figure 3.5). Oil flow rates would often increase after the sampling system was cleaned and a fresh tube was installed.

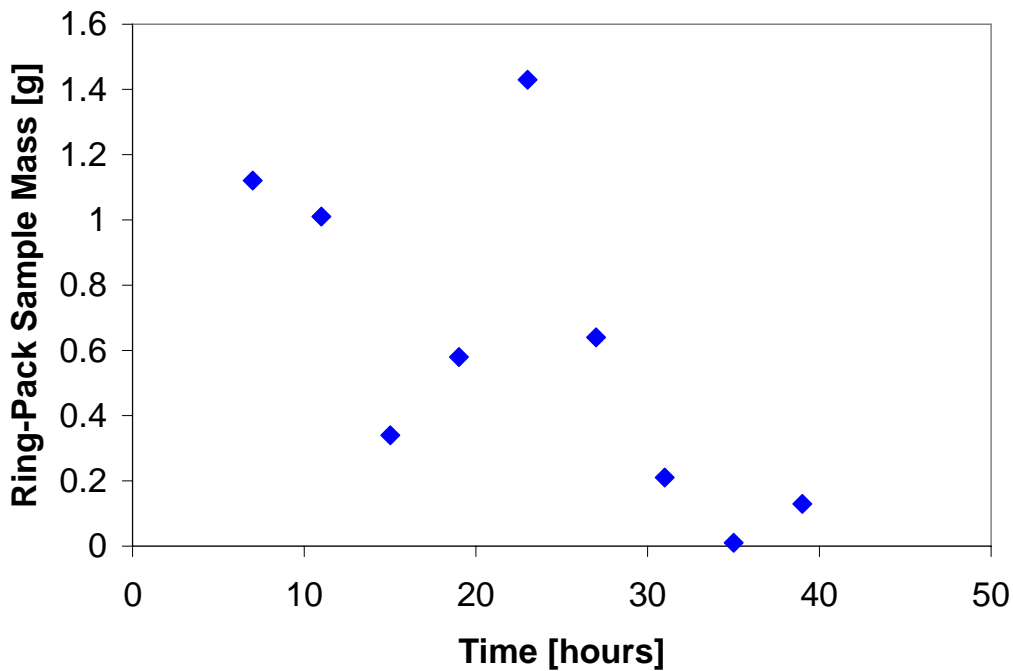


Figure 3.6 – The mass of oil samples collected in one hour by the piston ring pack sampling system, over the duration of a 40 hour experiment.

Elemental analysis of the deposits showed that they were primarily composed of carbon and metals from the lubricant additive package. Of the metals, zinc and phosphorus were found in the highest abundance, followed by calcium and magnesium. The preferential deposition of zinc and phosphorus may occur because these elements are associated with polar compounds that are attracted to surfaces.

3.1.2 Sump Oil Sampling

The degradation of the lubricant in the piston ring pack and on the cylinder liner is manifested as a slow change in the composition of the oil in the sump. In this study, oil samples were also extracted from the engine sump to track changes in crankcase lubricant composition over time.

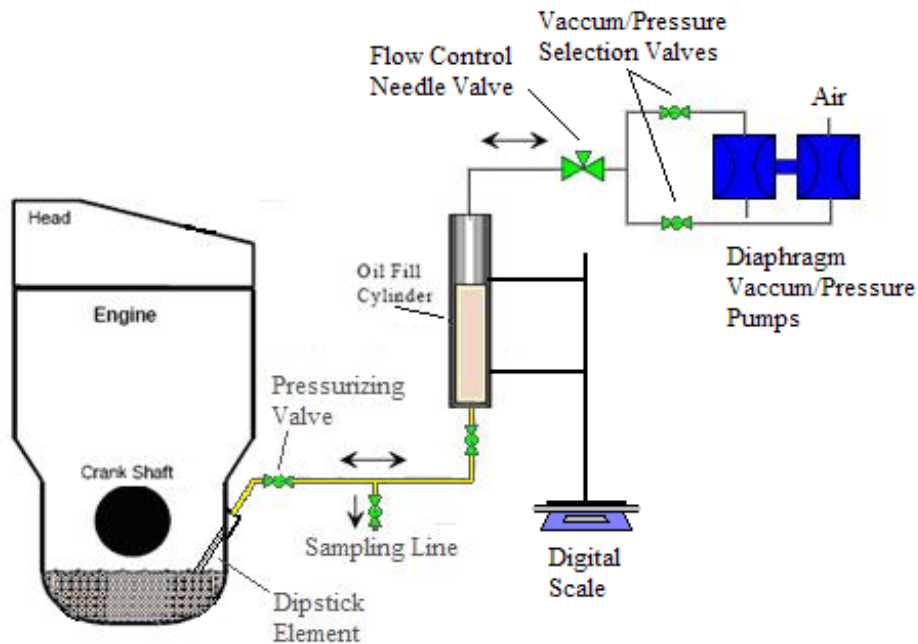


Figure 3.7 – A schematic of the sump oil sampling and oil consumption measurement system. Oil samples are collected after measuring the oil level in the sump.

A crankcase oil measurement system was constructed to take samples of the lubricant from the sump and track oil consumption during experiments. Oil was extracted from the sump through the dipstick hole in accordance with the procedure recommended in the

ASTM oil analysis standards [34,35,84,85,86]. The apparatus was based on the Cummins Gravity Feed System and the Cummins Smart Oil Consumption Measurement System [87]. A schematic of the system is shown in Figure 3.7. The system consisted of an external oil tank connected to the sump through a custom made dip stick element. To extract sample, oil was sucked through the dipstick element and into the tank by a vacuum pump. Sampling was performed in this manner to avoid the collection of heavy deposits that sometimes settle on the bottom of the oil pan when the lubricant is severely degraded. Figure 3.8 is a collection of annotated pictures of the system, including a detailed view of the dipstick element.



Figure 3.8 – Pictures of the sump oil sampling system.

3.1.2.1 Oil Consumption Measurement

An oil consumption measuring system was built in order to accurately correlate the ash emissions from the engine with oil composition measurements. The design and basic operation of the system was fairly simple. Before taking a measurement, the engine was stopped to prevent crankcase pressure effects on the measurements. Oil was then suctioned from the sump into a cylindrical container by a set of diaphragm air pumps mounted as one unit. Oil was removed from the crankcase until the level in the sump reached a predetermined baseline level. The weight of the cylinder (containing the oil)

was then recorded and make-up oil was added to the baseline oil level. Finally a pressure system was used to push the oil in the tank back into the engine.

This simple system proved to be accurate and extremely reliable means to measure oil consumption in a small single cylinder engine. Consecutive oil consumption measurements were repeatable to within ± 4 grams.

3.1.3 Valve Train Sampling

During this study, samples of valve train oil were obtained and analyzed to determine if the composition of the lubricant from this region is sufficiently different from the oil in the sump. The operating environment for the oil in the valve train is different from the conditions in the power cylinder. The predominant lubricating regime on the valve train is boundary lubrication; whereas hydrodynamic conditions dominate elsewhere.

All of the experiments involving valve train sampling were performed on a Cummins ISB, multicylinder diesel engine (6 cylinder, 2 intake and 2 exhaust valves per cylinder). This engine was selected because it featured a more modern valve train design than the one found in the Lister Petter engine.

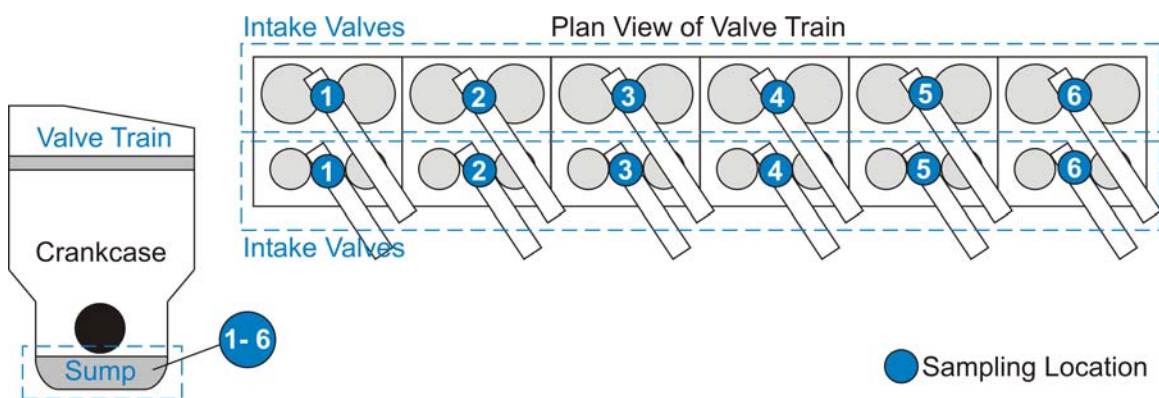


Figure 3.9 – The sampling locations in the valve train system. Lubricant was collected from the valve rockers and simultaneously from the sump.

Oil was sampled from several locations in the valve train. Figure 3.9 shows where oil was collected from the system. In a typical experiment, twelve oil samples were extracted from the valve train. Six samples were collected from the contact surface on the intake valve rockers. Another six samples were taken from the exhaust valve rockers. In addition, lubricant was sampled from the sump for comparison with the valve train oil. All oil samples were analyzed with Inductively Coupled Plasma (ICP) analysis and Fourier Transform Infrared (FTIR) spectroscopy. A statistical analysis was performed to determine with there was any significant composition differences between the oil in the sump and the valve train.

3.2 OIL ANALYSIS

The oil samples collected during this study were analyzed by several standardized techniques to determine the lubricant elemental composition, remaining useful life, and extent of contamination and degradation. Each form of analysis yields specific information about the sample and has limitations. The results of all the tests on an individual sample must be considered to assess the true condition of the oil.

3.2.1 Inductively Coupled Plasma (ICP) Analysis

Spectroscopy is utilized in this study to characterize the composition of lubricant samples collected from the test engine. One type, inductively-coupled plasma (ICP) spectroscopy, measures light in the visible and ultraviolet regions of the spectrum. ICP spectroscopy is used to measure the concentration of individual elements in the oil.

In this procedure, a diluted oil sample is passed through an argon gas plasma. The plasma is produced by induction and is maintained at a temperature of approximately 8000°C. In the upper region of the plasma, acquired energy is released as a result of the electronic transitions, and characteristic light emissions occur. Different elements produce different frequencies. The intensity of the light emitted is directly proportional to the concentration of the element.

The concentrations of up to 30 metallic elements can be measured simultaneously in a single ICP analysis, to an accuracy of ± 5 ppm. Most metallic elements found in used oil come from two main sources; the lubricant additive package and from the wear of engine components. Table 3.2 lists the origin of metallic elements detected in used oil samples.

Table 3.2 – Common sources of Elements found in ICP Analysis of Used Oil Samples

Element	Symbol	Source in Engine, or Oil
Calcium	Ca	Detergent additives
Magnesium	Mg	Detergent additives
Zinc	Zn	Anti-wear additive
Phosphorus	P	Anti-wear, anti-oxidant additives
Iron	Fe	Gears, roller bearings, cylinder liners, shafts
Copper	Cu	Bearings, brass/bronze bushes, gears
Chromium	Cr	Piston rings, roller bearings
Nickel	Ni	Roller bearings, camshafts and flowers, thrust washers, valve stems, valve guides
Molybdenum	Mo	Piston rings, solid additive
Aluminum	Al	Pistons, journal bearings, dirt
Tin	Sn	Bronze brushes, washers and gears
Lead	Pb	Journal bearings, grease
Silver	Ag	Journal bearings (seldom), silver solder
Sodium	Na	Internal coolant leaks, additive
Lithium	Li	Grease
Boron	B	Dispersant additive, internal coolant leak
Sulfur	S	Lubricant base stock, additives

ICP is one of the most versatile techniques for lubricant analysis, although it does have some limitations. For instance, the procedure is unable to analyze the composition of particles with sizes greater than 5 to 8 microns. All of the additive compounds in used oil may be characterized by ICP since they are at least an order of magnitude smaller than this size limitation. While this limit does not normally affect the detection of wear particles, there are times when large particles could be missed in an analysis. For example, wear particles generated due to fatigue tend to be abnormally large.

It is also generally not possible to measure additive depletion with ICP analysis. Take, for example, the detergent additive used to neutralize acids that accumulate in oil over time.

The concentrations of detergent compounds are reflected by calcium and magnesium levels. Neglecting volatilization, if the calcium level of both a new and a used oil were measured, they would be very similar, even though in the used oil the detergent has been depleted. The reason for this is that the amount of actual calcium in the oil has not changed. What has changed is the form, or compound, in which the calcium exists. Before being neutralized, the calcium was present in a compound with detergent properties. After being used, the calcium is still present, but now in an inactive form. Similar effects occur with other additives; therefore, ICP should not be used to measure additive depletion.

The ICP analysis in this study was performed by an independent laboratory in accordance with ASTM standards D4951 [84] and D5185 [85].

3.2.2 Total Base Number (TBN)

Total Base Number (TBN) quantifies the alkaline reserve of a lubricant available for the neutralization of acidic contaminants. The measurement consists of a titration procedure and is expressed in milligrams of potassium hydroxide per gram of oil (mg KOH/gram). Lubricants with higher TBN more effectively suspend wear-causing contaminants and reduce the corrosive effects of acids over an extended period of time.

There are several standard methods presently used to measure the TBN of new and used oil samples. Each method gives slightly different results depending upon the reagents used and the method for titration endpoint determination. The procedures account differently for the contribution of different additives to TBN (see Section 2.1.5). Three test standard ASTM methods are employed in this study to measure the TBN of oil samples; ASTM D2896 [34], D4739 [35] and D5984 [86].

The use of perchloric acid and a potentiometric titration in the ASTM D2896 test method [34] allows for a measurement of the TBN contribution from both detergent and dispersant additives. This procedure tends to yield the highest TBN levels for new and

used oil samples. D2896 is used in this study to measure the depletion of dispersant additives in an experimental lubricant with no detergents.

A hydrochloric acid titration is utilized in the ASTM D4739 test method [35] for determining the TBN of used oil samples. This weaker acid is preferentially neutralized only by detergent additives in the oil. As a result, TBN measurements with D4739 tend to be lower than those obtained with D2896. ASTM D4739 is used in this study to track the depletion of detergent additives in the lubricant.

In some circumstances, the accuracy of TBN measurements can be affected by an error in the determination of the titration endpoint. Most of the TBN measurements obtained during this study have been verified by the ASTM D5984 standard method [86]. This colorimetric titration procedure uses a different method for endpoint determination. The TBN values obtained by D-5984 are consistently between those obtained by D2896 and D-4739 [88,89,90].

3.2.3 Total Acid Number (TAN)

Total Acid Number (TAN) is a measure of lubricant acidity. It quantifies the amount of unneutralized (weak) acid in a lubricant. In a procedure similar to that used to determine TBN, the measurement of TAN involves a titration where the total acid content of 2 grams of oil is dissolved in a mixed solvent and completely neutralized by the gradual addition of an alcoholic solution of potassium hydroxide (KOH). The TAN of oil is defined as the number of milligrams of KOH needed to neutralize the acid constituents in 1 gram of the oil (mg KOH/gram).

In this study, TAN is determined with two standard ASTM test methods; ASTM D664 [91] and D974 [92]. These procedures mainly differ in the way that the titration endpoint is determined. ASTM D664 is a potentiometric titration method, which is accurate with most oil samples. ASTM D974 is colorimetric titration procedure, where the endpoint is determined by the use of a chemical indicator that changes color as soon as the acid is

completely neutralized. The results of both analysis methods have been shown to similar [89].

3.2.4 Four Ball Wear Test

The four ball wear test is a bench test originally developed to assess the capability of lubricating oils to prevent wear in highly loaded contacts under boundary lubrication, as can be experienced in ball bearings, or valve trains. It is often used as a screening test to determine if a sample of lubricant contains an active anti-wear additive.

In a four ball wear test, three metal balls are clamped together and covered with the test lubricant, while a rotating fourth ball is pressed against them in sliding contact (see Figure 3.10). This contact typically produces a wear scar, which is measured and recorded. The smaller the average wear scar, the better the wear protection provided by the lubricant.



Figure 3.10 – The contact geometry used during a four ball wear test.

Table 3.3 – Four Ball Wear Test Parameters

Test Parameters	
Speed (rpm)	1200 (± 60)
Temperature ($^{\circ}\text{C}$)	75 (± 1.7)
Load (kfg)	40 (± 0.2)
Duration (min)	60 (± 1.0)
Ball Specifications	
Ball Material	AISI-E52100
Hardness (HRc)	64-66 (Extra Polish)
Grade	25 (± 0.00005)
ANSI Spec B	3.12

All of the four ball wear tests in this study were performed by an independent laboratory in accordance with the ASTM D4172 standard [93]. The test parameters, with typical limits, are listed in Table 3.3.

The four ball wear tests performed in this study were conducted to obtain a preliminary evaluation of the anti-wear properties of oil samples under sliding contact. No attempts have been made to correlate the test results with any other contact regimes. In fact, it is not known if the results correlate with engine field performance. The relative performance of the oil samples can only be assured under the conditions of the four ball wear test.

3.2.5 Fourier Transform Infrared (FTIR) Spectroscopy

Infrared (IR) analysis is another type of spectroscopy routinely used to analyze oil samples. Unlike ICP spectrometry, it provides data on lubricant condition. This technique is applied to used engine oils to measure several useful degradation parameters, most of which are related directly or indirectly to combustion by-products. Infrared spectroscopy is also able to detect the presence of water and can be used on occasions to identify oil base stocks.

While ICP spectroscopy measures emissions of radiation of specific wavelength in the visible and ultraviolet regions of the electromagnetic spectrum, IR analysis involves the measurement of absorption of specific wavelengths of radiation in the infrared region. Various degradation by-products and contaminants found in oil have characteristic absorptions in specific regions of the infrared spectrum. A higher the level of degradation or contamination in the sample results in a higher the degree of absorption in the characteristic region.

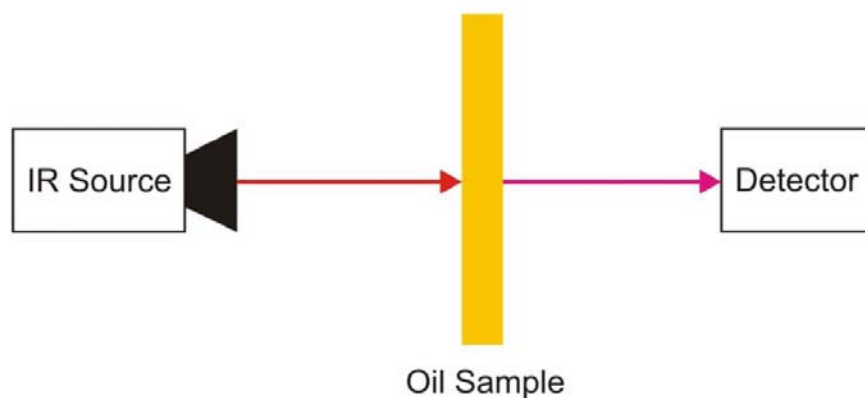


Figure 3.11 – In a typical FTIR analysis the oil sample is placed between the infrared source and detector. Infrared radiation must pass through the sample to be absorbed.

In a typical analysis, an oil sample is placed between an IR source and detector (see Figure 3.11). The amount of infrared radiation absorbed by the sample at each characteristic frequency is measured and can be directly related to the concentration of individual chemical species. The term FTIR spectroscopy refers to the specific manner in which the data is collected and converted from an interference pattern to the infrared spectrum of the sample.

A plot of absorbance versus wavelength is generated by the FTIR procedure. This spectrum can be analyzed to yield measurements for soot, oxidation, sulfates, nitrates and water in the sample. A typical spectrum of used oil is shown in Figure 3.12. The peaks in the spectrum correspond to the presence of specific chemical bonds, or functional groups in the sample. Figure 3.13 shows which functional groups can be resolved in the spectrum and their wavenumber positions. Table 3.4 summarizes the methodology used to analyze the spectrum and the reporting procedure use in this study.

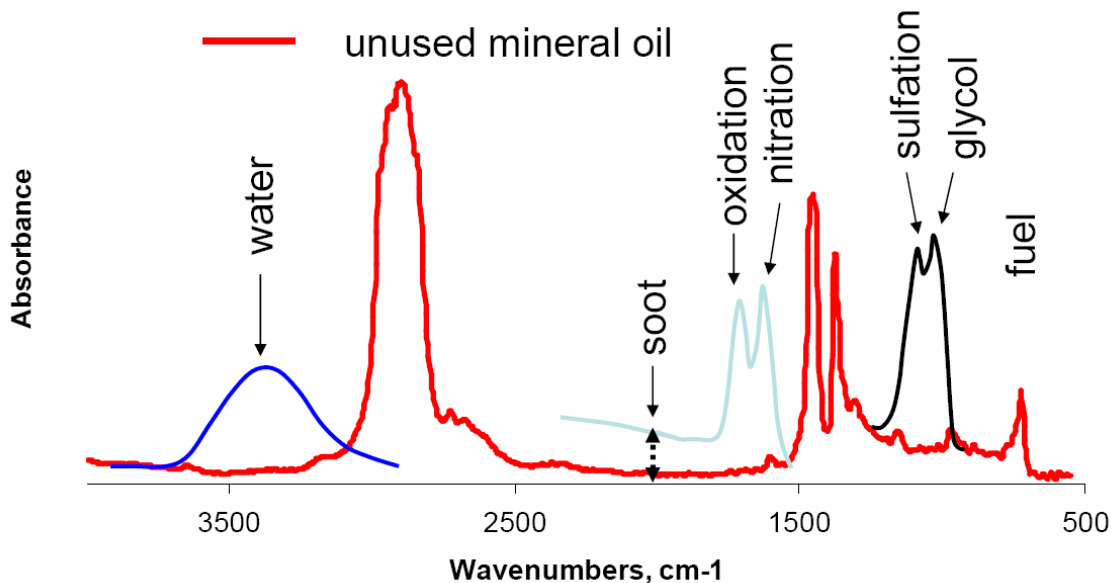


Figure 3.12 – A typical FTIR spectrum of used oil with peaks of interest labeled.

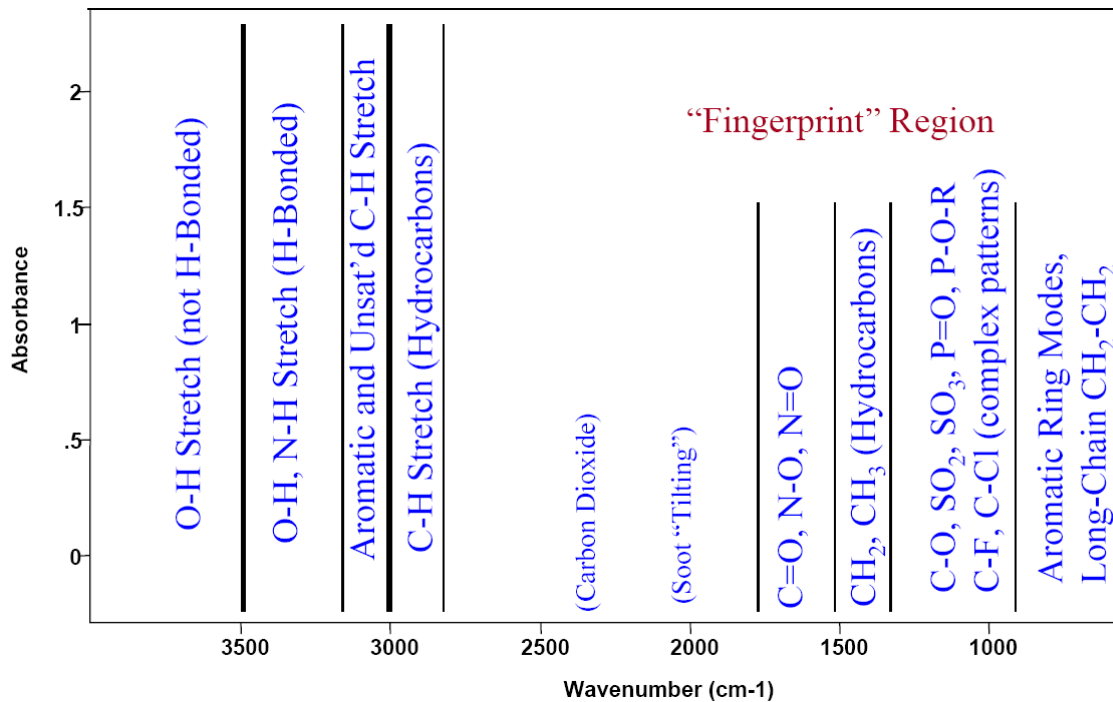


Figure 3.13 – Functional groups that correspond with absorbance peaks in FTIR spectra of used oil.

Table 3.4 – Diesel Lubricating Oil Condition Monitoring Parameters Used for Direct Trending and Reporting Procedure

Component	Measurement Area (cm⁻¹)	Baseline Points(s) (cm⁻¹)	Reporting
Water	Area 3500 to 3150	Minima 4000 to 3680 and 2200 to 1900	Report Value as Measured
Soot Loading	Absorbance Intensity at 2000	None	Value × 100
Oxidation	Area 1800 to 1670	Minima 2200 to 1900 and 650 to 550	Report Value as Measured
Nitration	Area 1650 to 1600	Minima 2200 to 1900 and 650 to 550	Report Value as Measured
Anti-wear Components	Area 1025 to 960	Minima 2200 to 1900 and 650 to 550	Report Value as Measured
Sulfate by-products	Area 1180 to 1120	Minima 2200 to 1900 and 650 to 550	Report Value as Measured
Diesel	Area 815 to 805	Minima 835 to 825 and 805 to 795	(Value + 2) × 100
Gasoline	Area 755 to 745	Minima 780 to 760 and 750 to 730	Report Value as Measured
Ethylene Glycol Coolant	Area 1100 to 1030	Minima 1130 to 1100 and 1030 to 1010	Report Value as Measured

3.3 IN-SITU FOURIER TRANSFORM INFRARED (FTIR) SPECTROSCOPY

While samples of lubricant from the piston ring pack and liner regions have been obtained in several studies, the accuracy of the measurements is unknown. The extraction technique utilized to obtain samples from these regions (including the system employed in this study) may alter the composition of samples due to abnormal interactions with blow-by gases, deposition, and changes in ring pack oil flow. Ring pack sampling systems may also alter residency times for the oil on the piston and liner. New diagnostics systems are needed that obtain in-situ measurements of lubricant composition, with minimal disturbance on the system.

An in-situ system employing diffuse infrared spectroscopy has already been employed to examine the composition of oil in the ring pack region [83]. Unfortunately, this system is

impractical due to its sensitivity to transient radiation from combustion, variations in oil film thickness and complicated triggering requirements. One objective in this study is to develop an in-situ system for measurements of lubricant composition that is robust, has sufficient accuracy and sensitivity.

For this study, a novel system was developed that measures the composition of the lubricant at the piston and liner interface utilizing Attenuated Total Reflectance (ATR) FTIR spectroscopy. A rudimentary schematic is shown in Figure 3.14. IR radiation was channeled to the cylinder liner by a probe mounted on the engine. Measurements were obtained off the surface of a zinc sulfide crystal, which was in direct contact with the lubricant in the piston ring pack region. Optical fibers, made of silver halide, coupled the crystal at the tip of the probe to an IR source and detector.

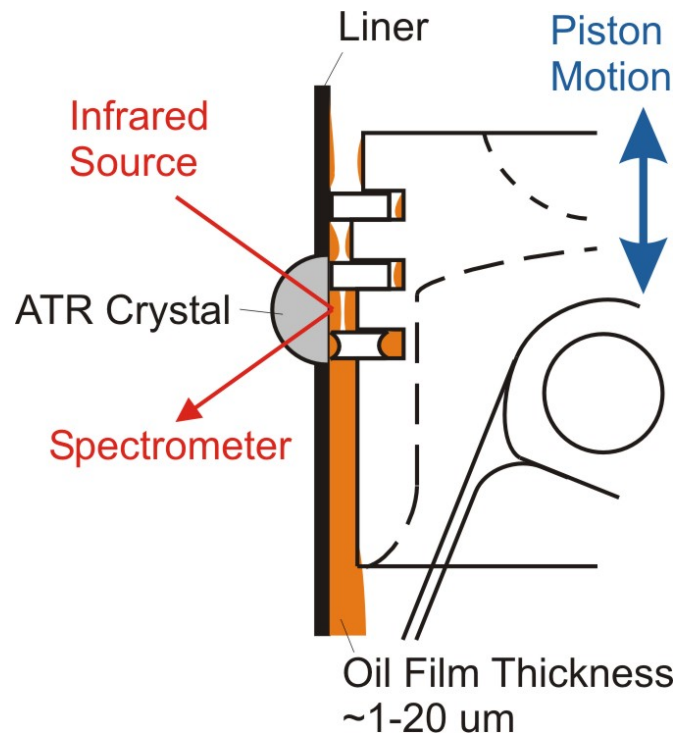


Figure 3.14 – A schematic of the FTIR measurement system. Infrared radiation is absorbed from the surface of a zinc sulfide crystal mounted on the cylinder liner.

3.3.1 Measurement Principle – Attenuated Total Reflectance (ATR)

Attenuated total reflectance (ATR) is a technique that may be used in conjunction with IR spectroscopy that enables substances to be examined directly in the solid or liquid state without sample preparation.

ATR relies on a property of total internal reflection called the *evanescent wave* (see Figure 3.15). A beam of infrared light is passed through an ATR crystal in such a way that it reflects at least once off the internal surface in contact with a sample. This reflection forms an evanescent wave which extends into the sample, typically by a few micrometres, and is partially absorbed. The beam is then collected by a detector as it exits the crystal [94].

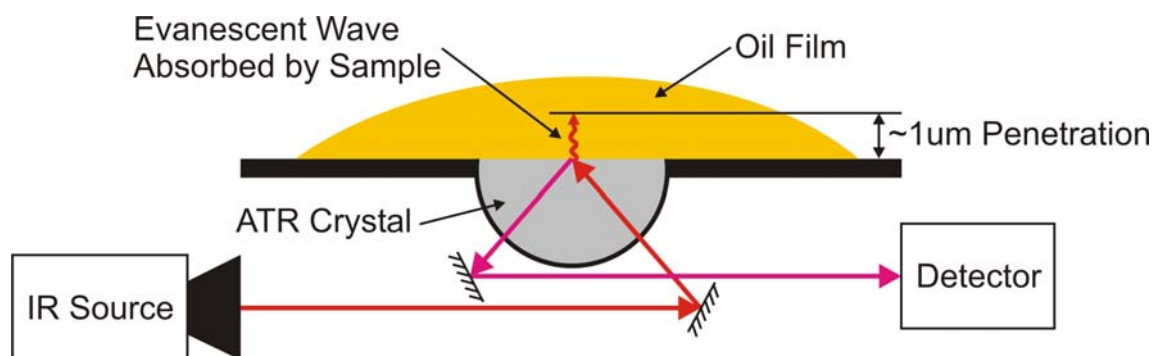


Figure 3.15 – The measurement principle for Attenuated Total Reflectance FTIR spectroscopy.

This evanescent effect occurs when the crystal is made of an optical material with a higher refractive index than the sample being studied. Good contact between the sample and the ATR crystal is required for repeatable measurements. In the case of a liquid sample, pouring a shallow coating amount over the surface of the crystal is sufficient.

Several factors must be considered while selecting an appropriate material for the ATR crystal, including the properties of the sample, operating environment and the infrared transmission properties of the crystal. Typical materials for ATR crystals include germanium, KRS-5 and zinc selenide, while silicon is ideal for use in the Far-IR region

of the electromagnetic spectrum. The excellent mechanical properties of diamond make it an ideal material for ATR, particularly when studying very hard solids, but the much higher cost means it is less widely used. Diamond crystals also absorb IR radiation in the spectral region that excites carbon (C-C) bonds. This property makes diamond a less desirable material for analyzing hydrocarbon samples.

3.3.2 ATR Probe Design

Figure 3.16 is an illustration of the probe body developed during this study. An ATR crystal made of highly pure zinc sulfide (trade name Cleartran™) was attached to one end of the probe. The crystal was secured onto the engine through a hole in the cylinder liner and was sealed by a high pressure fitting. The functions of the probe body were to hold the crystal in place, seal combustion gases inside the cylinder and provide cooling for the optical fibers. Silver halide fibers coupled the zinc sulfide crystal at the tip of the probe to the IR source and detector. The ATR was designed to be compatible with a Remspec™ FTIR system [95].

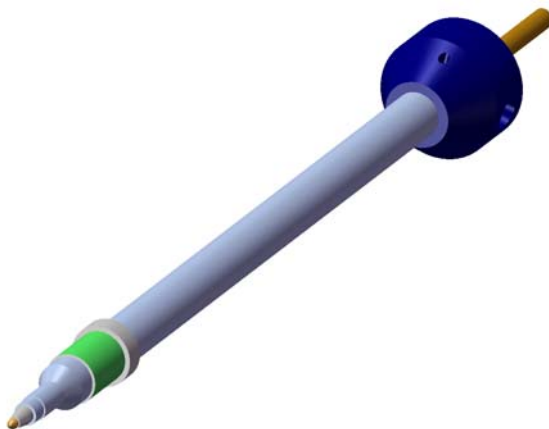


Figure 3.16 – A CAD rendering of the ATR probe developed for this study. The probe obtains FTIR measurements of lubricant composition at the piston and liner interface during engine operation.

The specifications of the probe are listed in Table 3.5. The ATR crystal was designed to make sensitive measurements of oil composition, while also withstanding the harsh

environment inside the cylinder. Detailed views of the probe tip are shown in Figure 3.17. The sampling end of the crystal had conical geometry with a 45° half angle. This shape provided two sampling surfaces (where infrared light reflects off the inner surface of the crystal). The long and thin shape of the crystal culminated IR light towards the sampling point by internal reflections off the outside walls. These design features made the crystal highly optically efficient. Zinc sulfide was selected as the crystal material due to its optical properties, temperature rating and cost. The index of refraction of zinc sulfide is sufficiently higher than that of oil, such that the penetration distance for the FTIR measurement was of the order of 1 micron. The material was also capable of withstanding continuous temperatures of over 350°C. The transmission properties of zinc sulfide are graphed in Figure 3.18. There are no absorbance peaks across the mid-IR wavelengths that could interfere with measurements.

Table 3.5 – ATR Probe Specifications

ATR Crystal	Zinc Sulfide (Cleartran™)
Crystal Geometry	90° Conical (2 Internal Reflections)
Index of Refraction	2.27
Maximum Useful Temperature	350°C
Melting Point	< 1000°C
Maximum Pressure	2 MPa
Optical Fibers	Silver Halide Bundle
Optical Fiber Geometry	7 Input Fibers, 12 Output Fibers
Maximum Fiber Temperature	60°C

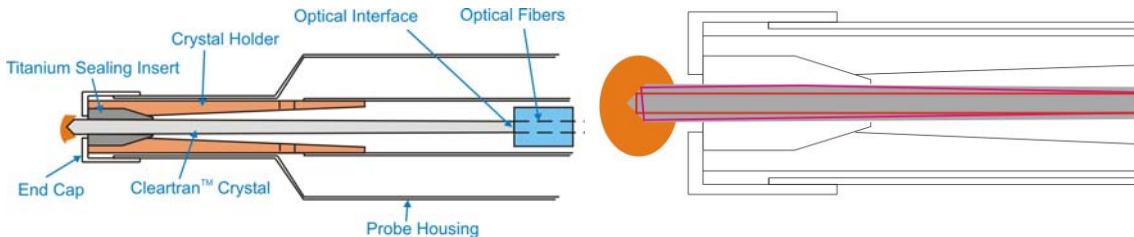


Figure 3.17 – The ATR crystal. *Left* – A cutaway of the probe tip and crystal mounting. *Right* – Internal reflections culminate the infrared radiation towards the probe tip. Two reflections occur at the sample location.

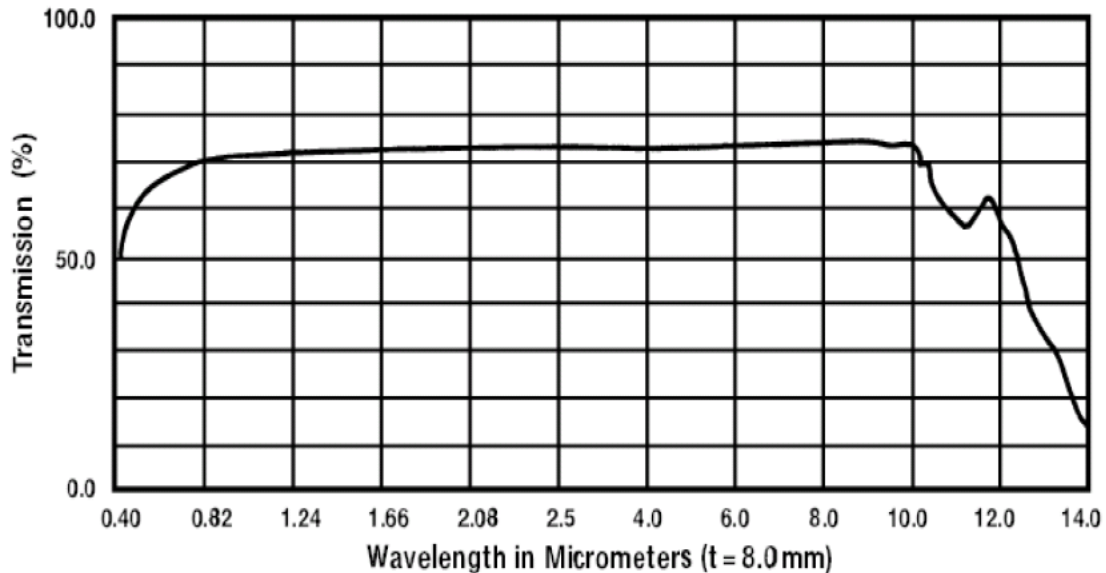


Figure 3.18 – The transmission properties of zinc sulfide are relatively constant across the wavelengths in the mid infrared range.

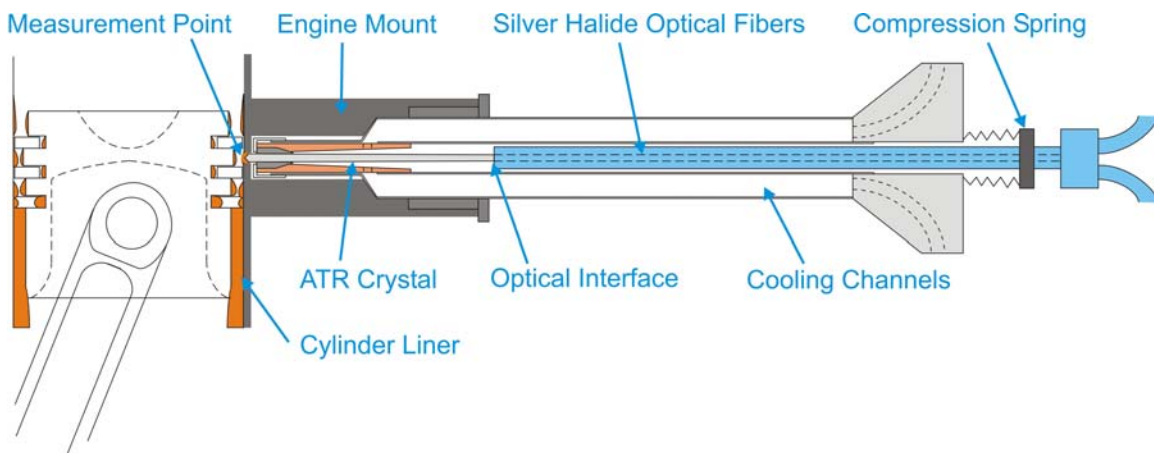


Figure 3.19 – A schematic of the ATR probe.

The optical fibers were the most fragile components in the system. They cannot withstand continuous temperatures above 60°C and degrade under harsh vibration. The probe body was designed to protect the fibers and ensure a good optical connection between the crystal and end of the fiber bundle. A cutaway view of the probe is illustrated in Figure 3.19. The optical fibers were held firmly against the end of the ATR crystal by a compression spring. Cooling channels delivered bottled nitrogen down the probe and then onto the surface of the ATR crystal. The cooling gas flowed over the fiber bundle and

then exited the probe in the back end. The temperature of gas at the outlet is monitored by a thermocouple and should not exceed 50°C when the fibers are inserted inside the probe. Coolant flow rate could be adjusted to prevent damage to the probe during use.

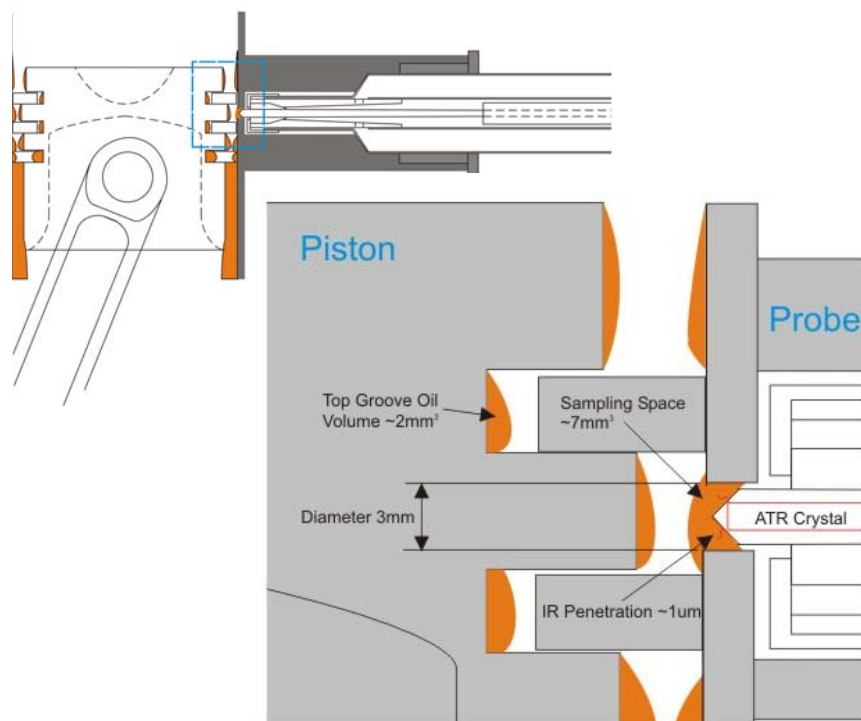


Figure 3.20 – An illustration of the sampling region.

The ATR probe is mounted directly on the engine cylinder just below the position of the top ring when the piston is in the top dead center. An enlargement of the sampling region is illustrated in Figure 3.20. The ATR crystal extends into the cylinder through a 3 millimeter diameter hole in the liner, and is in direct contact with the lubricant. During engine operation, lubricant from the piston and liner collect in the small void space around the probe. The volume of this void space is of the same order as the volume of oil normally found behind the top ring groove on the piston. The ATR probe enables sampling of oil at the piston and liner interface with minimal disturbance to the system. It also greatly simplifies the process for gathering spectra as complicated triggering systems are not required. A thin film of oil coats the crystal throughout the engine cycle, so continuous sample collection may be used to boost signal to noise ratio.

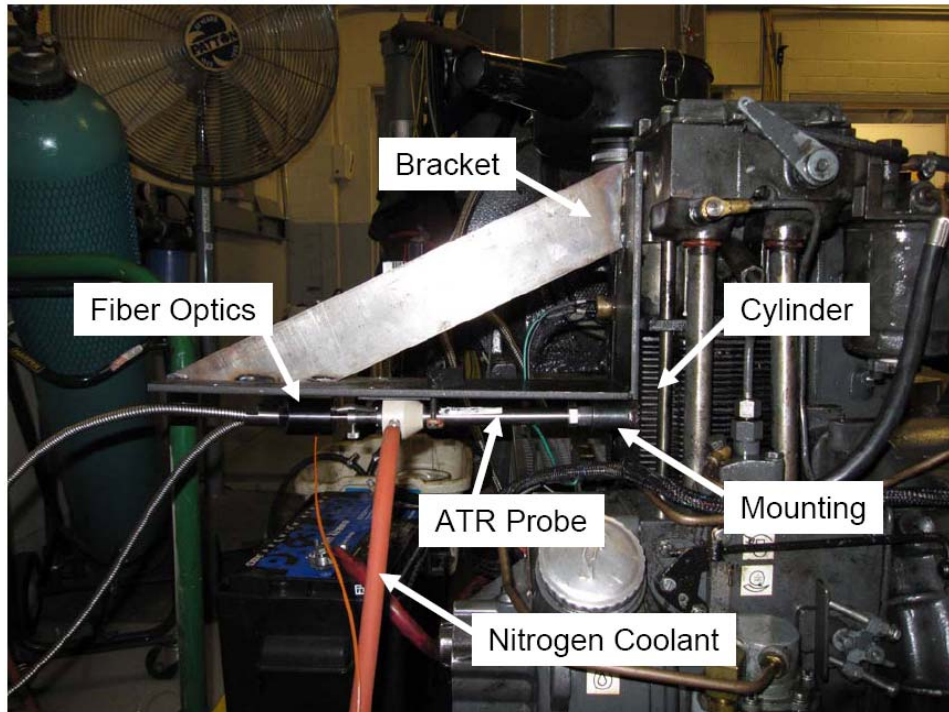


Figure 3.21 – A picture of the ATR probe attached to the engine.

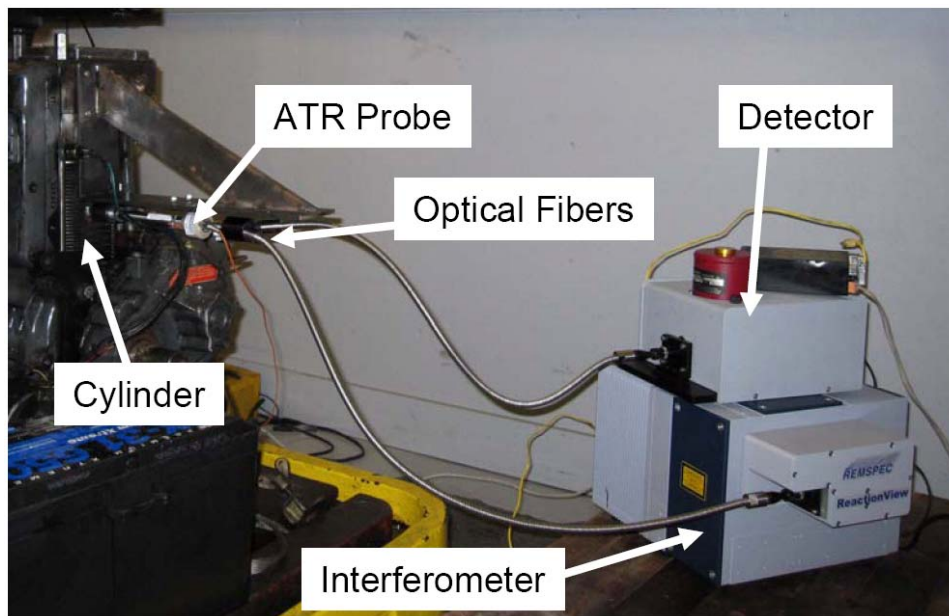


Figure 3.22 – A picture of the optics, interferometer and detector used in the ATR system.

Figures 3.21 and 3.22 are photographs of the ATR system test setup. The probe was mounted onto the side of the cylinder by a rigid high pressure seal. A steel bracket held the probe securely onto the side of the engine and reduced the amplitude of vibrations transferred through the probe. The IR source and detector used in this study was supplied by Remspec™ corporation. A ReactionView™ interferometer served as the IR source in the system. Spectra were captured by a highly sensitive mercury-cadmium-telluride (HgCdTe) detector, also supplied by Remspec™ corporation.

3.3.3 Measurement Procedure

The ATR system should be cleaned and recalibrated regularly. This procedure prevents the buildup of films on the crystal surface that may be detected in measurement even at thicknesses of less than 100 nanometers. Regular cleaning with a volatile solvent, such as dichloromethane, should maintain the sensitivity of the probe. The use of solvents on the inside of the probe, or on any plastic components must be avoided. The optical gain of the probe, fibers and assembled system should also be recalibrated regularly. Throughput of infrared radiation through the optical fibers can degrade over time due to vibration, or bending of the reinforced cables. The optical interface between the fibers and the end of the ATR crystal can also be optimized by rotating the fiber bundle in the probe until the gain is maximized.

A background spectrum must be obtained before any FTIR measurements can be taken. This reference is subtracted from all of the measured spectra, so it is critical that the crystal surface is clean and installed in the measurement location before obtaining the background. The engine should also be off while collecting a baseline. A good background improves the sensitivity of the measurement, so it should be collected over several minutes to maximize the signal to noise ratio.

Data can be collected after the system has been calibrated and a good background is obtained. As stated above, it is critical that the nitrogen coolant flow rate be adjusted to never exceed 50°C while the optical fibers are inserted in the probe. Extreme care must

be used while handling the probe, since bending the probe body can fracture the ATR crystal that is tightly fitted on the inside.

Table 3.6 – Measurement Parameters

Capture Rate	10 spectra/minute
Scan Rate	20 scans/second
Resolution	4 cm ⁻¹
Detector	HgCdTe

Table 3.6 lists the system settings used during this study to obtain measurements with the ATR probe. A spectrum of the used oil obtained with the ATR system at the piston and liner interface is shown in Figure 3.23. The lubricant was contaminated with biodiesel fuel, as indicated by the prominent ester peak. This data was measured 4.5 min after engine shutdown. The oscillations at about 2200 cm⁻¹ were caused by interactions in the silver halide optical fibers. Water was also found in the lubricant from condensation of exhaust water vapor on in-cylinder surfaces after engine shutdown. No spectrums obtained during engine operation indicated the presence of water in the lubricant.

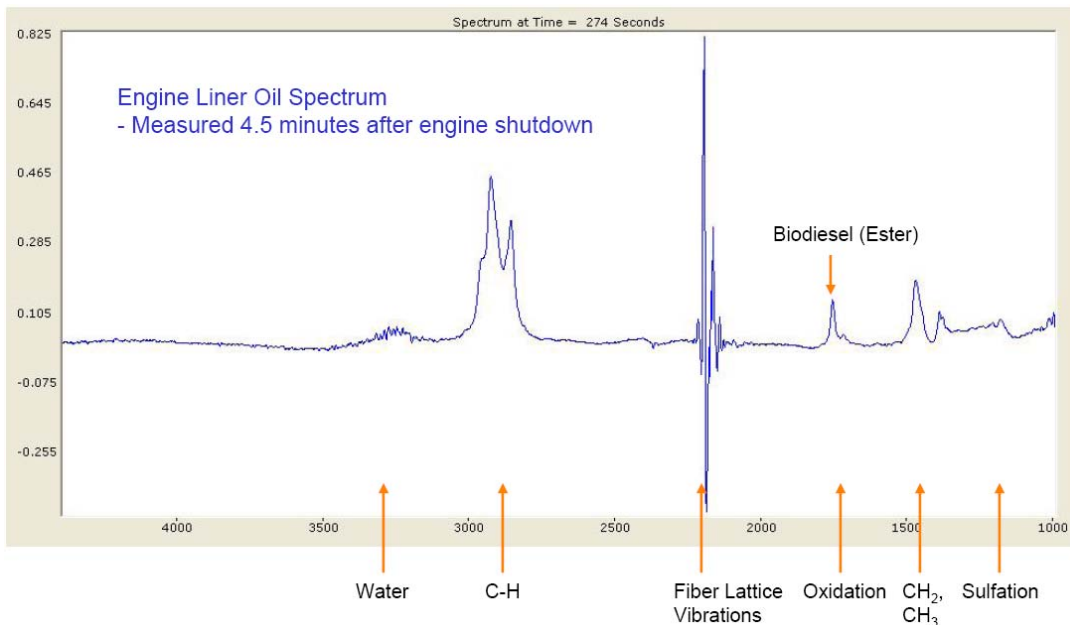


Figure 3.23 – A spectrum of used oil at the piston and line interface. The lubricant is contaminated with biodiesel fuel, as indicated by the prominent ester peak. This data was obtained 4.5 minutes after engine shutdown.

An example of the raw data collected by the ATR system during an experiment is shown in Figure 3.24. It is composed of a time series of FTIR spectra that combine to form a three dimensional surface. A view of the surface from above is shown in Figure 3.25. In this example, the system was activated before starting the engine. The engine was started at 30 seconds, and was shut down at 199 seconds. The time series is actually a collection of clean and noisy spectra (see Figure 3.26), with a usable FTIR spectrum occurring every 18 seconds (every third scan). The noise in the data is most likely caused by vibration at the interface between the ATR crystal and the fiber optics, and/or infrared interference from the combustion process and hot surfaces in the cylinder. Up to this point, the cause of the noise in the system output has not been verified, although vibration is the most likely source.

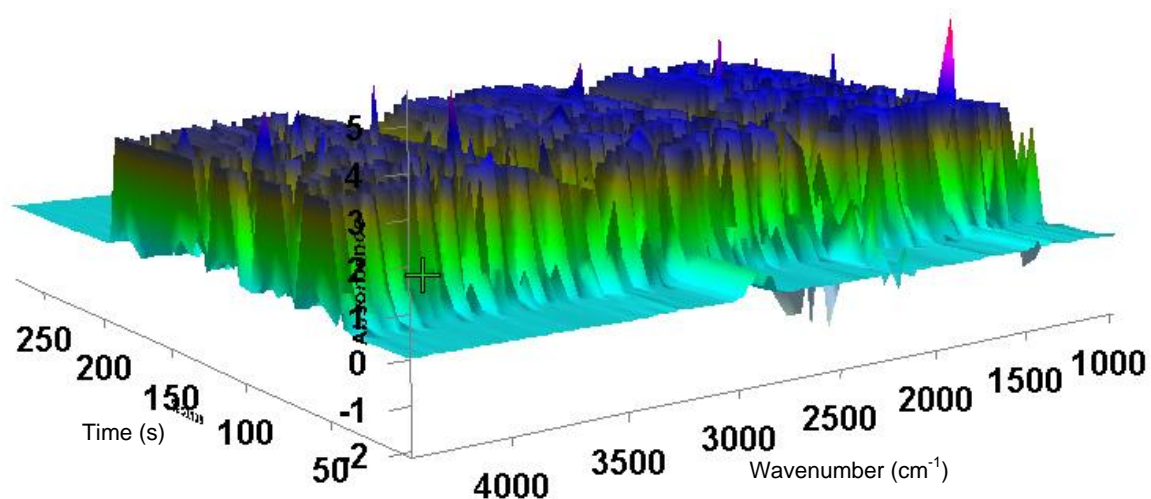


Figure 3.24 – Raw spectra collected by the ATR system. The engine starts at 30s and is shut down at 199 seconds. The vertical axis is in absorbance units.

Compositional changes in the lubricant are seen more clearly when the noisy spectra are removed from the time series. Figure 3.27 is the same data set shown in Figure 3.24 after removal of the noisy spectra. Changes in chemical composition are indicated by changes in the absorbance at specific wavelengths. Spectra obtained with ATR spectroscopy are interpreted the same manner as those measured by typical transmission spectroscopy (see Table 3.4).

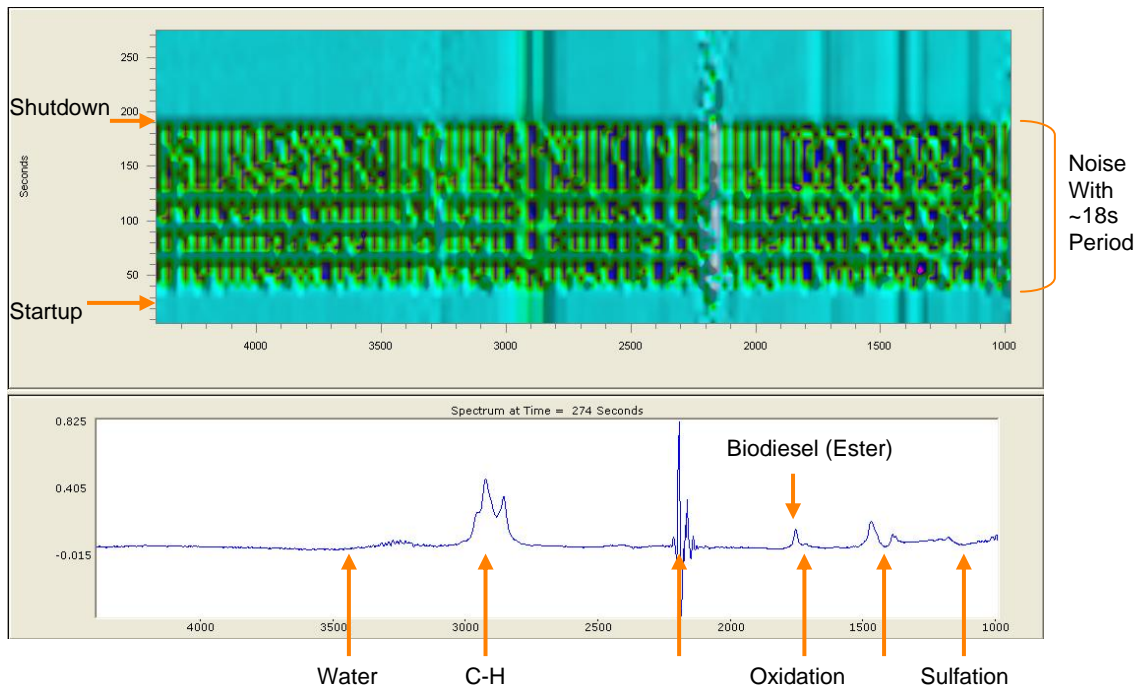


Figure 3.25 – The raw spectral time series viewed from above.

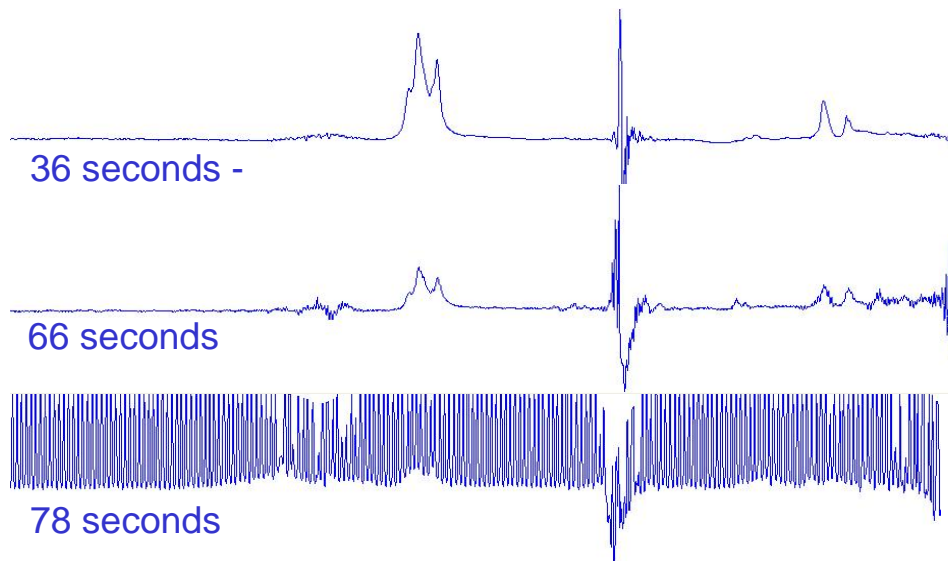


Figure 3.26 – Individual spectra obtained by the ATR system. The spectra obtained at start-up (36 seconds) and 66 seconds may be used to characterize the composition of the lubricant. The spectrum at 78 seconds is noisy and unusable.

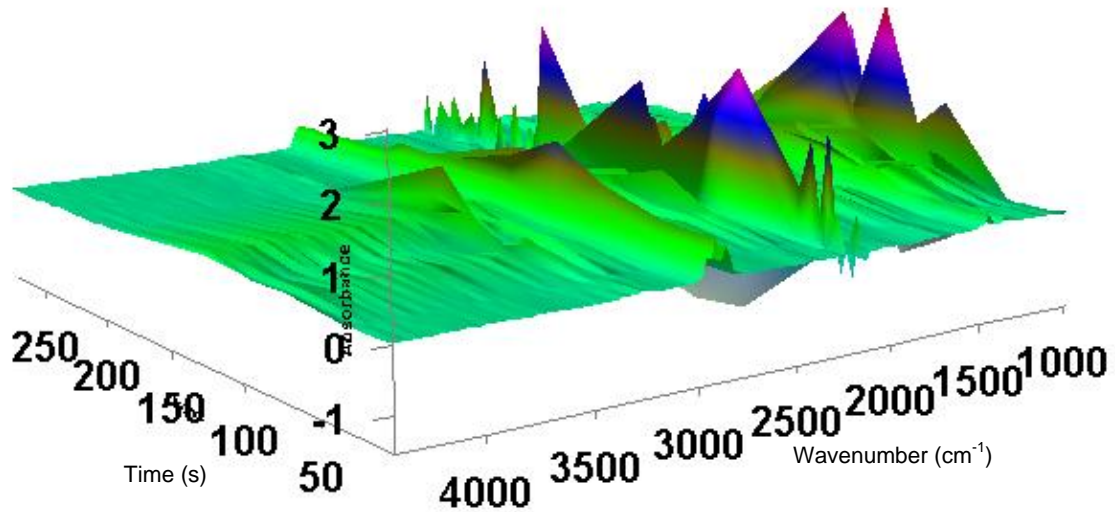


Figure 3.27 – The data series shown in Figure 3-21 after removal of the noisy spectra.

3.4 FILTER DEBRIS ANALYSIS

The oil filter is a potential sink for additive and engine wear metals in an engine. Debris collected by the filter also tends to be larger than the size limit for particles detected in ICP spectroscopy.

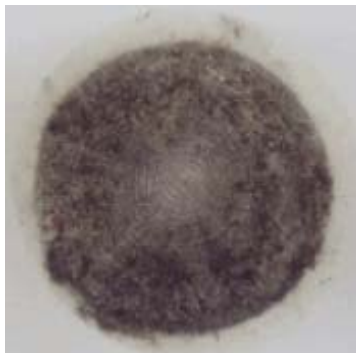


Figure 3.28 – A filter debris micro-patch obtained during the filter debris analysis procedure.

In this study, the material in oil filters was collected and analyzed by a process called filter debris analysis. An ultrasonic cleaner in combination with a pulsating backwash of oil and water was used to dislodge debris from oil filter elements and collect it on a 10

micron filter patch (see Figure 3.28). An inductive oil sensor in the cleaning system counted particle size and detected if individual particles were ferrous, or non-ferrous. X-Ray Fluorescence (XRF) analysis was utilized to characterize the elemental composition of the debris.

3.5 LUBRICANTS

Six different lubricants were used in this study; identified in this thesis as oils A to F. The relevant lubricant properties are listed in Table 3.7. The viscosity grade, volatility and additive package formulation were varied. Lubricants were selected with sulfated ash levels between 1.0% and 1.4%. There was also a range in volatility, as indicated by the mixture of SAE grades and the variation in the oil consumption rate. Oils A to E were commercially available diesel lubricants with full additive packages. Oil F was an experimental lubricant that did not contain detergent additives.

The additive packages in the lubricants were also varied. The concentrations of the metallic elements in the fresh oil as measured with ICP Spectroscopy, in accordance to [89], are shown in Table 3.8. Oil A has calcium and magnesium based detergent, whereas oils B and C contain calcium but not magnesium. Oils B and C have identical detergent and anti-wear additive formulations.

3.6 FUEL

The fuel used in this study was ultra low-sulfur diesel with a sulfur concentration of less than 15 ppm. The fuel was tested with ICP to ensure that the concentrations of all metallic contaminants were less than 1 ppm.

Table 3.7 – Lubricant Properties

Oil	A	B	C	D	E	F
Specification	CI-4 PLUS	CH-4	CH-4	CI-4 PLUS	CJ-4 LE	Zero Detergent
SAE Grade	15W40	30W	40W	40W	15W40	15W40
API Gravity	28.8	29.0	29.0	28.9	29.1	29.1
Viscosity @ 40°C [cSt]	125			146	125	
Viscosity @ 100°C [cSt]	15.1	10.9	14.4	14.9	15.7	15.2
Base Stock Group	II	II	II	II	II	I
Sulfated Ash [%] (D874)	1.41	1.0	1.0	1.35	1.0	0.057
TBN [mgKOH/g] (D2896)	12.2	7.3	7.3	10.2	9.6	5.5
TBN [mgKOH/g] (D4739)	10.5	6.3	6.4	9.5	6.5	0.5
Oil Consumption [g/hour]	6.1	5.5	3.5	3.55	5.1	5.7

Table 3.8 – Lubricant Elemental Analysis (D4951)

Oil	A	B	C	D	E	F
Calcium (Ca)	3123	2495	2495	3130	1432	0
Magnesium (Mg)	119	0	0	10	355	0
Zinc (Zn)	1546	1245	1231	1350	1389	0
Phosphorus (P)	1322	1050	1086	1490	1286	480
Boron (B)	207	0	0	130	586	0
Molybdenum (Mo)	52	0	0	102	77	0
Barium (Ba)	0	0	0	0	0	0
Sodium (Na)	0	0	0	0	0	0

3.7 LUBRICANT SPECIES TRANSPORT MODEL FRAMEWORK

A framework was developed to model the distribution of lubricant species inside the power cylinder. This mathematical framework was used to predict the emissions of ash-related species from the engine.

3.7.1 Modeling Approach

A mass balance approach was used to model changes in lubricant composition throughout the engine due to oil transport, contamination, oil consumption and chemical reactions. The system was separated into zones, and the composition of the lubricant throughout each zone was assumed to be uniform. The lubricant composition was represented as a collection of species, which can represent any distinct component in the formulation. The general case is shown in Figure 3.29. The schematic is a representation of a single zone that is in communication with the surrounding zones by oil transport (flows). The mass of individual species can also be affected directly by sources and sinks of mass in each zone.

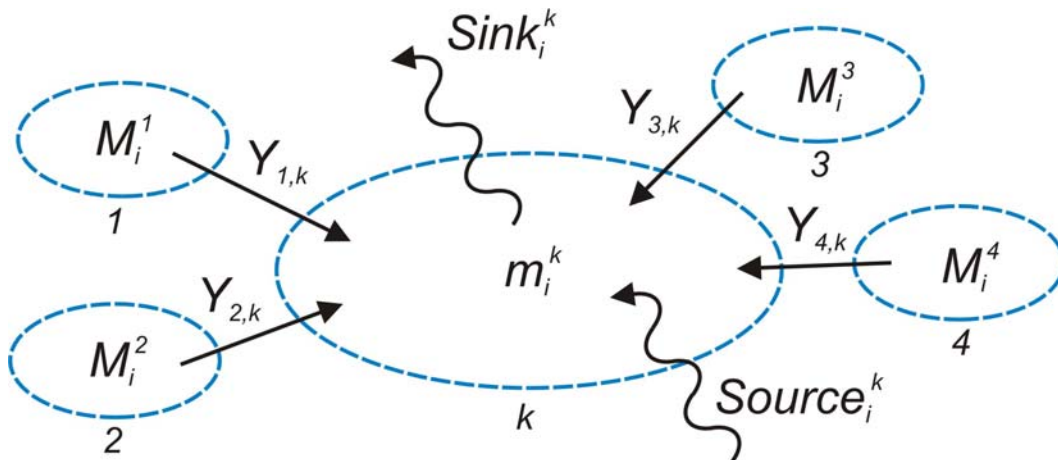


Figure 3.29 – A representation of a single zone in the lubricant species transport model. Each zone can communicate with any number of neighboring zones by oil transport. Chemical reactions are modeled as sources, or sinks of a species in each zone.

The mass, m , of each species, i , in each zone, k , was calculated by integrating the following equation:

$$\frac{dm_i^k}{dt} = \sum_{j=1}^L Y_{j,k} M_i^j + \text{source}_i^k - \text{sink}_i^k \quad (3.1)$$

Where, the subscript j indicates an interconnecting zone and $Y_{j,k}$ represents the flow rate of oil from zone j to k . The concentration of a species, i , in an interconnecting zone, j , is denoted as M_i^j . Sources and sinks for species in each zone were modeled as two additional terms in the equation. A rate of direct species addition into a zone (e.g. the rate of calcium addition due to oil addition into the sump, or chemical reaction) was expressed as source_i^k . Similarly, a rate of species removal from a zone (e.g. volatilization of base oil, or chemical reaction) is expressed as sink_i^k .

3.7.2 Model Framework

To analyze the data obtained in this study, a simple model of the power cylinder was created by dividing the system into three zones (see Figure 3.30):

1. The crankcase;
2. Ring pack; and
3. Combustion Chamber.

There is a flow of oil from the crankcase to the ring pack region. The majority of the lubricant supplied to the ring pack returns to the crankcase after residing for a period of time on the piston and the liner. Some oil is lost to the combustion chamber due to liquid oil consumption, or volatilization. These transient flows were modeled as steady flow rates between the zones. This approximation is valid for modeling time horizons that far exceed the residency times of oil in the system. The following approximations were made to simplify the model:

- Steady flows were assumed between the zones;
- A uniform lubricant composition was assumed in each zone;
- Deposition of lubricant components was neglected; and
- The net flow of oil in and out of the ring pack was zero (constant mass).

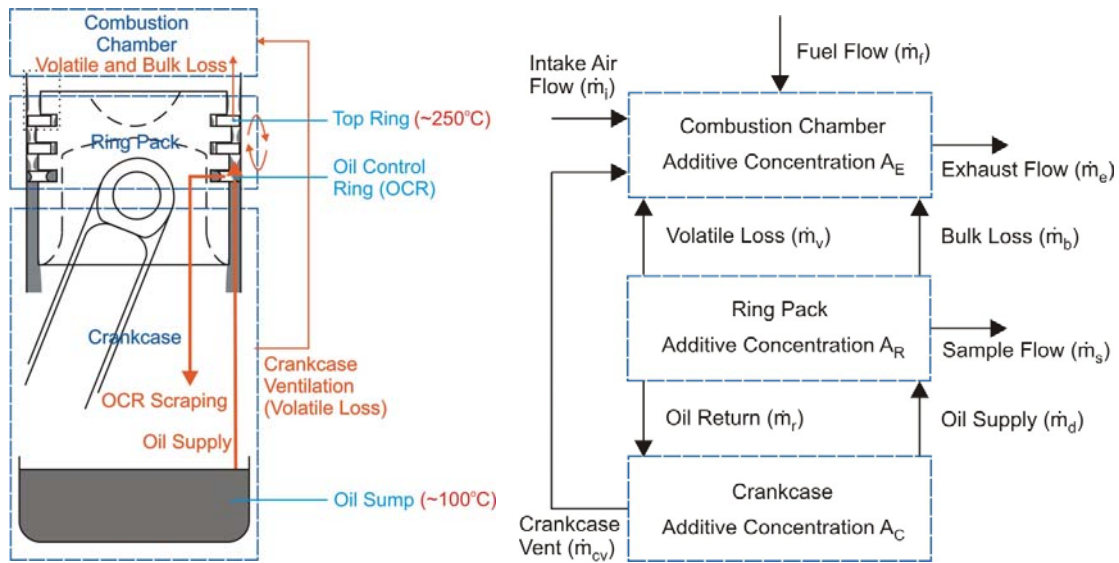


Figure 3.30 – A simple model of the power cylinder system. Left - Lubricant in the engine is separated into three zones. Right – The zones are interconnected by oil flows, many of which model the modes of oil consumption.

The composition of the lubricant in each zone was modeled as a combination of five species:

1. Base Oil (modeled as a collection of 15 sub-species);
2. Calcium;
3. Zinc
4. Phosphorus
5. Oxidation Products

Base oil was modeled as a mixture of 15 hydrocarbon sub-species, each with different molecular masses. Each species and sub-species was modeled by Equation 3.1. Changes in the lubricant composition with time were predicted by simultaneously integrating Equation 3.1 for all species and zones with a fourth order Runge-Kutta numerical scheme.

3.7.3 Base Oil Evaporation Model

Base oil evaporation has a strong effect on lubricant composition, especially in the piston ring pack region. In the current model, oil vaporization is modeled as a mass convection

problem using a similar approach as taken by [96]. Oil vapor at the surface of the liquid oil film is assumed to be carried away by the motion of the cylinder gases.

The oil is modeled as being composed of 15 hydrocarbon sub-species, each with its own thermophysical properties. The rate of oil vaporization from each zone can be computed by calculating the local instantaneous mass flux, integrating with time and then multiplying by the total effective area. The rate of oil consumption from the engine can be found by summing the volatilization from each zone. In a more compact form, the time averaged oil vaporization rate, OC , is found by:

$$OC = \sum_{k=1}^M \left[\frac{A_{eff,k}}{T} \sum_l^{15} \int m_{e,k,l}(t) dt \right] \quad (3.2)$$

Where, the average oil consumption is summed across all the zones and M is the total number of zones in the model. The instantaneous mass flux in a zone, k , for one of the oil sub-species (l) is denoted by $m_{e,k,l}$ and is a function of time, t . The mass flux is multiplied by the effective area of each zone, $A_{eff,k}$, and divided by the time period of interest, T .

3.7.4 Convection Model

A standard model for convective mass transport is used to evaluate the local instantaneous evaporative mass flux [97]:

$$m_{e,k,l}(t) = g_{k,l}(t) \cdot (mf_{s,k,l}(t) - mf_{\infty}) \quad (3.3)$$

Where, $g_{k,l}$ is the mass convection coefficient for a particular base oil sub-species, $mf_{s,k,l}$ is the mass fraction of oil vapor at the zone surface for that sub-species and mf_{∞} is the mass fraction of that species in the bulk gases surrounding the surface. Due to the large quantity of gases that surround surfaces in the engine, mf_{∞} is assumed to be zero. The vapor mass fraction at the oil film surface is computed from the local vapor pressure of the oil species of interest.

3.7.5 Oil Model

The oil is modeled as being composed of 15 pure hydrocarbon species to account for the complex volatility behavior of engine oils. The boiling point and mass fraction (relative to the liquid oil) for each species must be specified. This data can be taken from measured distillation curves for the oils used in this study (see Figure 3.31).

All of the necessary oil vapor properties can be computed after the boiling point and mass fraction for an oil sub-species is specified from the distillation curve (see Appendix B for details on property calculations). The mass fraction of each sub-species can be calculated from:

$$mf_{s,k,l}(t) = \left(\frac{\overline{mf_{\ell,k,l}}(t) \cdot P_{v,k,l}(T_{s,k})}{P_{c,k}(t)} \right) \left(\frac{MW_l}{MW_\infty} \right) \quad (3.4)$$

Where, $\overline{mf_{\ell,k,l}}$ is the *mole fraction* of the oil sub-species in the zone. $P_{v,k,l}(T_{s,k})$ is the vapor pressure of the oil film at the local instantaneous surface temperature in the zone. $P_{c,k}$ is the instantaneous pressure of the bulk cylinder gas, MW_l is the molecular weight of the oil sub-species, and MW_∞ the average molecular weight of the gas in the wall boundary layer. Since the total molar fraction of the oil species in the boundary layer gas is low, MW_∞ is taken to be the molecular weight of air.

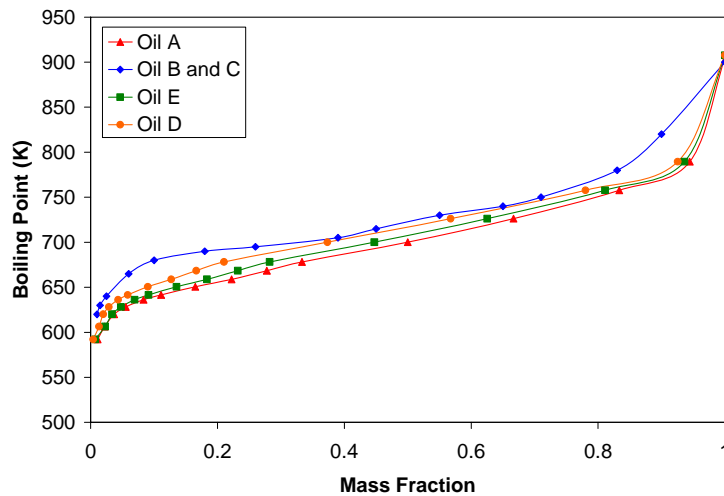


Figure 3.31 – Distillation curves for the oils used in this study.

3.7.6 Estimating the Convective Heat Transfer Coefficient

The mass convection coefficient is computed in this model using an analogy between heat and mass transfer. In such analyses, a heat convection coefficient, h , is computed from a Nusselt-Reynolds-Prandtl correlation [97]:

$$Nu = a \cdot Re^c \cdot Pr^d \quad (3.5)$$

Where,

$$\begin{aligned} Nu &= hL/k - \text{Nusselt number} \\ Re &= VL/\nu - \text{Reynolds number} \\ Pr &= \nu/\alpha - \text{Prandtl number} \\ L &- \text{Characteristic length} \\ V &- \text{Characteristic velocity} \\ k &- \text{Thermal conductivity} \\ \nu &- \text{Kinematic viscosity} \\ \alpha &- \text{Thermal diffusivity} \end{aligned} \quad (3.6)$$

Using the analogy between heat and mass transfer, the corresponding mass transfer relation is:

$$Sh = a \cdot Re^c \cdot Sc^d \quad (3.7)$$

Where,

$$\begin{aligned} Sh &= (gL)/(\rho D_{ah}) - \text{Sherwood number} \\ Re &= VL/\nu - \text{Reynolds number} \\ Sc &= \nu/ D_{ah} - \text{Schmidt number} \\ \rho &- \text{Density} \\ D_{ah} &- \text{Binary diffusion coefficient} \end{aligned} \quad (3.8)$$

For this analogy between heat and mass transfer to remain valid, the rate of oil vaporization must remain low enough for the process to be considered a low mass transfer rate convection process. Also, the temperature of oil film must not exceed the boiling point for any of the oil species for the given cylinder pressure. Boiling is an energy limited process and Equation 3.3 only applies for diffusion limited process.

Many attempts have been reported to determine appropriate values for the constants a , c , and d in Equations 3.5 and 3.7 (documented in [96]). Suggested values are:

$$a = 0.035 \text{ to } 0.13$$

$$c = 0.7 \text{ to } 0.8 \tag{3.9}$$

$$d = 0.667$$

(This page intentionally left blank)

CHAPTER 4 - IN-ENGINE DISTRIBUTION AND TRANSPORT OF ASH-RELATED SPECIES

4.0 INTRODUCTION

Lubricant interactions within the engine must be understood to predict the quantity and composition of ash-related compounds emitted in the exhaust of diesel engines. This information is essential to predict the effect of different lubricant formulations on DPFs and after treatment systems. Up to this point, studies focused on measuring the amount of ash-related elements in engine exhaust or collected in DPFs without examining the lubricant compositional changes in the engine. The preferential emission or retention of metallic elements from the additive package is related to the distribution and transport of ash-related compounds in the engine. In this study, changes in the elemental composition of the lubricant in the power cylinder of an operating diesel engine are measured. The objective is to ascertain how changes in the composition of the lubricant in the engine are related to the mass of ash emitted in the exhaust.

In the most basic sense, ash emissions are a direct result of oil consumption. Oil is consumed from several regions in a diesel engine including the power cylinder, crankcase ventilation system, turbocharger seals and valve guides. These components are all sources for lubricant ash-related compounds in the exhaust. In particular, the lubrication requirements and dynamics of the piston ring-pack result in oil loss through the power cylinder region that makes the major contribution to the total oil consumption in normally operating engines. As a result, the mechanisms for the consumption of various lubricant compounds in this region determine to a large extent the mass of lubricant-derived metallic elements in the exhaust stream.

A simplified representation of the oil flows in the power cylinder is illustrated in Figure 4.1. The majority of the lubricant is contained in the crankcase, where the temperature is typically about 100°C. An extremely small oil volume (of the order of a few tenths of a milliliter) is also contained in the crevices of the ring-pack. The oil in this

region is subjected to the highest temperatures due to its proximity to the combustion chamber. Temperatures exceeding 250°C in the top ring zone (TRZ) degrades the ring-pack oil during engine operation. To lubricate the piston rings and liner, oil is supplied from the crankcase onto the piston liner by splashing or sprays. Excess oil is returned to the crankcase by the oil control ring (OCR). A fraction of the oil supply is transported by various modes past the OCR and into the ring-pack where it mixes with the small volume of degraded oil in the ring grooves and on the face of the piston. Lubricant in the ring-pack is mixed on the piston face by several oil transport mechanisms examined in [6]. A large portion of this flow is returned to the crankcase through the ring grooves and by interaction with blow-by gas.

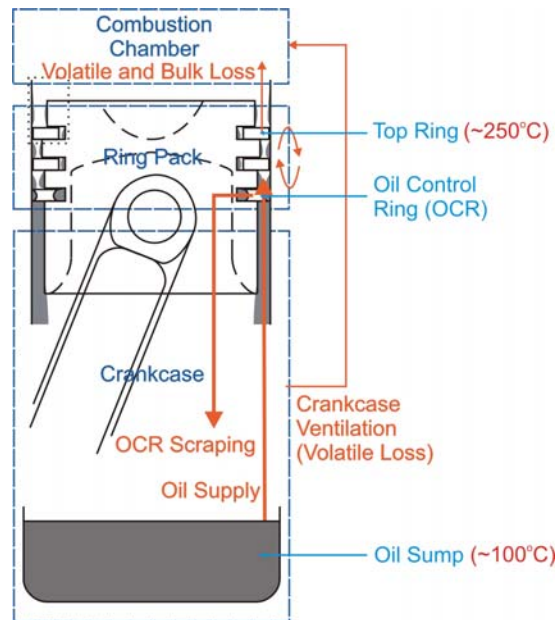


Figure 4.1 – A simplified representation of the oil flows in the power cylinder

This exchange between the crankcase and ring-pack is manifested as a slow degradation of the crankcase oil. Of the oil in the ring pack, only a small quantity is eventually transported to the top ring groove (TRG) of the piston, which is located behind the piston ring and is in the region in closest proximity to the combustion chamber. Oil flowing out of the TRG and onto the piston crown is often regarded as effectively lost by a number of oil consumption modes [6]. The mass of ash-related elements emitted from the power

cylinder and into the exhaust depends on the composition changes of the lubricant as it flows from the crankcase to the TRG.

The oil consumed from the power cylinder due to liquid oil transport is expected to have a similar composition as the lubricant in the TRG. In this study, ring pack sampling is employed to extract oil from the TRG during engine operation. Long duration engine tests are also conducted to examine the change in the crankcase oil composition with time due to volatilization and degradation of the oil in the ring pack. The concentration of ash-related elements in the ring pack samples are measured and related changes in the sump oil composition.

It has been suggested that deposition inside the engine may also be a significant factor affecting the emission of ash-related elements from the engine. In this study, filter debris analysis and the characterization of piston deposits is utilized to investigate if deposits in the engine are significant sinks for additive metals.

While these studies contribute an understanding of composition differences in engines, the accuracy of the measurements is unknown. The extraction technique used during ring pack sampling may alter the composition of samples due to abnormal interactions with blow-by gases, deposition, and changes in ring-pack oil flow. New diagnostics systems are needed that obtain in-situ measurements of lubricant composition with minimal disturbance on the system.

A novel system was developed during this study that takes in-situ measurements of the composition of the lubricant at the piston and liner interface with Fourier Transform Infrared (FTIR) spectroscopy. This system is used to obtain observations of the steady state lubricant composition of the oil at the piston ring zone. Tracer experiments are also performed to determine the residence time of the oil in that region, a parameter influencing ash emissions from the power cylinder.

In the final part of this chapter, the results of the sampling studies are used to develop a framework to model the distribution and transport of ash-related elements in the power cylinder. The resulting model formulation may be used to investigate alternatives to reduce ash emissions from diesel engines.

4.1 EXPERIMENTAL METHODOLOGY

In this study, a sampling system was employed to extract oil samples from the TRG of an operating heavy-duty diesel engine. Tests were conducted with three oils with different viscosities, volatilities and additive package formulations. The samples were analyzed for the concentrations of metallic elements in the additive package. This data was used to analyze the mechanisms for the transport of ash-related elements in the power cylinder.

4.1.1 Ring Pack Sampling Experiments

The ring pack sampling system, described in Section 3.2.1, was used to obtain oil from the TRZ of the piston during engine operation. Sampling systems have been used by several researchers [14, 15, 16] to obtain samples of the lubricant from the ring-pack of operating engines. The sampling system design used in this study was based on the apparatus constructed by [15] to measure base oil oxidation in a single-cylinder gasoline engine.

Oil was extracted from the engine via a small (1 mm diameter) hole drilled into the TRG of the piston. The sampling hole was situated on the anti-thrust face of the piston and was centered axially in the groove such that it was covered by the top ring at all times. The channel drilled into the piston was terminated on the piston under-crown by a fitting that incorporated a 0.5 mm restriction. Finally, a length of Teflon tubing connected the orifice to a sample collection point mounted outside the crankcase. Blow-by gases were vented before oil samples were collected in cooled glass sampling containers.

Liquid oil samples were obtained almost continuously during the experiments at sampling rates between 8 to 20 mg/min. During every engine cycle a small amount of oil was blown by the high pressure combustion gases into the sampling hole, through the tubing and then eventually into the sample collection vial. A minute fraction of the oil from inside the TRG was entrained as a mist and transported by the gas flow. In fact, the majority of the flow through the sampling tube was comprised of blow-by gases from the combustion chamber. The 0.5mm restriction limited the sampling rate, thereby minimizing the effect sampling had on the oil flows and residence times in the ring-pack. The interaction of the oil sample with blow-by gas during extraction is expected to have only a small effect on the sample composition. Oil in the ring-pack is normally subjected to high gas flow rates during engine operation.

Although the sampling system was subjected to high temperatures and forces during operation it remained functional for time periods exceeding 30 hours. The lifetime of the system was reduced by wear of the sampling tube, and blockage of the sampling hole or orifice. The limiting factor was often the formation of deposits in the system. Blockage resulted in a substantial reduction of the sampling rate or drastic changes in the composition of the TRG samples.

Sampling experiments were performed with three lubricants; oils A, B and C. Three 26 hour sampling experiments were conducted with each lubricant resulting in a total of 9 experiments. The engine ran continuously over the duration of each experiment at 100% of the rated full power and at 1800 rpm. Run duration was limited to 26 hours to reduce the effect of deposition in the sampling system. The sampling system was cleaned and the crankcase lubricant was changed with fresh oil using a double flush procedure before every experiment.

Crankcase oil samples were taken at the beginning and the end of each experiment. Total oil consumption over the 26 hour period was also measured. The crankcase oil supply was sufficient to last the span of each experiment, so no top-up oil was added.

Oil was continuously collected through the sampling system over each 26 hour period. However, only the TRG oil sampled between 7 and 19 hours was included in the analysis. The engine took 7 hours to stabilize, therefore, the lubricant collected in the first 7 hours was not considered representative of the actual steady state condition in the TRG. Oil samples extracted from the TRG after 19 hours were not included in the analysis to reduce the effect of sampling system deposition on the results. In the time period between 7 and 19 hours, four discrete TRZ samples were taken at 4 hour intervals. Lubricant was collected in individual sample vials over a 1 hour time period. The composition of each sample represented the average composition in the TRG over a 1 hr time period.

4.1.2 Long Duration Sampling Experiments

Long duration experiments were also conducted on the Lister Petter TR-1 to observe the changes in sump oil composition over time. Five 285 hour tests were performed, each with a different lubricant. The lengths of the tests corresponded with the oil drain interval of the engine. Oils A, B, C, D and E were used in these experiments. Samples were extracted at regular intervals throughout the tests and analyzed to measure changes in elemental composition.

Table 4.1 – Long Duration Engine Test Parameters

Engine	Lister Petter TR-1
Duration	285 hours
Engine Load	100% Full Power
Engine Speed	1800 rpm
Fuel	15 ppm Ultra Low Sulfur Diesel
Sump Temperature	100°C ($\pm 5^\circ\text{C}$)
Oil Filter	Standard Oil Filter

The test conditions used in the long duration engine tests are listed in Table 4.1. The engine ran at 100% full power and at a steady speed of 1800 rpm throughout all of the tests. An oil sump temperature of approximately 100°C was maintained over the duration of the tests. These test conditions induced the maximum rate of degradation in the crankcase lubricant.

Oil consumption was measured every 24 hours using the apparatus described in Section 3.2.2.1. The sump oil was topped up with fresh lubricant after each measurement. The rate of oil consumption varied significantly across all of the oils used in these experiments. Routine maintenance was also performed every 24 hours.

At the end of each test the oil filter was recovered and sent for filter debris analysis using the procedure described in Section 3.5. The objective of this work was to determine if the filter was a significant sink for ash-related elements inside the engine.

Samples of the sump oil (with a mass of approximately 17 grams) were extracted every 48 hours using the procedure recommended in the ASTM standards [84, 85]. The objective of these experiments was to determine how the elemental composition of the sump oil changed across an oil drain interval and relate these changes to quantity of the ash emitted by the engine.

4.1.3 Valve Train Sampling

Oil samples were also extracted from the valve train in a separate set of experiments to determine if the composition of the oil in that region was different than the sump oil. Samples were collected from the valve train of a Cummins ISB engine, using the procedure described in Section 3.2.3.

Prior to sampling from the engine, it was operated under a steady load and speed for over one hour to allow the system to stabilize. Six oil samples were extracted from the valve train and another six samples were taken from the sump.

The samples were analyzed to determine elemental and chemical composition. This data was used to make a comparison between the valve train and sump oil to determine if there were any significant differences. Elemental composition was determined by ICP spectroscopy (ASTM D5185) [85]. The valve train and sump oil samples were compared on the basis of calcium, aluminum, boron, iron, magnesium, phosphorus and zinc

concentrations. Chemical composition was determined with FTIR spectroscopy. The heights of several prominent peaks in the spectrum were used as the basis of comparison. These features in the spectrum are labeled in Figure 4.2.

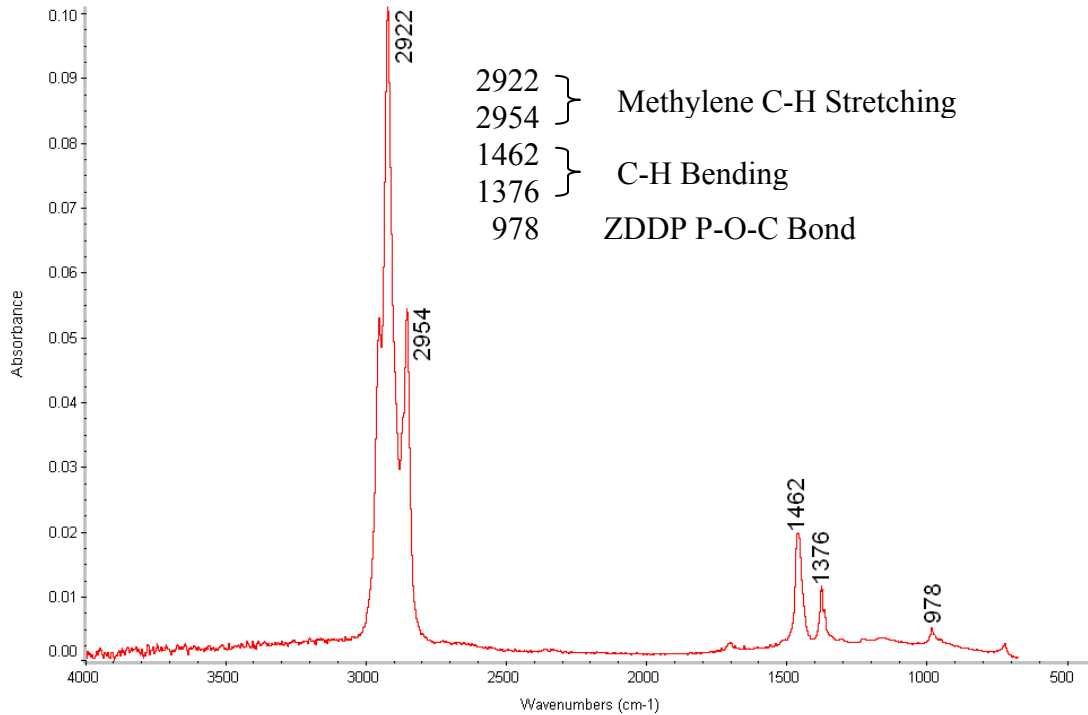


Figure 4.2 – The peaks used to compare the chemical composition of the valve train and sump oil.

4.1.4 In-Situ FTIR Measurements

In-situ measurements of the lubricant composition at the piston and liner interface were also obtained with the in-situ FTIR system described in Section 3.4. These measurements were used to determine the residence time for the oil in the ring pack, a critical parameter influencing the emissions of ash-related elements from engines.

The composition of the oil at the piston and liner interface was measured in two experiments. The test parameters are listed in Table 4.2. In the first experiment, the steady state composition of the lubricant was measured with the ATR probe. In the second experiment, a tracer (biodiesel) was added to the sump oil to facilitate a

measurement of the residence time at the probe location. In both experiments, the ATR system was initiated before starting the engine (as indicated in Table 4.2). The ATR system continued scanning for an extended period of time after engine shutdown.

Table 4.2 – FTIR Experimental Parameters

Experiment	1	2
Sump Oil	Oil F	Oil F + Biodiesel (B-100)
Run Time	282 seconds	169 seconds
Engine Startup Time	18 seconds	29 seconds
Engine Shutdown Time	300 seconds	198 seconds

The steady state composition of the lubricant at the piston and liner interface was observed in the first experiment. These measurements were compared to the FTIR spectrum of the sump oil. The purpose of this test was to determine if the ATR system could resolve differences between the liner and crankcase lubricant composition. The oxidation resistance of the zero-detergent oil (oil F) was also evaluated in the first experiment.

A biodiesel (B-100) tracer was mixed with the sump oil before commencing the second experiment. An estimation of the residence time for the oil around the probe was determined by tracking the emergence of a peak in the spectral time series consistent with the ester functional group found in biodiesel molecules. Biodiesel was selected as a tracer because it has a high volatility, is soluble in oil and is easily recognized in FTIR spectra. The ester peak at approximately 1750 cm^{-1} in an FTIR spectrum is a clear indication of the presence of biodiesel in a lubricant sample (see Figure 4.3).

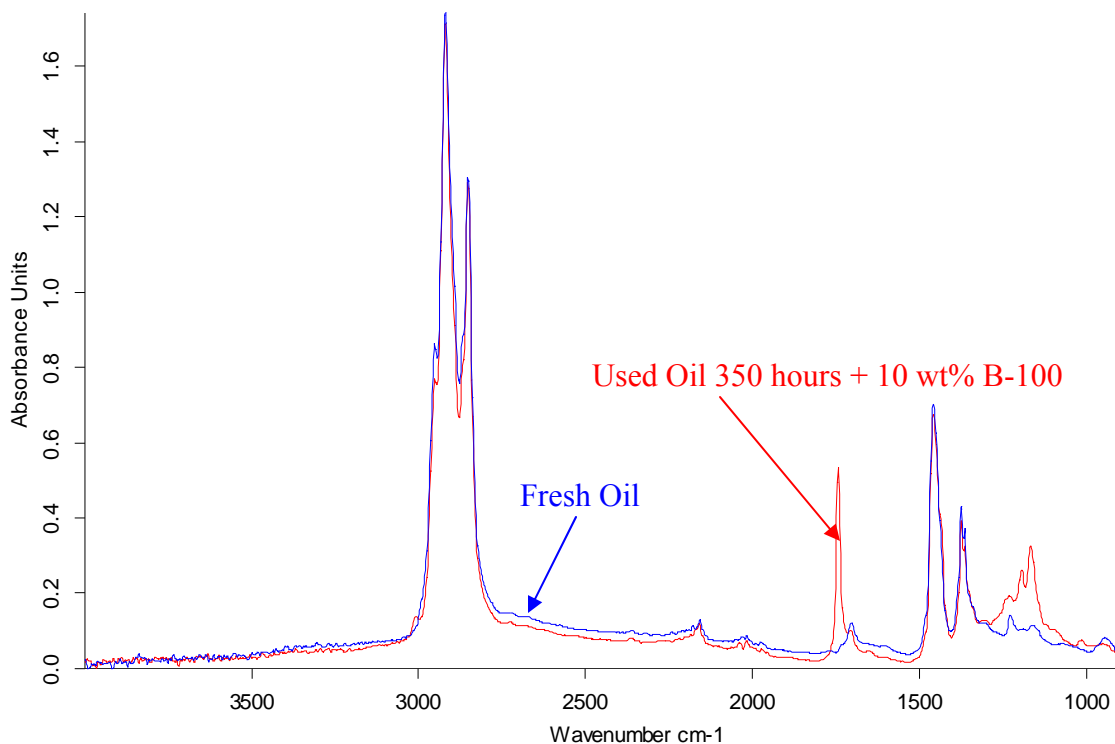


Figure 4.3 – Two FTIR spectra of engine oil measured with ATR spectroscopy. The blue spectrum is a fresh oil sample. The red spectrum is used oil aged for 350 hours with 10 wt% biodiesel. The presence of biodiesel is clearly indicated by the ester peak at approximately 1750 cm⁻¹.

4.1.5 Lubricant and Fuel Properties

Three different lubricants were used in the ring pack sampling experiments; identified in this paper as oils A, B and C. The relevant lubricant properties are listed in Table 4.3. The viscosity grade, volatility and additive package formulation were varied. Oil A was a multi-grade mineral base oil, and oils B and C were single-grade synthetic lubricants. Base stock volatility decreases from oil A to B to C as indicated by the mass loss measured with Thermo-Gravimetric Analysis (TGA) up to 300°C. The additive packages in the lubricants were also varied. The concentrations of the metallic elements in the fresh oil as measured with ICP are shown in Table 4.4. Oil A has calcium and magnesium based detergents, whereas oils B and C contain calcium, but not magnesium. Oils B and C have identical detergent and anti-wear additive formulations.

Table 4.3 – Properties of Lubricants Used in the Ring Pack Sampling Experiments

Property	Oil A	Oil B	Oil C
SAE Viscosity Grade	15W40	30W	40W
Sulfated Ash (%) [ASTM D874]	1.41	1.0	1.0
Viscosity @100°C (cSt)	15.1	10.9	14.4
Total Base Number (mgKOH/g)	12.2	7.3	7.3
Relative TGA 300°C Mass Loss	Highest	Intermediate	Lowest

Table 4.4 Fresh Oil Concentrations of Metallic Elements in the Lubricants Used in Ring Pack Sampling Experiments (ASTM D5185)

Element (ppm)	Oil A	Oil B	Oil C
Calcium	2644	2397	2442
Magnesium	310	--	--
Zinc	1494	1103	1137
Phosphorus	1201	929	940

Oils A, B, C, D and E were used in the long duration engine tests. The specifications for these lubricants are listed in Table 3.7. These oils were selected to represent a range of sulfated ash levels, volatilities and additive package formulations. The oil consumption rate also varied between all the lubricants.

Table 4.5 lists sulfated ash level and average oil consumption rate for all of the oils used in this study. Oil consumption modifies the elemental composition of the crankcase oil during engine operation. Oil consumption is highest for the most volatile lubricants. It is emphasized that a significant amount of evaporative oil consumption is expected in these experiments. High oil consumption rates result from the air cooled engine design and from the evaporation of light-end hydrocarbons in the fresh oil at the beginning of every experiment.

The fuel used in this study was low-sulfur diesel with a sulfur concentration of less than 15 ppm. The fuel was tested with ICP to ensure that the concentrations of all metal contaminants were less than 1 ppm.

Table 4.5 – The Sulfated Ash and Oil Consumption for the Lubricants Used in the Long Duration Engine Tests

Oil	A	B	C	D	E
Sulfated Ash (%) [D874]	1.41	1.0	1.0	1.35	1.0
Average Oil Consumption (g/hour)	6.1	5.5	3.5	3.55	5.1

4.1.6 Oil Sample Analysis

All oil samples collected during these experiments were analyzed by an independent laboratory for the concentrations of metallic elements with Inductively Coupled Plasma (ICP) Spectroscopy (ASTM D5185) [85]. Due to the limited sample size, all of the ring pack oil samples (approximately 1 gram per sample) were diluted three times (by mass) with a pure kerosene mixture prior to analysis. The maximum error associated with ICP measurements is considered to be $\pm 6\%$.

4.2 RESULTS

4.2.1 Ring Pack Oil Samples

Figure 4.4 shows a typical data set generated from a ring pack sampling experiment (with oil A). Large differences in the concentrations of corresponding additive metals are observed between the crankcase and the oil in the TRG. Substantially higher concentrations of additive elements are seen in the TRG samples. Oil samples extracted from the TRG are also noticeably thicker and darker than the crankcase oil, which indicates that the oil has been oxidized, has lost lighter hydrocarbon species from the base oil and has been heavily contaminated with soot. The concentrations of additive metals in the crankcase lubricant change during each experiment. The Metals associated with the detergent (i.e. calcium and magnesium) increased in concentration during all of the tests. However, the concentrations of the metals associated with the anti-wear

additives (i.e. zinc and phosphorous) remain essentially constant, or are only slightly reduced.

The effect of deposits in the sampling system was noticeable in several experiments where it was manifested as a gradual decrease of the concentrations of metals in the TRG samples. These changes in concentration became more pronounced when experiments were extended beyond 25 hours. A precipitous drop in metal concentration was sometimes observed for longer duration tests.

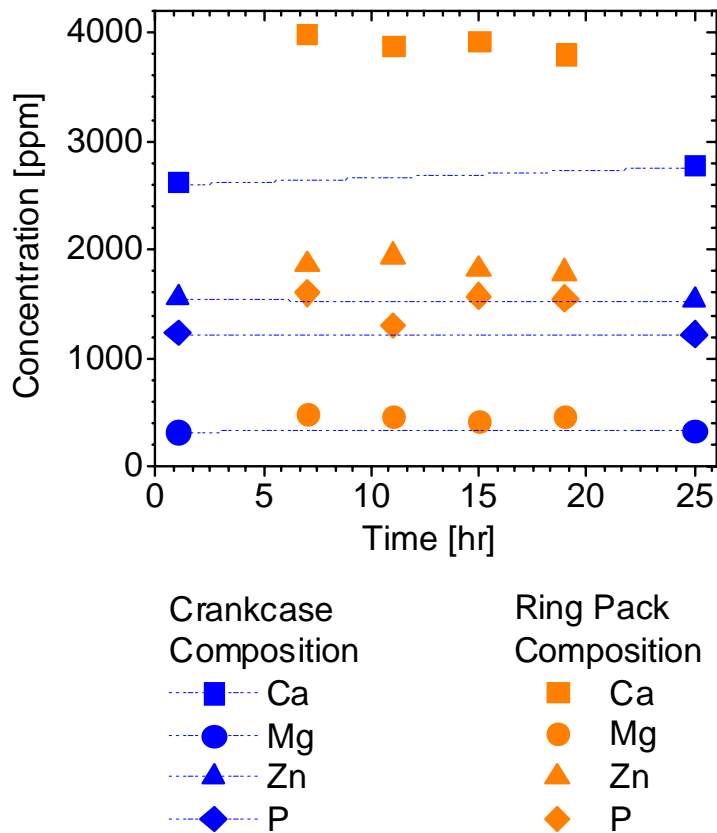


Figure 4.4 – Results from a typical ring pack sampling experiment with oil A.

These decreases in elemental concentrations may be related to the formation of deposits in the sampling system, causing partial blockage of the sampling tube. Sample composition could be modified due to filtration and absorption of additive compounds and degradation products by debris accumulated on the inner surfaces of the sampling

tube. As a result, the ring-pack sampling system cannot be used to collect representative samples from the TRG beyond 25 hours for this engine’s design and operating conditions. Accordingly, the sampling duration was limited to 19 hours and the sampling system was cleaned after each test to ensure that the impact of blockage on sample composition was minimized.

4.2.2 Top Ring Groove Enrichment

Ash-related elements were concentrated in the TRG samples relative to the composition of the crankcase lubricant. The increase in concentration may be expressed in dimensionless form as an enrichment factor. This parameter is defined as the concentration of an individual element in a TRG sample divided by the corresponding concentration in the crankcase oil when the sample is taken:

$$\text{Enrichment Factor}_i = \frac{\text{Concentration}_i \text{ in TRG Sample}}{\text{Concentration}_i \text{ in Sump}} \quad (4.1)$$

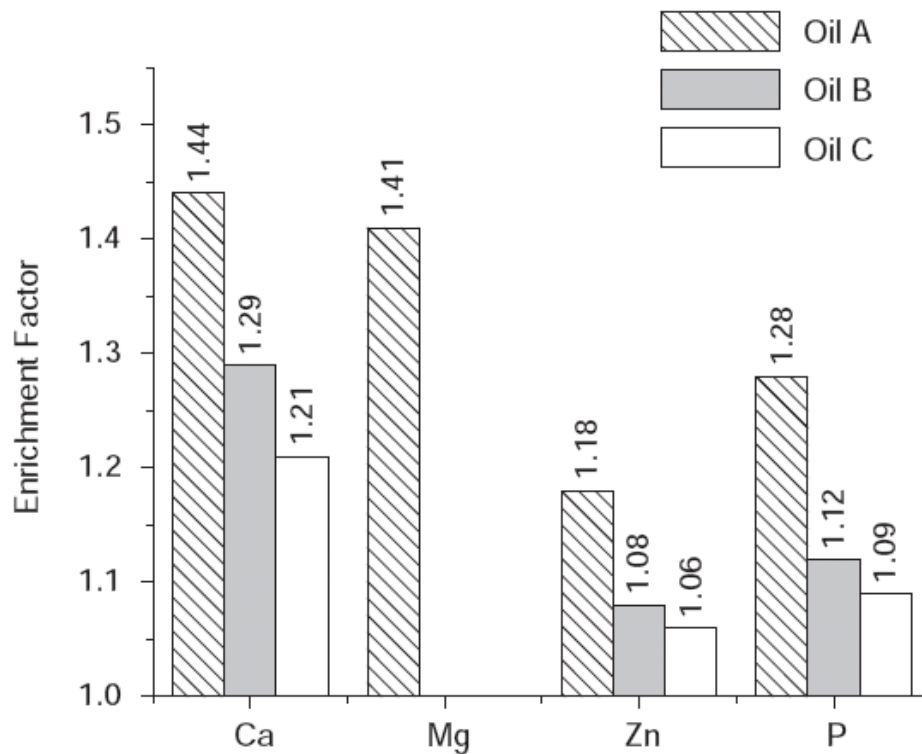


Figure 4.5 - The average enrichment factors of metallic element in TRG samples.

The enrichment factors for each element are shown graphically in Figure 4.5 with the variation in the results indicated by error bars representing the 95% confidence interval. Table 4.6 lists the average enrichment factors for the TRG samples. The results indicate that base oil volatility strongly affects the enrichment of additive metals in the TRG oil. Calcium is enriched to the highest degree for oil A, which has the highest volatility. The enrichment of calcium is reduced for the lower volatility oils. A marked difference in the enrichment of phosphorus and zinc is also seen between oil A and the synthetic oils (B and C).

Table 4.6 – TRG Sample Analysis Results

Element	Average Enrichment Factor		
	Oil A	Oil B	Oil C
Calcium	1.41	1.31	1.19
Magnesium	1.39	--	--
Zinc	1.20	1.06	1.03
Phosphorus	1.30	1.12	1.13

Figure 4.5 also shows that the degree of enrichment is different for each element. Calcium and magnesium are concentrated to the highest degree in the TRG samples. These elements are associated with detergent additives in the lubricant. The lowest enrichment factors are found for zinc and phosphorous, which are associated with ZDDP in the oil.

4.2.3 Crankcase Oil Analysis

The concentrations of metallic elements in the sump oil were measured at regular intervals during the long duration engine tests. The measured concentrations of calcium, zinc and phosphorus in the crankcase oil for the experiments with oils D and E are graphed in Figure 4.6. Different trends were exhibited in the elemental concentration data for each element.

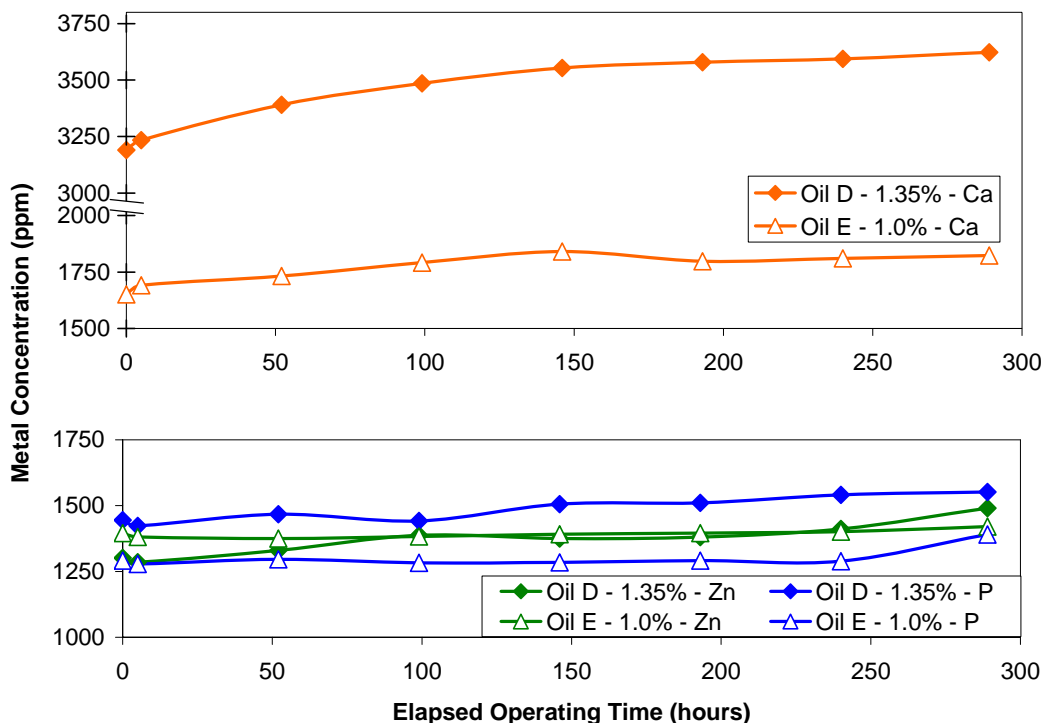


Figure 4.6 – The measured concentrations of calcium, zinc and phosphorus in the crankcase oil during the long duration engine tests. Results for oils D and E are shown.

The concentration of calcium in the sump oil samples increased slowly over the duration of the tests. This effect occurred due to the preferential volatilization of base oil hydrocarbons throughout the experiment. The calcium tended to remain in the lubricant because it was bound to over-based detergents, which are often considered to be involatile due to their high molecular mass and polar nature. Calcium also appeared to accumulate more readily in the lubricants with more volatile base oils. This effect can be seen by comparing the results for oils D and E in Figure 4.6. Oil D exhibited higher mass loss than oil E in TGA up to 300°C. The concentration of calcium also increased more rapidly in the beginning of the tests than the end. This effect was most likely caused by the volatilization and eventual depletion of lighter-end constituents in the fresh base oil at the beginning of the test.

A different behavior was observed for zinc and phosphorus, the elements associated with ZDDP. The concentration of these elements in the sump oil appeared to remain relatively

constant throughout the long duration tests. Only a slight increase in zinc and phosphorus concentrations was observed during the tests. In addition, the atomic ratio of zinc to phosphorus atoms in the used oil samples remained almost constant. If deposition is neglected, these results indicate that zinc and phosphorus must have volatilized from the lubricant during the tests. This condition is possible, since ZDDP is known to be much more volatile than detergent compounds [98].

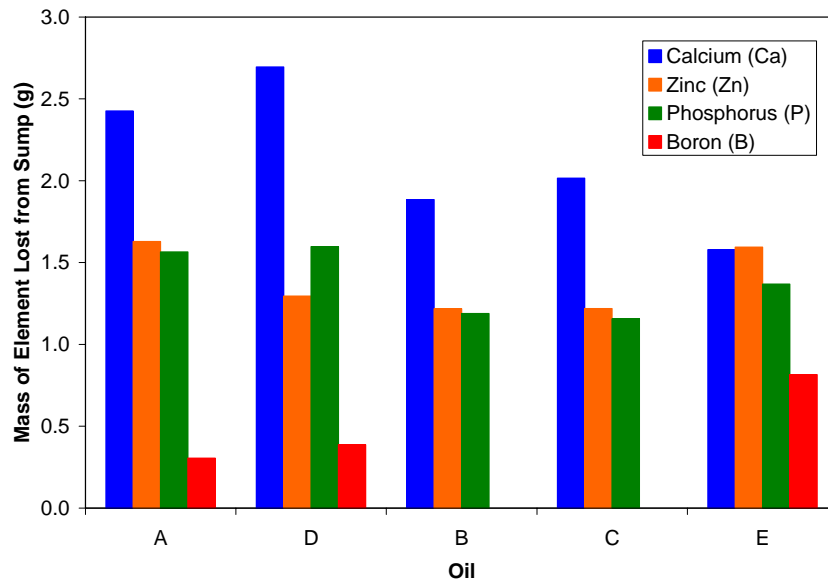


Figure 4.7 – The total mass lost for elements in the in the crankcase oil.

Figure 4.7 compares the mass loss of elements associated with lubricant-derived ash from the sump oil during the long duration tests. The mass of each element lost from the system was not in proportion to its concentration in the fresh oil. For oils A, B, C and D, the concentration of calcium in fresh lubricant is over twice the concentration of zinc and phosphorus (see Table 3.7). However, the mass of zinc and phosphorus lost from the crankcase oil is consistency greater than half the mass of calcium lost. This result implies that the elements associated with ZDDP are preferentially consumed from the crankcase oil during the tests.

4.2.4 Comparison of Actual and Expected Loss from the Crankcase

Figure 4.8 compares the measured mass loss from the crankcase oil of metallic additive elements (found in DPF ash) with the expected loss. The expected mass loss is defined by multiplying the total oil consumption with the fresh lubricant composition. This comparison shows if an element associated with lubricant-derived ash is preferentially depleted from, or retained in the crankcase oil. The actual mass loss equals the expected mass loss along the $x=y$ line. Data points above this line indicate that an element is preferentially consumed during an experiment. On the other hand, a point below the $x=y$ line shows that the element is preferentially retained in the crankcase oil. Boron is included in this comparison because although it is not found in ash collected from DPFs, it is a significant contributor to sulfated ash.

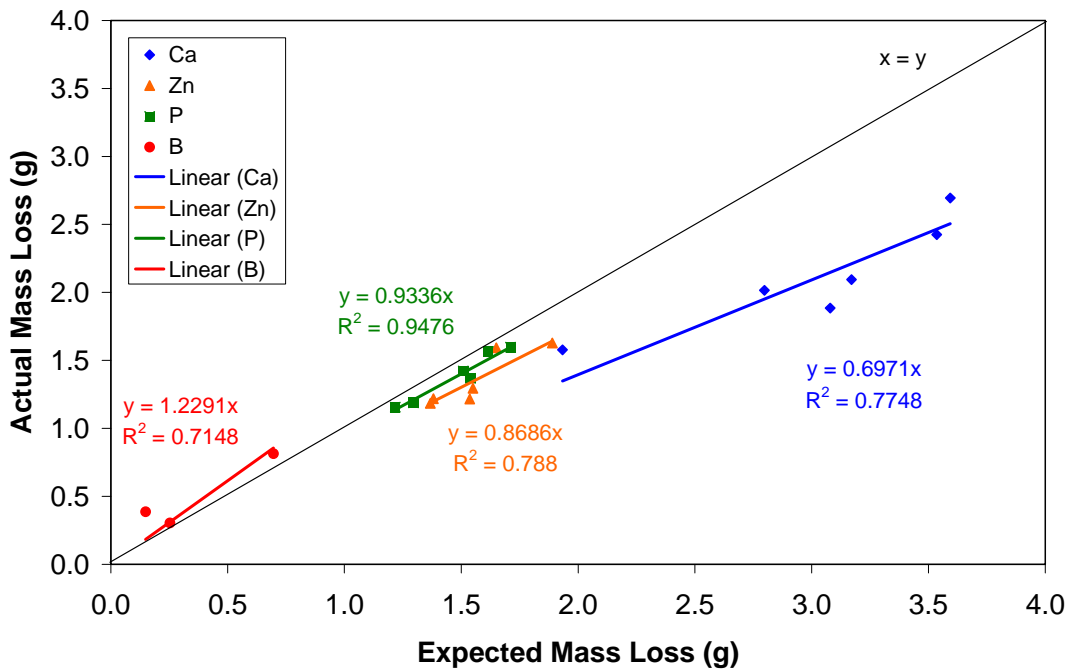


Figure 4.8 - A comparison of the actual and expected mass loss of ash-related elements from the crankcase oil.

Clear differences in the consumption characteristics of the detergent and the ZDDP elements were seen in the results. Although all of the detergent and ZDDP elements were

preferentially retained in the sump oil, Phosphorous and zinc were lost more readily than the calcium (as indicated by the proximity of data points to the $x=y$ line). These results are consistent with previous studies of diesel engine exhaust gas composition [4, 6]. The mass of calcium collected in typical engine exhaust is lower than expected. However, phosphorus and zinc are recovered in the exhaust at higher rates than calcium.

Linear curve fits are included in Figure 4.8. The equations approximate the data to a reasonable degree of accuracy even though the oils have different properties and additive package formulations. The y-intercepts in the equations were specified to pass through the origin, as it is assumed for this analysis that the only mode for elemental mass loss from the system is oil consumption, although this is not necessarily the case. The slope of the equation gives an estimation of the elemental emission rate. Table 4.7 lists the emission rates for all of the elements measured in this study. For instance, the data indicates that only about 70 percent of the calcium you would expect to be emitted, based on the oil consumption and fresh oil composition, is released into the exhaust. Much higher emission rates are observed for zinc and phosphorus. Boron is preferentially consumed from the lubricant, although it has never been found in DPF ash [4, 6].

Table 4.7 – Emission Rates for Elements Associated with DPF Ash

Element	Elemental Emission Rate
Calcium	0.697
Zinc	0.869
Phosphorus	0.994
Boron [†]	1.229

[†]Boron has never been found in DPF ash, although it contributes to sulfated ash

One possible explanation for the higher consumption rate of zinc and phosphorus from the crankcase oil is the higher volatility of ZDDP. In addition, at high temperatures ZDDP can thermally decompose into more volatile by-products that are even more likely to be depleted from the lubricant. Thermal decomposition of ZDDP has been observed by several researchers in the piston ring pack of diesel engines [14, 16].

4.2.5 Valve Train Oil Samples

A statistical analysis was used to determine if the composition of the lubricant in the valve train was significantly different than the sump oil. The mean valve train oil and sump oil composition was determined by averaging the ICP and FTIR analysis results for the six samples taken from each location. The standard deviations of each sample set were also determined. The analysis results (ICP and FTIR) and statistical analysis are summarized in Appendix C.

The ICP results were used to determine if there were any significant differences in elemental composition of the valve train and sump oil. A student t-Test was utilized to determine if variations in the valve train and sump oil sample compositions were statistically significant to a 95% confidence level (2-tail). The difference in the sample means ($\mu_v - \mu_s$) was assumed to have a normal distribution. For the student t-Test, the null hypothesis (H_o) was:

$$H_o: \text{The mean compositions of the valve train and sump oil samples are equal (i.e. } \mu_v - \mu_s = 0) \quad (4.1)$$

The difference in the mean elemental concentrations in the valve train and sump ($\mu_v - \mu_s$) are graphed in Figure 4.9. The largest differences in composition are observed in the concentrations of calcium, phosphorus and zinc. The concentrations of wear metals are almost identical in the valve train and sump.

In order to determine if these differences are statistically significant, they must be compared to the standard deviation of the samples via the student t-Test. The results of the t-Test are graphed in Figure 4.10. The t-Test significance for all of the elements tracked in these study was greater than 0.05. This result implies that the average concentrations of all the measured elements in the valve train and sump oil should be considered as equal to a confidence limit of 95% (19 times out of 20). There were no significant differences in the elemental composition of the valve train and crankcase lubricant.

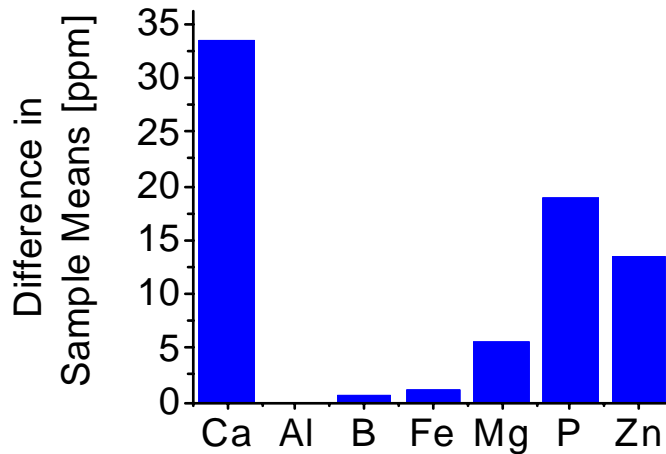


Figure 4.9 – The differences in the sample means ($\mu_v - \mu_s$) of elemental concentrations measured in the valve train and sump oil samples.

It should be noted, however, that the t-Test significance for phosphorus was close to the threshold. This result indicates that there may be a difference in the phosphorus concentration between the valve train and sump. This difference may occur due to the formation of antiwear films in the valve train, which are rich in phosphorus.

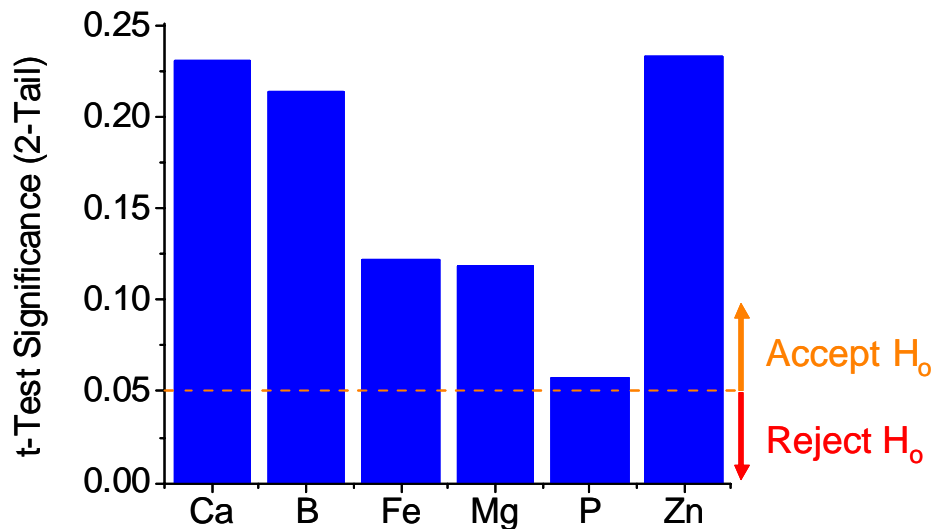


Figure 4.10 – Results of the student t-Test, comparing the valve train and sump oil elemental composition. A t-Test significance greater than 0.05 implies that the null hypothesis (H_0) can be accepted to a confidence level of 95%.

The FTIR results were also analyzed to determine if there were any significant differences in chemical composition of the valve train and sump oil. A similar procedure as above was used to compare the chemical composition of the valve train and sump oil samples. The differences in the mean chemical composition of the valve train and sump oil ($\mu_v - \mu_s$) are graphed in Figure 4.11. The largest difference in the measured chemical composition occurs at 1462 cm^{-1} in the FTIR spectrum.

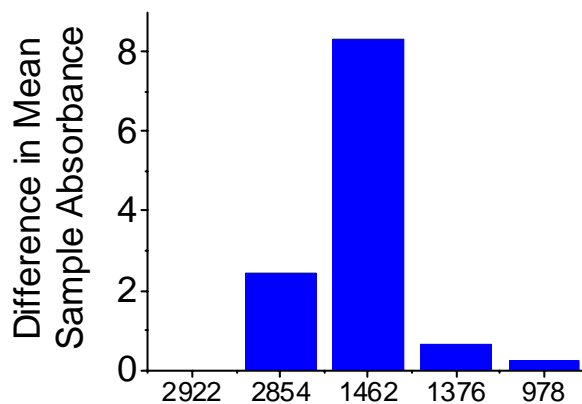


Figure 4.11 – The differences in the sample means ($\mu_v - \mu_s$) of FTIR absorbance (at specific wavenumbers) measured in the valve train and sump oil samples.

The results of a t-Test on the absorbance data is graphed in Figure 4.12. The t-Test significance for all of the elements tracked in these study was greater than 0.05. This result implies that the average chemical composition of the valve train and sump oil should be considered as equal to a confidence limit of 95% (19 times out of 20). There were no significant differences in the chemical composition of the valve train and crankcase lubricant.

The results of these experiments show that there are no measureable differences in the elemental and chemical composition of the valve train and sump oil. This conclusion indicates that the lubricant in the valve train and sump are well mixed by the high oil flow rate through the valve train/crank oil loop (see Figure 3.2).

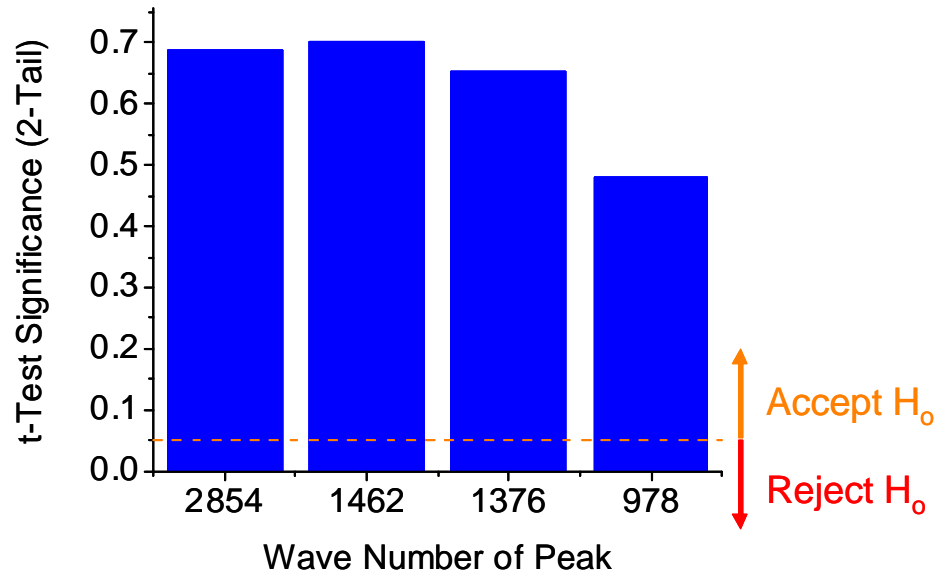


Figure 4.12 – Results of the student t-Test, comparing the valve train and sump oil chemical composition. A t-Test significance greater than 0.05 implies that the null hypothesis (H_0) can be accepted to a confidence level of 95%.

4.2.6 Filter Debris Analysis

Deposition of additive metals in the oil filter has been suggested as a possible explanation for why less ash is emitted from engines than expected based on the oil consumption rate and fresh oil composition. An analysis of the material in the oil filter was performed to determine if the filter is a significant sink for the metals that contribute to ash found in DPFs.

Three oil filters from the long duration engine tests were subjected to the filter debris analysis procedure. The debris was collected on micro-patches, weighed and analyzed for elemental composition with XRF. The average mass of debris collected from filters was 3.27 mg. About 85 percent of the mass was composed of metallic elements. The remaining 15 percent was composed of organic matter (i.e. carbon, sulfur and oxygen, etc).

The results of the XRF analysis for one filter are shown in Figure 4.13. Most of the material in the filter was wear debris. Iron was the element in highest abundance. Copper, from the bearing surfaces, was also found in the filter. Some trace elements from the additive package were also recovered, including calcium, zinc and phosphorus.

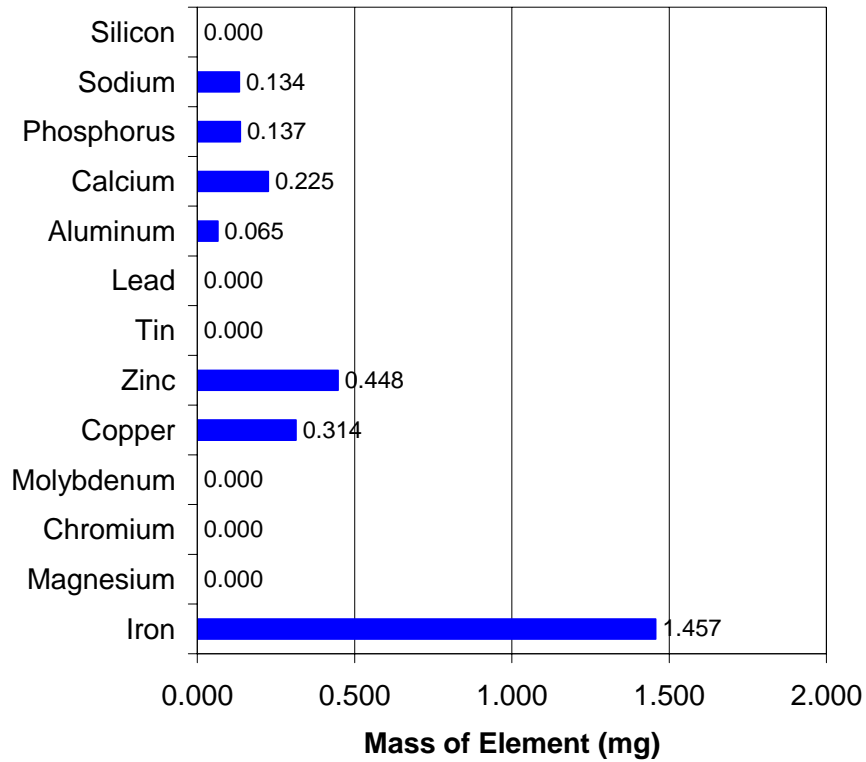


Figure 4.13 – The mass of individual elements in the debris trapped by a standard full-flow oil filter. The filter was used for 285 hours.

Table 4.8 compares the mass of elements found inside the oil filter with the amount in the crankcase oil at the end of a long duration engine test. For the elements that contribute to DPF ash, there is at least 10,000 times more material in the crankcase oil than trapped in the filter. Clearly, the oil filter is not a significant sink for ash-related elements in the engine system.

Table 4.8 – Comparison of the Mass of Elements in the Oil Filter and the Sump Oil[†]

Element	Mass in Filter (mg)	Mass in Sump (mg)	Element	Mass in Filter (mg)	Mass in Sump (mg)
Silicon	0	14	Tin	0	8
Sodium	0.134	0	Zinc	0.448	2700
Phosphorus	0.137	2800	Copper	0.314	255
Calcium	0.225	6600	Molybdenum	0	0
Aluminum	0.065	0	Chromium	0	7
Lead	0	6	Magnesium	0	18
--	--	--	Iron	1.457	219

[†]Note: Ash-related elements are lightly shaded

4.2.7 Characterization of In-Engine Deposits

The Deposits in the engine were also characterized to determine if they were a significant sink for ash-related elements. An analysis of piston deposits with XRF showed that the majority of the material was carbon, with a small amount of calcium, zinc and phosphorus. The mass of metallic elements in the deposit was insignificant compared to the total mass of ash-related elements in the crankcase oil. Piston deposits are unlikely to be a significant sink for additive metals in the engine system.

The deposits on the inside of the exhaust system were collected and characterized by [99] in a comprehensive study. These researchers found that only 1-2 percent of ash-related elements were captured by the exhaust system. Deposits are not a significant sink for ash-related elements in the engine system.

4.2.8 In-Situ Measurements at the Piston and Liner Interface

4.2.8.1 Ring Pack Oil Composition

Measurements of the ring pack oil composition under steady load operation were obtained with the in-situ ATR system. Multiple FTIR spectra were captured from the oil at the piston and liner interface. In-situ spectra of the lubricant in the piston ring zone and

in the sump are superimposed for comparison in Figure 4.14. The fingerprint region is shown between the wavenumbers 1850 to 1000 cm^{-1} .

The data showed significant differences in the composition of the lubricant in the piston ring zone and crankcase. A much higher concentration of carbonyl, a by-product of oxidation reactions, was found at the piston and liner interface. This result was expected due to the higher temperatures in that region of the engine. The lubricant in the piston ring zone was also found to be more contaminated with acidic compounds containing nitrates and sulfates. The sources of these contaminants were combustion and blow-by gases, which mix with the lubricant in the piston ring zone.

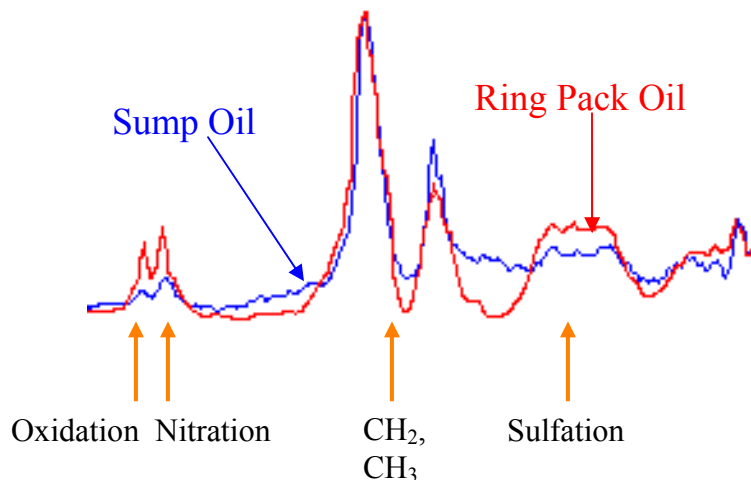


Figure 4.14 – In-situ FTIR spectra of the oil in the piston ring zone and sump. The fingerprint region between 1850 and 1000 cm^{-1} is shown.

4.2.8.2 Residence time

Experiments with a tracer compound were also performed to estimate the residence time of the oil in the piston ring zone. The concentration of the tracer (biodiesel), which was added initially to the crankcase oil, was measured as it mixed with the small quantity of lubricant in the piston ring zone (see Figure 4.15).

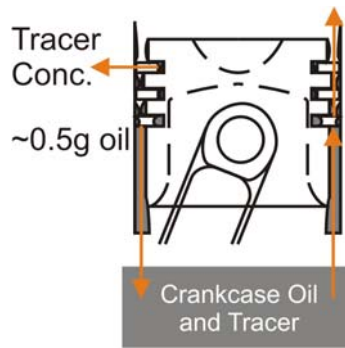


Figure 4.15 – The concentration of biodiesel was measured in-situ as it mixed with the oil in the piston ring zone.

The surface created by the FTIR spectra measured during the tracer experiment is shown in Figure 4.16. A new absorbance peak emerged in the spectra at 1760 cm^{-1} after engine startup. This peak indicated the presence of biodiesel (ester) in the oil at the piston ring zone. The concentration of biodiesel grew slowly over about 120 seconds, and then remained steady for the remainder of the experiment.

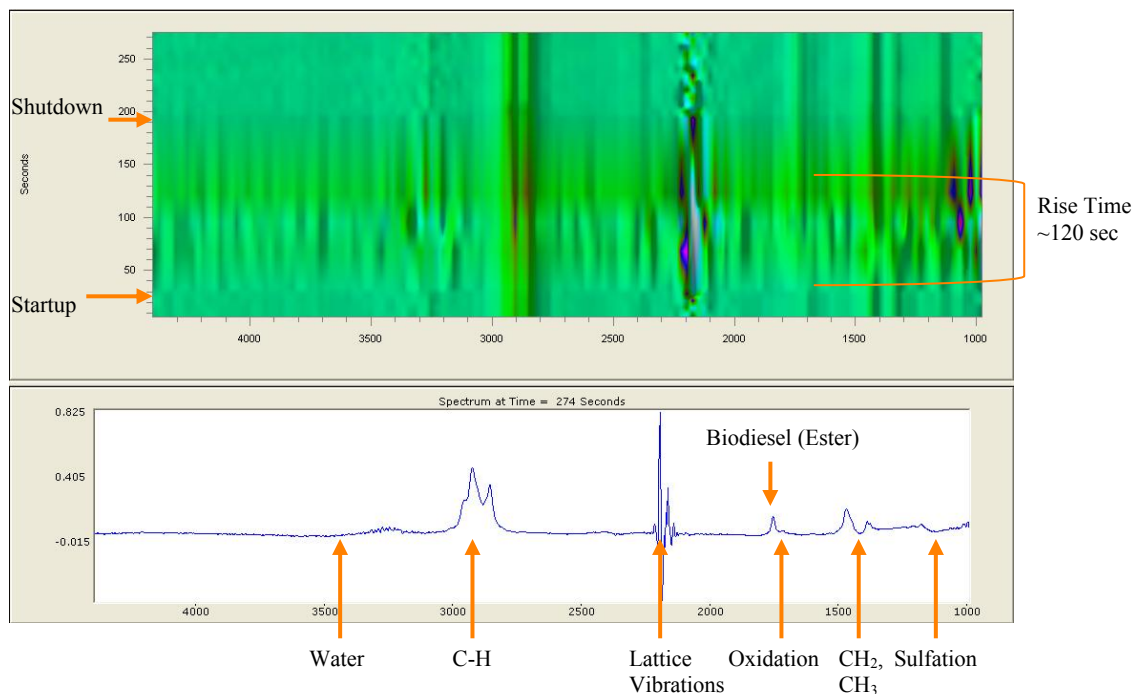


Figure 4.16 – A top view of the spectral time series recorded during the tracer experiment. The emergence of an ester peak is clearly visible at 1750 cm^{-1} .

Figure 4.17 graphs the measured height of the ester peak, in reference to a stable peak in the spectrum. The absorbance (or peak height) at 1750 cm^{-1} is directly proportional to the concentration of biodiesel in the oil at the piston ring zone. There is an exponential increase in biodiesel concentration beginning immediately after engine startup.

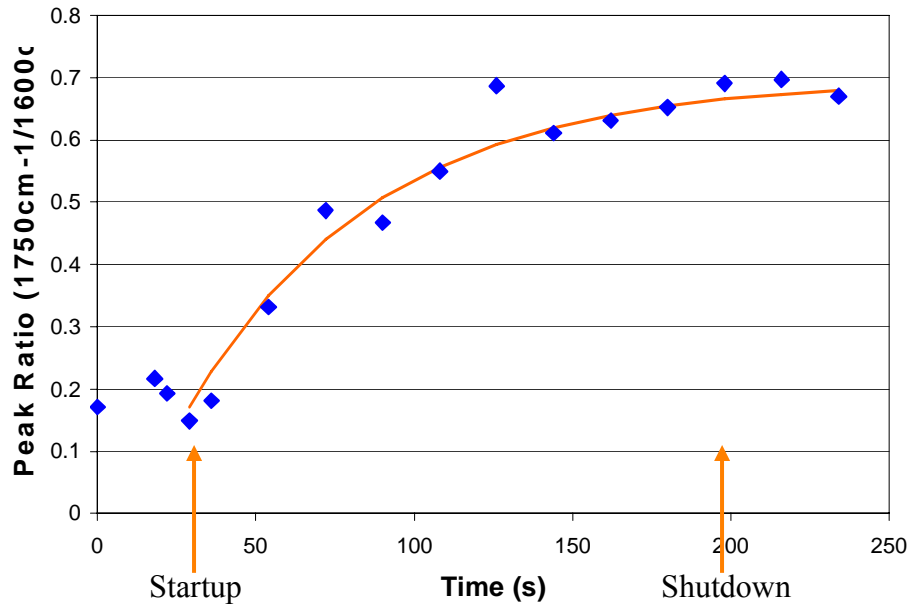


Figure 4.17 – The growth of the peak associated with biodiesel.

The residence time of the oil can be estimated from this data by applying a simple mixing model to represent the piston ring pack. The ring pack could be represented as a constant volume reservoir with a steady flow of oil at the inlet being supplied from the crankcase, and an equivalent outlet flow of oil returning to the sump. If the inlet flow were mixed with a tracer, the concentration of the tracer in the reservoir would increase exponentially according to the equation:

$$[\text{marker}]_{\text{ring pack}} = [\text{marker}]_{\text{sump}} \left(1 - \exp^{-\frac{t}{\tau_{\text{RingPack}}}} \right) \quad (4.2)$$

Where $[\text{marker}]$ is the concentration of the tracer in the ring pack, or sump, and τ_{RingPack} is the residence time for the tracer in the volume. A residence time of about 60 seconds is obtained when this model is fitted to the data. This result is consistent with the

measurements obtained by [14], who found a residence time of 3 minutes for the oil in the TRZ using sampling experiments also on a Lister Petter TR-1 engine.

4.3 ANALYSIS OF RESULTS

An analysis of the results of this study gives several insights into the mechanisms for the emission of ash-related elements into the exhaust. A mass balance can also be developed, which separates the sources and sinks inside the engine for ash-related elements. This knowledge assists in the development and validation of a framework to model of lubricant species distribution and transport inside diesel engines.

The majority of the material that forms ash in DPFs is emitted from the power cylinder system. In this system, the mechanisms of oil consumption and degradation in the piston ring-pack lead to the preferential consumption, or retention of metallic elements in the lubricant. This effect may be manifested in the sump oil elemental analysis results as differences in the speciated emission rates (see Figure 4.8).

Two oil consumption mechanisms are known to be important in transferring oil and additive metals from the TRG to the combustion chamber; liquid oil consumption, and evaporation. Liquid oil, with a composition close to that in the TRG, is lost to the combustion chamber by an inertia-driven throw-off process [9]. The second oil consumption mechanism involves evaporation of volatile lubricant components from the hot metal surfaces of the piston and entrainment in blow-by gases. The temperature of the piston and liner is often lower than would be required for rapid evaporation to occur. However, hot combustion gases reach the surface of the oil layer and surface temperatures may exceed 250°C. Evaporation tends to alter the composition of the lubricant in the TRG by preferentially removing the components with the highest vapour pressures (see Figure 4.5). Severe thermal and oxidative stresses are also imposed on the lubricant in this region. Under these conditions, a fraction of ZDDP is expected to thermally decompose into more volatile byproducts [20].

4.3.1 Estimated Ash Emissions

The emission of ash-related elements from the engine causes an accumulation of ash in DPF's as the metallic compounds are filtered out of the exhaust. Analysis of diesel exhaust emissions and the material found in DPFs has shown that the metallic compounds emitted from the engine are not necessarily in the same chemical form as the ash found in regenerated traps. High temperature regeneration oxidizes the metallic compounds, converting them into only a few compounds typically found in DPF ash. X-ray diffraction (XRD) analysis has shown that the majority of ash found in DPFs is made up of the following compounds [37]:

- Calcium Sulfate - CaSO_4
- Zinc Phosphates - $\text{Zn}_3(\text{PO}_4)_2$
- Zinc Magnesium Phosphates - $\text{Zn}_2\text{Mg}(\text{PO}_4)_2$

An estimation of the total ash emissions from the engine may be calculated by stipulating that the metallic elements emitted from the engine are ultimately incorporated into the typical compounds found in ash. It is assumed that all of the calcium, zinc and magnesium from the sump oil are captured by the DPF and transformed into calcium sulfate, zinc phosphate and zinc magnesium phosphate respectively. This assumption is valid since it has been shown that the DPF traps at least 99% of these elements [37]. Deposition inside the engine has also been shown to be negligible in this study.

Figure 4.18 graphs the estimated ash emissions for each lubricant, emitted during the long duration engine tests. This estimation is based on the measured elemental mass losses graphed in Figure 4.7. The vast majority of ash (approximately 70%) found in the DPF is composed of calcium sulfate, although calcium has the lowest elemental emission rate (see Figure 4.8). This result is consistent with several studies of DPF ash composition [7, 45, 37]. Ash containing zinc constitutes approximately 30% of the ash, although it represents a larger fraction of the ash from oils with 1.0% sulfated ash. The magnesium emitted from the engine is always found bound to zinc phosphates in DPF ash.

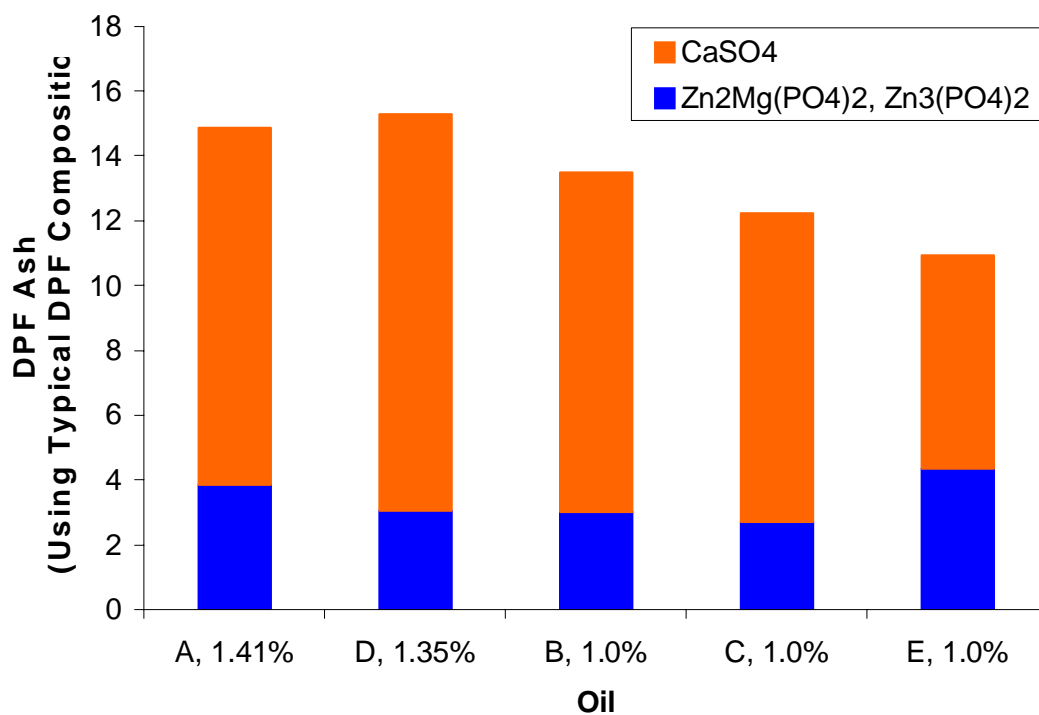


Figure 4.18 – The estimated composition of DPF ash that would result from the long duration engine tests.

Figure 4.19 compares the mass of DPF ash that would be produced during the long duration engine tests with the amount of ash expected based on the sulfated ash level of the fresh lubricant. For all of the lubricants, the sulfated ash measurement overestimates the total DPF ash. Only 75 percent of the ash you would expect based on sulfated ash would be found in the DPF. This result highlights the deficiencies in the use of sulfated ash as a measure of a lubricant’s potential impact on aftertreatment systems. Misrepresentation of oils occurs because the test fails to account for the actual recovery rates of elements. In addition, the composition of sulfated ash is significantly different from typical DPF ash.

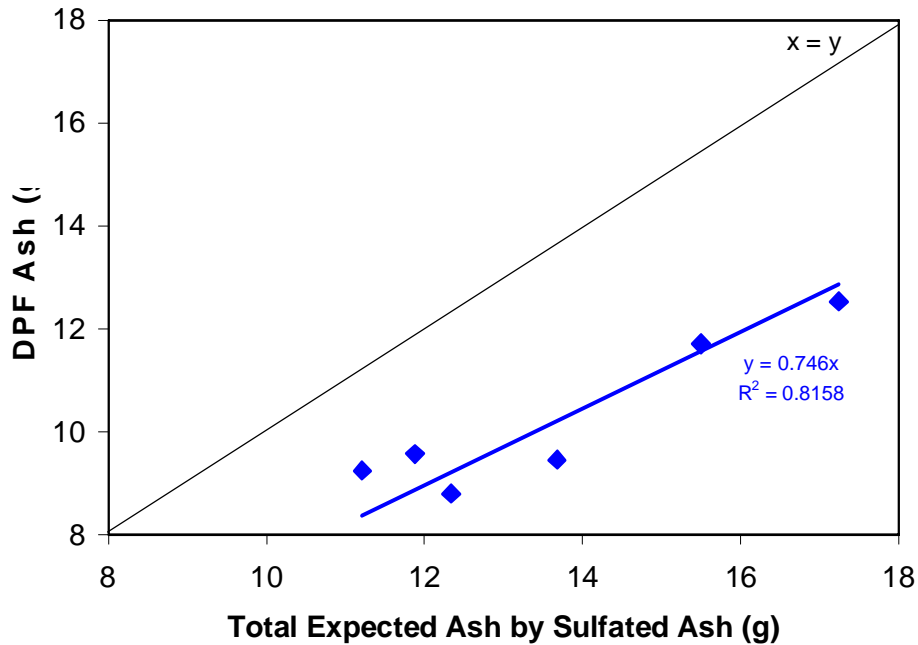


Figure 4.19 – A comparison of the estimated DPF ash with the total expected ash based on the sulfated ash level of the fresh lubricant.

4.3.2 Elemental Mass Balance

The results from this study can also be presented in the form of an elemental mass balance. This analysis accounts for the sources and fates of ash-related elements in the engine. There are only two sources for ash-related elements from the lubricant additive package; the fresh sump oil, and the makeup oil added due to oil consumption. When deposition is neglected (as it was shown to be insignificant), there are two sinks for ash-related elements; DPF ash, the used drain oil. In a complete mass balance, the sums of the sources and the sinks must be equal.

A mass balance for calcium is shown in Figure 4.20. A substantial portion of the calcium in the engine is retained in the sump and is eventually recovered from the drain oil. The remaining calcium is emitted from the engine by oil consumption. Almost all of the calcium emitted from the engine is trapped by the DPF, where it is oxidized to form calcium sulfate.

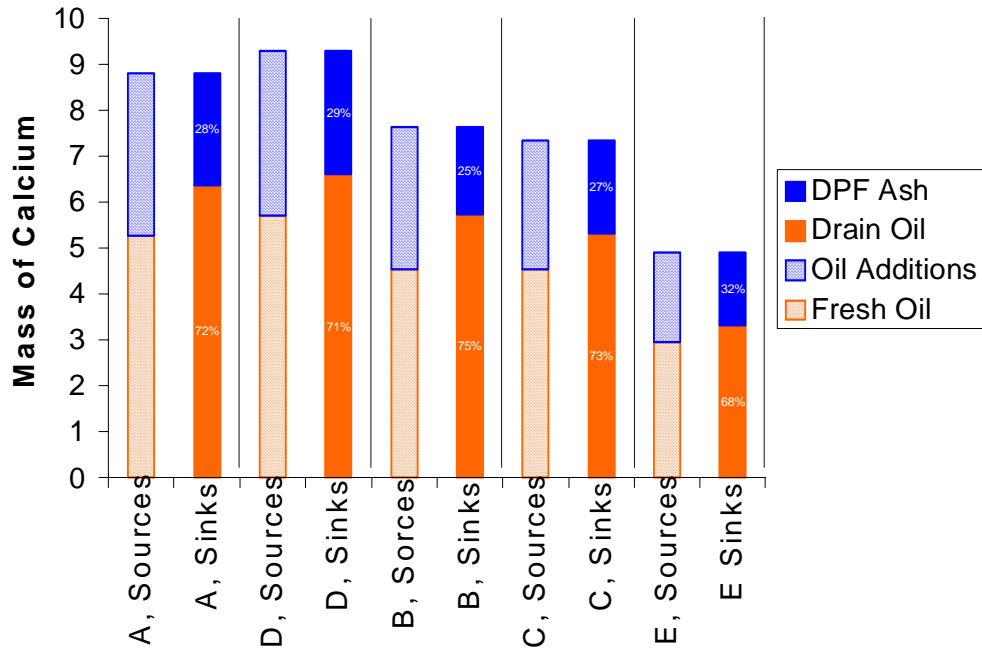


Figure 4.20 – A mass balance for calcium. The letters on the horizontal axis refer to the lubricants used in the long duration engine tests.

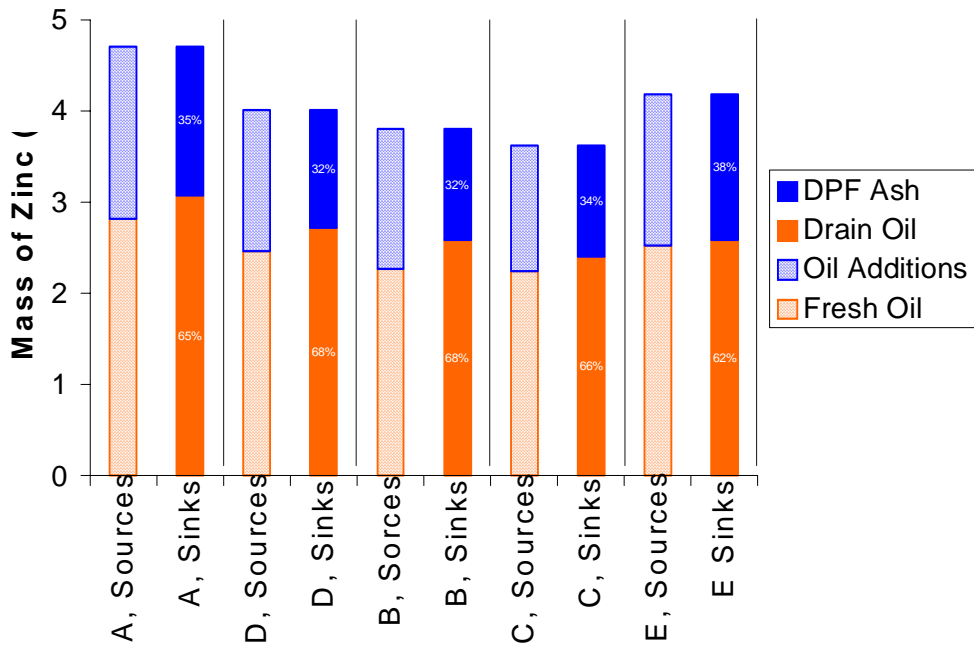


Figure 4.21 – A mass balance for zinc.

Similar trends are seen in the zinc mass balance (see Figure 4.21), although, a smaller fraction of the element is recovered in the drain oil. Most of the zinc emitted from the engine is trapped by the DPF and is recovered as zinc phosphate, or zinc magnesium phosphate.

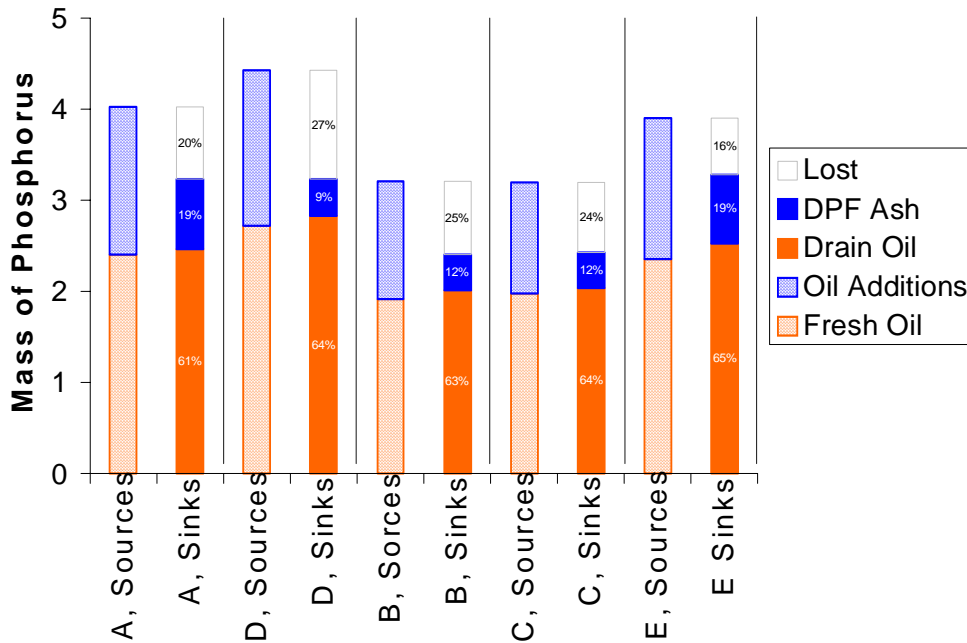


Figure 4.22 – A mass balance for phosphorus.

The mass balance for phosphorus is shown in Figure 4.22. Phosphorus accumulates in the sump oil to a lesser degree than calcium and zinc. A portion of the element is trapped in the DPF as zinc phosphate, or zinc magnesium phosphate. Surprisingly, a large fraction of the phosphorus is unaccounted for in the mass balance. It appears to be lost from the engine system. There are two possible additional fates for phosphorus:

- Penetration through the DPF; or
- Accumulation of phosphorus in the DPF substrate, or wash coat separate from ash in the channels of the filter.

Evidence that phosphorus is penetrating through the DPF has been collected by [37].

4.3.3 Source of Calcium and Magnesium in Exhaust

Liquid oil consumption is the only means for the transport of calcium and magnesium from the power cylinder to the exhaust stream, since detergents are considered to be involatile [4]. Liquid oil is lost from the piston crown immediately above in the TRG. In this region, the concentration of calcium in the lubricant is higher than in the sump, due to the preferential consumption of base oil by volatility (see Figure 4.5).

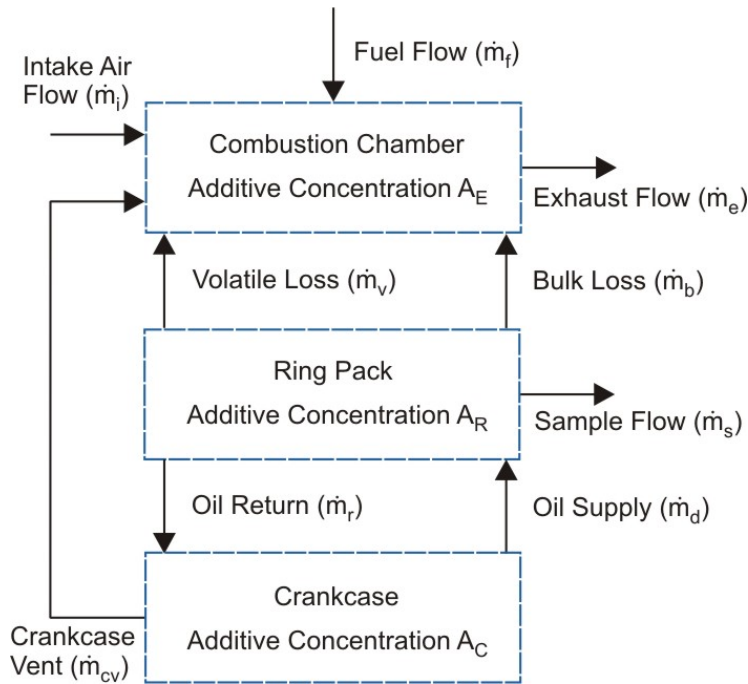


Figure 4.23 – A simplified model of the power cylinder system. The concentration of calcium in the TRG, measured with ring pack sampling, may be used to estimate the rate of bulk oil loss. This is the only mode for the emission of calcium into the exhaust.

A basic three-zone reactor model (illustrated in Figure 4.23) may be used to describe the transport of involatile additives from the crankcase to the exhaust [15, 16]. In this model, the measured enrichment of calcium is used to estimate the fractions of oil lost by liquid oil loss and volatility. The transient flows in the power cylinder are approximated as steady mass flow rates over the time period of interest. Uniform lubricant compositions are also assumed in the crankcase, ring-pack and combustion chamber zones. This simplification is appropriate for the crankcase oil because it is well mixed by the high

flow rate through the crankshaft and valve train lubrication loop. Deposition in the sump is also assumed to be insignificant. A well mixed assumption may not be appropriate for the ring-pack, however, because the oil mass in this region is subdivided on the piston surface by the piston lands and in grooves [56]. The oil flows between these may zones not be sufficient for substantial mixing to occur, therefore, considerable variations in lubricant composition may be present throughout ring pack. The lubricant in the TRG is expected to have the highest degradation and volatility loss due to its proximity to the combustion chamber and exposure to temperatures exceeding 250°C.

The average liquid oil consumption rate from the TRG can be estimated using the concentration of calcium in the TRG and the loss of calcium from the crankcase oil. The change in the mass of calcium in the crankcase lubricant depends on the mass flow rates of oil into and out of the sump and the concentrations of the species in those flows:

$$\frac{d(m_{CC}A_{CC,Ca})}{dt} = \dot{m}_r \beta A_{RP,Ca} - \dot{m}_d A_{CC,Ca} \quad (4.3)$$

Where the parameter β is included to represent that the composition of the oil returning to the crankcase from the ring pack is different than the composition of the oil measured in the samples extracted from the TRG. It accounts for the local differences in oil composition throughout the ring-pack, particularly between the TRG and the OCR. Another equation similar to (4.3) may be derived for the change in the total mass of a calcium in the ring pack:

$$\frac{d(m_{RP}A_{RP,Ca})}{dt} = \dot{m}_d A_{CC,Ca} - \dot{m}_r \beta A_{RP,Ca} - (\dot{m}_t + \dot{m}_s) A_{RP,Ca} \quad (4.4)$$

By combining Equations (4.3) and (4.4), and neglecting the change in the mass of calcium in the ring pack with time (since $m_{RP} \ll m_{CC}$), the average rate of liquid oil loss from the power cylinder may be estimated with:

$$\dot{m}_l = -\frac{1}{A_{RP,Ca}} \frac{d(m_{CC}A_{CC,Ca})}{dt} \quad (4.5)$$

It is emphasized that in this model the total liquid oil consumption depends on the concentration of calcium in the TRG, not the crankcase. This is because the oil is lost

from TRG, where the concentration of calcium is elevated due to the evaporation of the base oil.

The average total liquid and volatile oil consumption for the sampling experiments are compared in Figure 4.24, shown as a fraction of the total oil consumption. As expected, the total volatile loss increases with increasing oil volatility. Small differences in the average total loss of liquid oil are found between oils A, B and C. It should be noted that because fresh oil is used for each sampling experiment the volatilization rate is expected to be higher than in typical engines. A disproportionate amount of lower molecular weight base oil hydrocarbons with relatively high vapor pressures are lost from the oil in the first several hours of each test. The volatilization rate for an engine filled with used oil would probably be lower than that value measured in these experiments.

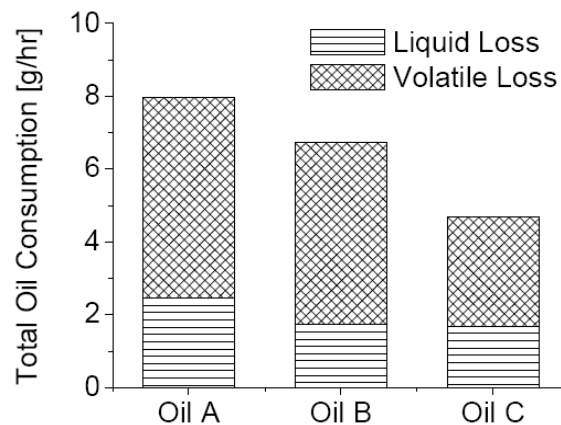


Figure 4.24 – The fractions of total volatile and liquid (bulk) oil consumption during the ring pack sampling experiments. High oil consumption rates occurred during these experiments due to the volatilization of light-end hydrocarbons from the fresh oil.

Volatilization of the base oil in the piston ring-pack concentrates the additive metals in the TRG, which affects the mass of ash-related elements emitted due to liquid oil consumption. The average volatilization rate from the ring-pack may be estimated by accounting for the change in the concentration of calcium as it is transporting in the lubricant from the crankcase to the TRG. Oil flows in the ring-pack change considerably throughout the engine cycle. The compositions of the samples extracted with the

sampling system represent the average condition in the TRG over the one hour sampling duration. Considering the average flows for the ring-pack zone, oil consumption by volatilization and liquid oil loss is balanced by net oil supply from the crankcase beyond the OCR:

$$\dot{m}_l + \dot{m}_v = \dot{m}_d - \dot{m}_r \quad (4.6)$$

Assuming that the concentration of calcium is constant over the measurement period and that any increase in the concentration of calcium relative to the crankcase oil is solely due to evaporation of the base oil (i.e. no deposition), a mass balance for calcium in the ring pack may be written as:

$$\dot{m}_d A_{CC,Ca} = \dot{m}_{RP,Ca} A_{RP,Ca} + \dot{m}_l A_{RP,Ca} \quad (4.7)$$

An expression for the average evaporation rate of base oil from the ring pack may be derived by combining Equations (4.6) and (4.7). It is expressed as a function of the enrichment factor of calcium species and the mass flow rate of oil delivered into the ring pack (above the OCR) from the crankcase:

$$\dot{m}_v = \dot{m}_d \left(1 - \frac{A_{CC,Ca}}{A_{RP,Ca}} \right) \quad (4.8)$$

The inverse of the concentration ratio in Equation (4.8) is the enrichment factor of calcium in the ring-pack samples. To find the fraction of oil consumed by liquid and volatile loss in the ring pack the mass flow rate of fresh oil delivered into the ring pack from the crankcase must be known. This parameter may be estimated if the residence time for oil in the ring pack is known. The residence time of oil in the ring pack has been measured to be approximately one to three minutes for this type of engine design. Assuming that the ring grooves are nominally 20% full of oil the oil delivery rate from the crank case into the ring pack and beyond the oil control ring is estimated to be 6.5 grams/hour.

Using the measured enrichment of calcium in the TRG samples and the approximate oil delivery rate, the relative fractions of oil lost from the ring pick due to volatilization and liquid loss are calculated and shown in Figure 4.25. It should be emphasized that the calculation of the vaporization rate is highly dependent on the assumed fresh oil delivery

rate. This analysis is intended to illustrate the mechanism by which the base oil is preferentially consumed from the ring pack and involatile species are concentrated in the oil.

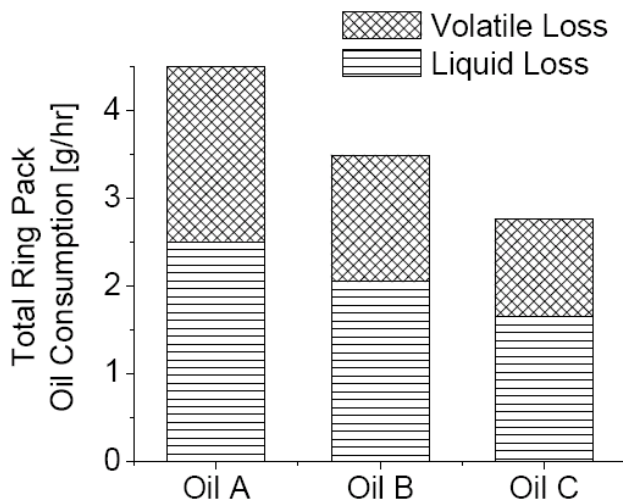


Figure 4.25 – The fractions of oil consumed by volatile and liquid (bulk) oil consumption from the piston ring pack region during the ring pack sampling experiments.

4.3.4 Source of Zinc and Phosphorus in Exhaust

Zinc and phosphorus are emitted from the engine due to both liquid and volatile oil consumption. The composition of the TRG samples reflects the action of these loss mechanisms. In the TRG samples, the enrichment factors for the ZDDP elements are consistently lower than the enrichment factors for the detergent elements. The lower enrichment factors for phosphorus arises primarily from the volatilization of unstable ZDDP thermal degradation products in the ring-pack region. Evaporation of phosphorus from lubricants at high temperatures has been observed in several studies and is examined in [98, 100].

The mass of evaporated phosphorus and zinc depends on a number of factors including the temperature and the lubricant formulation. The environment in the piston ring-pack tends to convert ZDDP into volatile products that may evaporate with the base oil. Fresh

oil often contains a blend of ZDDP in the neutral and basic forms. Neutral ZDDP is the active anti-wear and anti-oxidant additive. Basic ZDDP has a relatively high molecular weight and correspondingly, a low volatility. It is less active as an anti-wear additive at low temperatures. However, at piston temperatures, basic ZDDP is thermally unstable and is converted rapidly into the more volatile neutral form. Under the oxidizing conditions in the ring pack, ZDDP reacts and is converted into a disulphide which has been previously identified as a major degradation product in TRG oil samples [14]. The neutral ZDDP and the disulphide oxidation products have high vapour pressures, so they evaporate from the TRG. Deposition also tends to reduce the degree of enrichment for zinc relative to the detergent metals. Crown land deposits are known to attract zinc compounds from the lubricant in the TRG, although the measurements in this study show that this is not a significant sink for additive metals.

4.4 MODELING LUBRICANT SPECIES DISTRIBUTIONS AND TRANSPORT IN THE ENGINE

To further analyze the results of this study, a framework was developed to model the distribution and transport of ash-related lubricant species in the power cylinder. The model was formulated using the methodology outlined in Section 3.8. It was calibrated by comparing output to the results of the sampling experiments and the long duration engine tests. The resulting model may be used to investigate possible opportunities to reduce ash emissions from engines.

4.4.1 Power Cylinder Model

A schematic of the framework utilized to model the distribution and transport of ash-related species in the power cylinder is shown in Figure 4.26. Similar to the simple model shown in Figure 4.23, the power cylinder is separated into three zones; the crankcase, ring pack and combustion chamber. The majority of the lubricant in the system is contained in the crankcase (1850 grams), while the ring pack contains a constant oil mass of 0.5 grams. Table 4.9 lists the input parameters for each zone.

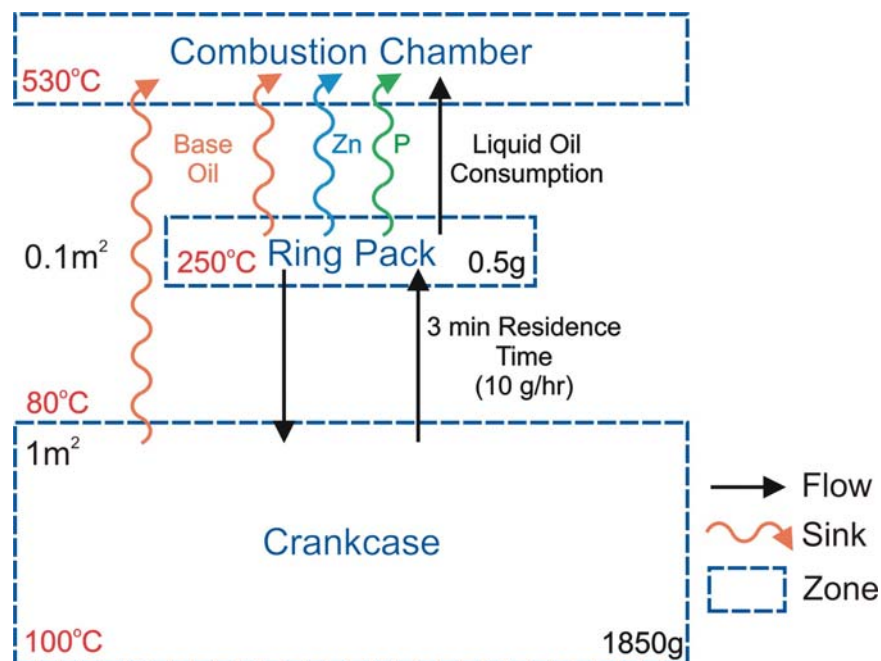


Figure 4.26 – A schematic of the framework used to model ash-related lubricant species distribution and transport in the power cylinder.

Table 4.9 – Specified Parameters for Each Zone

Region	Crankcase	Ring Pack	Combustion Chamber
Zone	1	2	3
Oil Mass (g)	1850	0.5 (constant)	0
Surface Temperature (°C)	100	250	N/A
Gas Temperature (°C)	80	530	530
Surface Area (m ²)	1	0.1	N/A

The complex network of transient flows in the power cylinder, are modeled as a set of simplified steady flows between the zones. This approximation is reasonable over the time scale of interest (several hours). Oil is supplied from the crankcase to the ring pack at a rate of 10 grams/hour. This flow rate corresponds with a residence time in the ring pack of 3 minutes. A portion of the flow is lost to the combustion chamber due to liquid oil consumption. The balance of the flow returns to the crankcase.

The sinks for lubricant species are also modeled in the framework. Volatilization of the base oil is modeled with the mass transfer equations presented in Sections 3.8.3 to 3.8.6. The thermal decomposition and volatilization of ZDDP are modeled as sinks for zinc and

phosphorus in the ring pack. The volatilization rate is a model input parameter that is calibrated from the experimental data.

4.4.2 Model Calibration

The power cylinder model was calibrated to fit the measurements of lubricant composition obtained during the ring pack sampling experiments and the long duration engine tests. The volatility of the zinc and phosphorus was adjusted until the predicted elemental emissions (see Figure 4.8) matched the measured values. Table 4.10 lists the specified values for zinc and phosphorus volatility. The volatility is different for each lubricant, which is not surprising since it depends on the type of ZDDP and the other additives used in the formulation [100]. The average volatilization rates for zinc and phosphorus were 0.290 and 0.416 (g/s) $\times 10^6$ respectively. These values are consistent with those measured by [98].

Table 4.10 – The Specified Volatility for Zinc and Phosphorus

Oil	Specified Volatility (g/s) $\times 10^6$		Volatility (mol/s) $\times 10^9$	
	Zinc	Phosphorus	Zinc	Phosphorus
A	0.293	0.471	4.48	15.21
B	0.304	0.427	4.65	13.79
C	0.313	0.403	4.79	13.01
D	0.249	0.385	3.81	12.43
E	0.289	0.392	4.42	12.66
Average	0.290	0.416	4.43	13.42
Std. Dev.	0.022	0.031	0.336	1.006

The calibrated model predicts the emissions of ash-related elements reasonably well. Figure 4.27 compares the model output with the experimental results. Linear curve fits are applied to the data to estimate the elemental emission rates predicted by the model. Table 4.11 lists the elemental emission rates obtain from the measurements and from the model output. The results match within 10 percent.

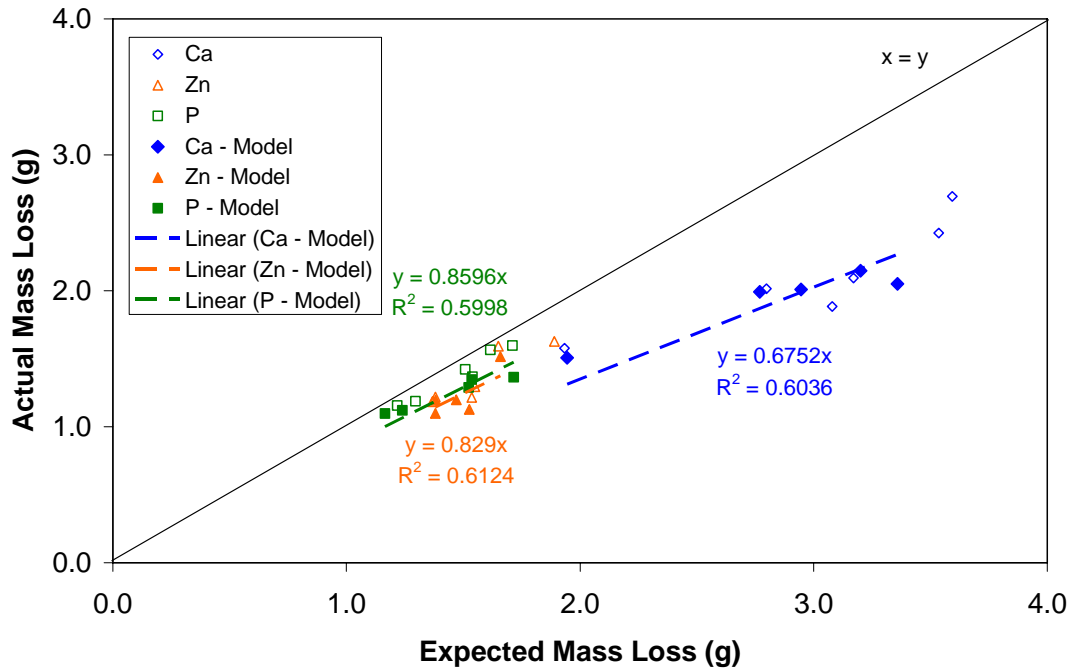


Figure 4.27 – A comparison of the elemental emissions, measured and from the model.

**Table 4.11 – Relative Elemental Emission Rates
(Measured and Predicted by the Model)**

Element	Measured (%)	Model Output (%)
Calcium	70	67
Zinc	87	83
Phosphorus	93	86

The model formulation also captures the distribution of lubricant species inside the engine. Figure 4.28 compares the model output with the measurements of lubricant species concentrations obtained during a ring pack sampling experiment with oil A. The model matches the measured data for the elements associated with the detergent (calcium and magnesium). The results for the elements associated with ZDDP (zinc and phosphorus) are not as accurately modeled. This discrepancy may occur because the complex degradation processes that influence the concentration of ZDDP in the ring pack are not modeled in the formulation. The concentrations of zinc and phosphorus could also be modified by deposition in the ring pack sampling system.

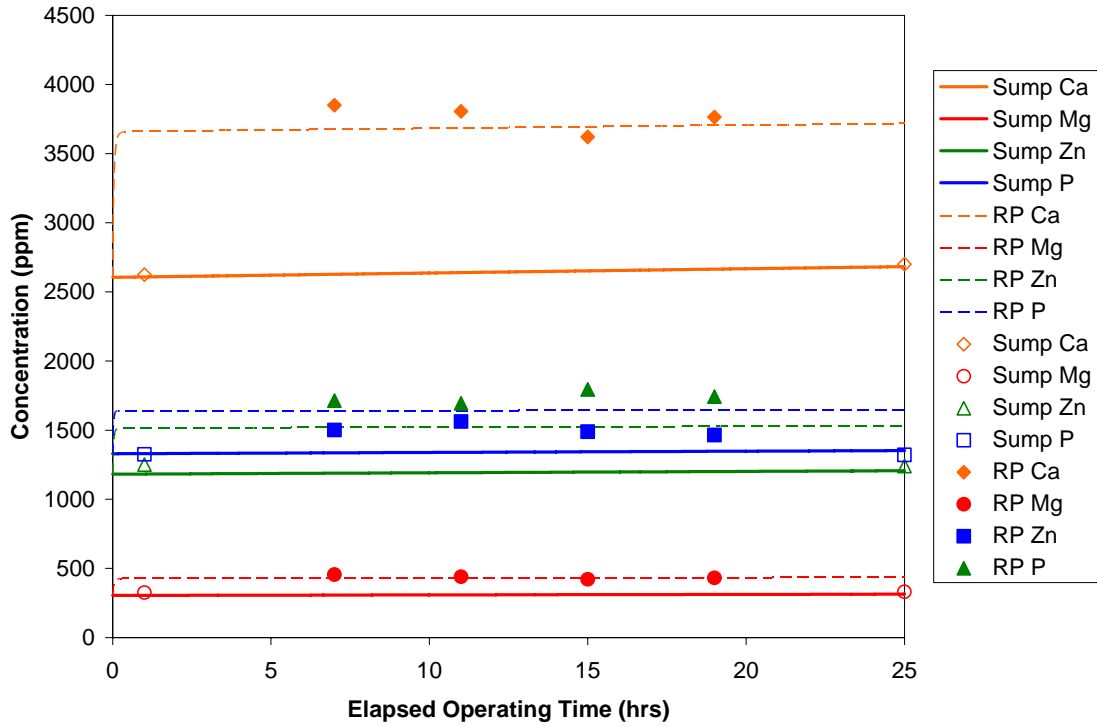


Figure 4.28 – The predicted species concentrations during a ring pack (RP) sampling experiment with oil A. The compositions of samples from the ring pack are also plotted.

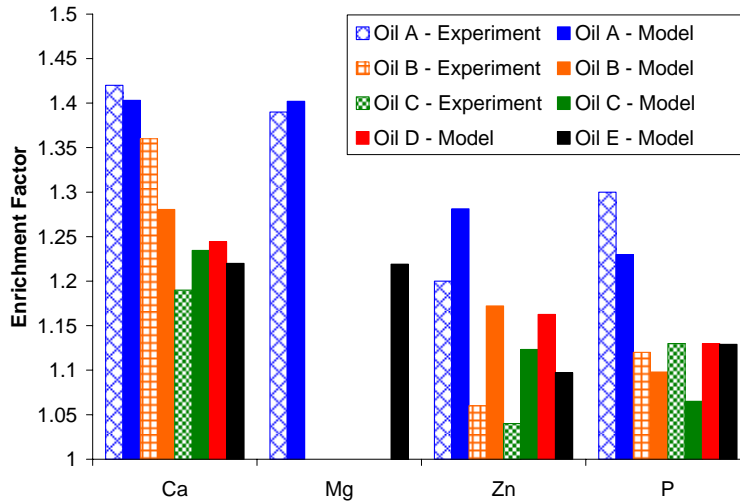


Figure 4.29 – A comparison of the measured enrichment factors and those predicted by the model.

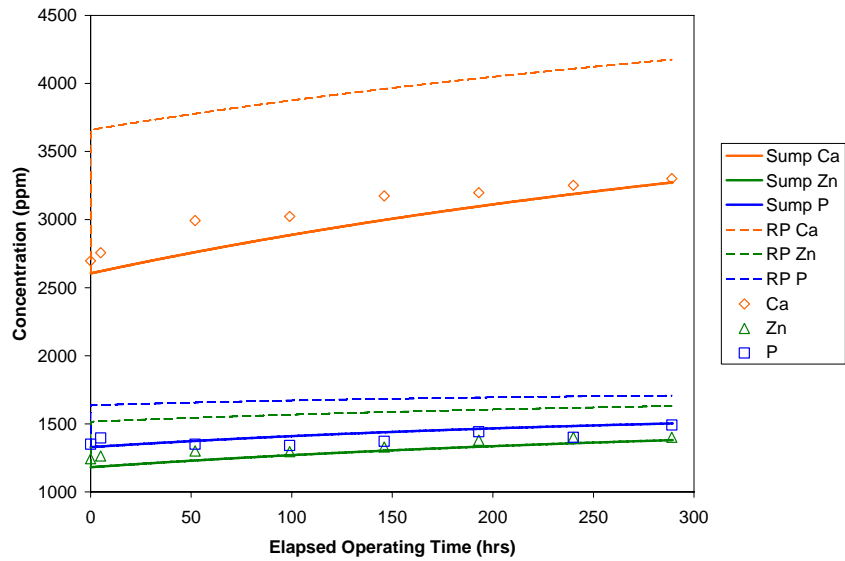


Figure 4.30 – A comparison of the sump oil composition for oil A measured in the long duration engine tests and predicted by the model.

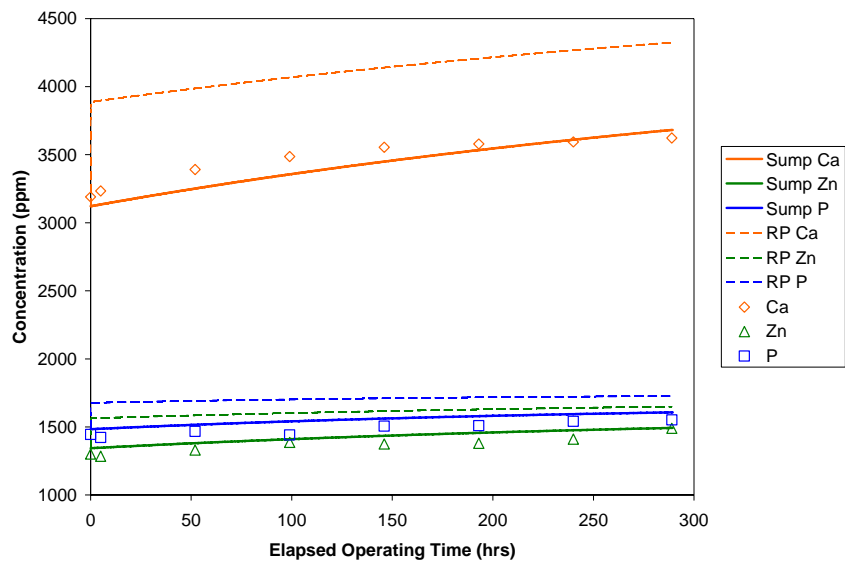


Figure 4.31 – A comparison of the sump oil composition for oil D measured in the long duration engine tests and predicted by the model.

Figure 4.29 compares the measured enrichment factors for the ash-related elements with those predicted by the model. The model fits the measured data reasonably well for calcium, zinc and phosphorus. However, the model consistently over estimates the

enrichment factor for zinc. This result suggests that deposition inside the sampling system may be preferentially removing zinc from the samples.

A comparison of the model output and measurements of sump oil composition for oils A and D are shown in Figures 4.30 and 4.31 respectively. The model captures the changes in sump oil composition over time. Although, the initial rapid increase in the calcium concentration does not appear in the output. The increase in the concentration of calcium occurs due to the volatilization of light end hydrocarbons in the base oil, especially in the ring pack zone (see Figure 4.32). It is expected that the accuracy of the model would improve if the ring pack were modeled as several zones.

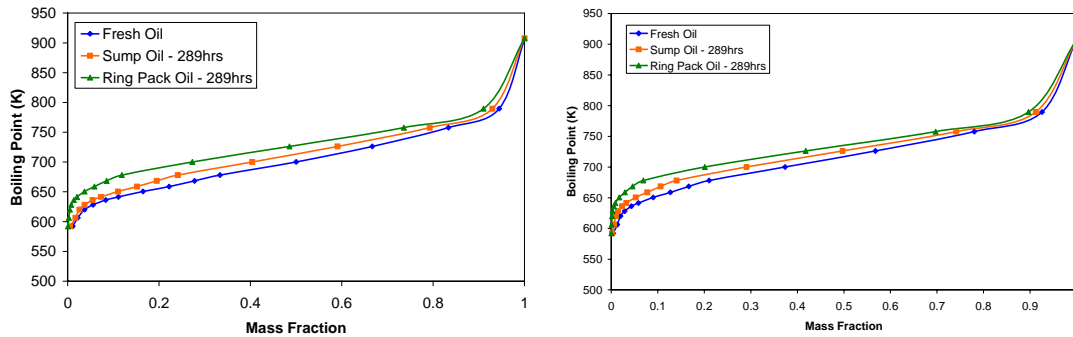


Figure 4.32 – The predicted distillation curves for base oil in the sump and ring pack after 289 hours of engine operation (*Left* - Oil A, *Right* - Oil D). The curves shift to the left due to preferential volatilization of lighter hydrocarbons in the mixture.

4.4.3 Alternatives for Reducing Ash Emissions

There may be alternatives for reducing ash emissions beyond simply reducing the oil consumption rate, or the concentration of ash-related species in the fresh lubricant. In this section, the effects on ash emissions of reduced base oil volatility, or shortened ring pack residence time are analyzed with the model framework.

4.4.3.1 Effect of Reduced Base Oil Volatility

A possible alternative for reducing ash emissions is to design lubricants with lower volatility base oils. This change may lower the enrichment of ash-related elements in the ring pack, thereby reducing the concentration of metallic elements in the lubricant lost by liquid oil consumption.

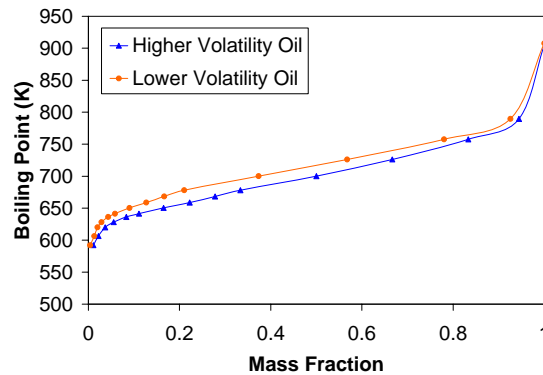


Figure 4.33 – Base oil distillation curves. The higher volatility oil has a NOACK volatility of 15%. The lower volatility oil has a NOACK volatility of 11%.

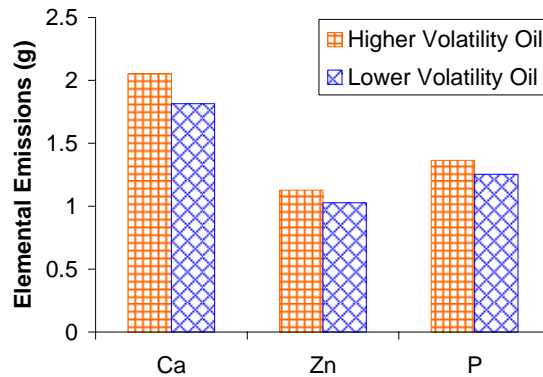


Figure 4.34 – Predicted elemental emissions with higher and lower volatility base oils.

The effect of lower volatility base oil was analyzed with the lubricant species distribution and transport model. Two lubricants with identical elemental compositions were modeled with different base oil volatilities (15% and 11% NOACK volatility). The base oil distillation curves are shown in Figure 4.33. Reduced ash emissions were predicted with

the lower volatility base oil (see Figure 4.34). The elemental emissions of calcium, zinc and phosphorus were expected to be reduced by 12, 9 and 8 percent respectively.

4.4.3.2 Effect of Shortened Ring Pack Residence time

Another possible alternative for reducing ash emissions is to reduce the residence time of the lubricant in the piston ring pack. Similar as reducing base oil volatility, this change may lower the enrichment of ash-related elements in the ring pack, thereby reducing the concentration of metallic elements in the lubricant lost by liquid oil consumption.

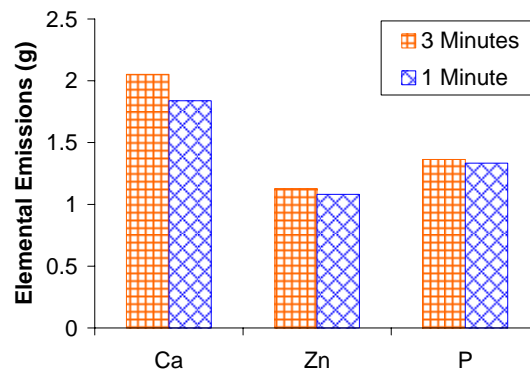


Figure 4.35 - Elemental emissions for ring pack residence times of 3 and 1 minute.

The power cylinder model predicted the ash emissions for ring pack residence times of 3 minutes and 1 minute. The results are summarized in Figure 4.35. Shortening the residence time by 2 minutes reduced elemental emissions of calcium, zinc and phosphorus by 10, 4 and 2 percent respectively.

4.5 CONCLUSIONS

In this study, changes in the elemental composition of the lubricant in the power cylinder of an operating diesel engine are measured. The objective is to ascertain what effect these changes in composition have on the mass of ash-related elements lost from the crankcase and emitted in the exhaust. The following conclusions may be made based on measurements taken in this study:

Crankcase Oil Sampling

- Detergent metals (calcium and magnesium) are preferentially retained in the crankcase oil.
- ZDDP metals (zinc and phosphorus) are emitted at a higher rate into the exhaust.

Ring Pack Oil Sampling

- All additive metals are concentrated in the ring pack region.
- Detergent compounds are concentrated to a higher degree than anti-wear additives (ZDDP) in ring pack oil samples.
- The volatilization of light-end hydrocarbons concentrates calcium and magnesium in the top ring zone.
- Ring-pack volatility increases the concentration of metals in the liquid oil that is lost to the combustion chamber.
- The concentration of zinc and phosphorus in the ring pack is influenced by:
 - evaporation of volatile hydrocarbons
 - volatilization of ZDDP thermal degradation products

In-Situ FTIR Measurements at the Piston and Liner Interface

- In-situ measurements show that the liner oil is degraded significantly due to:
 - Contamination with combustion gases (sulfates and nitrates), acids, soot
 - Oxidation due to high oil temperatures
- For this engine, the oil flows through the piston liner region has a residence time (τ) of approximately 1 minute. The residence time in the piston ring pack is about 3 minutes.

Valve Train Sampling and Filter Debris Analysis

- Deposition of additive metals in the valve train and oil filter is negligible.

Mass Balance

- Emissions of calcium contribute the majority of DFP ash (calcium sulfate).

- During these experiments, 16-27% of the phosphorus in the lubricant appears to be lost through the DPF, or accumulates in the substrate and washcoat separate from the ash in the channel.

Sulfated Ash Balance

- Sulfated ash is an unreliable measure of potential ash emissions from a lubricant.
- The procedure fails to account for elemental emission rates, and the actual composition of DPF ash.

Lubricant Species Distribution and Transport Model

- The calibrated model framework developed in this study predicts emissions and the distribution of ash-related elements reasonably well.
- Beyond simply reducing the oil consumption rate, or the concentration of ash-related species in the fresh lubricant, elemental emissions may be reduced by:
 - Reformulating lubricants with lower volatility base oils
 - Shortening the residence time for oil in the piston ring pack

(This page intentionally left blank)

CHAPTER 5 - FILTER CONDITIONING AS A POTENTIAL MEANS TO REDUCE ADDITIVE REQUIREMENTS

5.0 INTRODUCTION

Acids are the source of many lubricant-related problems in diesel engines. During normal engine operation, the lubricant is exposed to combustion gases containing nitrogen, sulfur and carbon-based acids. Weak organic (carbon) acids also accumulate in the lubricant due to oxidation of the base oil. Severe problems can occur if these acids remain in the oil and are not neutralized. The accumulation of weak organic acids in the oil can cause engine wear and corrosion, high lubricant viscosity, sludge, varnish and piston deposits. In several cases the capacity of the oil to neutralize and control acids determines the lubricant lifetime and the oil drain interval.

Acid control remains an important issue especially in modern diesel engines employing advanced emission control technologies [10]. The high EGR rate used by these engines increases the exposure of the lubricant to combustion acids and induces more severe oxidation. However, this increase in acid contamination is balanced by a reduction in the amount of sulfur based acids [11]. The change to ultra-low-sulfur diesel fuel reduces the concentration of sulfur dioxide in exhaust gases. The widespread use of biodiesel fuel is especially concerning. Hydrolysis of the esters in biodiesel increases the weak acid concentration in the lubricant, which in turn accelerates the rate of lubricant degradation, and promotes engine wear and corrosion [12, 13].

Considerable research and development has focused on optimizing additive packages to control lubricant acidity and protect components from wear. Dispersants and over-based detergent additives are typically used in diesel lubricants to neutralize acids. These additives are effective; however, new lubricant specifications limit the amount of ash containing additive that can be used in formulations. The recent API CJ-4 specification requires a sulfated ash level at or below 1.0 percent [2]. There is insufficient data to demonstrate that ash-containing anti-wear additives at a lower concentration than current

prevalent levels can provide sufficient wear protection. Therefore, the concentration of over-based detergents is reduced in these oils because they are the only other significant source of ash. This change decreases the acid neutralization capacity of the lubricant, so the lengths of oil drain intervals have remained constant at best [9].

5.1 CURRENT ALTERNATIVE TECHNOLOGIES

Several systems have been developed to extend oil drain intervals. Filters that slowly release lubricant additives and by-pass filtration are two technologies currently used to extend oil drain intervals and enhance engine protection. Slow release filters incorporate a gelled additive package consisting of detergents, dispersants and antioxidants. The filter discharges these components into the oil to replenish depleted additives. Unfortunately, in most designs there is limited control over the release rate, so additives are released at times when they are not necessarily required by the engine. The accumulation of additives in the oil also increases ash content and circumvents API CJ-4 specifications. By-pass filtration is also used to extend oil drain intervals. This technology mechanically removes particles too small to be trapped by standard oil filters. However, acidic contaminants are not trapped by the filter, so they remain in the lubricant. By-pass filtration only increases oil drain interval in those cases where particulate contamination determines the oil drain interval.

5.2 STRONG BASE FILTER

This part of the thesis explores the effectiveness of an innovative strong base oil filter technology that supplements the acid control function typically performed by detergent and dispersant additives. The filter interacts chemically with the lubricant to sequester acidic contaminants. This approach is unique compared to other additive technologies because it has the ability to induce a chemical change in the lubricant without releasing compounds into the oil. The experiments in this study are designed to investigate the effect of the strong base filter on lubricant life and engine protection.

The strong base filter sequesters unneutralized weak acids, or already neutralized strong acids from the lubricant. It consists of a standard full-flow filter element impregnated with magnesium oxide particles. The lubricant in the main oil circuit interacts with the strong base as it is pumped through the filter. Acids are transferred from the lubricant to the surface of the base where they are immobilized.

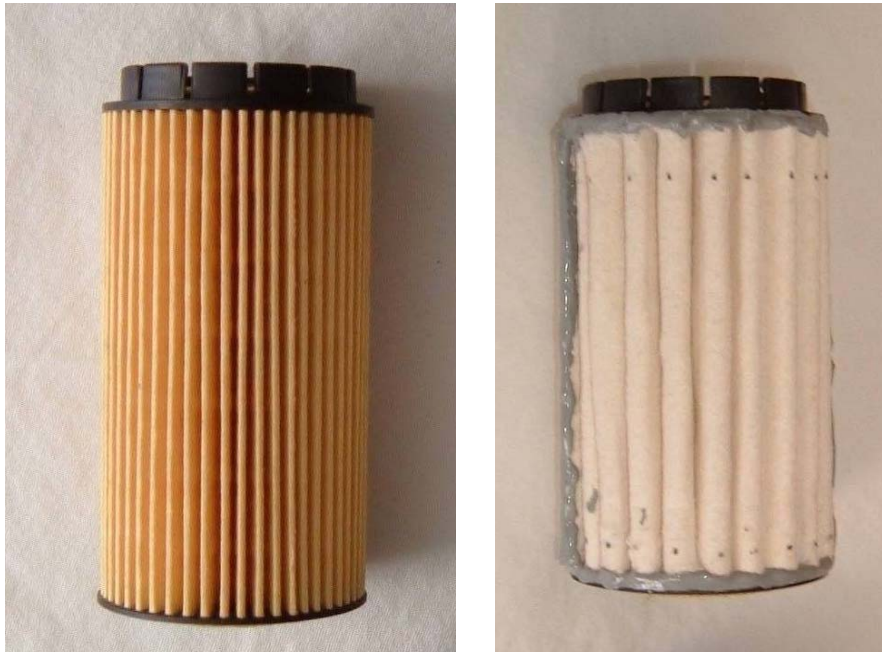


Figure 5.1 – *Left* - The standard filter element. *Right* - The prototype strong base filter. Both filters are full-flow 20 micron filter elements and are reinforced with stainless steel mesh.

The strong base filter element has a geometry similar to a standard full flow filter (see Figure 5.1). It consists of standard 20 μm filter paper impregnated with magnesium oxide particles. Figure 5.2 is an image of standard filter paper, taken by a Transmission Electron Microscope (TEM). A highly magnified view of the filter paper in the strong base filter is shown in Figure 5.3. An elemental analysis of one of the base particles, collected with an Environmental Scanning Electron Microscope (ESEM), is shown in Figure 5.4. The particles consist of only magnesium oxide and have a primary particle size of approximately 5 μm . They are bound to the paper fibers in such a way that they are not released into the lubricant during normal use. This design maximizes the contact

area between the lubricant and the strong base, increasing the acid neutralization rate. However, the magnesium oxide particles in the paper occupy sites that store the contaminants trapped by standard filters. Therefore, it is expected that a strong base filter will have less capacity to store dirt collected from the lubricant, and perhaps a shorter filter life.

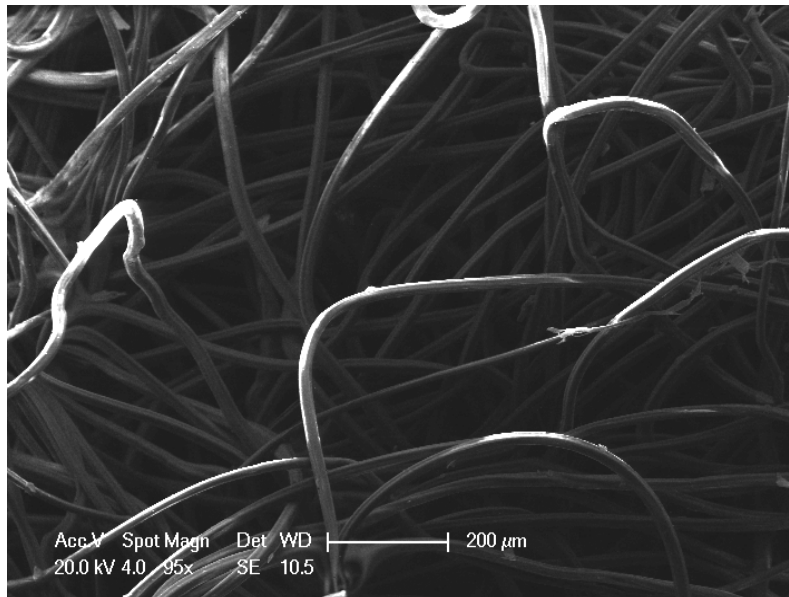


Figure 5.2 – A TEM image of standard (20 micron) filter paper.

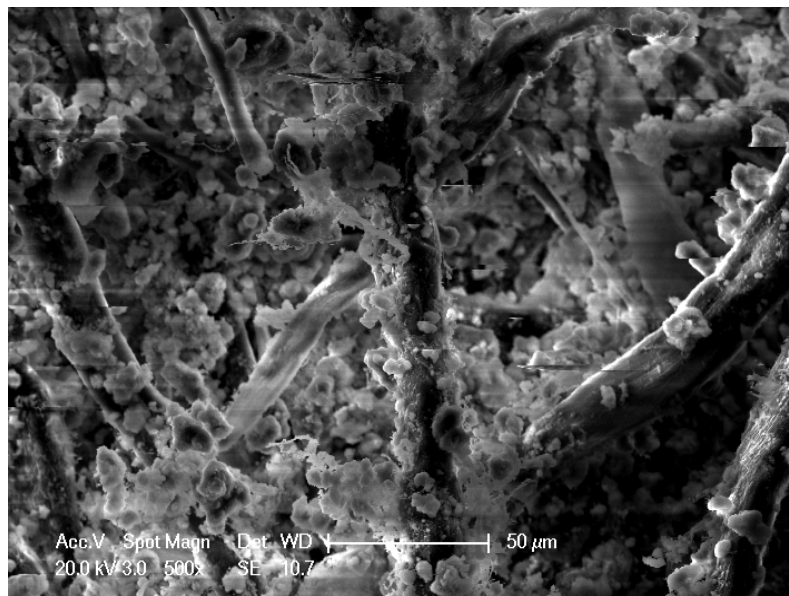


Figure 5.3 – A TEM image of the filter paper in the strong base filter.

The transfer of acid to the filter is reported in prior literature. One source [101] reports photo acoustic IR measurements on the strong base elements in an experimental filter, which found strong absorbances of alkyl sulphates from a sulfur-free and zero-detergent oil in a 1G2 engine. For this test the fuel used contained 4,000 ppm sulfur. In the engine tests reported in this paper using CI-4 PLUS lubricant, the concentration of calcium in the used lubricant increased by approximately the amount that would be expected from losing the volatile components of the oil. It is believed that the only components of the lubricant that are removed from the lubricant and sequestered in the filter are unneutralized weak acids and already neutralized strong acids. The useful life of the strong base filter is set by the capacity of the filter to sequester acids.

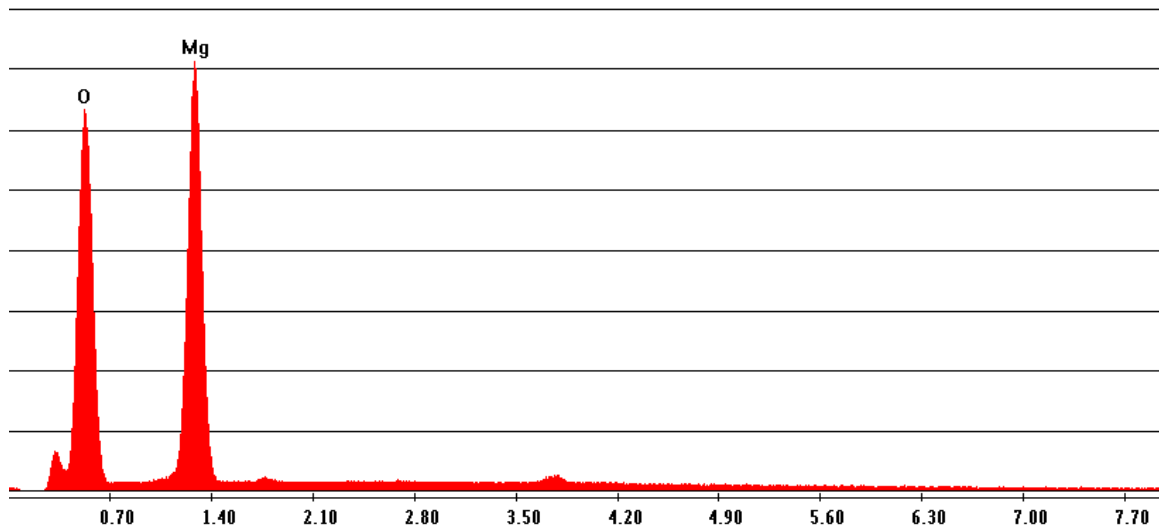


Figure 5.4 – Elemental analysis with ESEM of a strong base particle in the filter. The particles are primarily composed of magnesium oxide.

5.3 EFFECT ON AFTERTREATMENT SYSTEM DURABILITY

Modern engines are fitted with DPF's to reduce particulate emissions. The inorganic compounds in lubricant additive packages (i.e. detergents and ZDDP) form ash when oil transported past the piston rings is burned in the combustion chamber. The ash accumulates in the DPF and degrades the durability of the system. There is also a

detrimental effect on fuel consumption, due to an increased exhaust restriction and more frequent regenerations [7].

A strong base filter could be used in combination with a lubricant containing no detergent additives to minimize the detrimental effects of ash on DPF's. In this system, the acidic contaminants are neutralized only on the filter. Less ash would be expected in the DPF because the lubricant would contain a lower concentration of inorganic compounds. It may also be possible to offer an zero-detergent lubricant that provides adequate engine protection while maximizing the durability of the DPF.

In this study, the strong base filter is tested with an experimental zero-detergent lubricant. The objective of these tests is to determine if the filter performs the acid control function when used with oil formulated without over-based detergent additives. An engine utilizing a zero-detergent oil is expected to have significantly lower ash emissions and improved aftertreatment system durability.

5.4 EXPERIMENTAL APPROACH

In this study, the effect of oil conditioning with the strong base filter was assessed by comparing the level of oil degradation in four long duration tests with the Lister Petter TR-1 engine. Two tests were conducted with an experimental lubricant formulated with no over-based detergent additives. The other two tests used a fully formulated lubricant conforming to API CI-4 PLUS specifications.

Two experiments were conducted with each lubricant. One test was a baseline case with a standard (chemically inert) oil filter. A strong base filter was used in the second test. The standard and strong base filters were fitted to the engine using a Racor™ screw-on-type housing (see Figure 5.5). No modifications to the oil circuit were required to use the strong base filter.



Figure 5.5 – Both filter elements were mounted in a Racor™ full-flow housing. Both filters contained identical oil volumes and similar flow profiles.

Oil samples were extracted from the engine at regular intervals. Standardized oil analysis techniques were used to measure lubricant condition and determine what effects filter conditioning had on oil degradation.

5.4.1 Test Procedure

Four long duration engine experiments were performed to observe the effect of strong base filter conditioning on lubricant degradation. The test conditions used in the experiments are summarized in Table 5.1.

Table 5.1 – Engine Test Parameters

Parameter	Test 1	Test 2	Test 3	Test 4
Lubricant	Zero-detergent, SAE 15W40		API CI-4 PLUS, SAE 40W	
Oil Filter	Strong Base Filter	Standard Oil Filter	Standard Oil Filter	Strong Base Filter
Test Duration	300 hours	82 hours	318 hours	750 hours
Oil Consumption	5.103 g/hour	5.59 g/hour	3.61 g/hour	3.51 g/hour
Engine Load	100% Full Power			
Engine Speed	1800 rpm			
Fuel	Ultra Low Sulfur Diesel			

The first set of tests was performed with the zero-detergent lubricant. In Test 1, a strong base filter was used for 300 hours of operating time (approximately equivalent to the oil drain interval recommended by the OEM). This experiment demonstrated the effect of oil conditioning on a lubricant containing no strong base reserve. In Test 2, a standard (chemically inert) filter was employed for 82 hours of operating time. This experiment represented the baseline case and exhibits the consequences of operating an engine with no strong base reserve. The test was halted at 82 hours to prevent severe wear and corrosion of engine components due to a rapid increase in lubricant acidity.

The second set of tests was performed with a lubricant conforming to API CI-4 PLUS specifications. In Test 3, a standard (chemically inert) filter was used for 318 hours of operating time. This experiment represented the baseline case and demonstrated the expected level of oil degradation over a standard oil drain interval. In Test 4, a strong base filter was employed for 750 hours of operating time (over twice the standard oil drain interval). A comparison of this experiment with the baseline case shows the effect of filter conditioning on the degradation of a fully formulated lubricant.

Engine load was maintained at 100 percent full power for the duration of the tests. This power level exposed the lubricant to the most severe operating conditions and accelerated the rate of oil degradation.

The condition of the sump oil and the engine was similar at the beginning of all the tests. The crankcase lubricant was recharged with 1.95 kg of fresh oil using a triple flush procedure. The engine was also rebuilt before each test, which included a replacement of the main bearing surfaces.

Routine maintenance of the engine was performed every 24 hours. Oil consumption was monitored at these times using a gravimetric method. Fresh top-up oil was added after every measurement to maintain the mass of sump oil in the engine. Fuel consumption and oil sump temperature were also recorded every 24 hours. This data was used to verify that the engine conditions in the experiments were identical.

Sump oil samples were extracted from the engine every 48 hours. The first oil sample was extracted at 5 hours to allow the fresh oil to mix and ensure a uniform lubricant composition. The recommended ASTM sampling procedure was used in this study. A vacuum system was employed to pull 17 gram oil samples from the sump through the dipstick guide hole. Just enough lubricant was extracted to satisfy the minimum volume requirements of the oil analysis tests. The amount of fresh makeup oil addition was reduced by following this procedure.

5.4.2 Lubricant and Fuel Properties

The zero-detergent and CI-4 PLUS oils lubricants used in this study were oils D and F, respectively, found in Table 3.7. Relevant lubricant specifications are listed in Table 5.2. The sulfated ash levels of the zero-detergent and the CI-4 PLUS lubricants were 0.057 percent and 1.35 percent respectively.

Table 5.2 – Lubricant Properties

Property	Zero-detergent	CI-4 PLUS
Oil	D	F
SAE Grade	15W40	40W
API Gravity	29.1	28.9
Viscosity at 40°C (cSt)	125	146
Viscosity at 100°C (cSt)	15.2	14.9
Sulfated Ash (%) [ASTM D874]	0.057	1.35
TBN (mg KOH/g) [ASTM D2896]	5.6	10.2

The concentrations of metallic elements in the fresh oil are listed in Table 5.3. Lubricants with low magnesium content were selected so any leaching of strong base filter material (magnesium oxide) could be detected in the used oil samples.

**Table 5.3 – Fresh Lubricant Elemental Analysis
(ASTM D4951)**

Element	Concentration (ppm)	
	Zero-detergent	CI-4 PLUS
Calcium	0	3130
Magnesium	0	10
Zinc	0	1350
Phosphorus	480	1490
Barium	0	160

The additive package in the zero-detergent oil had a relatively simple composition (summarized in Table 5.4). It was formulated specifically for this study and was not optimized for this application. The lubricant contained a dispersant additive, an antiwear additive and a viscosity modifier. The base oil was a blend of Americas Core Group I 150/600. A PIBSA/PAM dispersant was used, which comprised approximately 10 percent of the formulation. Antiwear protection was provided by a proprietary blend of ashless phosphorus and sulfur containing additives.

Table 5.4 – A Description of the Components in the Zero-Detergent Oil

Component	Description
Base Oil	Blend of Americas Core Group I
Detergent	None
Dispersant	PIBSA/PAM (~10% of formulation)
Antiwear	Ashless phosphorus and sulfur containing additives
Additional Corrosion Inhibitors	None

The CI-4 PLUS lubricant was selected to minimize the oil consumption rate. This single weight and high viscosity lubricant was chosen after several tests with different lubricants. A low volatility lubricant was chosen to limit fresh oil addition and reduce the accumulation of nonvolatile detergent additives in the oil. The zero-detergent oil was a 15W40 lubricant and was provided by another party.

Ultra low sulfur diesel fuel was used with a sulfur concentration less than 15 ppm. This fuel is currently used by all on-highway diesel vehicles in the United States. A lower sulfur concentration limits sulfur dioxide emissions and reduces sulfuric acid contamination of the lubricant.

5.4.3 Oil Sample Analysis

All oil samples were analyzed by independent laboratories to assess the level of oil degradation. Standardized tests were employed to measure lubricant acidity, remaining base reserve, lubricant oxidation, viscosity and engine wear. Four ball wear tests were also performed with the drain oil extracted at the ends of all the tests to assess the remaining amount of antiwear protection.

In some cases, tests were repeated due to errors in the first round of analysis. It was not possible to obtain a complete set of data from retested samples due to the limited volume of oil in the samples.

The samples from each individual test were collected and sent out for analysis as a batch. The engine was triple flushed with the next oil to be tested. Zero time analytical results from the standard and strong base filter differ by less than the standard deviation of the test. Each batch of samples may have been analyzed by a different technician and used a different batch of reagents. Conclusions from the data are not based on the values of individual data points, but on the slopes of the respective lines on which a least squares analysis can be conducted. The statistical significance and confidence limits for the slopes derived from the least squares analyses are listed in Appendix D.

5.5 RESULTS

The results obtained from the long duration engine tests showed that the strong base filter has a significant effect on lubricant acidity and degradation.

5.5.1 Test Conditions

Identical engine operating conditions were used in all of the tests. In this study, differences in lubricant condition were induced by changing the lubricant formulation (i.e. zero-detergent oil versus CI-4 PLUS oil), or from the action of the strong base filter. During the tests, the oil consumption rate, oil temperature, fuel consumption, and soot loading were measured periodically to monitor the operating environment and contaminant loading of the lubricant. An analysis of this data showed that the mean oil temperatures in Tests 1 and 2 were slightly different and that higher oil consumption occurred with the zero-detergent oil.

There were also small variations in the average oil consumption rates between tests. Figure 5.6 graphs the total oil consumption during the experiments. The average oil consumption rate in each test is listed in Table 5.1. With the CI-4 PLUS lubricant, a slightly higher rate of oil consumption occurred in the test with the standard filter (Test 3). As a result, an increased rate of oil degradation would be expected in the test with the strong base filter due to smaller oil additions (Test 4).

Lubricant composition had an effect on the oil consumption rate. The average oil consumption for the tests with the zero-detergent oil and the tests with the CI-4 PLUS lubricant was 5.81 g/hour and 3.56 g/hour respectively. This disparity was most likely caused by differences in base oil volatility. The main objective of this study is to examine the effect of filter conditioning. The difference in the average oil consumption of the zero-detergent and CI-4 PLUS oils complicates a direct comparison of lubricant performance.

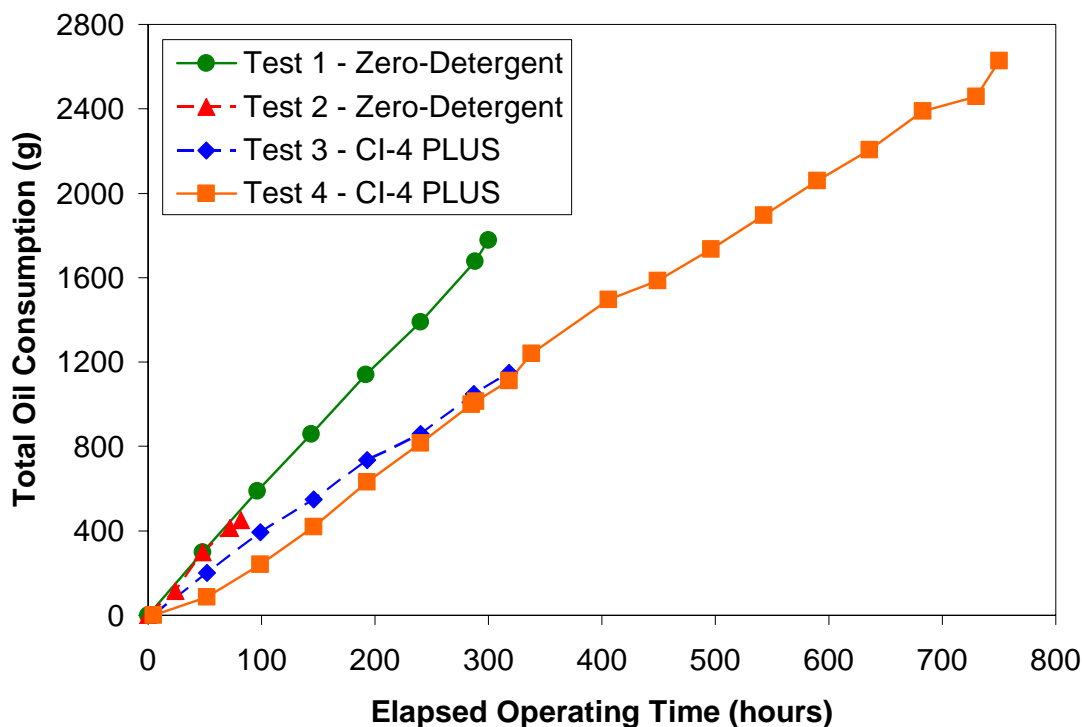


Figure 5.6 – Total oil consumption.

The rate of lubricant degradation is correlated with oil temperature and engine load [15]. These conditions must be equivalent for all the tests, in order to make good comparisons. Tables 5.5 and 5.6 list the mean oil temperatures and fuel consumption for tests with the zero-detergent and the CI-4 PLUS oils. The proximity of the mean oil temperature to the boiling point of water leads to the conclusion that there is not an aqueous phase present and that the neutralization reactions are occurring in a hydrocarbon environment.

Fluctuations in the oil temperature were caused by changes in ambient temperature and were amplified because the engine is air cooled. There was also some variability in the fuel consumption rates measured during the tests. The differences in the mean oil temperature and fuel consumption of Tests 3 and 4 (CI-4 PLUS) were statistically insignificant. There was a statistically significant difference in the mean oil temperatures of Tests 1 and 2 (zero-detergent). As a result, a slightly higher rate of oxidation would be expected in Test 2.

Table 5.5 – A Comparison of the Conditions in the Tests with Zero-Detergent Oil

	Test 1 – Strong Base Filter	Test 2 – Standard Filter
Mean Oil Temperature (°C)	94.2	100.0
Standard Deviation of Oil Temperature (°C)	1.72	1.63
Difference in Mean Oil Temperature - t-Test Significance (2 tail)	2.0x10 ⁻⁴ (Statistically Significant)	
Mean Fuel Consumption (USgal/hr)	0.58	0.56
Standard Deviation of Fuel Consumption (USgal/hr)	0.047	0.042
Difference in Mean Fuel Consumption - t-Test Significance (2 tail)	0.256 (Statistically Insignificant)	

Table 5.6 – A Comparison of the Conditions in the Tests with CI-4 PLUS Oil

	Test 4 – Strong Base Filter	Test 3 – Standard Filter
Mean Oil Temperature (°C)	101.0	98.5
Standard Deviation of Oil Temperature (°C)	4.40	3.89
Difference in Mean Oil Temperature - t-Test Significance (2 tail)	0.206 (Statistically Insignificant)	
Mean Fuel Consumption (USgal/hr)	0.54	0.57
Standard Deviation of Fuel Consumption (USgal/hr)	0.049	0.034
Difference in Mean Fuel Consumption - t-Test Significance (2 tail)	0.263 (Statistically Insignificant)	

Figure 5.7 compares the soot loading in the lubricant at several points during the experiments. The oil is exposed to similar contaminant loading during all the tests. It is reasonable to conclude that for all of the experiments, the oil is exposed to similar quantities of combustion acids.

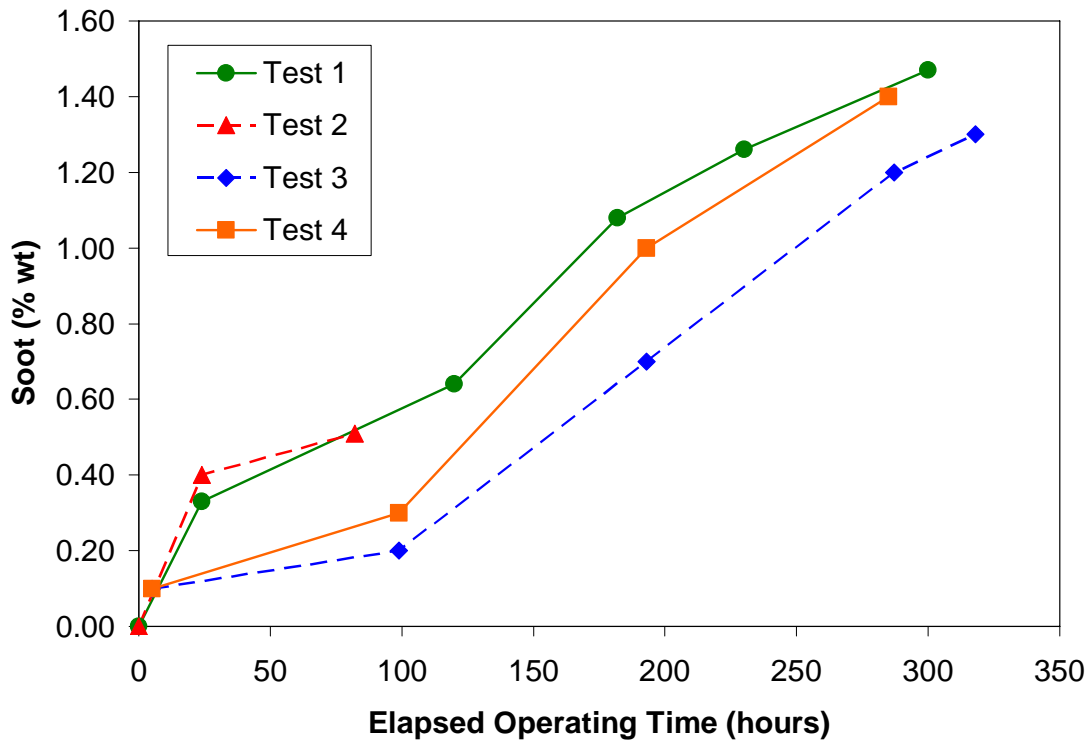


Figure 5.7 – Oil soot content in the first 300 hours, measured with FTIR.

It is not believed that the strong base filter has any effect on soot contamination. If the soot particles carried an acidic charge they might be removed by the strong base filter, but we have seen no data to support this conclusion.

5.5.2 Mobility of Strong Base Material

Figure 5.8 shows the concentration of magnesium in the used CI-4 PLUS oil samples, corrected for base oil volatility. The fresh lubricant contains a small amount of magnesium (8 ppm). For the test with the standard filter, the concentration of magnesium at the beginning and end of the test is equal. There is a small (3 ppm) increase in the

concentration of magnesium during the extended test with the strong base filter. Furthermore, negligible levels of magnesium are detected during the tests with zero-detergent oil.

These results show that the strong base (magnesium oxide) remains in the filter during use. The observed increase in magnesium concentration is caused by the addition of makeup oil throughout the test. An insignificant amount of base is transferred from the filter to the oil. Any reductions in lubricant acidity must be caused by the neutralization of acids on the filter surface, as opposed to a release of strong base into the lubricant.

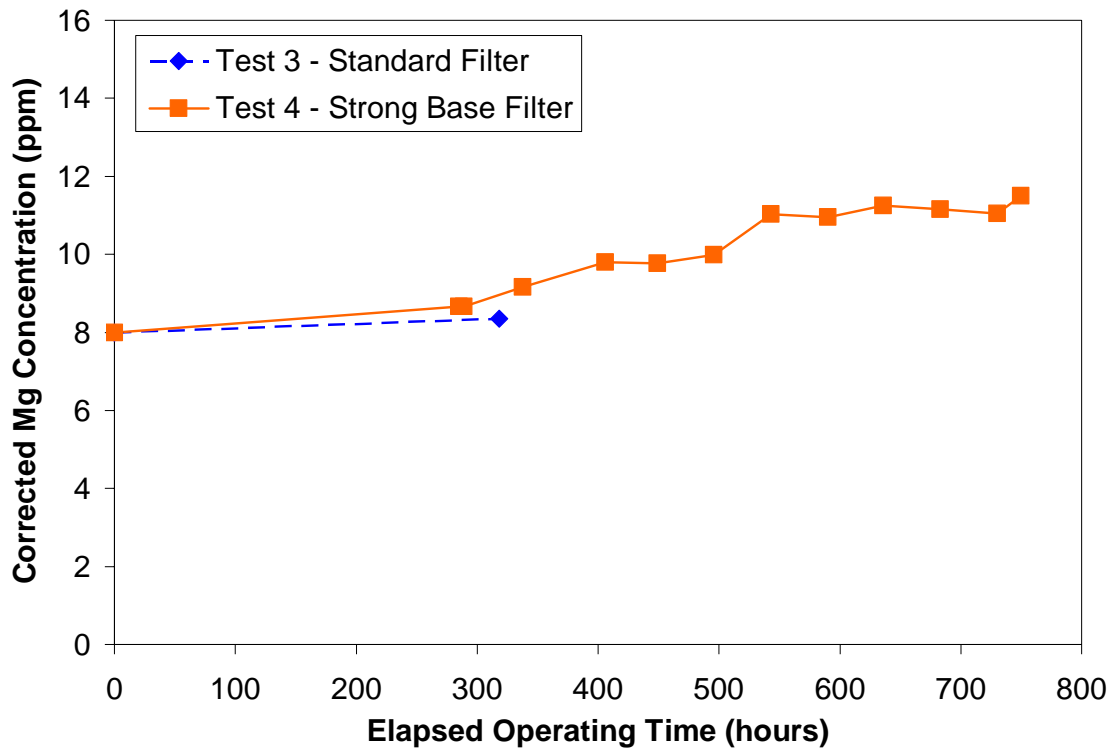


Figure 5.8 – The concentration of magnesium measured with ICP (ASTM D5185).

5.5.3 Lubricant Acidity

Lubricant acidity is a key indicator used to determine the timing of an oil change. Low acidity levels must be maintained to ensure adequate protection of engine components.

An acidic environment can cause corrosion, lubricant oxidation, viscosity increase and engine wear.

5.5.3.1 Total Acid Number (TAN)

Total acid number (TAN) measurements are often used to quantify the level of lubricant acidity. An increasing TAN indicates higher lubricant acidity. TAN measures the quantity of unneutralized acid in an oil sample. TAN combines the acidic contribution from two sources; lubricant additives and unneutralized acidic contaminants (i.e. combustion acids and organic acids).

Figure 5.9 graphs the TAN of the used oil samples. The TAN of the zero-detergent oil samples was obtained with two test methods. In the test with the standard filter (Test 2) there is a rapid increase in TAN due to the lack of a strong base reserve in the system capable of neutralizing excess acid. The weak base in the lubricant (i.e. dispersant) is consumed rapidly as acids accumulate in the oil. Severe corrosion and engine wear could occur if the test were extended beyond 82 hours. In Test 1, the rate of acidification is decreased by approximately a factor of three with the strong base filter. This result indicates that the strong base filter absorbs acidic contaminants in the oil. The strong base filter provides the only source of reserve alkalinity for oil with no detergent. The observed decrease in TAN could only occur when there is a transfer of acid from association with the dispersant to the filter surface.

TAN of the used CI-4 PLUS oil samples is also plotted in Figure 5.9. In these cases, the TAN measures the amount of acid that is not efficiently neutralized by the detergent (i.e. organic acids). A linear increase in TAN is seen in Tests 3 and 4. The rate of TAN increase is substantially reduced by the strong base filter. It appears that the strong base filter decreases the quantity of organic acid in the used oil.

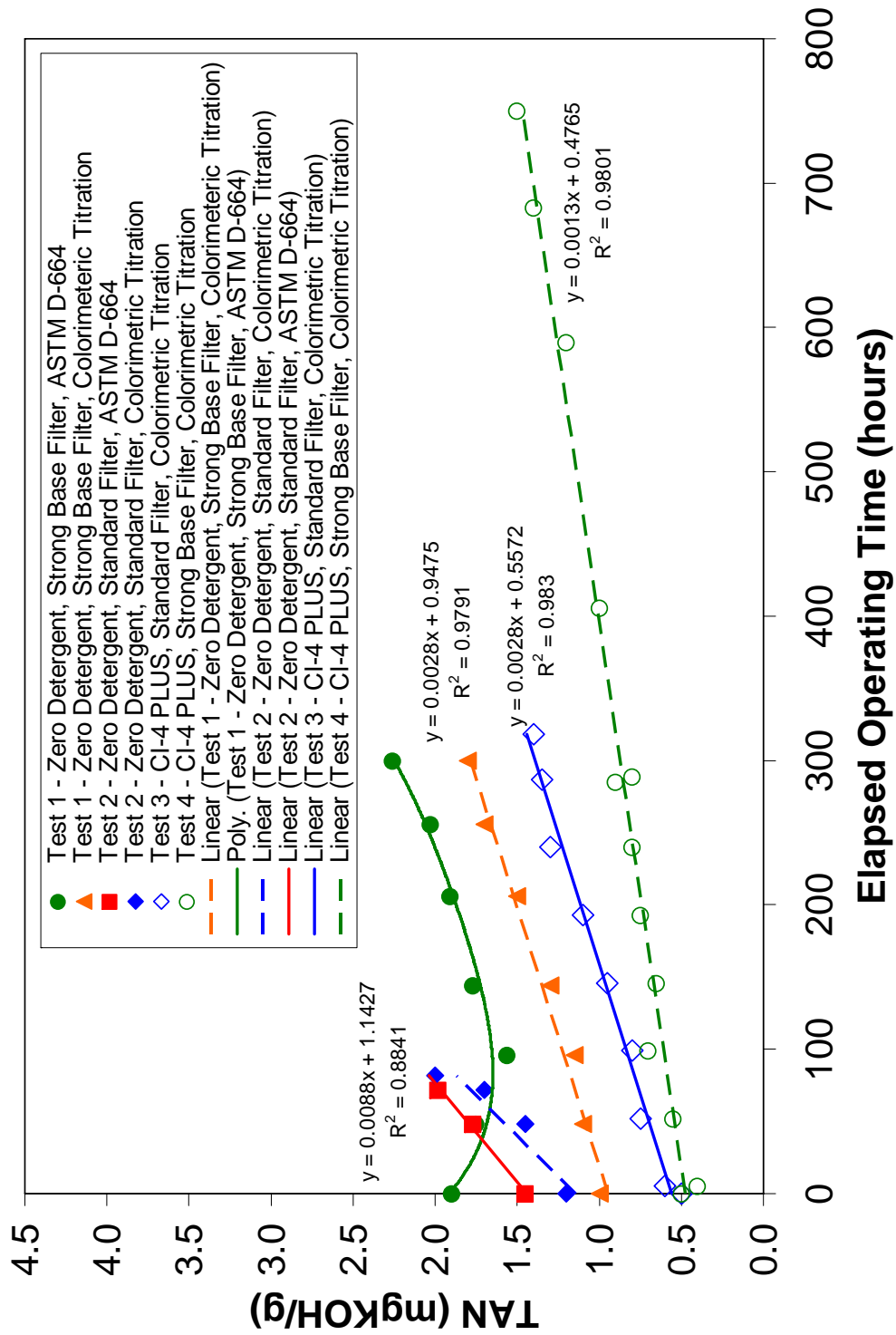


Figure 5.9 – TAN of the zero-detergent and CI-4 PLUS oil samples measured with ASTM D-664 and colorimetric titration.

One interpretation from this result is that the strong base in the filter has less steric hindrance than detergent additives to the neutralization of hindered organic acids. The sterically restricted surfactant shield of an over-based detergent colloid is a barrier to the neutralization of organic acids. The surface of the strong base in the filter is not hindered by a surfactant shield. As a result, the strong base filter is a more effective neutralization site for organic acids. More organic acid is neutralized with the filter and the TAN is reduced. Lubricant conditioning with the strong base filter decreases the concentration of acids in the lubricant and maintains a less corrosive environment in the engine.

5.5.3.2 pH Measurements

The pH of used oil samples are graphed in Figure 5.10. A lower pH level implies a higher lubricant acidity. There is a linear decline in pH for all of the tests. The rate of pH decline is higher with the zero-detergent oil. Therefore, the CI-4 PLUS lubricant maintains a less corrosive environment.

The lowest pH measurements are obtained from samples extracted during the tests with the zero-detergent oil. The most rapid decrease in pH is seen in Test 2, with zero-detergent oil and a standard filter. This result was expected due to the lack of a strong base reserve in the system and is consistent with the TAN measurements. The rate of pH decline is reduced significantly with the strong base filter (Test 1). A comparison of the pH data for the zero-detergent oil tests shows that the rate of pH decline is about three times lower with the strong base filter. This result is further evidence that the strong base filter is absorbing acidic contaminants from the lubricant

Higher pH levels are observed in the tests with the CI-4 PLUS lubricant. This result indicates that the fully formulated lubricant maintains a lower acidity environment in the engine. A significant improvement in the pH is observed with the CI-4 PLUS lubricant and the standard filter (Test 3). The increase in pH is most likely due to the presence of the basic over-based detergent in the oil. The strong base filter further reduces lubricant acidity levels (Test 4). A comparison of the pH data from the experiments with the fully

formulated lubricant shows that the strong base filter slows the rate of pH decline by about a factor of two. The strong base filter reduces the acidity of fully formulated lubricants and maintains a less corrosive environment in the engine by absorbing acidic contaminants.

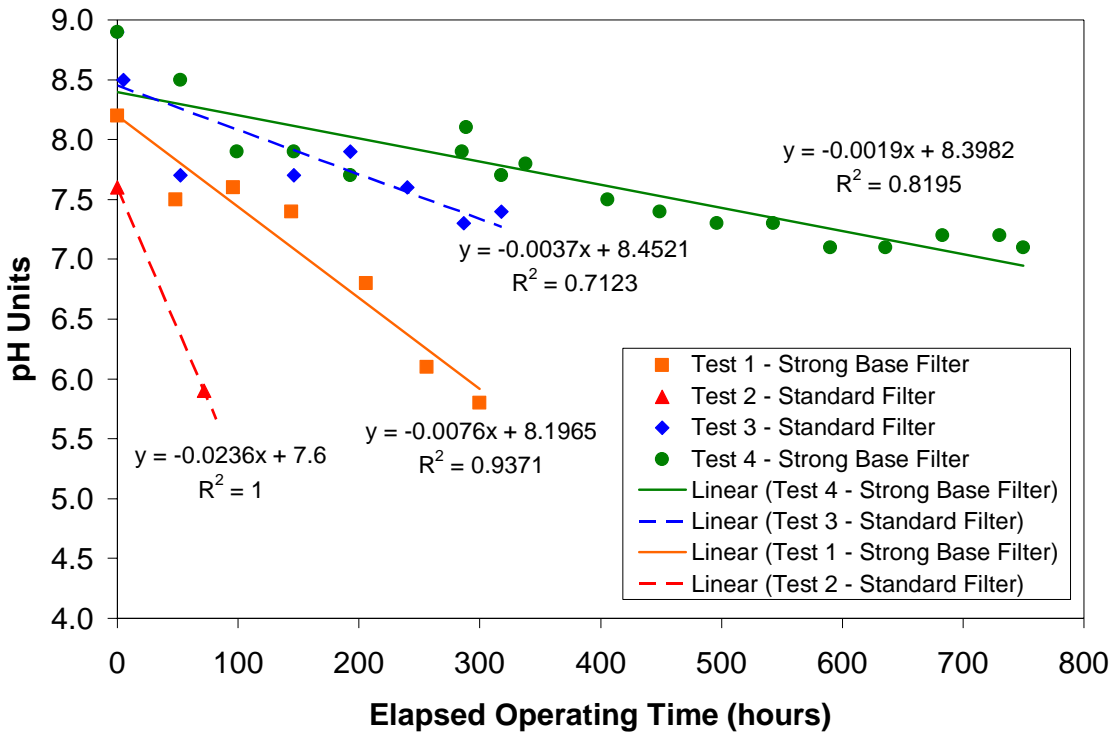


Figure 5.10 - Lubricant acidity measured in pH units.

5.5.4 Total Base Number (TBN) Retention

Total base number (TBN) is a measure of the remaining alkaline reserve in a lubricant. When acids contaminate a lubricant, they are typically neutralized by dispersant and detergent additives. A TBN of zero indicates that these additives no longer have sufficient capacity to neutralize acids. Severe corrosion and wear can result if TBN is allowed to decline below a minimum level [20]. For this reason, TBN is often used as an indicator to determine when to change the oil.

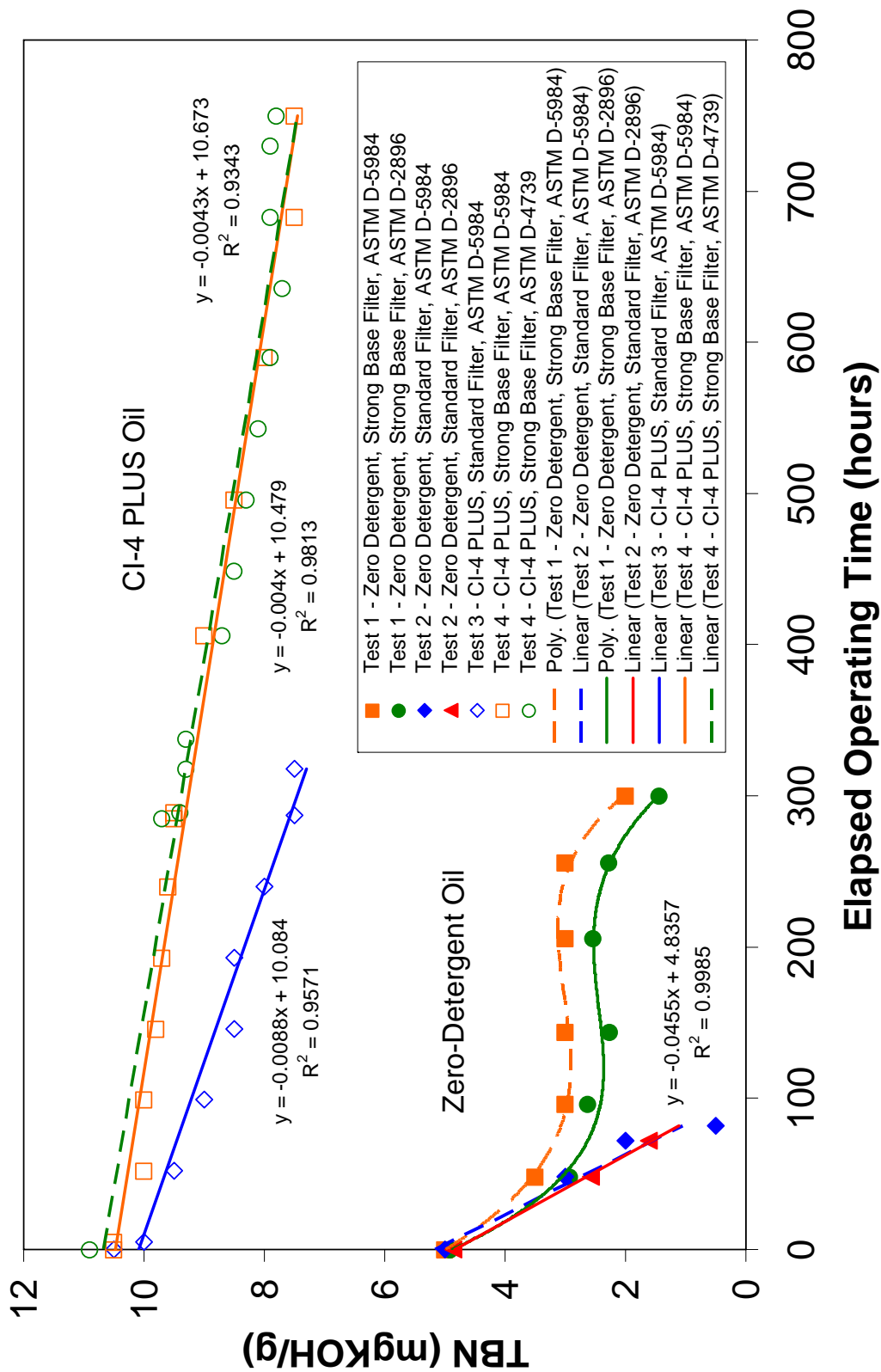


Figure 5.11 – TBN retention for the tests with the zero-detergent and CI-4 PLUS oils.

The TBN of the zero-detergent oil samples are plotted in the lower portion of Figure 5.11. Each sample was measured for TBN using two standard test methods (ASTM D-2896 and ASTM D-5984). Dispersant additives contribute the majority of the TBN in the zero-detergent oil. In these cases, the TBN measures the unused acid neutralization capacity of the dispersant.

TBN results from the tests with the zero-detergent oil give insights into a possible mechanism for acid transfer to the strong base filter. In Test 2, TBN rapidly declines as the dispersant neutralizes acids and is depleted. TBN retention is extended substantially in Test 1, when the strong base filter is used with the zero-detergent oil. There is an initial drop in the TBN as the dispersant neutralizes acids and neutral acid:dispersant complexes increase in concentration. Eventually the TBN plateaus at approximately 3 mgKOH/gram-oil. In this region, there is an approximate balance in the rate of transfer of neutralized acid from the acid:dispersant complex to the strong base in the filter and the rate of formation of acid:dispersant complex at the piston ring zone. Finally, after 250 hours a drop in the TBN is observed, which indicates that the rate of acid transfer to the filter is slowing. This decline could be caused by the consumption of neutralization sites on the filter, or by a loss of dispersancy in the lubricant. Acidic contaminants could be transferred to the strong base filter by the dispersant. The strong base filter may extend the TBN retention of zero-detergent oil by regenerating acid:dispersant complexes and absorbing acids.

The TBN of the CI-4 PLUS oil samples are also plotted in Figure 5.11. Each sample was tested with ASTM D-4739 and ASTM D-5984. These analysis methods measure the remaining capacity to neutralize strong acids, and measure the contribution mostly from the remaining unneutralized detergent. A linear curve fit to the data results in high 2 values exceeding 0.93.

The strong base filter has a large effect on TBN retention. In the tests with CI-4 PLUS oil, the rate of TBN depletion is reduced by about one half when the strong base filter is installed in the oil circuit. The over-based detergent neutralizes acids at a slower rate. The

strong base filter must be neutralizing at least half of the acidic contaminants entering the lubricant. Clearly, the strong base filter augments the acid control function of the detergent.

5.5.5 Lubricant Oxidation

Figure 5.12 plots the oxidation level of the used oil samples taken during the tests with the CI-4 PLUS lubricant. The oxidation level is measured with FTIR spectroscopy and is related to the concentration of carboxylic (organic) acids in the samples.

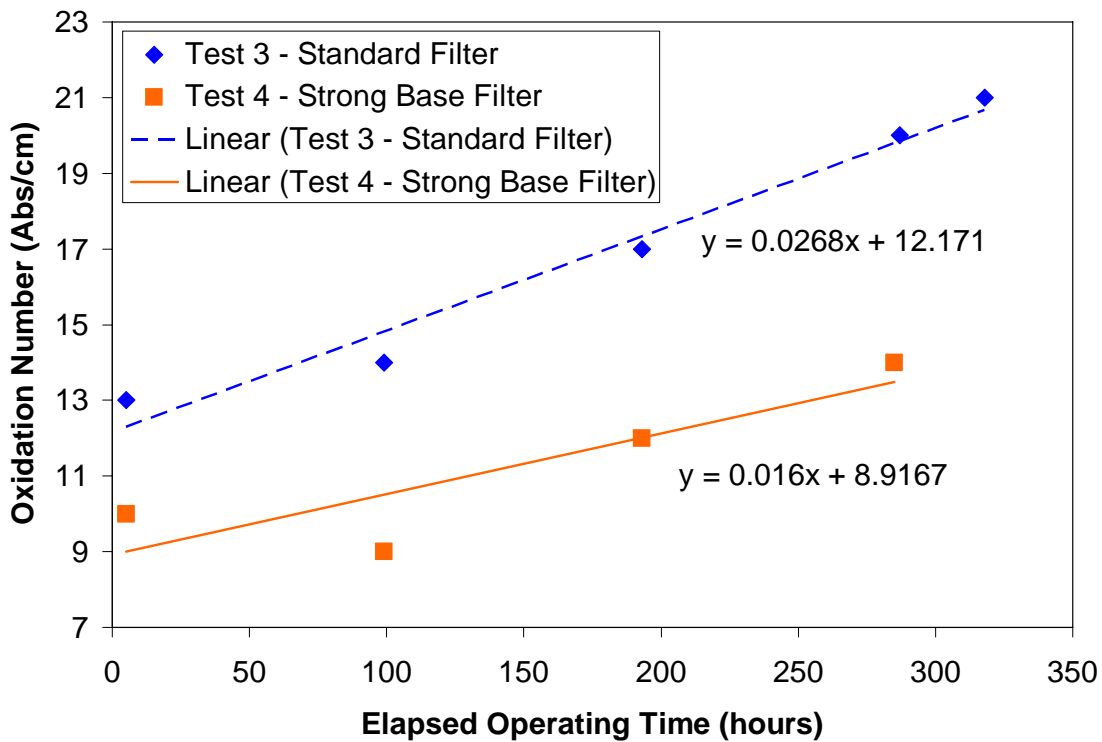


Figure 5.12 – Oil oxidation in the tests with the CI-4 PLUS oil, measured with FTIR analysis.

The concentration of organic acids increases at a slower rate with the strong base filter. This result could be caused by two effects; a lower oxidation rate due to lower acidity, or removal of carboxylic acids by the filter. It should be noted that the shift in the initial oxidation level is most likely caused by baseline shifting of the FTIR spectrum.

5.5.6 Viscosity

Viscosity is a critical property of the lubricant that affects friction and wear in the engine. It is important to maintain the viscosity of the lubricant over the duration of the oil drain interval. Viscosity increase can be caused by oxidation, soot contamination, or sludging. A large change in viscosity is often a symptom of severe oil degradation.

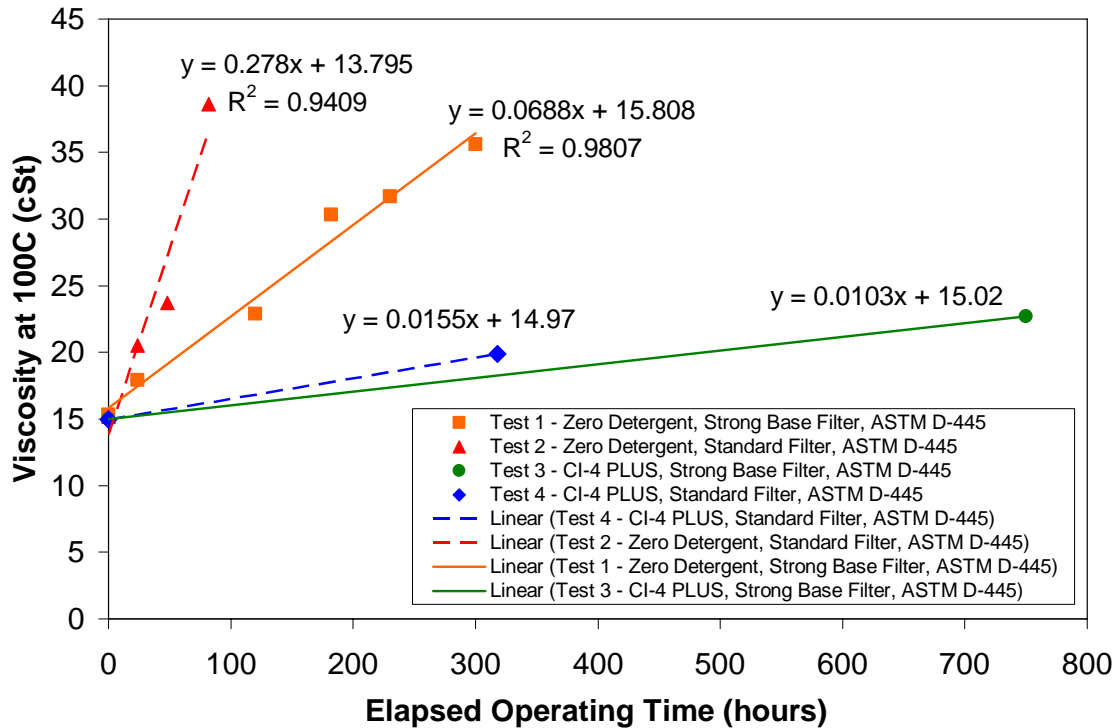


Figure 5.13 – Viscosity of zero-detergent oil samples.

The viscosity of the oil samples taken during the tests with the zero-detergent oil are graphed in Figure 5.13. There is a linear increase in viscosity to over twice the initial value in both tests. A rapid increase in viscosity is observed in Test 2, when the zero-detergent oil is used with a standard filter. A slower rate of viscosity increase is observed with the strong base filter (Test 1). The rate of viscosity increase is lowered by over two thirds with the strong base filter. Oil conditioning with the strong base filter decreases the rate of oil thickening in the zero-detergent oil tests, thereby extending the lifetime of the oil.

Viscosity measurements from the tests with the CI-4 PLUS lubricant are also plotted in Figure 5.13. The viscosity is measured at the beginning and end of the experiments. Less oil thickening is observed with the CI-4 PLUS oil than with the zero-detergent oil. This result is expected because the CI-4 PLUS oil is a fully formulated lubricant that complies with API specifications. On the other hand, the additive package of the zero-detergent oil is not optimized.

For the CI-4 PLUS tests, the rate of viscosity increase can be estimated by assuming that trend is linear. The rate of oil thickening is approximately one third lower when the strong base filter is used. The lower rate of viscosity increase with the strong base filter may be related to the lower rate of oxidation, measured by FTIR, shown in Figure 5.12. It is not believed that the difference in the rate of viscosity change is related to soot formation in that the amount of soot for the tests with either filter is not high enough to have a significant effect on viscosity.

5.5.7 Wear Metal Analysis

Antiwear and corrosion protection are essential functions of the lubricant. Adequate wear protection must be maintained over the entire oil drain interval. It is well known that wear and corrosion is reduced in lubricants with lower acidity. The strong base filter may have an indirect effect on engine wear by reducing lubricant acidity and slowing the oxidation rate. Reduced oxidation may also preserve the antiwear additive (ZDDP) in the oil.

An accepted method for monitoring engine wear is to measure the concentration of wear metals accumulating in used engine oil. Wear debris not captured by the oil filter tends to remain dispersed in the engine oil. In this study, the concentration of metallic elements in the used oil samples is measured with inductively coupled plasma (ICP) analysis (ASTM D-4951). The measured concentrations are corrected for base oil volatility by multiplying by the factor that normalizes the calcium content in the sample to the calcium content of the fresh lubricant.

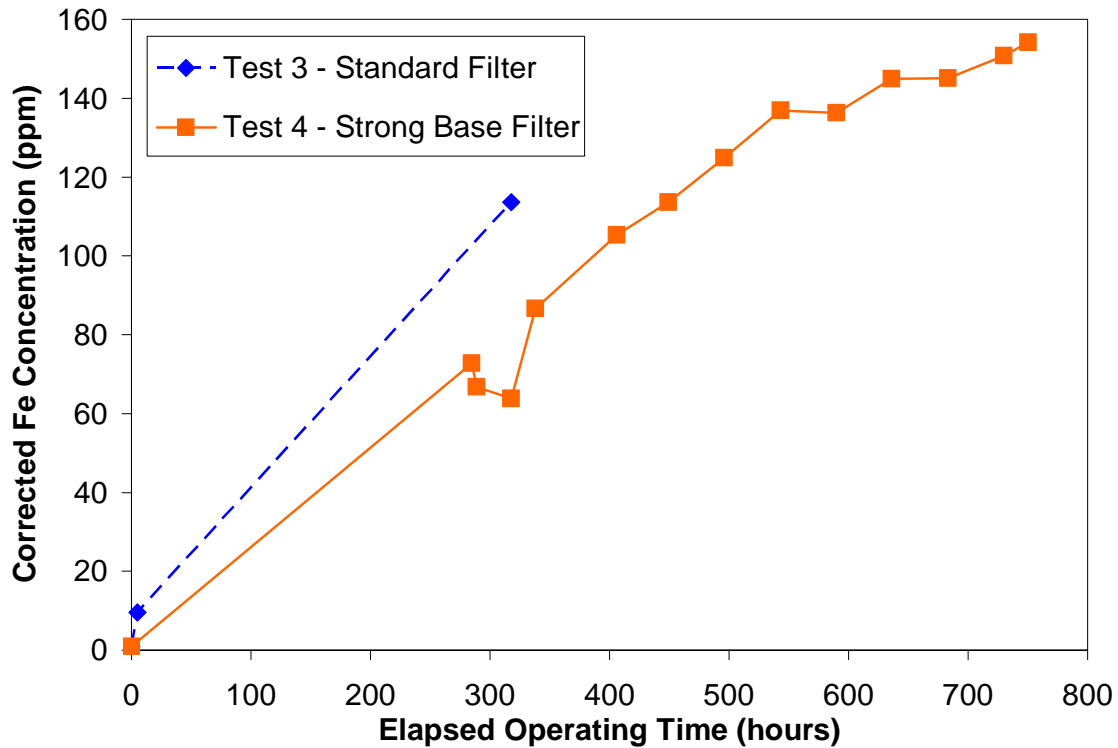


Figure 5.14 – The concentration of iron in the CI-4 PLUS oil samples measured with ICP (ASTM D5185).

Figure 5.14 graphs the concentration of iron in the used oil samples from the test with the CI-4 PLUS lubricant (Test 3 and 4). Iron is the most abundant wear metal in the used oil samples. The concentration of iron increases linearly in both tests. There is no indication of an increasing wear rate in the test with the strong base filter even though the oil drain interval is doubled. In fact, an apparent reduction in wear is seen at 318 hours with the strong base filter.

Similar levels of iron are observed in the zero-detergent oil samples (see Figure 5.15). Use of the zero-detergent oil without a strong base filter could induce catastrophic wear in the engine. An increasing rate of iron accumulation may have occurred in Test 2, although there are only a few data points to show this trend. The test with the strong base filter (Test 1) exhibits a similar trend as seen with the fully formulated CI-4 PLUS lubricant. This result suggests that the ashless antiwear additive in the zero-detergent oil is at least as effective as ZDDP in the CI-4 PLUS formulation. Although, the strong base

filter must be used with the zero-detergent oil to prevent severe corrosion and wear in the engine.

Engine bearings and piston rings are susceptible to acidic attack and corrosion. Figure 5.16 graphs the concentrations of copper and chromium in the used CI-4 PLUS oil samples. Copper accumulates in oil due to corrosion and wear of the main bearing surfaces. Chromium is most often found in the piston rings. The concentration of copper decreases in the second half of the test. This drop in the lubricant concentration is commonly observed in extended duration engine tests late in the test cycle. It is believed to be related to the low solubility of copper complexes formed when a threshold concentration of copper is reached. Again, it appears that the strong base filter prevents an increase in the wear rate over the duration of the extended test. Wear rates are also lower when the strong base filter is used.

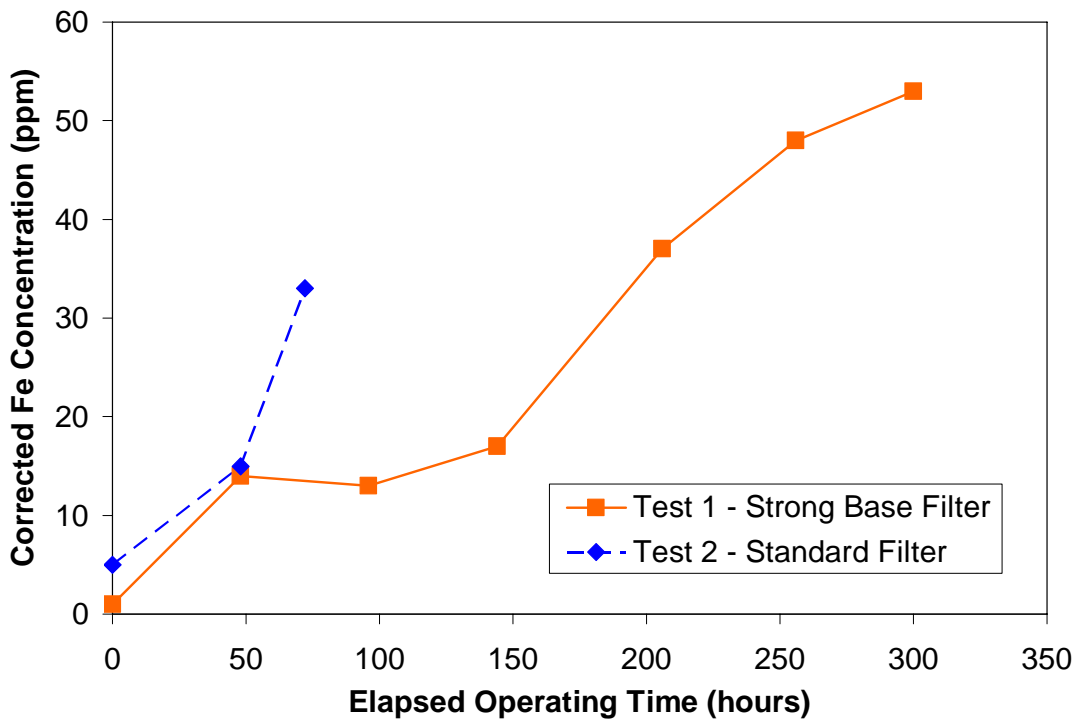


Figure 5.15 – The concentration of iron in the zero-detergent oil samples measured with ICP.

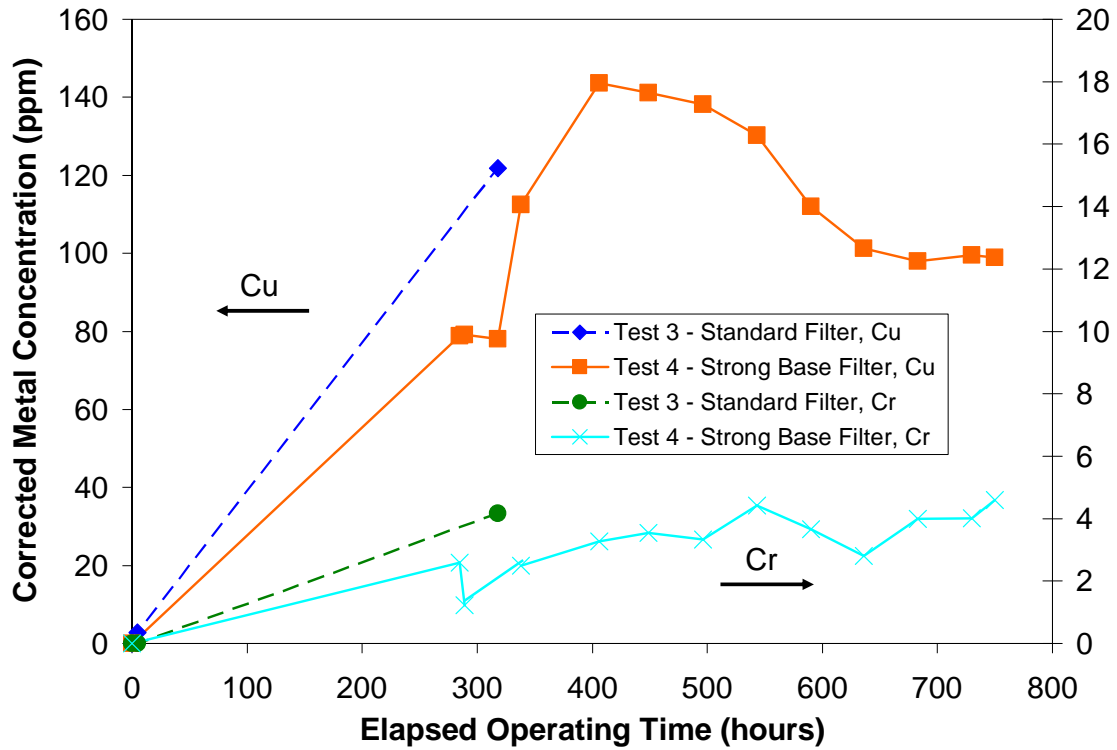


Figure 5.16 – The concentration of copper and chromium in the CI-4 PLUS oil samples measured with ICP.

The concentrations of copper and chromium in the zero-detergent oil samples are plotted in Figure 5.17. The amount of wear in the test with the zero-detergent oil and the strong base filter (Test 1) is equivalent to the amount seen in the test with the fully formulated lubricant and the standard filter (Test 3). The concentrations of copper and chromium at 300 hours in Test 1 are similar to those seen in Test 3 at 318 hours. Again, an increasing wear rate is observed in Test 2, although there are only a small number of data points to show the trend. Low rates of copper and chromium wear are observed when the strong base filter is employed with the zero-detergent lubricant.

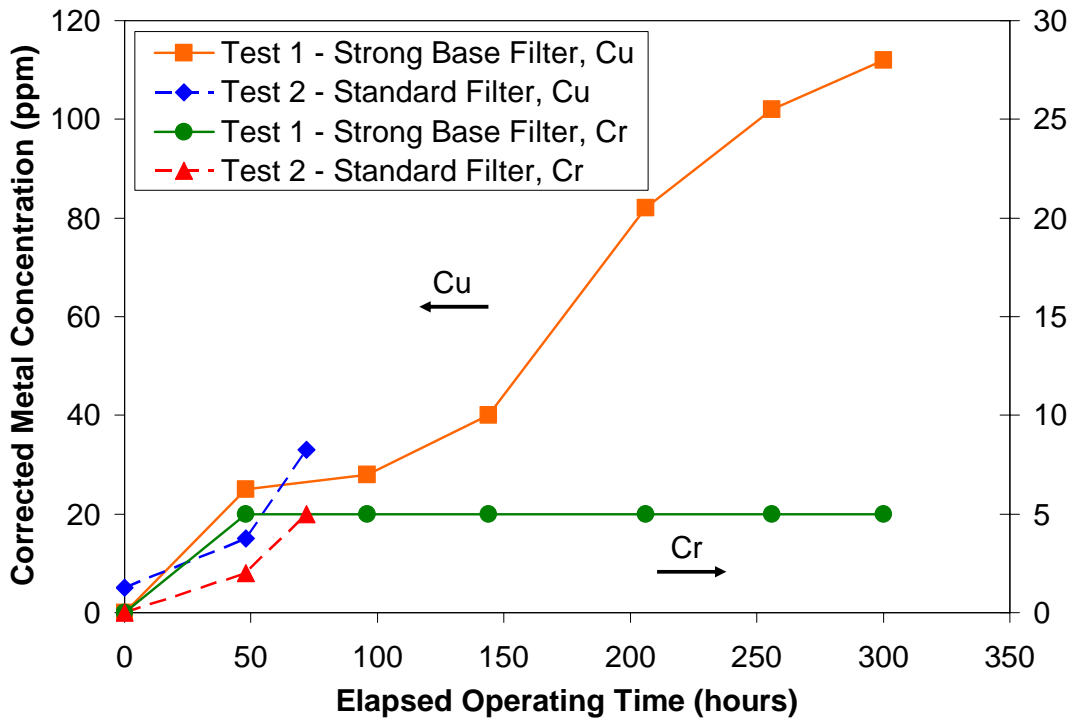


Figure 5.17 – The concentration of copper and chromium in the zero-detergent oil samples measured with ICP.

Figure 5.18 shows the concentration of tin and lead in the samples from the tests with the CI-4 PLUS oil. The lead on bearing surfaces is the most sensitive engine component to acidic attack and corrosion. Lead is worn from the bearings at a constant rate in both tests. The strong base filter prevents an increase in the wear rate of all metals over the duration of the extended test. Lower wear rates are also observed when lubricant acidity is reduced by the strong base filter.

Lead corrosion is more severe in the tests with the zero-detergent oil (see Figure 5.19). An order of magnitude increase in lead is found in the zero-detergent oil samples probably due to the increased lubricant acidity (see Figure 5.10) and a lack of corrosion inhibitors in the formulation. After more development, it may be possible to formulate a zero-detergent oil for use with the strong base filter that provides the same level of engine protection as a CI-4 PLUS lubricant.

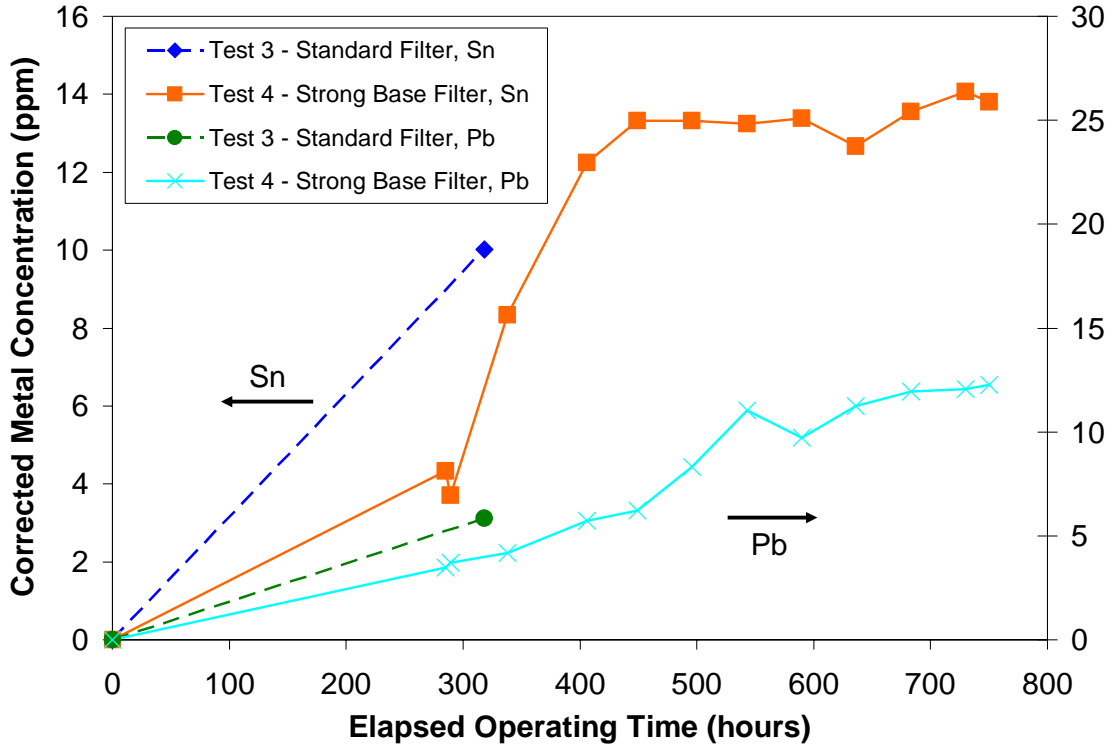


Figure 5.18 – The concentration of tin and lead in the CI-4 PLUS oil samples measured with ICP.

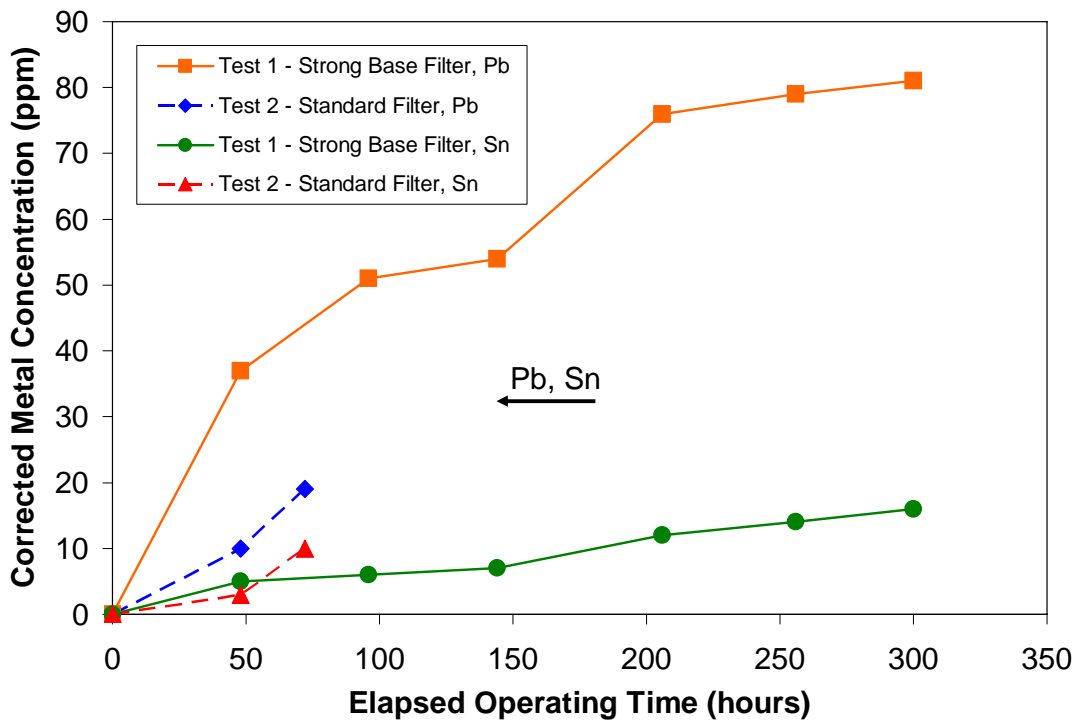


Figure 5.19 – The concentration of tin and lead in the zero-detergent oil samples measured with ICP.

5.5.8 Four Ball Wear Tests

Four ball wear tests (ASTM D-4172) are used to assess the protection against rubbing wear provided by fresh and used oils. Figure 5.20 compares the average depth of wear scars produced during four ball wear tests with the used oil. The tests were performed with used drain oil from the endpoints of the experiments, and with the fresh lubricant. It was not possible to run four ball wear tests with intermediate samples because the sample volume was inadequate. A smaller wear scar indicates that the lubricant used in the test provides better antiwear performance.

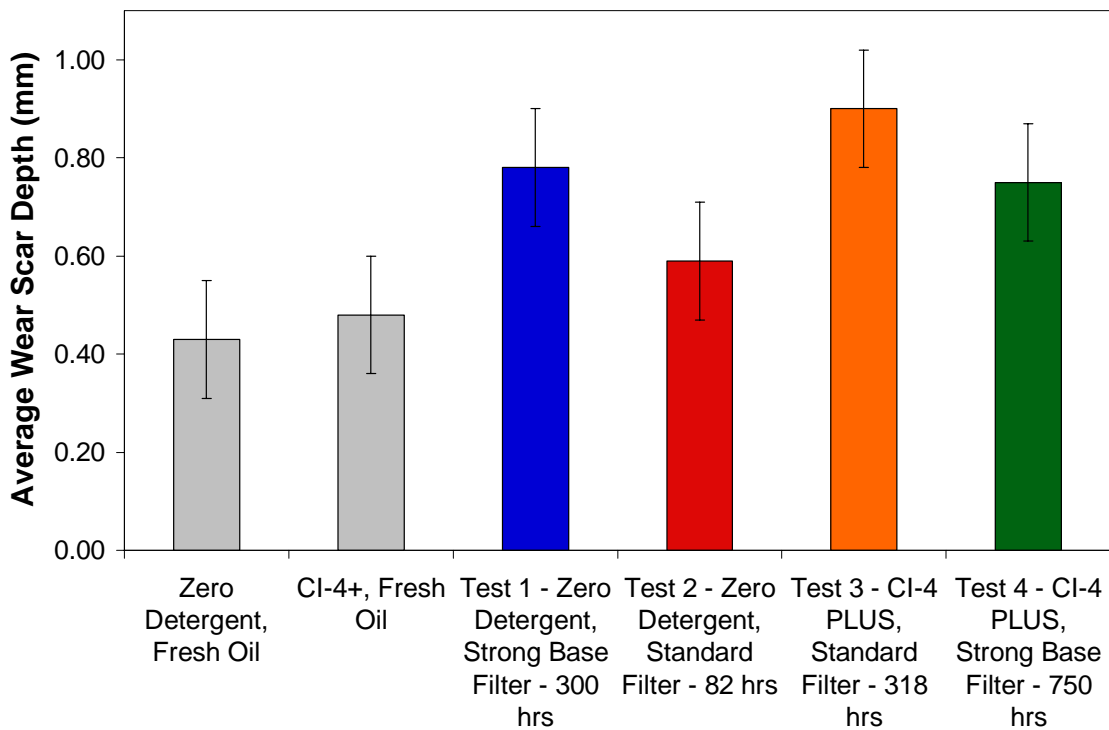


Figure 5.20 – Four ball wear test results.

With the CI-4 PLUS lubricant, the largest wear scar is observed with the used oil aged with the standard filter. Oil aged with the strong base filter offers equivalent wear protection even though the oil is aged for over twice the length of time. As expected, the fresh oil gave superior antiwear protection. This data indicates that the strong base filter may have a beneficial effect on engine wear.

In the four ball wear tests with the zero-detergent oil, the fresh lubricant offers the most protection against rubbing wear. A substantial increase in wear is observed with the oil aged for only 82 hours with the standard filter (Test 2). The deepest wear scar occurs when the oil from Test 1 is used (strong base filter, 300 hours).

An additional observation can be made by comparing the four ball wear results of Tests 1 and 3. The oil used in these tests was aged for an almost equal length of time and have approximately the same soot content (see Figure 5.7). Rubbing wear protection provided by the zero-detergent oil aged with a strong base filter (Test 1) and the CI-4 PLUS oil aged with a standard filter (Test 3) are comparable. The ashless antiwear additive in the zero-detergent oil appears to be as effective as ZDDP in these tests. This result suggests that the zero-detergent oil used with the strong base filter could provide the equivalent rubbing wear protection as a fully formulated lubricant with high sulfated ash content.

5.5.9 Filter Capacity and Efficiency

When the engine tests were terminated, the strong base filters were evaluated for particle removal capacity and efficiency using ISO 4548-12 (1st Edition 2000). In the tests utilizing the zero-detergent lubricant, the usable contaminant holding capacity of the strong base filter had been reached and the filter was considered spent. This result is typical of a filter exposed to a lubricant which has reached the end of its useful life. In the tests using the CI-4 plus lubricant, the filter displayed a Beta ratio of 10 (90% efficient) for particles larger than 15 microns at the termination of the filter test (10 psi). More than half of the total contaminant holding capacity of the filter remained.

5.6 ANALYSIS OF RESULTS

Under the test conditions used in this study, the strong base filter had a significant effect on lubricant properties. Lubricant conditioning via the strong base in the filter lowered lubricant acidity, extended the base reserve, reduced oxidation and improved wear and corrosion protection.

The results show that the strong base filter enhances the acid control function typically performed by over-based detergent additives. A portion of the acidic contaminants entering the lubricant are absorbed by the strong base filter. The acid absorption rate is dependent on a number of factors, including reaction kinetics, acid type and the formulation of the sump oil. The fraction of acids in the lubricant absorbed by the strong base filter can be estimated from the results of this study.

It may be possible to use the acid absorbing capacity of a strong base filter as a substitute for the over-based detergent in a lubricant. This lower ash oil would reduce the rate of ash accumulation in DPFs and could potentially reduce piston deposits as demonstrated in the 1G2 tests reported in [101]. The results of the current study also show that oil conditioning has the potential to extend oil drain intervals. The strong base filter improves TBN retention of fully formulated lubricants, reduces TAN, improves viscosity and could have a beneficial effect on corrosion and wear.

5.6.1 Proposed Mechanism

A mechanism for the action of a strong base filter has been previously proposed [101]. The authors propose that the strong base filter sequesters acids from a neutralized combustion acid-dispersant complex and unneutralized weak acids. The proposed acid transfer mechanism is illustrated in Figure 5.21. The majority of acids enter the lubricant in the piston ring zone. In this region, the oil is exposed to acidic combustion gases and high temperatures (greater than 250°C) that induce severe oxidation rates. Polar acidic contaminants in the oil are temporarily neutralized by dispersant additives. This

interaction between the weak base and the acid creates neutral dispersant-acid complexes that are soluble in the oil. A fraction of these salts may be transported to the filter where the acid could be transferred to the strong base and be immobilized on the filter surface. In the process, the dispersant additives would be restored and released to travel back to the piston ring zone, where they neutralize more acids.

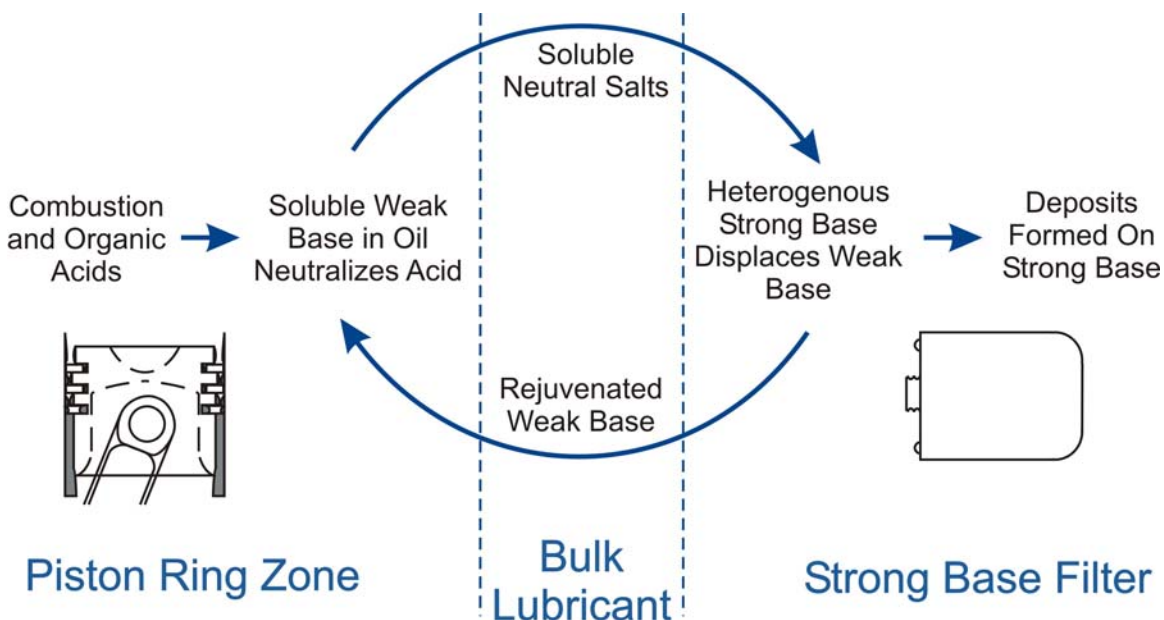


Figure 5.21 – The proposed mechanism for acid transfer to the strong base filter.

This cyclic process maintains the dispersant concentration in the oil and extends the alkaline reserve provided by over-based detergents. The filter may also reduce the lubricant acidity by neutralizing weak organic acids. Filter conditioning could decrease the rate of lubricant degradation and extend the lifetime of the oil.

The results of this study are consistent with this proposed mechanism. The strong base filter is the only source of strong base reserve for the zero-detergent oil system used in this study. It absorbs acids transferred to the filter surface by the dispersant additives. Acid transfer to the filter rejuvenates the dispersant in the lubricant. Figure 5.11 plots the TBN of the zero-detergent oil with and without filter conditioning. In these cases, the available dispersant additives contribute the majority of the TBN in the oil. There is a

plateau in the data in the case with the strong base filter. In this region, the rate of acid neutralization by the dispersant must be approximately equal to the rate of acid absorption on the filter. The majority of acidic contaminants in the zero-detergent oil are neutralized by the strong base filter.

Over-based detergents are most often used as a strong base reserve in fully formulated diesel lubricants. The detergent competes with the strong base in the filter to neutralize acids when the filter is used with a fully formulated lubricant. The fraction of acids absorbed by the filter depends upon the relative transfer rates of acid to the filter and the detergent. The difference in the slopes of the CI-4 PLUS curves in Figure 5.11 show that, in this study, approximately half of the acid typically neutralized by the detergent is removed from the lubricant by the strong base in the filter.

Acidic contaminants are more likely to be absorbed and neutralized by the filter when favorable kinetics conditions exist and when the contaminants are weak organic acids. The results also indicate that the strong base filter slows the weak-acid induced auto-catalytic nature of the oxidation process.

5.6.2 Effect On Lubricant Acidity

Oil conditioning with the strong base filter lowers lubricant acidity and improves TBN retention. The filter absorbs acids from the lubricant, and may regenerate acid:dispersant complexes. Under the test conditions used in this study, the rate of acid absorption appears to be approximately equal to the neutralization rate of over-based detergent additives. In addition, the strong base filter appears to have a higher affinity for weak acids (i.e. oxidation by-products) than does the detergent.

5.6.2.1 Proposed Acid Transfer Mechanism

Based upon prior proposals, it seems reasonable that acidic contaminants are initially neutralized by dispersant additives, a reaction that forms soluble neutral salts in the bulk

lubricant. The consumption of dispersant additives is manifested as a drop in TBN during the zero-detergent oil test with the strong base filter (see Figure 5.11). An initial drop in TBN occurs as the dispersant is consumed and the concentration of neutral dispersant-acid complexes increases. The neutralization of acids by this weak base is essential to prevent corrosion of engine components, especially in the piston ring zone.

The strong base filter may regenerate acid:dispersant complexes by displacing the weak base and absorbing the acid on the filter surface. The rate of dispersant regeneration and acid absorption accelerates with increasing concentration of dispersant-acid complexes in the oil. The plateau in TBN (see Figure 5.11) occurs perhaps when the rate of dispersant regeneration is equal to the acid neutralization rate.

The transfer of acids to the strong base filter should continue as long as unneutralized base is available on the filter surface and free dispersants are present in the oil to neutralize acid. The strong base in the filter can be consumed by neutralization, or physically blocked by particles filtered from the oil. Dispersants are depleted by the formation of associations with other contaminants in the lubricant (e.g. soot). The sequestration capacity of the strong base filter limits the duration of its effectiveness. Experiments to determine the lifetime of the filter were beyond the scope of this study.

5.6.2.2 Acid Neutralization Rate

The results also give insights into the rate of acid neutralization on the filter surface. The acid absorption rate is a key performance measure for the filter. Figure 5.11 shows that approximately half of the acids normally neutralized by detergent additives are absorbed by the strong base filter. This result implies that the rate of acid transfer to the strong base filter must be approximately equal to the rate of neutralization by the detergent additives. The physical characteristics of the strong base in the filter enhance its receptivity to acid. A high transfer rate is ensured by reducing steric hindrance between acids and the strong base, and by maximizing the surface area of the reactive surface.

Steric hindrance affects the rate of acid-base reactions in lubricants. Colloidally dispersed over-based detergent additives consist of a kernel of strong base surrounded by a surfactant shield. Similarly, polar contaminants in the lubricant are also encircled by dispersant additives. These layers create a steric hindrance to reactions between the acids in the lubricant and the base in detergent additives. The reaction rate between acids and the soluble base is reduced.

The construction of the strong base filter may reduce steric hindrance between the reactants. Absence of the surfactant shield on the filter surface may reduce the effect of steric hindrance and increase the reaction rate on the strong base filter. Surface area is another factor affecting the reaction rate. The strong base filter is constructed to maximize the area of the reactive surface and maximize contact between the lubricant and the strong base. The combination of a low steric hindrance and a high surface area in the filter results in a rate of acid transfer and neutralization almost equal to that seen with detergent additives.

5.6.2.3 Neutralization of Oxidation By-Products

It is well known that typical detergent additives react less completely with high molecular weight organic acids [102]. Detergent additives react more readily with the more acidic combustion acids [10, 102]. Accumulation of organic acids in the lubricant is often a primary factor that triggers an oil change.

The results of this study suggest that organic acids are more readily neutralized by the strong base filter than by detergent additives. TAN measurements (see Figure 5.9) show that the concentration of unneutralized acids (mostly organic acids) is lower when the strong base filter is utilized. The pH data (see Figure 5.10) confirms this result.

The oxidation data from the tests with the CI-4 PLUS oil (see Figure 5.12) shows that the filter absorbs oxidation by-products. It is reasonable to assume that the base oil oxidation rates in both tests were similar because the mean oil temperatures were equal. The

reduced acidity levels seen in this study can only occur if the strong base filter is absorbing oxidation by-products that are not normally neutralized by detergent additives. An enhanced ability to neutralize organic acids is beneficial in modern diesel engines where oil oxidation and lubricant acidity are important concerns. Engines fitted with advanced emission control systems are fueled with ultra-low-sulfur diesel fuel, so the exposure of the lubricant to sulfuric acid is drastically reduced by over 90 percent. However, these engines typically employ high EGR rates, which give a greater opportunity for combustion acids to mix with the lubricant. More critically, EGR increases the temperature of the lubricant and accelerates the oxidation rate [10]. A strong base filter with an enhanced ability to neutralize organic acids is particularly well suited for use in engines employing emission control technology.

The widespread use of bio-diesel increases the importance of a means to neutralize weak organic acids because biodiesel has a measurable TAN and because it hydrolyzes in the sump to produce additional weak organic acids [103]. The results of this study indicate that the strong base filter absorbs the acids originating from biodiesel dilution of the oil.

5.6.3 Effect on Lubricant Viscosity

Oil conditioning with the strong base filter reduced oxidation and slowed the rate of viscosity increase. Lower viscosity was observed in the tests with the fully formulated lubricant and the zero-detergent oil (see Figure 5.13).

Lubricant thickening occurs due to oxidation, polymerization of the base oil and by soot contamination. Higher lubricant acidity causes more severe oxidation in the absence of antioxidants. The strong base filter decreases the rate of viscosity increase by sequestering acids and lowering lubricant acidity. This effect is apparent during the tests with the zero-detergent oil (see Figures 5.9 and 5.13). There is a rapid increase in lubricant acidity and viscosity during the test with the standard filter (Test 2). Oil conditioning with a strong base filter substantially lowers lubricant acidity and slows the rate of viscosity increase.

Soot contamination is another important cause of oil thickening and may determine the timing of an oil change. In this study, the strong base filter appears to have no measurable effect on the amount of soot in the lubricant (see Figure 5.7); however, it may improve dispersancy by absorbing acidic contaminants and regenerating dispersants.

5.6.4 Effect on Corrosion and Wear

The results of this study indicate that corrosion and wear has the potential to be reduced in engines fitted with a strong base filter. Less wear than expected occurred in four ball wear tests performed with oil conditioned by the strong base filter (see Figure 5.20). Lower concentrations of wear metals were also found in used oil conditioned by the strong base filter (see Figure 5.14-5.19). Corrosion occurs in regions where the lubricant is acidic. Lubricant acidity is reduced with the strong base filter. This effect inhibits corrosive wear.

In four ball tests with the fully formulated lubricant, the oil aged with the strong base filter demonstrated equivalent antiwear performance to the oil aged with the standard filter (see Figure 5.20). This result was especially surprising because the oil used with the strong base filter was aged for over twice the length of time (750 hours versus 318 hours). In addition, wear metal analysis showed no increase in the wear rate over the duration of the extended test.

One possible explanation for this result is that oil conditioning preserves the antiwear additive in the lubricant. ZDDP is a dual purpose additive, protecting engine components from wear and functioning as an antioxidant. It is consumed by oxidation of the lubricant. Oil conditioning decreases the rate of oxidation. Therefore, it is reasonable to expect that more ZDDP is available for antiwear protection in the used oil conditioned by the strong base filter.

5.6.5 Effect on Aftertreatment System Durability

Under the test conditions used in this study, the strong base filter is capable of performing the acid neutralization function of over-based detergent additives. This capability may be used in a zero-detergent oil system to provide a strong base reserve for the neutralization of acids. A zero-detergent lubricant contains no metallic compounds that contribute to ash; the substance that fouls aftertreatment systems.

An experimental zero-detergent lubricant is tested in this study. Rapid oil degradation occurs when this oil is used with a standard filter. Severe corrosion and wear would damage the engine after only a short period of time. Lubricant conditioning with the strong base filter has a substantial effect on the rate of oil degradation. The results are promising, although more development and testing is required to create a zero-detergent lubricant with the same level of engine protection as a fully formulated lubricant.

The beneficial effects of filter conditioning on the zero-detergent oil are demonstrated in Tests 1 and 2. TBN is preserved by the absorption of acids on the filter surface and the regeneration of dispersant additives. TAN is reduced because the filter has an affinity for weak organic acids. The rate of oil thickening is also reduced. Four ball wear tests also suggest that in these experiments, the zero-detergent oil aged with the strong base filter has the equivalent antiwear performance as the CI-4 PLUS oil aged with a standard filter. Several concerning trends were also apparent in the results. Higher lubricant acidity was observed in all of the tests with the zero-detergent oil. Higher concentrations of lead were found in the used oil samples; a condition that indicates the onset of bearing corrosion. An unacceptable increase in viscosity also occurred in the tests with the zero-detergent oil. These problems can most likely be corrected by altering the formulation of the oil.

5.6.6 Effect on Oil Drain Interval

The results of this study suggest that the strong base filter may be used to extend oil drain intervals in diesel engines employing lubricants with high sulfated ash levels. The filter

provides additional alkaline reserve to the engine and reduces lubricant acidity. These effects delay the point when TAN exceeds TBN in the lubricant, a situation that often triggers an oil change [20]. Lower acidity levels also delay the onset of autocatalytic oxidation in the oil and reduce corrosion of engine components. These benefits may extend the lifetime of engine oil.

The results of this study show that oil conditioning with a strong base filter could be used as a means to minimize lubricant ash requirements and extend oil drain intervals.

5.7 CONCLUSIONS

An innovative filter technology that sequesters acidic contaminants in the lubricant was tested in this study. Four long duration engine tests were performed to investigate the effect of filter conditioning on the lubricant degradation. The following results were obtained:

- Under the test conditions used in this study, the strong base filter had a significant and beneficial effect on the rate of oil degradation.
- The strong base filter reduced lubricant acidity by absorbing acidic contaminants in the lubricant.
- There was a substantial improvement in TBN retention.
- From the relative slopes in the TBN results, it may be concluded that the rate of acid transfer to the strong base filter was approximately equal to the rate of neutralization by detergent additives.
- An apparent directional difference in engine wear and corrosion was observed with the strong base filter, based upon metal concentrations.
- The zero-detergent oil (formulated with ashless antiwear additives) and the CI-4 PLUS oil provide similar levels of wear protection after aging with the strong base filter.

- The benefits of filter conditioning could be used to extend oil drain interval, or lower lubricant ash requirements, which would result in improved aftertreatment system durability.

(This page intentionally left blank)

CHAPTER 6 – CONCLUSIONS AND RECOMMENDATIONS

6.0 CONCLUSIONS

This thesis examined the in-engine sources for lubricant-derived ash found in diesel aftertreatment systems. A novel oil filter technology was also demonstrated that has the potential to significantly reduce additive requirements in oil, and the related emissions of ash-related elements.

The distribution and composition of ash-related elements in the engine was measured in sampling experiments and with in-situ measurements of lubricant composition. A novel diagnostics system, employing FTIR-ATR spectroscopy, was developed to obtain in-situ measurements of lubricant composition at the piston and liner interface.

A modeling effort complemented the experimental work and served to demonstrate the mechanisms for the emission of metallic elements into the exhaust. A model framework of lubricant composition changes in the power cylinder system was shown to be in reasonable agreement with the measurements obtained during the sampling experiments. This work will assist lubricant formulators in the development of diesel engine oils that adequately protect engine components, while minimizing impact on aftertreatment systems.

6.0.1 In-Engine Distribution and Transport of Ash-Related Species

In the first chapter of this thesis, the sources of lubricant-derived ash were explored with sampling experiments and in-situ measurements of lubricant composition in a single cylinder diesel engine. Samples were obtained from the three regions in the engine to determine the distribution of ash-related elements.

Experiments with a ring pack sampling system showed that all of the metallic elements found in DPF ash are concentrated in the top ring zone (TRZ). The metallic elements

found in detergent additives (calcium and magnesium) are concentrated to a higher degree than the elements in ZDDP (zinc and phosphorus). These variations in the enrichment of metallic species were caused by differences in the volatility of additive compounds. For instance, the thermal degradation of ZDDP at high temperatures increased the rate of zinc and phosphorus volatilization from the piston ring pack.

Measurements of lubricant composition with a novel in-situ FTIR system at the piston and liner interface showed that the lubricant in the TRZ is more severely oxidized than the sump oil. It is also heavily contaminated with sulfates, nitrates and combustion acids. In tracer experiments, the residence time of oil in the piston ring zone was estimated to be between one to three minutes.

An elemental ash balance for ash-related elements showed that deposition is not a significant sink for ash-related elements in the engine. A large portion of the calcium and zinc accumulates in the sump oil due to preferential volatilization of light end hydrocarbons in the base oil. The results from the sampling experiments were analyzed to obtain estimated emission rates for ash-related elements. Emissions of calcium result in the majority (approximately 70%) of ash found in DPFs.

In the final part of the chapter, the understanding derived from the sampling experiments was incorporated into a framework to model the distribution and transport of ash-related species in the power cylinder. The model formulation fit experimental results to a reasonable degree of accuracy. This tool may be used in future work to design lubricants with reduced impact on aftertreatment systems.

6.0.2 Filter Conditioning as a Potential Means to Reduce Additive Requirements

In the second chapter of this thesis, a novel filter technology was demonstrated that sequesters acids in the lubricant without releasing any compounds into the oil. The strong base filter immobilizes combustion acids and oxidation by-products on the filter paper as

the oil passes through it in the main oil circuit of the engine. This system has the potential to supplement, or replace detergent additives, the primary source of ash in DPFs.

Long duration engine tests demonstrated the effects of filter conditioning with the strong base filter. The filter was effective with both a fully formulated CI-4 PLUS oil and an experimental lubricant containing no detergent additives. The strong base filter significantly reduced lubricant acidity over the duration of the tests. It also improved the TBN retention of engine oil. Measurements of lubricant oxidation and viscosity confirmed that the strong base filter reduces the rate of oil degradation. There is also some evidence the filter has a beneficial effect on engine wear.

From an analysis of the results, a proposed mechanism for the operation of the strong base filter was proposed. The filter appears to regenerate weak bases (i.e. detergent additives) in the lubricant by an ion exchange at the filter surface, which results in the absorption of acids. The restored base is free to return to the piston ring zone and neutralize more acidic species. This process may be used to supplement or replace detergent additives in lubricant formulations. Use of the strong base filter is a potential means to reduce additive requirements in lubricant formulations and the related ash emissions from diesel engines.

6.1 RECOMMENDATIONS

The following three actions are recommended to OEMs and lubricant formulators, based on the analysis of the results. These measures have the potential to significantly reduce the emission of ash-related species from the engine and limit the mass of lubricant-derived ash that collects in aftertreatment systems:

1. *Focus on reducing the rate of loss of unvaporized oil and concentration of ash-related species of oil in the piston-ring-zone* – The results of this and several other studies clearly show that emissions of lubricant-derived ash are a direct result of both oil consumed and the composition of oil at the point of loss. The majority of ash

emissions are caused by consumption of liquid oil in the piston ring pack, where additive metals are concentrated. Concentration of additive metals in the piston ring zone (PRZ) can be reduced by more rapid fresh oil replenishment to the PRZ and by lower base oil volatility. Liquid oil consumption is also the only mode for calcium to enter the exhaust. The measurements taken during this thesis show that calcium sulfate is approximately 70 percent of the ash expected in DPFs.

2. *Investigate the possibility of further reducing calcium detergents in lubricant formulations* – As stated above, calcium is the source of the vast amount of ash found in DPFs. There would be significant reductions in ash emissions if detergents were removed from lubricant formulations. Although, the detergent performs an essential function in the oil that cannot be easily replaced with other additive compounds. Drastic reductions in oil change intervals and engine protection would result from the removal of detergents from engine oil. Alternatives for the detergent, such as the strong base filter or ashless detergents, must be developed to supplement or replace detergent additives in lubricant formulations.
3. *A more representative alternative to the Sulfated Ash test (ASTM D874) is needed to characterize the potential impact of lubricant formulations on aftertreatment systems* – The results this study show that the sulfated ash measurement does not correlate well with the emissions of ash-related elements from lubricants. The test consistently over estimates potential ash emissions. Sulfated ash also has a different composition from the ash found in DPFs (i.e. Boron is contained in sulfated ash, but has never been found in DPF ash). As a result, the concentration of beneficial additives that do not contribute to DPF ash are constrained by the sulfated ash requirements in lubricant specifications. A more representative test method will help formulators create lubricants that are optimized for enhanced protection of engine components, while also minimizing the impact on DPFs. One possible alternative to the sulfated ash test is described below. The proposed test is based on the ideas developed in this thesis.

6.1.1 Percent Ash Measurement

One of the recommendations of this study was the development of a more representative test to characterize the impact of lubricant formulations on aftertreatment systems. This section describes a test procedure, called the percent ash measurement, which could be used as an alternative to sulfated ash (ASTM D874).

Sulfated ash overestimates the potential ash emissions from a lubricant in large part because the procedure neglects the specific emission rates of ash-related elements. Sulfated ash also has a different chemical composition than the ash typically found in aftertreatment systems. For instance boron contributes to sulfated ash, but has never been found in the ash that collects in DPFs. In fact, the results in this study show that the sulfated ash test overestimates ash by over 30 percent. These discrepancies restrict the ability of lubricant formulators to develop lubricants with enhanced properties, or lengthened oil drain intervals.

The percent ash measurement combines an analytical procedure with performance tests. The contribution to DPF ash of each additive in the lubricant is assessed, and then combined to estimate the potential ash from a lubricant formulation. The ash intensity, $\%Ash_{additive}$, of each additive can be determined with the following calculation:

$$\%Ash_{additive} = \left(\begin{array}{c} wt\%_{element} \\ \times \text{Emission Rate}_{element} \\ \times \text{Ash Composition Factor}_{element} \end{array} \right) \quad (6.1)$$

Where the subscript, *element*, refers the ash-related element in the additive that is captured by the DPF. This formulation accounts for the contribution of each additive to DPF ash due to the concentration of the associated ash-related element in the fresh lubricant, the ash emissions of associated ash-related elements and the composition of the ash in the DPF. The concentration of the associated ash-related elements in the fresh lubricant may be determined with ICP analysis. The elemental emission rate may be determined from long duration engine tests similar to the ones conducted in this study. Finally, the ash composition factor may be determined by analyzing the composition of

ash produced from accelerated ash loading experiments. Experiments can be performed using the apparatus developed by [37] and a lubricant containing only the additive of interest. Table 6.1 lists additives that are known to contribute to DPF, the associated elemental emission rate and the ash composition factor.

Table 6.2 compares the sulfated ash and percent ash measurements for the lubricants used in this study. The percent ash measurements are consistently lower than the sulfated ash values. The procedure also reveals differences between the lubricant formulations even for the oils with 1.0 percent sulfated ash.

Table 6.1 – Parameters Used in a Percent Ash Calculation for Selected Additives

Additive	Associated Ash Compound	<i>element</i>	Elemental Emission Rate ($\frac{\text{g}_{\text{element}}}{\text{g}_{\text{element}}}$)	Ash Composition Factor ($\frac{\text{g}_{\text{ash}}}{\text{g}_{\text{element}}}$)
Calcium Detergent	CaSO ₄	Calcium	0.697	3.40
ZDDP with only Calcium Detergent	Zn ₃ (PO ₄) ₂	Zinc	0.869	1.98
ZDDP with Magnesium Detergent	Zn ₂ Mg(PO ₄) ₂	Zinc	0.869	2.64

Table 6.2 – Comparison of Sulfated Ash and Percent Ash Measurements

Oil	A	B	C	D	E	F
Sulfated Ash (%)	1.41	1.00	1.00	1.35	1.00	0.057
Percent Ash (%)	0.889	0.713	0.824	0.933	0.805	0.000

6.2 RECOMMENDATIONS FOR FUTURE WORK

While the contents of this thesis advances knowledge of lubricant interactions in diesel engines and emissions of ash-related species, there are several opportunities for future work in these areas.

6.2.1 In-Situ FTIR Measurements of Lubricant Composition

In this thesis, a novel FTIR system was developed for in-situ measurements of lubricant composition at the piston liner interface. The system was demonstrated in steady state and tracer experiments.

In the future, the FTIR system may be used to evaluate new lubricant formulations with reduced concentrations of additives. For instance, it is expected that there would be increased oxidation in the piston ring zone if only detergent and ZDDP levels were lowered in lubricant formulations. Carefully balanced formulations with increased concentrations of ashless additives can be developed to control lubricant degradation. However, ashless additives are typically less cost effective and less developed than traditional additives. The in-situ FTIR system may be used in parametric experiments to find the minimum levels of additives required to control oxidation in the piston ring zone.

6.2.2 Lubricant Species Distribution and Transport Model

The formulation developed during this thesis to model lubricant species distributions and transport in the power cylinder matched experimental measurements reasonably well. To improve the accuracy and utility of the model, several phenomena could be added to the model formulation.

The current model represents that piston ring pack as a single zone with a uniform lubricant composition. In reality, this region of the engine contains several distinct volumes with varying amounts of oil. The lubricant also interacts with combustion and blow-by gases, and flows between volumes on the piston surface and cylinder liner.

The model could be reformulated to include a multi-zone representation of the piston ring pack (see Figure 6.1). This approach has already been implemented by [63] to model base oil volatilization from the ring pack.

A more challenging project involves modeling the transport of lubricant between all of the zones in the ring pack and liquid oil consumption. Possible mechanisms for oil transport in this region include inertia, gas dragging, ring pumping, ring scraping and ring carrying along the cylinder liner. The paths for flows between the zones include the piston lands, through the ring grooves, through the ring gap and along the liner. All of these aspects should be modeled for an accurate representation of lubricant composition in the piston ring pack. These additions should improve the accuracy of model output.

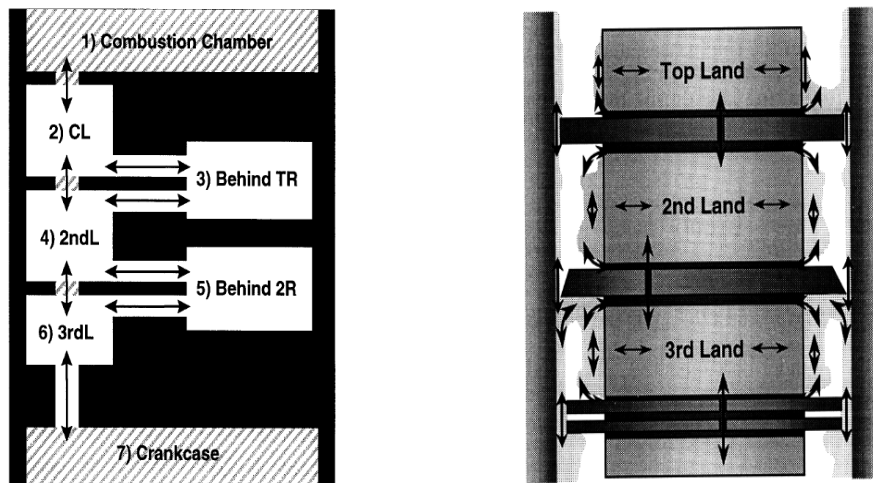


Figure 6.1 – Left - A schematic of a multi-zone representation of the piston ring pack.
Right - The modes for oil transport through the piston ring pack [96].

6.2.3 Lubricant Conditioning with the Strong Base Filter

In the experiments performed during this thesis, the strong base filter demonstrated that it is effective and it absorbs acids in the lubricant. The carefully controlled experiments also showed that that the novel technology has the potential to supplement, or replace detergent additives in lubricant formulations.

In future experiments and field tests, the strong base filter should be evaluated on multi-cylinder engines with large oil sump capacities. It should also be shown that the filter has sufficient capacity to remove large contaminants (i.e. dirt, agglomerations of soot, wear shards) from the oil over an extended drain interval.

The zero detergent oil formulated for this study was formulated solely for experimental use. A great deal of development is required before a lubricant containing no detergent can be used in conjunction with the strong base filter, to ensure adequate engine protection.

6.2.4 In-Situ Raman Spectroscopy

Raman spectroscopy is a technique used to study the vibrational, rotational, and other low-frequency modes in a system. Spectra result from inelastic, or Raman scattering, of monochromatic light generated by a laser. Most Raman systems use lasers in the visible (512 nm and 785 nm), or near-infrared range (1064 nm). The information that can be obtained is similar to FTIR spectroscopy, and in some cases can be complementary due to resonances with some samples.

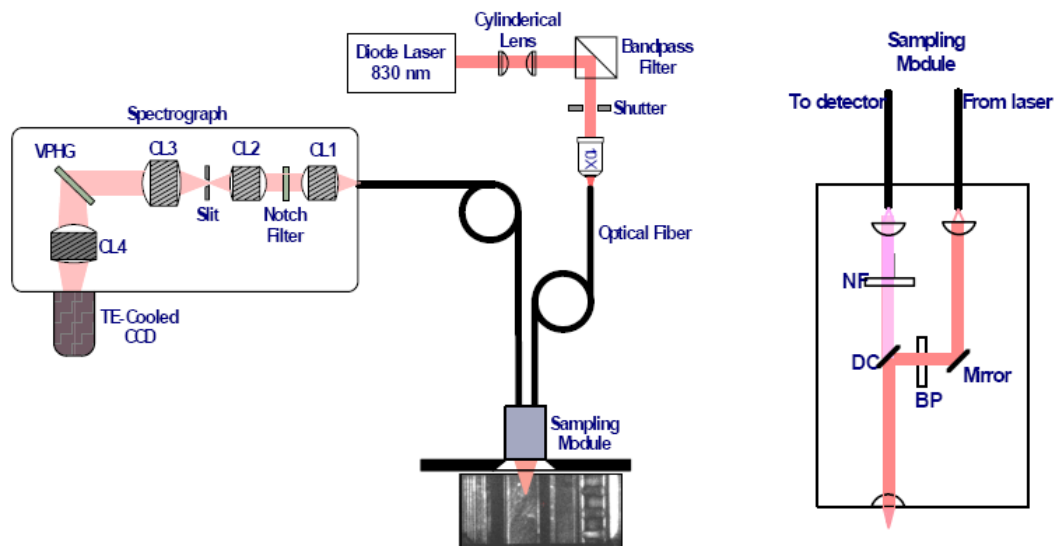


Figure 6.2 – The configuration of a proposed Raman system for in-situ measurements of lubricant composition in the power cylinder.

Implementation of Raman spectroscopy for in-situ measurements in engines is relatively simple compared to an ATR system. The configuration of a proposed single-point system is shown in Figure 6.2. Monochromatic light enters the cylinder through a small quartz

window in the liner. Back-scattered light is collected and processed by a spectrometer. Components may be coupled with standard optical fibers.

6.2.1.1 Ultraviolet Raman Spectroscopy

Previous attempts to analyze diesel oil samples with Raman spectroscopy have failed due to fluorescence interference (at 514 nm and 785 nm) and heating effects (at 1064 nm). The majority of this interference is caused by the strongly absorbing characteristics of soot in the oil.

During this thesis, it was discovered that UV Raman spectroscopy can be used to eliminate this interference because the excitation wavelength is sufficiently outside the range where organic molecules fluoresce. A custom UV Raman system with an excitation of 193 nm was used to analyze a sample of used diesel oil with a soot content of 1.8%. What was obtained is, to the knowledge of the author, the first example of a Raman spectrum of used diesel oil with no fluorescence interference.

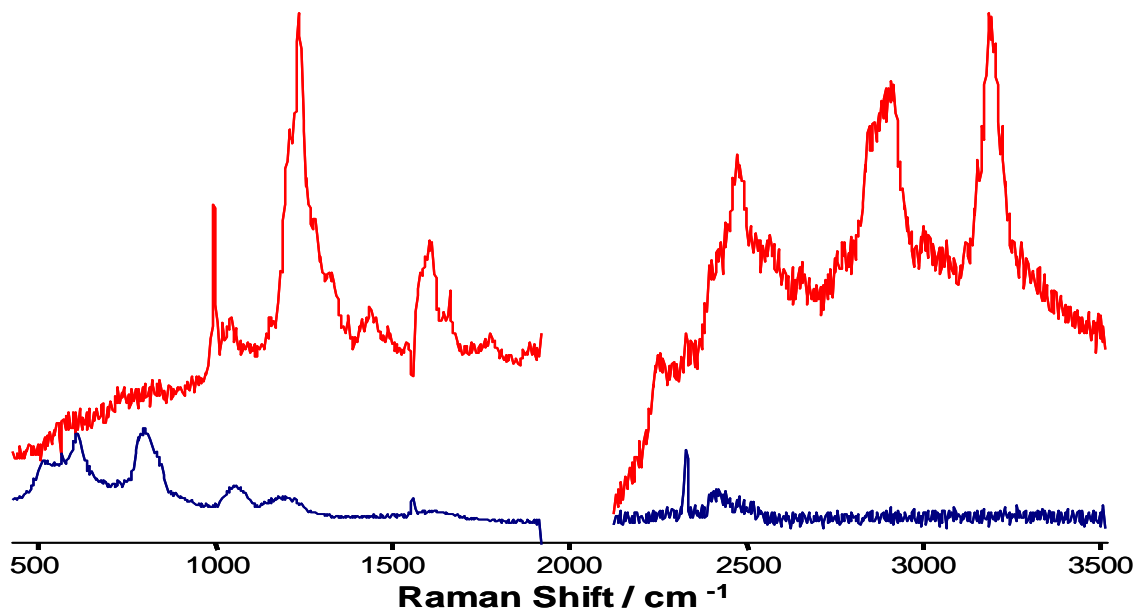


Figure 6.3 – Raman spectra of used diesel engine oil with high soot content (1.8%), measured with deep UV (193 nm) laser excitation. *Red* – Used Oil Spectrum, *Blue* – Spectrum of quartz sample container subtracted from the raw spectrum.

A UV Raman spectrum of used diesel oil is shown in Figure 6.3. A number of clearly defined peaks are present, which could be used to analyze the composition of the sample, although, more research is needed to characterize the spectrum.

A possible interpretation of the spectrum can be proposed based on direct trending from the FTIR spectrum of used oil. Possible spectral correlations in the fingerprint region are labeled in Figure 6.4. Peaks may correspond to bonds in ZDDP and antioxidants, nitration, sulphation and oxidation. UV Raman spectroscopy is a promising alternative to FTIR spectroscopy for in-situ analysis of the lubricant at the piston and liner interface. The technique should be pursued in future studies of lubricant composition in the power cylinder system.

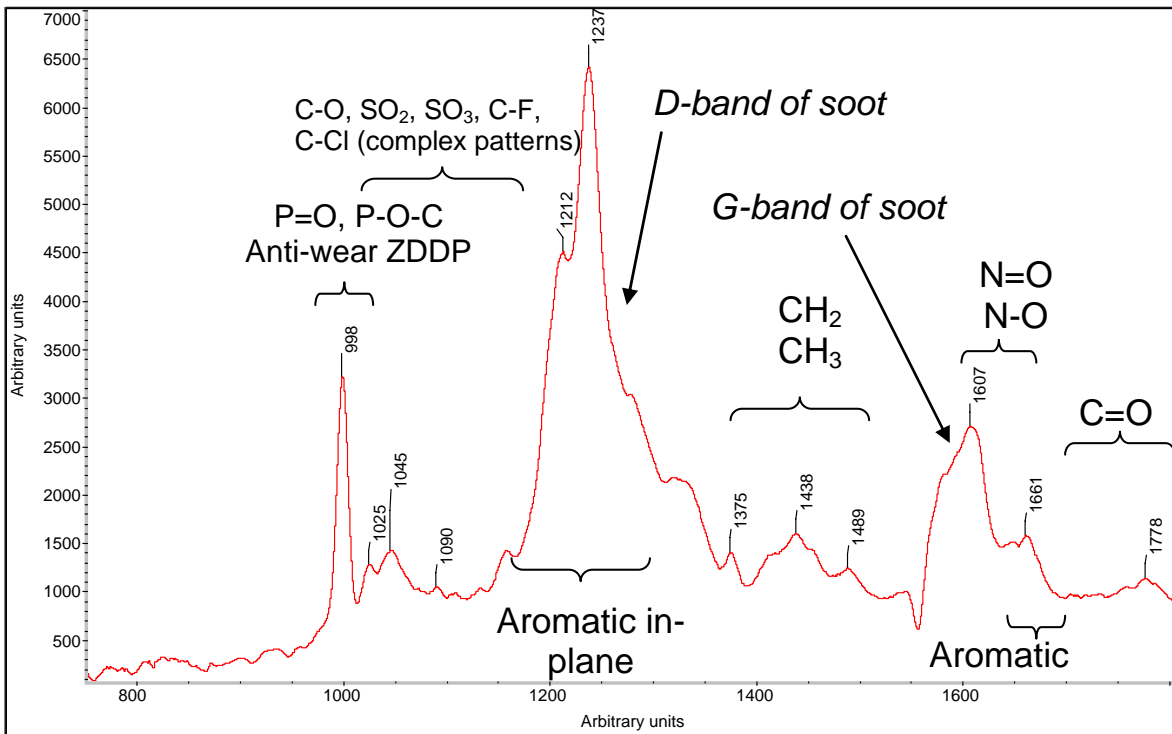


Figure 6.3 - The possible spectral correlations in the fingerprint region of the UV Raman spectrum of used diesel engine oil.

(This page intentionally left blank)

REFERENCES

- [1] Bardasz E., Mackney D., Britton N., Kleinscheck G., Olofsson K., Murray I. and Walker A. Investigations of the interactions between lubricant-derived species and aftertreatment systems on a state-of-the-art heavy duty diesel engine. SAE 2003-01-1963, 2003.
- [2] McGeehan J.A., Moritz J., Shank G., Kennedy S., et al., API CJ-4: Diesel Oil Category for Pre-2007 Engines and New Low Emission Engines Using Cooled Exhaust Gas Recirculation and Diesel Particulate Filters. SAE 2007-01-1966, 2007.
- [3] Kurihara I., Takeshima S. and Yashima H. Development of Low-Ash Type Heavy Duty Diesel Engine Oil for After-Treatment Devices, SAE 2004-01-1955, 2004.
- [4] Givens W.A., Buck W.H., Jackson A., Kaldor A., Hertzberg A. Moehrmann W., Mueller-Lunz S., Pelz N. and Wenninger G. Lubricant formulation effects on transfer of elements to exhaust after-treatment system components. SAE 2003-01-3109, 2003.
- [5] Takeuchi Y., Hirano S., Kanauchi M., Ohkubo H., Nakazato M., Sutherland M. and Van Dam W. The impact of diesel engine lubricants on deposit formation in diesel particulate filters. SAE 2003-01-1870, 2003.
- [6] DOE. Advanced Petroleum-Based Fuels – Diesel Emissions Control (APBF-DEC): Lubricant Project Phase 1 – Final Report, 2007.
- [7] Bardasz E.A., Cowling S., Panesar A., Durham J., and Tadrous T.N. “Effects of Lubricant Derived Chemistries on Performance of the Catalyzed Diesel Particulate Filters”, SAE Paper, 2005-01-2168, 2005.
- [8] McGeehan J.A., Moritz J., Shank G., Kennedy S., et al., 2007, “API CJ-4: Diesel Oil Category for Pre-2007 Engines and New Low Emission Engines Using Cooled Exhaust Gas Recirculation and Diesel Particulate Filters.”, SAE Paper, 2007-01-1966, 2007.
- [9] Van Dam W., Feijens deVries, Van Leeuwen J.A., and Narasaki K., 2007, “Modern Heavy Duty Diesel Engine Oils with Lower TBN Showing Excellent Performance”, SAE Paper, 2007-01-3999, 2007.
- [10] Burk W.M., Domonkos B.D., Donnelly K., Duncan D.A., et al., 2007, “Are the Traditional Methods for Determining Depletion of Total Base Number Providing Adequate Engine Protection?”, SAE Paper, 2007-01-4001, 2007.
- [11] Van Dam W., Narasaki K., and Martinez J., 2006, “Diesel Engines Using Low Sulfur Fuel Showing Excellent Performance and Durability with Reduced TBN

- Lubricants”, SAE Paper, 2006-01-3437, 2006.
- [12] Devlin C.C., Passut C.A., Campbell R.L., and Jao T.C., “Biodiesel Fuel Effect on Diesel Engine Lubrication”, SAE Paper , 2008-01-2375, 2008.
- [13] Fang H.L., Whitacre S.D., Yamaguchi E.S., and Boons M., 2007, “Biodiesel Impact on Wear Protection of Engine Oils”, SAE Paper, 2007-01-4141, 2007.
- [14] Saville S.B., Gainey F.D., Cupples S.D., Fox M.F. and Picken D.J., A study of lubricant condition in the piston ring zone of single-cylinder diesel engines under typical Operating Conditions. SAE 881586, 1988.
- [15] Lee, P. M., Priest, M., Stark, M. S., Wilkinson, J. J., Lindsay-Smith, J. R., Gamble, R., Hammond, C. J., Taylor, R. I. and Chung, S. Lubricant degradation studies using a single cylinder research engine, in *Proc. World Tribology Congress III*, Abstract WTC2005-64373, 2005, 2.
- [16] Fox M.F., Jones C.J., Picken D.J. and Stow C.G. The “limits of lubrication” concept applied to the piston ring zone lubrication of modern engines. *Tribology Letters* 3, 1, 1997, 99-106.
- [17] Boschert, T. "The Lubricant Contribution to Future Low Emission Engine Design", Diesel Particulate and NOx Emissions Course (University of Leeds), Ann Arbor, MI, October 2002.
- [18] McGeehan, J., Yeh, S., Rutherford, J., Couch, M., Otterholm, B., Hinz, A., and Walker, A. Analysis of DPF Incombustible Materials from Volvo Trucks Using DPF-SCR-Urea With API CJ-4 and API CI-4 PLUS Oils, SAE Paper 2009-01-1781, 2009.
- [19] Pawlak, Z. *Tribochemistry of Lubricating Oils*, Elsevier, Amsterdam, 2003.
- [20] Bardasz E.A., and Lamb G.D., “Additives for Crankcase Lubricant Applications”, *Lubricant Additives Chemistry and Applications*, ed. Rudnick L.R., Marcel Dekker Inc., pp. 387-429.
- [21] Van Dam, W., et al. "The Impact of Detergent Chemistry on TBN Retention", *Tribotest Journal*, 6(3), 2000, pp. 227-240.
- [22] Barnes, A. M., Bartle, K. D., Thibon, V. R. A. “A Review of ZDDPs: Characterisation and Role in the Lubricating Oil,” *Tribology International*, Vol. 34, 2000, pp. 389-395.
- [23] Fujita, H., Spikes, H. A. “The Formation of Zinc Dithiophosphate Antiwear Films,” *Journ. Engi. Tribology*, Vol. 218, 2004, pp.265-277.
- [24] Spikes, H. “The History and Mechanisms of ZDDP,” *Tribology Letters*, Vol.

- 17, 2004, pp. 469-489.
- [25] Harrison, P. G., Kikabhai, T. "Proton and Phosphorous-31 Nuclear Magnetic Resonance Study of Zinc(II) O,O'-Dialkyl Dithiophosphates in Solution," J. Chem. Soc. Dalton Transactions, 1987, pp. 807-814.
- [26] Kariya, H.A. "Development of a Multi-Regime Tribometer and Investigation of Zinc Dialkyldithiophosphate Tribofilm Development in the Presence of Overbased Calcium Sulfonate" M.S. Thesis, Massachusetts Institute of Technology, 2009.
- [27] Masuko, M., et al. "Influence of chemical and physical contaminants on the antiwear performance of model automotive engine oil", Proc. IMechE Part J: J. Engineering Tribology, 220, 2006, pp. 455-462.
- [28] Ullmann. "Lubricants and lubrication", *Ullmann's Encyclopedia of Industrial Chemistry*, John Wiley & Sons, New York, 2009.
- [29] Bosch, R.J., et al. "Continued Studies of the Causes of Engine Oil Phosphorus Volatility - Part 2", SAE Technical Paper 2007-01-1073, 2007.
- [30] Zhang, Z., et al. "Effects of Mo-Containing Dispersants on the Function of ZDDP: Chemistry and Tribology", Tribology Transactions, 50, 2007, pp. 58-67.
- [31] Wang, Y., et al., "Investigation on phenyl-borated hydroxyalkyldithiocarbamate as multi-functional lubricating additive with high hydrolytic stability and anti-oxidation", Proc. IMechE Part J: J. Engineering Tribology, 222, pp. 133-140, 2008.
- [32] Zheng, Z., et al., "Synthesis, hydrolytic stability and tribological properties of novel borate esters containing nitrogen as lubricant additives", Wear, 222, pp. 135-144, 2008.
- [33] Hu, J.-Q., et al. "Synergistic Tribological Performances of Borate Additive in Lubricants", Journal of ASTM International, 2007, 4(8).
- [34] ASTM D2896 - 07a, Standard Test Method for Base Number of Petroleum Products by Potentiometric Perchloric Acid Titration, ASTM International, 2007.
- [35] ASTM D4739 - 08e1, Standard Test Method for Base Number Determination by Potentiometric Hydrochloric Acid Titration, ASTM International, 2009.
- [36] Mogaka, Z.N., Wong, V.W., and Shahed, S.M. "Performance and Regeneration Characteristics of a Cellular Ceramic Diesel Particulate Trap," SAE 820272, 1982.
- [37] Sappok, A. The Nature of Lubricant-Derived Ash-Related Emissions and Their Impact on Diesel Aftertreatment System Performance, PhD Thesis,

Massachusetts Institute of Technology, 2009.

- [38] Cheng, S.S. “Rolling Regeneration Trap for Diesel Particulate Control,” SAE 2003-01-3178, 2003.
- [39] Manufacturers of Emission Controls Association (MECA): “Diesel Particulate Filter Maintenance: Current Practices and Experience,” Washington D.C., 2005.
- [40] Aravelli, K., and Heibel, A. “Improved Lifetime Pressure Drop Management for Robust Cordierite (RC) Filters with Asymmetric Cell Technology (ACT)”, SAE 2007-01-0920, 2007.
- [41] Britton, N., Sutton, M., Otterholm, B., Tengstrom, P., Frennfelt, C., Walker, A., and Murray, I. “Investigations into Lubricant Blocking of Diesel Particulate Filters”, SAE 2004-01-3013, 2004.
- [42] Warner, J., Johnson, J., Bagley, S., and Huynh, C. “Effects of Catalyzed Particulate Filter on Emissions from a Diesel Engine: Chemical Characterization Data and Particulate Emissions Measured with Thermal Optical and Gravimetric Methods”, SAE 2003-01-0049, 2003.
- [43] Kimura, K., Lynskey, M., Corrigan, E., Hickman, D., Wang, J., Fang, H., and Chatterjee, S., “Real World Study of Diesel Particulate Filter Ash Accumulation in Heavy-Duty Diesel Trucks”, SAE 2006-01-3257, 2006.
- [44] Allansson, R., Blakeman, P., Cooper, B., Phillips, P., Thoss, J., and Walker, A. “The Use of Continuously Regenerating Trap (CRTTM) to Control Particulate Emissions: Minimizing the Impact of Sulfur Poisoning”, SAE 2002-01-1271, 2002.
- [45] Nemoto, S., Kishi, Y., Matsuura, K., Miura, M., Togawaw, S., Ishikawa, T., Hashimoto, T., and Yamazaki, T. “Impact of Oil-Derived Ash on Continuous Regeneration-Type Diesel Particulate Filter-JCAPII Oil WG Report”, SAE 2004-01-1887, 2004.
- [46] Bunting, B., More, K., Lewis, S., and Toops, T. “Phosphorous Poisoning and Phosphorous Exhaust Chemistry with Diesel Oxidation Catalysts”, SAE 2005-01-1758, 2005.
- [47] Bardasz, E., Antoon, F., Schiferl, E., Wang, J., and Totten, W. “The Impact of Lubricant Derived Sulfur Species on Efficiency and Durability of Diesel NOx Adsorbers”, SAE 2004-01-3011, 2004.
- [48] Gaiser, G., and Mucha, P. “Prediction of Pressure Drop in Diesel Particulate Filters Considering Ash Deposition and Partial Regenerations”, SAE 2004-01-0158, 2004.

- [49] Bodek, K.M., Wong, V.W. The Effects of Sulfated Ash, Phosphorus and Sulfur on Diesel Asftertreatment Systems – A Review, SAE Paper 2007-01-1922, 2007.
- [50] Advanced Petroleum Based Fuels – Diesel Emission Control (APBF-DEC), Lubricants Project, Phase I Report, 2004.
- [51] McGeehan, J.A., Yeh, S., Couch, M., Hinz, A., Otterholm, B., Walker, A., and Blakeman, P. On The Road to 2010 Emissions: Field Test Results and Analysis with DPF-SCR System and Ultra Low Sulfur Diesel Fuel, SAE Paper 2005-01-3716, 2005.
- [52] Asanuma, T. "Effect of Sulfur-Free and Aromatics-Free Diesel Fuel on Vehicle Exhaust Emissions Using Simultaneous PM and NOx Reduction System", SAE Technical Paper 2003-01-1865, 2003.
- [53] DaCosta, H.F.M., Silver, R. "Thermal and Chemical Aging of Diesel Particulate Filters", SAE Technical Paper 2007-01-1266, 2007.
- [54] McGeehan, J.A., et al. API CJ-4: Diesel Oil Category for Both Legacy Engines and Low Emission Engines Using Diesel Particulate Filters, SAE Paper 2006-01-3439, 2006.
- [55] Kurihara, I., et al., 2004. "Development of Low-Ash-Type, Heavy-Duty Diesel Engine Oil for After-Treatment Devices", SAE Technical Paper 2004-01-1955.
- [56] Thirouard B. and Tian T. Oil transport in the piston ring pack (part I): identification and characterization of the main oil transport mechanisms, SAE 2003-01-1952, 2003.
- [57] Taylor, R.I. Transient effects in engines operating under steady speeds and loads, in *Proc. Of the 30th Leeds-Lyon Symposium on Tribology, Transient Processes in Tribology*, 2004, pp. 123-131.
- [58] Wong, V.W., Thomas, B.C., Watson, S.A.G. Bridging Macroscopic Lubricant Transport and Surface Tribochemical Investigations in Reciprocating Engines, Part J - Journal of Engineering Tribology, 221, 2007, pp. 183-193.
- [59] Dowson, D., Economou, P.N., Ruddy, B.L., Strachan, P.J., and Baker, A.J.S. Piston ring lubrication, part II, theoretical analysis of a single ring and a complete ring pack, in *Proc ASME Winter Annual Meeting*, 1979.
- [60] Wong, V.W., Tian, T., Lang, H., Ryan, J.P., Sekiya, Y., Kobayashi, Y., and Aoyama, S. A numerical model of piston secondary motion and piston slap in partially flooded elastohydrodynamic skirt lubrication, SAE Paper 940696, 1994.

- [61] Tian, T. Modeling the performance of the piston ring-pack in internal combustion engines. Ph.D. Thesis, Department of Mechanical Engineering, MIT, June 1997.
- [62] Tian, T., Noordzij, L.B., Wong, V.W., and Heywood, J.B. Modeling piston-ring dynamics, Blowby, and Ring-Twist Effects, *ASME, J. Eng. Gas Turbines Power*, 120(4), pp. 843-854.
- [63] Audette, W.E. Estimation of Oil Consumption Due to In-Cylinder Vaporization in Internal Combustion Engines, PhD Thesis, Massachusetts Institute of Technology, 1997.
- [64] Yilmaz, E. Sources and Characteristics of Oil Consumption in a Spark-Ignition Engine, PhD Thesis, Massachusetts Institute of Technology, 2003.
- [65] Inagaki, H., Saito, A., Murakami, M., and Konomi, T.: "Development of Two-Dimensional Oil Film Thickness Distribution Measuring System", SAE paper 952346, 1995.
- [66] Thirouard, B., Tian, T., and Hart, D. P.: "Investigation of Oil Transport Mechanisms in the Piston Ring Pack of a Single Cylinder Diesel Engine, Using Two Dimensional Laser Induced Fluorescence", SAE paper 982658, 1998.
- [67] Nakashima, K., Ishihara, S., and Urano, K. "Influence of Piston Ring Gaps on Lubricant Oil Flow into the Combustion Chamber", SAE paper 952546, 1995.
- [68] Saito, K., Igashira, T., and Nakada, M.: "Analysis of Oil Consumption by Observing Oil Behavior around Piston Ring Using a Glass Cylinder Engine", SAE paper 892107, 1989.
- [69] Hill, S., H., Sytsma, S., J. A Systems Approach to Oil Consumption, SAE paper 910743, 1991.
- [70] Froelund, K. Real-Time Steady-State Measurement of PCV-Contribution to Oil Consumption on Ford 4.6 L SI-Engine, SAE paper 2000-01-2876, 2000.
- [71] Orrin, D. S., and Coles, B. W. Effects of Engine Oil Composition on Oil Consumption, SAE paper 710141, 1971.
- [72] Stewart, R. M., and Saely, T. W. The Relationship between Oil Viscosity Engine Performance - A Literature Search, SAE paper 770372, 1977.
- [73] Furuhashi, S., Hiruma, M., and Yoshida, H. An Increase of Engine Oil Consumption at High Temperature of Piston and Cylinder, SAE paper 810976, 1981.
- [74] Wahiduzzaman S., Keribar, R., Dursunkaya, Z., and Kelley, F. A.: "A Model for Evaporative Consumption of Lubricating Oil in Reciprocating Engines", SAE

paper 922202, 1992.

- [75] De Petris, C., Gigilio, V., and Police, G.: "A Mathematical Model of the Evaporation of the Oil Film Deposited on the Cylinder Surface of IC Engines", SAE paper 972920, 1997.
- [76] Audette III, W. E., and Wong, V. W.: "A Model for Estimating Oil Vaporization from the Cylinder Liner as a Contributing Mechanism to Engine Oil Consumption", SAE paper 1999-01-1520, 1999.
- [77] Richard, G.P. "Lubricant Properties in the Diesel Engines Piston Ring Zone", Proc. 9th Leeds-Lyon Symposium on Tribology: Tribology of Reciprocating Engines, 1982, pp. 171-175.
- [78] Bush, G.P., Fox, M.F., Picken, D.J., Butcher, L.F. "Composition of Lubricating Oil in the Upper Ring Zone of an Internal Combustion Engine", Tribology International, Vol. 24, 4, 1991, pp. 231-233.
- [79] Picken, D.J., Seare, K.D.R., Thompson, A.L., Fox, M.F., Preston, W.H. "Lubricating Oil - Extraction and Chemical Analysis", Experimental Methods in Engine Research and Development '91, IMechE Seminar, HQ, December, 1991, pp. 115-120.
- [80] Iwakata, K., Onodera, Y., Mihara, K., Ohkawa, Y. "Nitro Oxidation of Lubricating Oil in Heavy-Duty Diesel Engine", SAE Technical Papers, SAE Paper 932839, 1993.
- [81] Fox, M. "Ring Zone Lubrication: Implications for Reduced Emissions and Enhanced Engine Life", The Tribology of Internal Combustion Engines, Professional Engineering Publications, 1997, pp. 69-91.
- [82] Moritani, H., Nozawa, Y. "Investigation on Oil Degradation in Piston Second-Land Region of Gasoline Engine", Japanese Journal of Tribology, Vol. 44, No. 4, 1999, pp. 435-446.
- [83] Nattrass, S.R., Thompson, D.M., McCann, H. "First In-Situ Measurement of Lubricant Degradation in the Ring Pack of a Running Engine", SAE Technical Papers, SAE Paper 942026, 1994.
- [84] ASTM D4951 – 09, Standard Test Method for Determination of Additive Elements in Lubricating Oils by Inductively Coupled Plasma Atomic Emission Spectrometry, ASTM International, 2009.
- [85] ASTM D5185 – 09, Standard Test Method for Determination of Additive Elements, Wear Metals, and Contaminants in Used Lubricating Oils and Determination of Selected Elements in Base Oils by Inductively Coupled Plasma Atomic Emission Spectrometry (ICP-AES), ASTM International, 2009.

- [86] ASTM D5984 - 97(2007), Standard Test Method for Semi-Quantitative Field Test Method for Base Number in New and Used Lubricants by Color-Indicator Titration, ASTM International, 2007.
- [87] Weng, W. Cummins Smart Oil Consumption Measurement System, SAE Paper, 2000-01-0927, 2000.
- [88] Finch, S. Evaluation of a Field Test Method for Total Base Number Determination in Lube Oils, DTR-12-03, Dexsil Corporation.
- [89] Finch, S. Evaluation of Field Methods for TBN and TAN in Oils, DTR-14-01, Dexsil Corporation.
- [90] Finch, S. TBN Analysis of Lubricants Using Non-Hazardous Solvents, DTR-14-02, Dexsil Corporation.
- [91] ASTM D664 - 09a, Standard Test Method for Acid Number of Petroleum Products by Potentiometric Titration, ASTM International, 2009.
- [92] ASTM D974 – 08, Standard Test Method for Acid and Base Number by Color-Indicator Titration, ASTM International, 2008.
- [93] ASTM D4172 - 94(2004)e1, Standard Test Method for Wear Preventive Characteristics of Lubricating Fluid (Four-Ball Method), ASTM International, 2004.
- [94] Harrick, N.J. *Internal Reflection Spectroscopy*, John Wiley and Sons Inc, 1967.
- [95] Thompson, M. In-Situ Reaction Monitoring: Tracking an Intermediate, Remspec Corporation, 2008.
- [96] Audette W.H. Estimation of Oil Consumption Due to In-Cylinder Vaporization in Internal Combustion Engines, M.A. Thesis, Massachusetts Institute of Technology, 1999.
- [97] Incropera, F., DeWitt, D. *Fundamentals Of Heat Transfer*, Third Edition, John Wiley & Sons, New York, NY, 1990.
- [98] Selby, T.W. Development and Significance of the Phosphorus Emission Index of Engine Oils, *Proceedings of 13th International Colloquium - Lubricants, Materials, and Lubrication Engineering*, Esslingen, Germany, pp. 93-102, 2002.
- [99] Manni, M., Pedicillo, A., Del Piero, G., and Previde Massara, E. An Experimental Evaluation of the Impact of Lubricating Oils and Fuels on Diesel Particulate Filters, SAE Paper, 2007-01-1925, 2007.
- [100] Selby T.W., Bosch R.J. and Fee D.C. Phosphorus additive chemistry and its effects on the phosphorus volatility of engine oils. *Elemental Analysis*

Symposium, ASTM D02, Tampa, FL, December 8, 2004.

- [101] US Patent 5,164,101, "Method for Reducing Piston Deposits", November 17, 1992.
- [102] Van Dam W., Broderick D.H., Freerks R.L., and Small V.R., Willis W.W., 1997, "TBN Retention – Are We Missing the Point?", SAE Paper, 972950.
- [103] Sugiyama G., Maeda A., and Nagai K., 2007, "Oxidation Degradation and Acid Generation in Diesel Fuel Containing 5% FAME", SAE/JSAE Paper, 2007-01-2027/20077154.
- [104] Wilhoit, R. C., Zwolinski, B.J. *Handbook of Vapor Pressures and Heats of Vaporization of Hydrocarbons and Related Compounds*. Thermodynamics Research Center, Texas A&M University, College Station, TX, 1971.
- [105] Gallant, R.W., Yaws, C.L. *Physical Properties of Hydrocarbons and Other Chemicals*. Gulf Publishing Company, Houston, TX, 1993.

(This page intentionally left blank)

APPENDIX A – ESTIMATING SULFATED ASH WITH ELEMENTAL WEIGHTING FACTORS

The sulfated ash level of a lubricant can be estimated by applying the elemental weighting factors listed in Table A-1. A summation of each elemental contribution (*i*) to sulfated ash is performed according to the equation:

$$\text{sulfated ash} = \sum_i [\text{Elemental \%}]_i \times (\text{Weighting Factor})_i \quad (\text{A.1})$$

This method was used to estimate the sulfated ash in the lubricants used in this study. Lubricant properties are listing in Tables 3-7 and 3-8. The calculation is summarized in Tables A-2 and A-3. The estimations of sulfated ash are in good agreement with the measured values.

Table A.1 – Elemental Weighting Factors

Element	Multiply Element Percentage By:
Calcium	3.4
Magnesium	4.95
Zinc	1.5
Barium	1.7
Sodium	3.09
Lead	1.464
Boron	3.22
Potassium	2.33
Lithium	7.92
Manganese	1.291
Molybdenum	1.5
Copper	1.252

Table A.2 – Elemental Percentages of Lubricant Species that Contribute of Sulfated Ash

Oil	A	B	C	D	E	F
Calcium (Ca)	0.312	0.250	0.250	0.313	0.143	0.000
Magnesium (Mg)	0.012	0.000	0.000	0.001	0.036	0.000
Zinc (Zn)	0.155	0.125	0.123	0.135	0.139	0.000
Barium (Ba)	0.000	0.000	0.000	0.000	0.000	0.000
Sodium (Na)	0.000	0.000	0.000	0.000	0.000	0.000
Phosphorus (P)	0.132	0.105	0.109	0.149	0.129	0.048
Boron (B)	0.021	0.000	0.000	0.013	0.059	0.000

Table A.3 Calculation of Estimated Sulfated Ash Percentage

Oil	A	B	C	D	E	F
Elemental Contribution to Sulfated Ash						
Calcium (Ca)	1.062	0.848	0.848	1.064	0.487	0.000
Magnesium (Mg)	0.059	0.000	0.000	0.005	0.176	0.000
Zinc (Zn)	0.232	0.187	0.185	0.203	0.208	0.000
Barium (Ba)	0.000	0.000	0.000	0.000	0.000	0.000
Sodium (Na)	0.000	0.000	0.000	0.000	0.000	0.000
Phosphorus (P)	0.000	0.000	0.000	0.000	0.000	0.000
Boron (B)	0.067	0.000	0.000	0.042	0.189	0.000
Calcium (Ca)	0.008	0.000	0.000	0.015	0.012	0.000
Estimated Sulfated Ash (%)	1.427	1.035	1.033	1.329	1.071	0.000
Measured Sulfated Ash (%)	1.410	1.000	1.000	1.350	1.000	0.057

APPENDIX B – CALCULATING BASE OIL PROPERTIES

This procedure is taken directly from [96].

The first task necessary to compute the oil properties required by the lubricant species transport model is to translate the data given by an oil distillation curve into useful information regarding the properties of the various species that compose base oil.

It is assumed that all the components in base oil are pure paraffin hydrocarbons. Using tabulated information from Wilhoit and Zwolinski [104], the molecular weight of such hydrocarbons can be reasonably correlated to the hydrocarbon's boiling point by:

$$MW = (6.28 \times 10^{-6}) \cdot T_{bp}^3 + (-4.61 \times 10^{-3}) \cdot T_{bp}^2 + (1.953) \cdot T_{bp} - 99.93 \quad (\text{B.1})$$

Where MW is the specie's molecular weight (kg/kmol) and T_{bp} is the specie's boiling point (C) as reported from the distillation curve. This correlation is fitted to tabulated data over a temperature range of 460K through 900K.

All the other necessary thermo-physical properties can be calculated once the molecular weight is known. For a pure paraffin hydrocarbon, the chemical structure is completely defined once the molecular weight is known. Since paraffin hydrocarbons have no branches, the chemical shape is that of a long string and the number of hydrogen atoms is exactly 12 times the number of carbon atoms plus 2 more to terminate both ends of the chain.

The vapor pressure can be computed knowing the chemical composition and the local instantaneous temperature of the liquid oil [104]:

$$\log_{10}(VP) = A - \frac{B}{C + (T_l - 273)} \quad (\text{B.2})$$

Where VP is the vapor pressure (mm Hg), T_l is the temperature of the liquid at its exposed surface (Kelvin), and A , B , and C are the Antoine constants which are tabulated by oil species.

Assuming a paraffin structure, the constants are correlated to the oil specie's molecular weight by:

$$\begin{aligned}
 A &= (4.40 \times 10^{-10}) \cdot MW^3 + (-1.10 \times 10^{-6}) \cdot MW^2 + (1.04 \times 10^{-3}) \cdot MW - 6.85 \\
 B &= (1.91 \times 10^{-6}) \cdot MW^3 + (-4.78 \times 10^{-3}) \cdot MW^2 + (4.51) \cdot MW - 1.06 \times 10^3 \\
 C &= (-1.15 \times 10^{-7}) \cdot MW^3 + (4.03 \times 10^{-4}) \cdot MW^2 + (-6.02 \times 10^{-1}) \cdot MW - 2.72 \times 10^2
 \end{aligned} \tag{B.3}$$

As before, these correlations are fitted to tabulated data. The source data was taken over the MW range of 310 kg/kmol to 842 kg/kmol.

Note that Equation B.2 becomes unbounded as the sum (C+T) approaches zero. In order for a species in the piston or liner oil to reach this temperature, however, the vapor pressure will have passed the point where it exceeds the total pressure within the cylinder. When this happens, the species will boil and the resulting mass transfer is no longer diffusion limited (as this model assumes) but is, instead, energy limited. The physics of the boiling process are not included in the current model. In the results shown in this thesis, the temperature of the liquid oil was never high enough to cause any species to boil.

In addition to the oil properties, the thermo-physical gas properties necessary to calculate vaporization are calculated using thermodynamic tables for air. In all cases, both the instantaneous cylinder pressure and the instantaneous boundary layer film temperature are used for evaluating the gas properties. Due to the low mass fraction of the oil vapor in the air, this should be a reasonably valid assumption.

The binary diffusion constant of a given oil species through air was computed using an algorithm presented in [105].

APPENDIX C – STATISTICAL ANALYSIS OF VALVE TRAIN OIL SAMPLES

Table C.1 – Valve Train and Sump Oil ICP Data

Metal	Sump Sample Mean (ppm)	Valve Train Sample Mean (ppm)	Sump Sample Std. Dev. (ppm)	Valve Train Sample Std. Dev. (ppm)
Calcium	2443.33	2409.83	27.15	39.09
Aluminum	6.00	6.00	0.00	0.00
Boron	20.00	20.67	0.00	0.82
Iron	15.33	16.50	0.58	1.05
Magnesium	262.67	257.00	4.73	4.43
Phosphorus	1163.00	1144.17	8.54	12.75
Zinc	1347.00	1333.50	9.85	16.15

Table C.2 – Valve Train and Sump Oil FTIR Data

Wave Number (cm⁻¹)	Sump Sample Mean (Absorbance)	Valve Train Sample Mean (Absorbance)	Sump Sample Std. Dev. (Absorbance)	Valve Train Sample Std. Dev. (Absorbance)
2922	0.0590	0.0590	0.0000	0.0000
2854	0.0330	0.0327	0.0009	0.0081
1462	0.0175	0.0176	0.0003	0.0003
1376	0.0069	0.0069	0.0003	0.0002
978	0.0014	0.0014	0.0000	0.0000

APPENDIX D – STATISTICAL SIGNIFICANCE OF TRENDS IN FILTER TEST RESULTS

The conclusions of this study are based on relative slopes, which have been statistically tested to show that they are valid. Following is a list of the relevant linear regression statistics.

Table D.1 – Summary of Regression Parameters

Figure	Filter	ASTM Test	Slope	p-Value [‡]	90% Confidence Interval		R ²
					Lower	Upper	
5.9	Strong Base	D664	0.002779	2.15E-05	0.002313	0.003245	0.979137
5.9	Standard	D664	0.008807	0.05971	-0.00089	0.018506	0.884145
5.9	Strong Base	D664	0.001326	1.06E-10	0.001223	0.001428	0.98005
5.9	Standard	D664	0.002787	1.87E-07	0.002525	0.00305	0.983022
5.10	Strong Base	pH	-0.02361	N/A	-0.02361	-0.02361	1.0
5.10	Standard	pH	-0.0076	0.000344	-0.00986	-0.00533	0.937141
5.10	Strong Base	pH	-0.00194	2.42E-07	-0.00233	-0.00154	0.819489
5.10	Standard	pH	-0.00372	0.008418	-0.0056	-0.00184	0.712303
5.11	Strong Base	D4739	-0.0043	1.87172E-08	-0.004888	-0.003714	0.934276
5.11	Strong Base	D5984	-0.00404	9.66318E-12	-0.004325	-0.003752	0.98132
5.11	Standard	D5984	-0.00877	4.83902E-06	-0.0100	-0.0074	0.957104
5.12	Strong Base	FTIR	0.0160365	0.127924961	-0.00254	0.034617	0.760514
5.12	Standard	FTIR	0.0267660	0.0019901	0.02061	0.032922	0.972142
5.13	Strong Base	D445	0.06875	0.000141	0.055355	0.082146	0.980682
5.13	Standard	D445	0.278041	0.029988	0.066076	0.490006	0.940922

[‡]p-Values below 0.05 indicate that the linear dependence represented by the slope can be considered to be statistically significant.